*Journal of Cardiovascular Magnetic Resonance* (2006) **8,** 211–300

ISSN: 1097-6647 print / 1532-429X online
DOI: 10.1080/10976640500479029

Taylor & Francis
Taylor & Francis Group

# Saturday Posters

## 430. THE USEFULNESS OF STRESS PERFUSION MR USING SSFP SEQUENCE FOR THE EVALUATION OF MYOCARDIAL ISCHEMIA: EXPERIENCES IN 167 CASES

**Sang Il Choi,[1] Hyuk-Jae Jang,[1] Dong-Ju Choi,[1] Cheong Lim,[1] Tae-Hwan Lim.[2]** [1]***Seoul National University Bundang Hospital, Seong-Nam, Republic of Korea,*** [2]***Asan Medical Center, University of Ulsan, Seoul, Republic of Korea.***

*Introduction:* Recently, myocardial magnetic resonance (MR) perfusion imaging using saturation-recovery steady-state free precession sequence (SR-SSFP) has been proven to provide high signal-to-noise ratio and contrast-to-noise ratio comparing with fast gradient techniques.

*Purpose:* To determine the usefulness and accuracy stress myocardial MR perfusion imaging using SR-SSFP for depiction of myocardial ischemia in patients with ischemic heart disease.

*Methods:* One hundred sixty-seven patients underwent first-pass contrast-enhanced myocardial MR imaging at rest and adenosine-induced stress by using a 1.5-T cardiac MR imaging unit (Intera CV release 10; Philips Medical Systems, Best, Netherlands) equipped with high-performance gradients and a five-element phased-array cardiac coil. The first-pass MR perfusion (2744/1372 msec: TR/TE, 50° flip angle, 256 × 256 matrix, 8 mm section thickness, 8–12 mm intersection gap) were acquired with a gradient echo sequence by using saturation-recovery steady-state free precession sequence (SR-SSFP). Coronary angiography was performed in 113 patients. Image analyses were performed to compare the diagnostic accuracies of MR imaging, with coronary angiography as the reference standard.

*Results:* During the MR exam, minor side effects were occurred as chest discomfort (n = 33), dyspnea (n = 5), and facial flushing (n = 1). The overall sensitivity of MR imaging for depicting at least one coronary artery with significant stenosis was 96% (82 of 85 patients). The sensitivities of MR imaging for depiction of single-, double-, and triple-vessel stenoses were 87% (13 of 15 patients), 96% (25 of 26 patients), and 100% (51 of 51 patients), respectively. The specificity of MR imaging for identification of patients with significant coronary artery stenoses was 78% (18 of 23 patients).

*Conclusions:* Stress myocardial MR perfusion imaging using SR-SSFP sequence is safe and useful for the detection of ischemia in patient with ischemic heart disease.

## 431. IMPROVED CORONARY MR ANGIOGRAPHY AT 3T USING ADIABATIC T2 PREP

**Nezafat Reza,[1] Matthias Stuber,[2] Ronald Ouwerkerk,[2] Milind Desai,[1] Ahmed Gharib,[1] Roderick Pettigrew.[1]** [1]***National Institute of Health, DHHS, Bethesda, MD, USA,*** [2]***Johns Hopkins University, Baltimore, MD, USA.***

*Introduction:* Coronary magnetic resonance angiography (MRA) at 1.5T has shown promise for the assessment of significant coronary artery disease. However, low SNR limits the utilization of this imaging technique for more distal and branching vessels at 1.5T. At a higher magnetic field strength, an improved SNR is expected. However, enhanced effect of magnetic field susceptibility leads to off-resonance effects, while $B_1$ inhomogeneity, and increased specific absorption rate are additional limitations that have to be considered. This combination results in non-uniform magnetization preparation by the standard composite MLEV weighted $T_2$ Preparation ($T_2$Prep) sequence used for coronary MRA. A new adiabatic refocusing $T_2$ Prep sequence is presented, in which the magnetization is tipped into the transverse plane with a hard RF pulse and refocused using a pair of adiabatic fast-passage RF pulses. The isochromats are subsequently returned to the longitudinal axis using a hard RF pulse. Numerical simulations predict an excellent suppression of artifacts originating from $B_1$ inhomogeneity while achieving good contrast enhancement between coronary arteries and surrounding tissue. This was confirmed by an in-vivo study, in which coronary MR angiograms was obtained without a $T_2$ Prep, with a conventional MLEV weighted $T_2$ Prep and the proposed adiabatic $T_2$ Prep.

*Methods:* Numerical simulations were performed to study the effect of B1 and B0 variation on the magnetization response to the sequence. In vivo coronary experiments were performed on normal volunteers (N = 15) with no known cardiovascular disease. All experiments were performed on Philips 3T Intera system. A free-breathing ECG gated, fat suppressed, 3D segmented gradient-echo image was acquired using a 2D-selective navigator signal. Imaging parameters were as follows: FOV = 27 cm, TR = 7.5 ms, TE = 2.1 ms, Matrix size = 384, slice thickness = 3 mm. In order to study the effect of T2Prep, we compared the results by doing the experiments without application of T2Prep, using two composite MLEV pulse, and with adiabatic T2Prep.

*Results:* Figures 1 and 2 demonstrate the longitudinal magnetization, $M_z/M_{eq}$, calculated from the numerical simulation of the Bloch equations for arterial and venous blood and for the myocardium for two conventional MLEV weighted composite

TABLE 1
Statistical Comparison: Effect of adiabatic T2Prep, MLEV weighted composite T2Prep and no T2Prep.

| | Adiabatic $T_2$ | Standard $T_2$ | No $T_2$ | $P_{c1c2}$ | $P_{c1c3}$ | $P_{c2c3}$ |
|---|---|---|---|---|---|---|
| $SNR_{blood}$ | $16.54 \pm 3.37$ | $16.97 \pm 4.21$ | $19.61 \pm 4.63$ | NS | <0.01 | <0.01 |
| $CNR_{blood\text{-}muscle}$ | $14.73 \pm 3.36$ | $13.17 \pm 4.37$ | $10.40 \pm 4.34$ | NS | <0.002 | <0.06 |
| Vessel Sharpness | $38.6 \pm 4.0$ | $36.5 \pm 6.0$ | $32.9 \pm 6.0$ | NS | <0.01 | NS |
| Visual Grading | $2.93 \pm 0.25$ | $1.8 \pm 0.56$ | $2.93 \pm 0.25$ | <0.0001 | NS | <0.0001 |

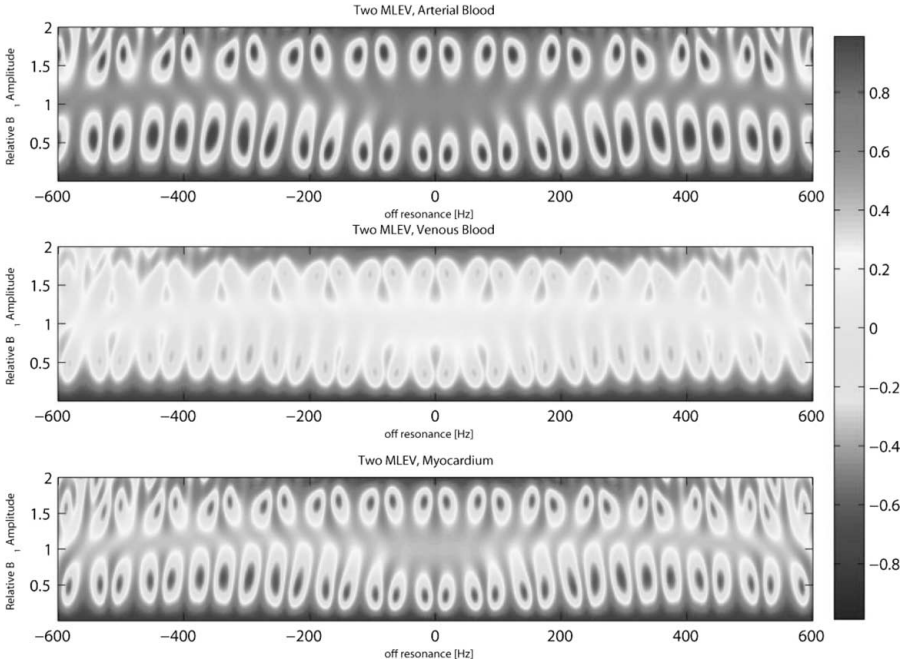


FIG. 1. Mz/Meq after experiencing MLEV weighted T2Prep.

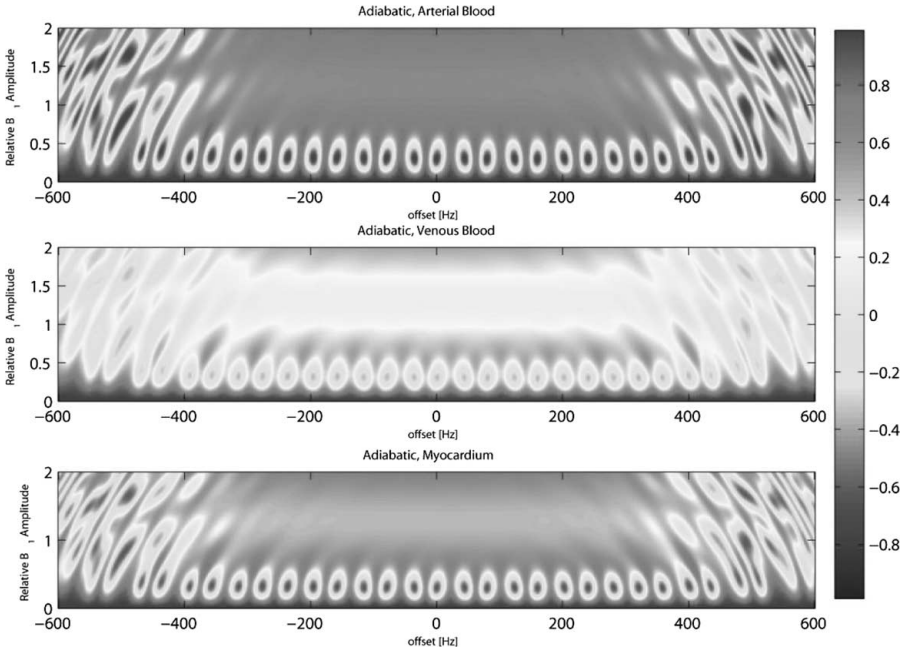


FIG. 2. Mz/Meq after adiabatic T2Prep.

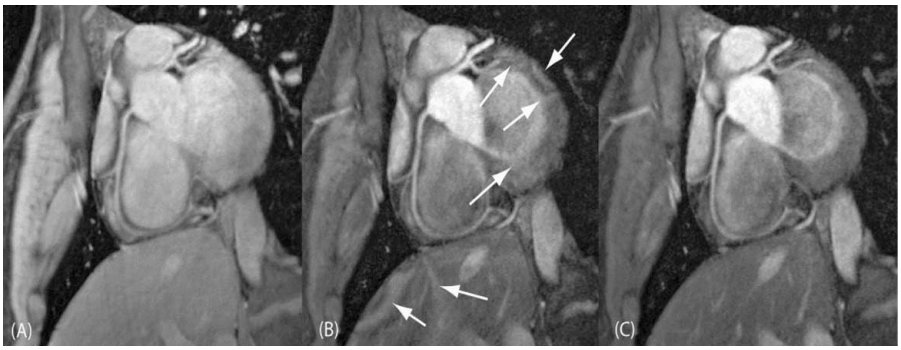


FIG. 3. Example RCA acquired with (A) no T2 Prep (B) MLEV T2Prep (C) adiabatic T2Prep.

refocussing pulses and adiabatic pulses. The colormap in the image corresponds to the normalized longitudinal magnetization after the $T_2$Prep sequence as a function of off-resonance and normalized B1 amplitude. In an ideal field with no inhomogeneity, the magnetization should return to the equilibrium state with a loss in magnitude only due to relaxation. These results demonstrate that the magnetization does not consistently and fully return to its equilibrium in the presence of strong B1 inhomogeneity with MLEV composite pulses compared to the adiabatic T2Prep. Sample reformatted images of the RCA are shown in Fig. 3. The coronary MRA image in Fig. 3A was acquired without any $T_2$Prep. The image shows no artifacts with no or minor contrast between coronary arteries and the surrounding tissue. Fig. 3B and 3C shows the same image acquired with the standard $T_2$ Prep and adiabatic T2 Prep sequence. An enhanced artifact level is visible in the liver, myocardium and the coronary arteries, as indicated by the arrows. Statistical comparisons of both objective and subjective measures are shown in Table 1.

*Conclusion:* In this study, a novel $T_2$Prep contrast enhancement scheme for coronary MRA at 3T was proposed. The results suggest that the new technique not only yields an improved CNR similar to the conventional T2 Prep, but also successfully removes the image artifacts originating from B1 and B0 inhomogeneity without exceeding the SAR limit.

## 432. QUANTITATIVE DUAL-BOLUS FIRST-PASS STRESS CMR OUTPERFORMS QUALITATIVE ANALYSIS FOR LOCALIZING CORONARY ARTERY DISEASE

**Patrick Antkowiak, BS, Frederick H. Epstein, PhD, Kiran Nandular, MD, John M. Christopher, RT, Jennifer R. Hunter, RN, Christopher M. Kramer, MD.** ***University of Virginia, Charlottesville, VA, USA.***

*Introduction:* Dual-bolus first-pass CMR with deconvolution analysis was recently shown to be highly accurate for quantitative perfusion imaging in canines with coronary artery occlusion or intracoronary adenosine infusion (1). In dual bolus imaging, a low dose bolus is used to image the undistorted arterial input function (AIF) and a high dose bolus is used to image the myocardial tissue function (TF) with high signal-to-noise ratio. We performed an initial evaluation of this quantitative technique for detecting coronary artery disease (CAD) in patients in comparison to qualitative analysis.

*Methods:* Eleven patients (7 male, 4 female, ages 67 $\pm$ 13) with suspected CAD based on an abnormal stress Sestamibi examination were imaged by CMR and x-ray angiography within 25 $\pm$ 17 days of each other. CMR studies were performed at 1.5T on either a Sonata or Avanto scanner (Siemens Medical Solutions). First-pass CMR was performed during adenosine infusion (140 $\mu$g/kg/min $\times$ 5 minutes) and again 10 minutes later at rest using a hybrid gradient-echo/echo-planar imaging sequence either with (N = 3) or without (N = 8) TSENSE. Both at stress and rest, first-pass data were acquired using Gd-DTPA bolus injections of 0.01 mmol/kg and 0.1 mmol/kg at 4 mL/sec followed by 20 cc of saline flush at 4 mL/sec. Specific parameters included number of slices = 3 (short axis at base, midventricle, and apex), a nonselective 90° saturation pulse followed by an 80 ms delay, field of view = 340–400 $\times$ 212–360 mm, matrix = 128 $\times$ 80, slice thickness = 8 mm, flip angle = 25°, TR = 5.6–6.2 ms, TE = 1.3 ms, and echo train length = 4. Both qualitative and quantitative analyses were performed in a standard 16 segment model of the left ventricle. For quantitation, Fermi function deconvolution analysis was used to compute perfusion reserve (PR) in both transmural and subendocardial segments. Perfusion reserve was compared to x-ray angiography for each patient and for each sector. For angiography, a patient or sector was defined as ischemic if the supplying coronary artery had a 50% or greater stenosis. Receiver-operator characteristic (ROC) analysis was performed for the sector-wise PR analysis using x-ray angiography as the gold standard.

*Results:* Example time-intensity curves from one patient during vasodilation are shown in Fig. 1 demonstrating TF curves in normal and ischemic segments as well as the scaled AIF curve. X-ray angiography detected significant coronary stenoses in 7 of the 11 patients. On a per-patient basis, quantitative dual-bolus CMR using a threshold of PR < 1.8 to indicate ischemia detected 7 of 7 patients with significant CAD, 3 of 4 without, with 1 false positive study, resulting in a sensitivity of 100%, a specificity of

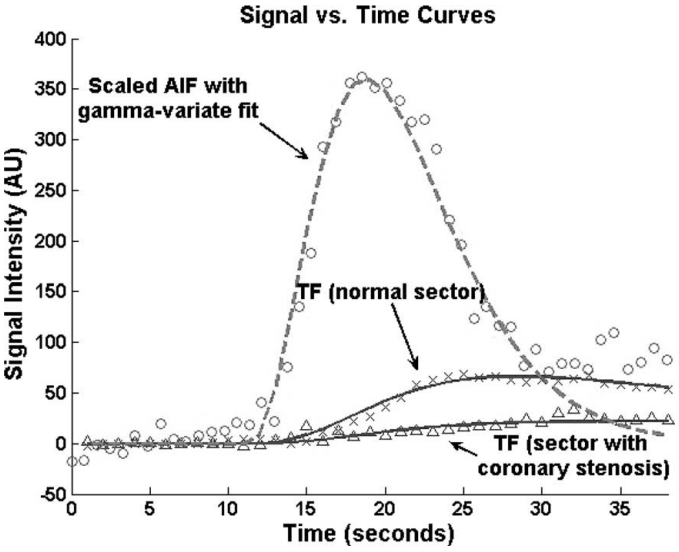


FIG. 1.

75%, and an overall accuracy of 91%. The qualitative analysis detected 6 of 7 patients with significant CAD, 3 of 4 without, with 1 false positive and 1 false negative, resulting in a sensitivity of 86%, a specificity of 75%, and an overall accuracy of 82%. ROC analysis of the sector-by-sector comparison yielded an area under the curve of 0.85 for the PR in subendocardial segments and 0.74 for PR in transmural segments. For 176 total subendocardial segments, using PR $< 1.8$ to indicate ischemia, quantitative dual bolus CMR had a sensitivity of 74%, specificity of 81%, and an overall accuracy of 78%. The overall accuracy of the qualitative by sector analysis was 64%.

*Conclusions:* Initial clinical results using quantitative dual-bolus first-pass CMR demonstrate excellent accuracy on a per-patient basis for the identification of significant CAD. In addition, the segmental quantitative analysis performs better than qualitative analysis for identification of the specific coronary artery territory involved.

## REFERENCE

1. Christian, et al. Radiology 2004;232:677–684.

## 433. CORONARY ARTERY MAGNETIC RESONANCE ANGIOGRAPHY (MRA): A COMPARISON BETWEEN WHOLE-HEART AND VOLUME-TARGETED METHODS USING NAVIGATOR-GATED, $T_2$-PREPARED SSFP SEQUENCE

**Xiaoming Bi, MS,[1] Vibhas Deshpande, PhD,[2] Debiao Li, PhD.[1]** [1]***Northwestern University, Chicago, IL, USA,*** [2]***Siemens Medical Solutions, Erlangen, Germany.***

*Introduction:* Whole-heart MRA method has recently been employed to visualize all major coronary arteries within one single measurement (1). Compared to conventional volume-targeted method, this technique has the potential of depicting distal potions of coronary arteries better as a result of increased volume coverage. In addition, the load of imaging orientation planning is reduced. However, heart rate alteration and respiratory drift of the subject over the long imaging time of a whole-heart scan may potentially lead to blurring of the coronary vessels. In this study, coronary MRA using whole-heart and volume-targeted methods are compared in healthy subjects. The resulting signal-to-noise ratio (SNR), contrast-to-noise ratio (CNR), depicted vessel length, vessel diameter, and vessel sharpness are evaluated.

*Method:* Ten healthy volunteers were scanned on a 1.5T Siemens scanner (Avanto) using an ECG-triggered, navigator-gated and tracked (6 mm window, tracking factor $= 0.6$), fat saturated, segmented SSFP sequence with T2 preparation (40 msec) (2). The trigger delay time and width of the data acquisition window were determined using a cine scan. For whole-heart imaging, 44 transverse slices were collected and sinc-interpolated into 88 slices of 1.3 mm thickness. Oblique planes for volume-targeted imaging were determined based on whole-heart images. Two separated targeted scans were then performed to depict the left anterior descending (LAD) artery and right coronary artery (RCA), respectively. For each of the volume-targeted scans, 16 slices were collected and interpolated into 32 slices. Spatial resolution was identical between whole-heart and volume-targeted scans for each subject. The in-plane pixel size ranged from $0.9 \times 0.9$ mm$^2$ to $1.3 \times 1.3$ mm$^2$. The acquisition duration for one whole-heart scan was $282 \pm 30$ accepted heartbeats. Corresponding values for RCA- and LAD-targeted scans were $117 \pm 21$ and $116 \pm 24$, respectively. Other imaging parameters included: TR/TE $= 3.7/1.7$ mm; flip angle $= 90^\circ$; lines per heartbeat $= 25$–$33$; readout bandwidth $= 870$ Hz/pixel. Blood signal intensity, myocardial signal intensity, and background noise were measured from raw images for SNR and CNR calculation (3). Lengths of depicted coronary arteries,

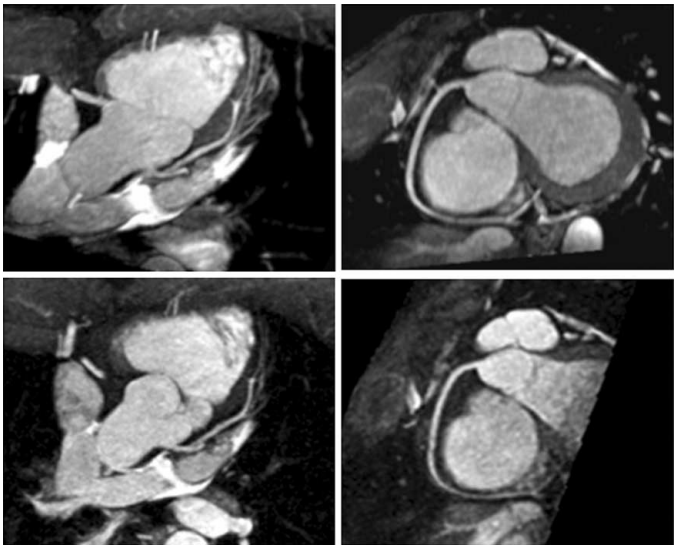

FIG. 1. LAD and RCA images acquired from the same volume using whole-heart (top row) and volume-targeted (bottom row) methods.

TABLE 1
Comparison of measured results using whole-heart and volume-targeted methods

| Imaging method | Whole-heart | RCA-targeted | LAD-targeted |
|---|---|---|---|
| SNR | 22.9 ± 8.0 | 18.8 ± 6.0* | 20.7 ± 7.1 |
| CNR | 10.9 ± 4.9 | 12.6 ± 5.6 | 12.7 ± 6.1 |
| Imaging time (min) | 12.2 ± 4.0 | 3.8 ± 1.4* | 3.5 ± 1.3* |

| | RCA | | LAD | |
|---|---|---|---|---|
| Coronary artery | Whole-heart | RCA-targeted | Whole-heart | LAD-targeted |
| Depicted length (mm) | 13.35 ± 3.91 | 10.96 ± 2.58* | 10.52 ± 1.66 | 8.65 ± 1.79* |
| Vessel diameter (mm) | 2.84 ± 0.59 | 2.64 ± 0.81 | 2.55 ± 0.52 | 2.42 ± 0.50 |
| Vessel Sharpness | 0.65 ± 0.26 | 0.84 ± 0.22* | 0.78 ± 0.23 | 0.90 ± 0.20* |

*$p < 0.05$.

lumen diameter and vessel sharpness were measured using a previously described method (4). All statistical results are presented as mean ± standard deviation. Comparisons between the whole-heart and volume-targeted results were performed using a paired t-test with two-tailed p-value smaller than 0.05 considered to be statistically significant.

*Results:* Coronary arteries are well depicted using both whole-heart and volume-targeted methods. Fig. 1 illustrates the LAD and RCA images acquired in one volunteer. Measured results of the SNR, CNR, depicted vessel length, vessel diameter and sharpness are summarized in Table 1. No significant difference is observed in SNR, CNR and vessel diameter using these two methods except that the SNR is lower for targeted RCA scan. Depicted lengths of LAD and RCA are significantly higher using the whole-heart method. Vessel sharpness is higher using the volume-targeted method for both arteries.

*Discussion:* Whole-heart scan increases the depicted lengths of coronary arteries at the cost of imaging time and vessel sharpness. Variations of heart rate and respiratory shift can be the potential reason for such decreased vessel sharpness. Parallel imaging technique should be employed to decrease imaging time in future studies. In addition, relatively low-resolution whole-heart scan can be combined with high-resolution volume-targeted scan for identification and examination of diseased coronary arteries.

## REFERENCES

1. Weber OM, et al. MRM 2003;50:1223–1228.
2. Shea SM, et al. JMRI 2002;15:597–602.
3. Stuber M, et al. MRM 2002;48:425–429.
4. Li D, et al. Radiology 2001;219:270–277.

## 434. IMAGE-BASED TRACKING AND PREDICTION OF CORONARY MOTION FOR CORONARY MR ANGIOGRAPHY

**Maneesh Dewan, MS,[1] Gregory D. Hager, PhD,[1] Christine H. Lorenz, PhD.[2]** [1]***Johns Hopkins University, Baltimore, MD, USA,*** [2]***Siemens Corporate Research, Baltimore, MD, USA.***

*Introduction:* Robust imaging of the coronary arteries is challenging due to the complex motion of these arteries induced by both cardiac and respiratory motion. Many state of the art methods work reasonably well in healthy volunteers, but there have been few techniques published that have been shown to work well in larger patient populations. One factor may be that these approaches make a simple, but often false, assumption that diaphragm motion and/or bulk cardiac motion is well correlated with the motion of the coronary arteries. We propose a method to overcome some of the current limitations by measuring coronary motion directly. The proximal LAD moves primarily in plane (z) in a short-axis view, while the LCX and RCA move in plane primarily in the x-y plane in a 4-chamber view. The basic idea behind the approach can be understood from Fig. 1. The motion of the coronary arteries can be tracked using real-time imaging (image-based navigators) in specific orientations (short axis and 4-chamber views) which can then be used to predict the acquisition window and coronary location for high resolution imaging with slice correction.

*Methods: MR Acquisition:* Based on Fourier analysis of coronary motion from high temporal and spatial resolution cine images, a frame rate of 15 frames/sec was considered adequate for capturing the main components of motion for this application. We acquired real time TrueFISP images in the short axis, coronal, and 4-chamber views in 5 volunteers with the following parameters: TR/TE/FL 1.7–2.7/0.85–1.35/50–55, GRAPPA ×2, in plane resolution 1.5–2.4 mm inplane, slice thickness 8 mm, 10–15 frames/sec for approximately 750 frames during

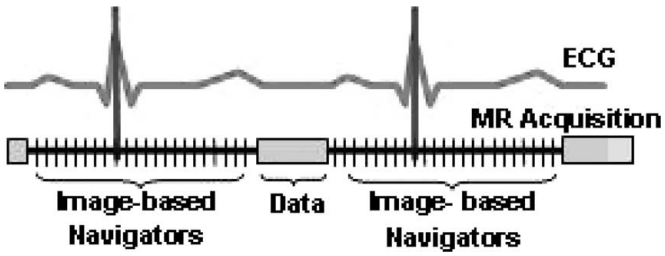


FIG. 1. Basic sequence-timing diagram involving Image-based navigators to track the motion of the coronary arteries.

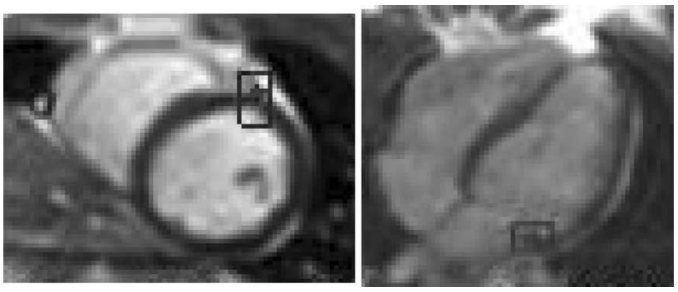

FIG. 2. These images show the tracked LAD and LCX grooves respectively.

free breathing on a 1.5T scanner (Espree, Siemens). *Tracking:* In real-time images (both the short axis and four chamber views), the coronary artery is not visible throughout the entire cardiac cycle, but grooves where the coronary arteries sit are clearly visible (Fig. 2), and were used as a surrogate. The tracking algorithms developed are variations of normalized cross-correlaton and sum of squares differences with multiple templates. *Variability:* Systolic and diastolic periods were determined for each heartbeat and variability over the exam was measured. In addition, the respiratory component of coronary motion was extracted from the total heart motion via Fourier-based filtering on the coronal views. The difference between respiratory motion estimated as 0.6*diaphragm motion and the motion extracted from the actual total coronary motion were compared, (1) over all timepoints, and (2) during mid-diastole at end-expiration with an acceptance window of ±2.5 mm.

*Results:* Tracking results were assessed visually and were in good agreement with the exception of occasional misaligned frames in early diastole during rapid motion. Fig. 3 shows longitudinal motion of the LCX over more than 700 frames. Systolic and diastolic periods varied significantly over the duration of the exam, with systolic periods (mean—380 to 400 ms, stddev—48 to 62 ms) varying less than diastolic (mean—610 to 900 ms, stddev—66 to 87 ms) as expected. The root mean squared error between the estimated and extracted respiratory component of coronary motion ranged from 0.95 to 1.34 mm across 5 subjects (Fig. 4). During the diastolic end-expiratory phases, root mean squared error ranged from 0.47 to 1.19 mm.

*Discussion:* Based on the prelimary results, image based tracking of coronary motion appears feasible, and the beat-to-beat variation in coronary motion and diastolic period warrant a more subject specific approach. The advantage of the proposed method is that there are no assumptions about the motion of the coronary artery. Future work will include validation of both the tracking and prediction accuracy by integrating the approach into the data acquisition.

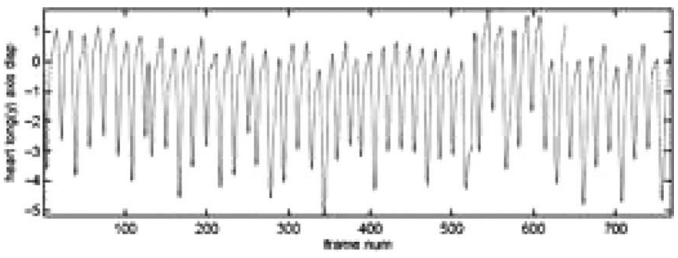


FIG. 3. Coronary motion.

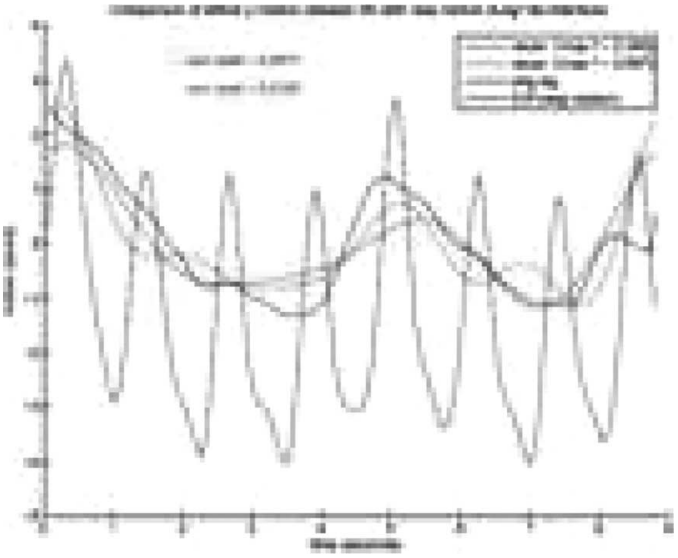

FIG. 4.

## 435. PERFUSION AND WALL MOTION DURING HIGH DOSE DIPYRIDAMOLE MAGNETIC RESONANCE FOR THE DETECTION OF CORONARY ARTERY DISEASE: A HEAD-TO-HEAD COMPARISON

**Elisabetta Strata, Alessandro Pingitore, Eugenio Picano, Barbara Scattini, Giovanni Donato Aquaro, Gianluca Di Bella, Daniele De Marchi, Massimo Lombardi.** ***Institute of Clinical Phisiology, Pisa, Italy.***

*Introduction:* Dipyridamole (D) stress test induces both reversible perfusion defects and wall motion abnormalities in patients with coronary artery disease (CAD). Cardiac magnetic resonance (CMR) can assess both perfusion and wall motion changes during D.

*Purpose:* To compare the diagnostic accuracy of perfusion and wall motion during D-CMR in patients with chest pain syndrome.

*Methods:* Thirty-nine pts (age 63± years, 25 males) with chest pain syndrome underwent D with CMR. High dose D test (0.84 mg/kg in 10 minutes) was used. Quantitative signal intensity upslope was evaluated at rest and after D as a measure of myocardial perfusion. A perfusion reserve index (PRI) was calculated as the ratio between D and rest upslope and perfusion positivity criterion was a PRI value <1.5 in at least 2 contiguous myocardial segments. Wall motion score (WMS, from 1 = normal to 4 = dyskinetic) was evaluated at baseline and peak stress and wall motion positivity criterion was a segmental

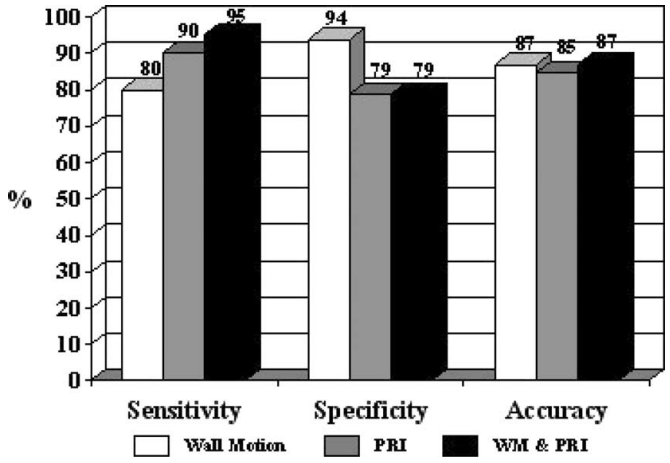


FIG. 1.

score increase of at least 1 grade in at least 2 segments. All patients underwent coronary angiography independently of test results.

*Results:* D infusion was fully administered in all patients without major or limiting side effects. Significant CAD (>50% diameter reduction in at least one major coronary vessel by coronary angiography) was found in 20 patients: 7 had single- and 13 multi-vessel disease. During D, 16 patients had typical chest pain. Overall diagnostic accuracy was similar for wall motion and perfusion changes—with a trend to higher specificity for wall motion and a trend to better sensitivity for perfusion changes (Fig. 1).

*Conclusions:* D-CMR is safe and feasible. Perfusion and wall motion abnormalities evaluated in the same time during D infusion have similar diagnostic accuracy, with perfusion having higher sensitivity that is counterbalanced by the higher specificity of wall motion abnormalities.

## 436. CMR ASSESSMENT OF DIASTOLIC FUNCTION IN MYOCARDIAL IRON LOADING

**Gillian C. Smith, MSc,[1] Mark A. Tanner, MBBS,[1] Tim J. Cannell, B. Apl. Biol,[1] Renzo Galanello, MD,[2] Dudley J. Pennell, MD.[1]** [1]***Royal Brompton Hospital, London, United Kingdom,*** [2]***Ospedale Microcitemico, Cagliari, Italy.***

*Introduction:* Heart failure secondary to cardiac siderosis is the most common cause of death in patients with thalassemia major (TM). Systolic dysfunction occurs at an advanced stage of cardiac iron loading, and it would therefore be desirable to identify markers of myocardial dysfunction that occur early in the disease process. Diastolic abnormalities can be identified by CMR and might occur at milder degrees of myocardial iron loading (as quantified by T2*).

*Purpose:* To assess diastolic function in mild to moderate myocardial iron overload.

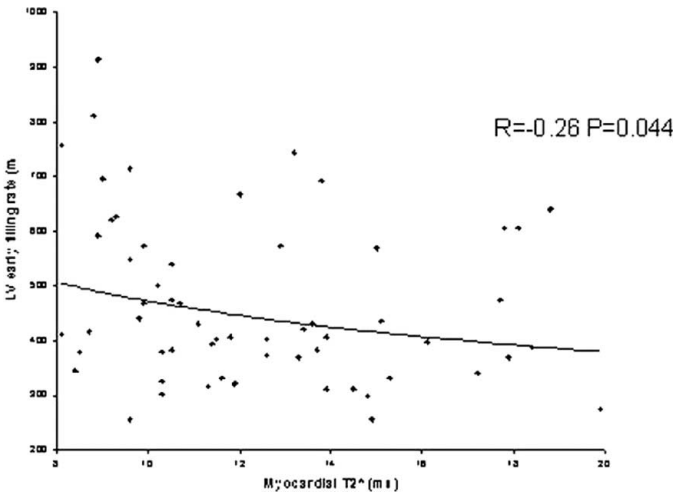


FIG. 1.

*Methods:* Myocardial T2* was assessed in 167 patients with TM using our mobile CMR scanner (1.5T Siemens Sonata) in Cagliari, Italy. Patients were aged 18–42 ($30 \pm 5.3$ years). 65 patients (27 male, 28 female, age $30 \pm 5.2$ years) with mild to moderate cardiac iron loading (T2* 8–20 ms) were invited back for further CMR assessment. Cine images were acquired using a retrospectively gated high temporal resolution SSFP sequence and filling parameters assessed using a semi-automated analysis package (LV tools © Cardiovascular Imaging Solutions, London, UK). 5 patients were excluded due to sinus tachycardia.

*Results:* There was a weak negative correlation between myocardial T2* and the peak E filling rate ($R = -0.26$, $p = 0.044$) and the E/A ratio ($R = -0.30$, $p = 0.022$) There was a weak positive correlation between myocardial T2* and LV ejection fraction($R = 0.280$, $P = 0.022$) (Figs. 1, 2, and 3). There was no correlation between myocardial T2* and peak A, E deceleration rate or E deceleration time.

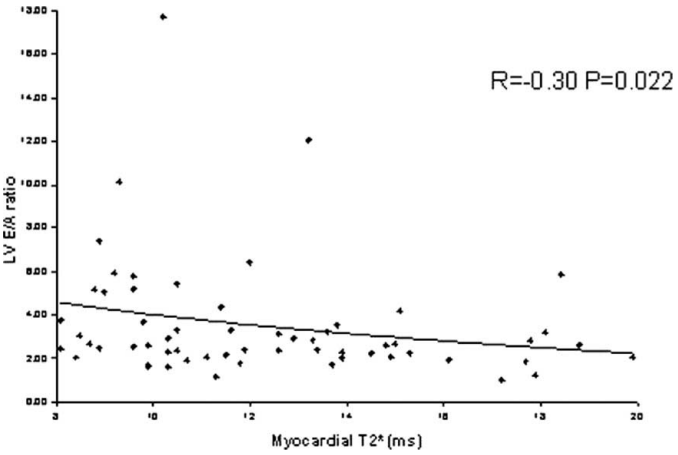


FIG. 2.

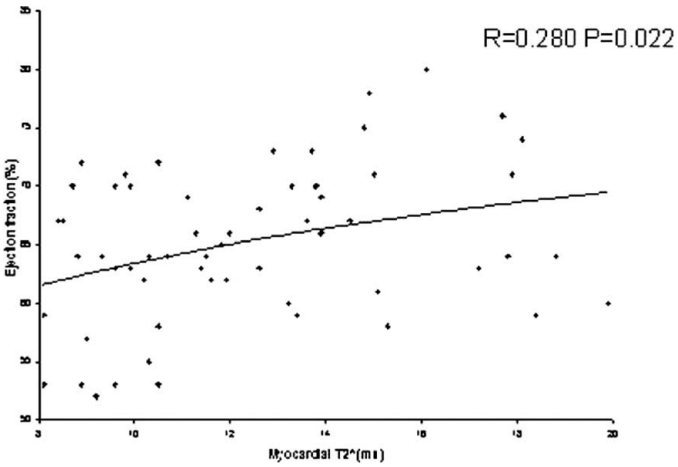


FIG. 3.

*Conclusions:* Diastolic function parameters are only weakly related to myocardial iron loading and are unlikely to have a useful role in the detection of early cardiac siderosis.

## 437. ASSESSMENT OF MITRAL REGURGITATION BY CMR DERIVED REGURGITANT VOLUME AND FRACTION; IS IT SUPERIOR TO ECHOCARDIOGRAPHIC ERO?

**Ketheswaram Caruppannan, MD, Mark Doyle, PhD, June Yamrozik, Ronald Williams, Vikas K. Rathi, MD, Diane A. Vido, Geetha Rayarao, Robert W. W. Biederman, MD.** ***Allegheny General Hospital, Pittsburgh, PA, USA.***

*Introduction:* Recently, the contribution that mitral regurgitation (MR) adds to human morbidity and mortality has been the focus of considerable attention by echocardiography (Echo). Yet, estimation of MR by Echo has been primarily limited to quantification of effective regurgitant orifice area (ERO) derived via geometric assumptions from proximal isovelocity surface area (PISA). Well described limitations of PISA exist, namely assumption of hemispheroidal concentric velocity spheres, nonlaminar flow profiles, multiple lobes of flow acceleration unappreciated by 2D measures, and eccentric jets. It has been shown that cardiovascular MRI (CMR) provides more accurate and reproducible formal quantitation of MR regurgitant volume ($Reg_{vol}$) and regurgitant fraction ($Reg_{fract}$), using more intuitive approaches. However, conventionally, CMR measurements have traditionally been derived from a phase velocity mapping (PVM) plane placed at the mitral orifice to quantify total thru-plane flow. This technique works best in central, non-eccentric jets, and is limited by incorporation of the LV outflow tract in the systolic flow and mitral-plane systolic descent which is not easily integrated when quantifying regurgitant fraction.

*Hypothesis:* We hypothesize that the incorporation of one additional PVM plane at the level of the aortic valve when combined with standard 3D LV volumetrics will accurately, rapidly and easily quantitate MR without reliance on the geometric assumptions of echo, and are verifiable in a phantom model.

*Method:* 1) A phantom flow pump (CardioFlow 1000, Shelley, Inc, Toronto) with a calibrated servometer was used with PVM to correlate quantitated flow (mL/s) against calibrated flow. 2) Thirty-five subjects (35) incorporating 14 normals average age 43, range 14 to 62, and 21 patients with varying degrees of MR (trace $-4+$), average age 60, range 25 to 83) underwent a 3D FIESTA LV volumetric 1.5T CMR (CV/i,GE, Milwaukee, WI) study with an additional trans-aortic thru-plane PVM acquisition to quantitate LV stroke volume (SV). Exclusion criteria include aortic regurgitation (AR) and any intracardiac shunt lesion. Subtraction of the volumetic derived SV ($SV_{3D}$) from the PVM derived SV ($SV_{PVM}$) yields, in the absence of AR or shunt, mitral regurgitant volume. Regurgitant fraction was defined as ($SV_{3D}$- $SV_{PVM}$/ $SV_{3D)}$.

*Results:* The correlation of flow between the phantom model and PVM was 0.98 ($p = <0.001$) varying over a physiologic range of clinical flow waveforms, including jet flow. The correlation in the controls between $SV_{3D}$ and $SV_{PVM}$ was $75 \pm 9$ vs $70 \pm 10$ mL, respectively, ($r = 0.88$, $p = <0.001$). All 35 subjects completed the study in $35 \pm 10$ minutes. The addition of the aortic PVM slice added $2 \pm 0.2$ min. The resultant 3D EF ranged from 13 to 76%. On an individual basis, the regurgitant volume was easily quantified as was the regurgitant fraction. The range of $Reg_{vol}$ and $Reg_{fract}$ was 15 mL to 56 mL and 15 to 47%, respectively, while encompassing the broad range of clinical MR from trace to severe. Quantitative MR was highly correlated with clinical qualitative findings from FIESTA imaging ($r = 0.9$). No geometric assumptions were required to derive either $Reg_{vol}$ or $Reg_{fract}$.

*Conclusion:* While recently shown to be prognostic in conveying additive morbidity and mortality to patients, echocardiographic derived effective mitral valve regurgitant orifice (ERO) relies on several arithmatic and geometric assumptions that are known not to be universally true. CMR derived quantitation of mitral regurgitant volume and regurgitant fraction using aortic PVM in conjunction with 3D quantified LV stroke volume permit accurate, rapid and easily obtained, non-assumption based clinical metrics without requirements for assessing the mitral orifice, often subject to errors and erroneous in eccentric jets. Given the additional *ex vivo* and *in vivo* validation by our independent measurement of PVM flow phantoms, this technique intuitively may supercede the accuracy and difficulty of echocardiographically derived ERO.

## 438. QUANTITATIVE MYOCARDIAL PERFUSION RESERVE IN PATIENTS PREDICTS THE SEVERITY OF GRADED CORONARY ARTERY STENOSIS DETERMINED BY ANGIOGRAM

**Christopher Klassen, MD, PHD,[1] Prasad Panse, MD,[1] Minh Nguyen, MD,[1] Kuran Kareti, MD,[1] Norbert Wilke, MD,[1] Michael Jerosh-Herold, PHD.[2]** [1] ***University***

***of Florida/Shands Jacksonville, Jacksonville, FL, USA, [2] University of Oregon, Portland, OR, USA.***

*Introduction:* Quantitative MR perfusion reserve has been validated in several previous studies to determine the severity of coronary artery disease (CAD). Previous reports have determined a cut-off value from 1.1 to 1.5 for severe CAD defined as a stenosis of >75%.

*Purpose:* Our purpose was first to measure quantitative myocardial perfusion reserve using constrained deconvolution of the signal intensity versus time curves utilizing a Fermi-function model with a $\gamma$-variate fit in patients with known coronary artery disease (CAD). Then correlate this with the visually estimated grade of coronary stenosis determined by coronary angiography. The second purpose was to develop cut-off values for myocardial perfusion reserve that can be used clinically to determine significant stenosis.

*Methods:* Magnetic resonance first pass perfusion (MRFPP) imaging was performed in 40 patients with known CAD (ages 34–78) that also had coronary angiography. MR first pass perfusion imaging was obtained at rest and during adenosine infusion (140 mcgs/kg/min) using a 1.5 Tesla Siemens MR scanner and Turbo-flash sequence. They were then analyzed by a quantitative method to find the absolute myocardial perfusion reserve (ratio of blood flow during adenosine with that during rest) in 8 radial sectors of the left ventricular myocardium for each slice. During coronary angiography, epicardial arteries were visually graded according to stenosis severity. Myocardial perfusion reserve was compared to stenosis grade for each sector and each patient. The sensitivity, specificity, positive predictive value (PPV), and negative predictive value (NPV) of MR perfusion reserve were derived per sector and per patient.

*Results:* The sensitivity, specificity, PPV, and NPV for myocardial perfusion reserve on a per sector basis to detect severe stenosis, defined as ≥75% area or collateralized myocardium as determined visually from coronary angiograms were 66.3%, 91.6%, 55.6%, and 94.5%. A per patient analysis showed sensitivity, specificity, PPV, and NPV to be 92.9%, 69.2%, 61.9%, and 94.7%. Collateralized myocardium assessed by angiography could be distinguished from regions with <50% area stenosis, and a trend was seen to distinguish collateralized myocardium from regions with 50–75% and 90–100% but not 75–90% stenosis. Regions with 0–25% and 25–50% stenosis could be distinguished from each other and from all other levels of CAD severity. The cutoff for severe CAD (>75% stenosis) as determined by receiver operating characteristics analysis was ≤1.45 for the perfusion reserve. Using this cut-off the probability that severe CAD is not present in a sector when the MRFPP reserve >1.45 is 94.5%. The figure panel demonstrates the relationship between myocardial perfusion reserve and stenosis severity.

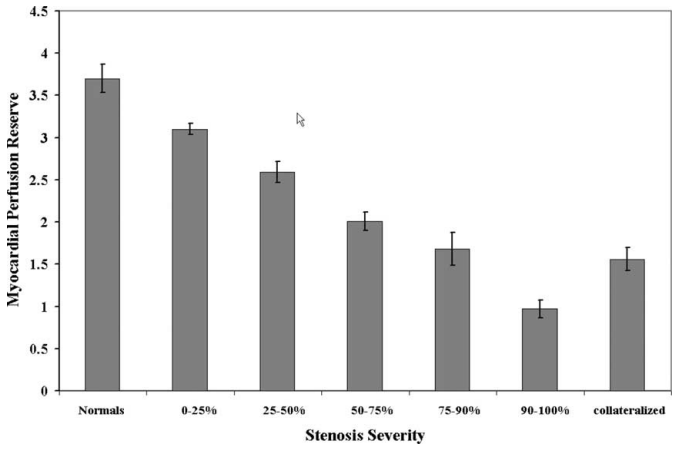


FIG. 1.

*Conclusions:* MRFPP can differentiate collateralized from normal myocardium and suggests its perfusion is similar to regions with 75–90% stenosis. This analysis also indicates that 95% of patients with negative results from magnetic resonance testing will not have severe lesions upon coronary angiography. This technique may be able to exclude patients from unnecessary intervention if no myocardial sectors have an absolute perfusion reserve less than 1.5.

## REFERENCES

1. Wilke N, Jerosch-Herold M, Wang Y, Huang Y, Christensen BV, Stillman AE, Ugurbil K, McDonald K, Wilson RF. Myocardial perfusion reserve: assessment with multisection, quantitative, first-pass MR imaging. Radiology 1997;204:373–384.
2. Kraitchman DL, Wilke N, Hexeberg E, Jerosch-Herold M, Wang Y, Parrish TB, Chang CN, Zhang Y, Bache RJ, Axel L. Myocardial perfusion and function in dogs with moderate coronary stenosis. Magn Reson Med. 1996;35:771–780.

## 439. CARDIOVASCULAR MAGNETIC RESONANCE (CMR) IMAGING OF LEFT VENTRICULAR DIASTOLIC DYSFUNCTION IN PATIENTS WITH FABRY DISEASE

**Christoph F. Juli,[1] Charles R. Peebles,[2] Johannes M. Froehlich,[1] Urs Widmer,[3] Christoph L. Zollikofer,[1] Klaus U. Wentz,[1] Boris P. Eckhardt.[1] [1] *Cantonal Hospital Winterthur, Winterthur, Switzerland,* [2] *University Hospital, Dept. Cardiothoracic Radiology, Southampton, United Kingdom,* [3] *University Hospital, Dept. of Internal Medicine, Zürich, Switzerland.***

*Introduction:* Fabry's disease (FD) commonly presents as non-obstructive left ventricular (LV) hypertrophic cardiomyopathy (HCM). LV systolic function is preserved in the majority of cases.

*Purpose:* We analysed LV time volume curves (TVC) from FD pts for evidence of diastolic dysfunction in relation to their LV myocardial mass.

*Methods:* Thirty FD pts, 12 female (f), 18 male (m), aged 17–64 yrs, underwent CMR imaging on a 1.5T MR scanner.

Pts were divided into three groups: G1 (n = 17)—normal LV mass&geometry (NLV), G2 (n = 6)—concentric remodelling 5pts, septal hypertrophy + NLV 1 pt, G3 (n = 7)—LV hypertrophy (LVH). G2&3 included pts with additional causes for LVH. We performed TVC analysis on stacks of sequentially acquired LV short axis (SA) cine images (T2-SSFP-TFE-sequence) covering the whole LV. Contours were drawn manually (Philips ViewForum Workstation Rel. 4.2) to outline the LV cavity according to the method described by (1) Lorenz et al. 1990. LV TVCs were generated. A 7 phase cardiac cycle (CC) model was used for TVC analysis. The TVC values and curve profiles from the FD pts were compared with those from a group of 10 healthy volunteers (5 males/5 females aged 27–60 yrs).

*Results:* The controls showed a heart rate (HR) range of 48–73 beats per minute (BPM) at rest, resulting in a TVC time resolution (25 frames per cardiac cycle) of 33–51 ms per frame. In the FD pts HR ranged between 49–83 BPM, with a TVC time resolution of 30–51 ms per frame. Using the 7 phase cardiac cycle model, we found in the controls, that the slow ejection phase starts at 29.1–33.4% of the CC. This is also seen in the majority of pts with FD and reflects relatively preserved systolic function (average EF: controls = 61%, G1 = 62%, G2&3 = 72%). G1 pts showed a rapid diastolic filling phase within the range (35%–54% CC length) seen in the controls. The average TVC curve profile of G1 matches the one of the controls. The average G2 TVC curve shows significantly ($p = 0.04$; 2 sided t-test) reduced early diastolic filling (phase 6). Phase 6 is abnormally lengthened in 61% of G2 pts and in 61% G3 pts. The average TVC curve profile of G3 shows even slower early diastolic filling than G2.

*Conclusions:* Two distinct TVC patterns are seen in FD pts. Those with normal LV mass and geometry do not have diastolic dysfunction. In pts with concentric remodelling and pts with increased LV mass early diastolic filling gets progressively worse reflecting diastolic dysfunction. The degree of diastolic dysfunction in FD pts is related to LV mass.

## REFERENCE

1. Lorenz, et al. 1990.

## 440. IN AORTIC STENOSIS, IS THERE A GENDER DISPARITY?

**Robert W. W. Biederman, MD,[1] Vikas K. Rathi, MD,[1] Tarun Tewatia, MD,[1] Valerie Bress,[1] Diane A. Vido,[1] June Yamrozik,[1] Ronald Williams,[1] Geetha Rayarao,[1] James A. Magovern, MD,[1] Nahaniel Reichek, MD,[2] Mark Doyle, PhD.[1]** [1]***Allegheny General Hospital, Pittsburgh, PA, USA,*** [2]***St. Francis Hospital, Roslyn, NY, USA.***

*Introduction:* Differences in ventricular hypertrophic responses in women vs. men have been described in severe aortic stenosis (AS), despite similar presentation with respect to symptoms, gradients and aortic valve areas. Women are often regarded as hyper-responders to the afterload of AS and have been described as exhibiting "exuberant hypertrophy" implying an absolute increase in LV mass compared to men. Women typically have small, thick, hyperdynamic LV's, while men have larger, relatively thin, mildly impaired hearts. Given these geometric disparities, neither 1D nor 2D measurements, such as wall thickness or LVEDD, are accurate gender neutral descriptors of LV geometry in AS.

*Hypothesis:* We hypothesize that 3D metrics integrate LV geometry more appropriately and describe LVH in a gender neutral manner, resolving the disparate observations concerning exuberant LVH by 1 and 2D measurements in women.

*Methods:* Patients (29, 15 F, age 73 ± 12) presenting with severe symptomatic AS underwent cardiac MRI (CMR) pre and post AVR (6 ± 1 months). Cine MR data were interrogated to extract 3D LV mass and volume. Tagged data characterized 2D circumferential strain (%S). Patients with >2+ AR or MR were excluded.

*Results:* All 29 patients survived AVR, with 24 available for follow up. In women vs. men, LVM normalized to BSA (LVMI) was approximately 25% lower at baseline (78 ± 17 vs. 107 ± 20 g/m$^2$, $p < 0.001$) and post AVR (67 ± 14 vs. 86 ± 18 g/m$^2$, $p < 0.001$), while %S was approximately 33% higher in women vs. men at baseline (22 ± 10 vs. 16 ± 9%, $p < 0.001$) and post AVR (24 ± 10 vs. 18 ± 9%, $p < 0.01$). However, when normalizing the LVM using 3D measured EDV, women vs. men were equivalent both at baseline (1.36 ± 0.48 vs. 1.35 ± 0.67 g/mL, $p = 0.9$) and post AVR (1.13 ± 0.35 vs. 1.19 ± 0.23 g/mL, $p = 0.7$).

*Conclusion:* In response to AS, women exhibit increased myocardial strain compared to men, which dramatically contrasted with the lower degree of ventricular hypertrophy when normalized by BSA, congruent with a hyperdynamic exuberant response but incongruent with exaggerated LVH. When utilizing integrated LV geometry and measures of LV volume by 3D CMR, apparent differences of LVH between women vs. men were resolved both pre and post AVR and were shown to manifest and regress symmetrically, nullifying the concept of "exuberant LVH."

## 441. PHYSIOLOGICAL AND CLINICAL CONSEQUENCES OF RELIEF OF RIGHT VENTRICULAR OUTFLOW TRACT OBSTRUCTION LATE AFTER REPAIR OF CONGENITAL HEART DEFECTS

**Louise Coats, MRCP,[1] Sachin Khambadkone, MD, MRCP,[1] Graham Derrick, MRCP,[1] Shanker Sridharan, MRCP,[1] Silvia Schievano, MEng,[1] Rod Jones, MSc,[1] John Deanfield, MRCP,[1] Denis Pellerin, MD, PhD,[2] Philipp Bonhoeffer, MD,[1] Andrew Taylor, MD MRCP FRCR.[1]** [1]***Great Ormond Street Hospital for Children, London, United Kingdom,*** [2]***The Heart Hospital, London, United Kingdom.***

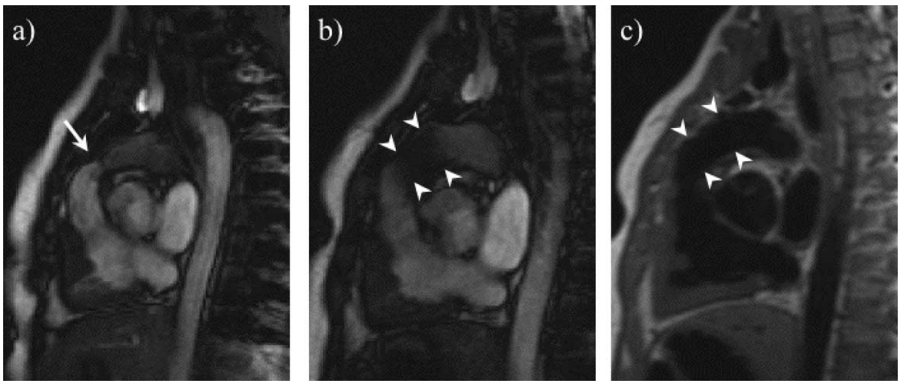


FIG. 1. a, RVOT balanced SSFP images before valve stent. Pulmonary conduit narrowing (arrow). b, RVOT balanced SSFP image after valve stent. Signal artifact from metallic component of the PPVI (arrowheads). c, RVOT "blackblood" turbo spin echo showing widely patent stent.

*Background:* RVOTO is a common problem in patients with repaired congenital heart disease. Percutaneous pulmonary valve implantation (PPVI) can now be used to treat homograft/conduit stenosis effectively and provides a unique model with which to study the physiological response of the heart without the confounding effects of cardiopulmonary bypass.

*Purpose:* The purpose of this study was to investigate the clinical and physiological response to relief of right ventricular outflow tract obstruction (RVOTO) late after repair of complex congenital heart disease.

*Method:* We studied 18 patients who underwent PPVI for late RVOTO (72% male, median age 20 years (range 9–51), 56% tetralogy of Fallot or subtype) from a total population of 93. All patients had RVOTO (peak RVOT gradient >50 mmHg on echocardiography) without clinically important pulmonary regurgitation (pulmonary regurgitant fraction <10% on magnetic resonance (MR) imaging or <mild pulmonary regurgitation on echocardiography). Cardiopulmonary exercise testing, tissue Doppler echocardiography and MR imaging were performed before and within 50 days after the procedure.

*Results:* PPVI reduced both the gradient across the RVOT (51.4 to 21.7 mmHg, $p < 0.001$) and RV systolic pressure (72.8 to 47.3 mmHg, $p < 0.001$) at catheterization. Symptoms and aerobic (25.7 to 28.9 ml/kg/min, $p = 0.002$) and anaerobic (14.4 to 16.2 mL/kg/min, $p = 0.002$) exercise capacity improved. On tissue Doppler imaging, systolic velocity improved at both the tricuspid annulus (4.8 to 5.3 m/sec, $p = 0.05$) and the mitral annulus (4.7 to 5.5 m/sec, $p = 0.01$) with no change in isovolumic acceleration. MR showed a reduction in RV end diastolic volume (99.9 to 89.7 mLs/m$^2$, $p < 0.001$) and an improvement in RV ejection fraction (48.0 to 56.8%, $p = 0.01$). Left ventricular ejection fraction also improved (62.6 to 65.8%, $p = 0.03$).

*Conclusion:* Relief of late RVOTO in patients with congenital heart disease results in rapid subjective and objective clinical improvement. This is associated with recovery of right and left ventricular function that is a direct result of the change in loading conditions.

## 442. INTERNAL, NOT EXTERNAL, VENTRICULAR ENERGY UTILIZATION MEASURED BY MRI, COUPLED WITH CORONARY ARTERY DISEASE, ASSESS RISK IN WOMEN: THE NHLBI-SPONSORED WOMEN'S ISCHEMIA SYNDROME EVALUATION (WISE) STUDY

**Mark Doyle, PhD,[1] Gerald M. Pohost, MD,[2] Leslee J. Shaw, PhD,[3] George Sopko, MD,[4] Eduardo Kortright, PhD,[5] Diane A. Vido,[1] Sheryl F. Kelsey, PhD,[6] B. Delia Johnson, PhD,[6] William J. Rogers, MD,[7] Steven E. Reis, MD,[8] Marian B. Olson, PhD,[8] Barry L. Sharaf, MD,[9] Carl J. Pepine, MD,[10] Sunil Mankad, MD,[1] Robert W. W. Biederman, MD.[1]** ***[1] Allegheny General Hospital, Pittsburgh, PA, USA, [2] University of Southern California, Los Angeles, CA, USA, [3] ACRI, Atlanta, GA, USA, [4] NIH/NHLBI, Washington, DC, USA, [5] University of New Orleans, New Orleans, LA, USA, [6] Epidemiology Data Center, Pittsburgh, PA, USA, [7] University of Alabama at Birmingham, Birmingham, AL, USA, [8] University of Pittsburgh Medical Center, Pittsburgh, PA, USA, [9] Rhode Island Hospital, Providence, RI, USA, [10] University of Florida, Gainesville, FL, USA.***

*Introduction:* The prognostic value of external and internal energy expenditure by the left ventricle (LV) has previously not been described in women with suspected myocardial ischemia. Here, the effect of epicardial coronary artery disease (CAD) and myocardial perfusion on these two variables is reported.

*Hypothesis:* We hypothesize that exaggerated internal energy expenditure by the LV increases risk of adverse events in the presence of epicardial CAD and myocardial ischemia.

*Methods:* Women (127), mean age 57.7 ± 11.3 yr, underwent quantitative coronary angiography (QCA) and MRI evaluation of myocardial perfusion and LV function. Using MRI measurements of LV volumes, maximal aortic elastance (Eam), internal baseline energy (BE) and external stroke work (SW) were calculated. Indices of LV efficiency were taken as the ejection fraction (EF) and the ratio of SW to total work (SW plus BE). Severity of CAD was determined by QCA and severity of myocardial

ischemia was assessed by MRI perfusion level. Adverse events were studied during follow-up (38 ± 14 months). Cox regression modeling was used to determine independent predictors of events.

*Results:* There were 49 adverse events (39%). Work and ejection efficiency were strongly correlated with each other ($r = 0.96$, $p < 0.001$) and each was moderately related to CAD severity ($r = 0.19$, and $r = 0.22$, $p < 0.05$, respectively). No relationship was found between efficiency indices and myocardial perfusion. Variables individually associated with adverse events were: EF, work efficiency, Eam, internal BE, external SW, myocardial perfusion level, and severity of CAD. Multivariable analyses demonstrated that internal BE, Eam, myocardial perfusion level and severity of CAD significantly contributed to adverse events ($p < 0.001$).

*Conclusions:* In women with suspected myocardial ischemia, external energy expenditure and ventricular efficiency indices were weakly prognostic, whereas exaggerated internal energy utilization by the LV in the presence of epicardial CAD and/or myocardial ischemia were strongly and independently associated with adverse events. A comprehensive evaluation of risk requires assessment of the epicardial coronary arteries, myocardial perfusion, and internal energy utilization by the left ventricle.

## 443. COMBINED CORONARY ARTERY IMAGING, MYOCARDIAL PERFUSION AND DELAYED ENHANCEMENT IN PATIENTS WITH SUSPECTED CORONARY ARTERY DISEASE

**Christoph Klein,[1] Thomas Kokocinski,[1] Rolf Gebker, Dr.,[1] Bernhard Schnackenburg, PHD,[2] Eckart Fleck, Prof.,[1] Eike Nagel.[1] [1]*German Heart Institute Berlin, Berlin, Germany,* [2]*Philips Medical Systems, Hamburg, Germany.***

*Introduction:* MRI offers a combination of functional studies for the detection of ischemia (hemodynamic relevance), detection and quantification of myocardial infarction as well as coronary angiography (morphological assessment).

*Purpose:* Aim of the study was to evaluate the feasibility and diagnostic accuracy of the combination of stress (adenosine) perfusion (PERF), delayed enhancement (DE) and coronary angiography (MRCA).

*Methods:* Thirty-five patients with suspected CAD underwent MR imaging including LV-function, MRCA (SSFP turbogradient, SENSE factor 1.7, spatial resolution 0.7 × 0.7 × .0.9 mm, T2 prep, fat suppression, trigger delay and temporal resolution adjusted to individual diastolic coronary rest period, TE /TR 2.3/4.6, FA 100°), stress PERF (adenosine 140 $\mu$g/min/kg body weight), rest PERF (SSFP, TE/TR 2.7/1.4, FA 50°, 1 saturation prepulse per slice, 3 slices per heart beat) and DE (3D inversion recovery technique, TE/TR 2.8/6.6, FA 15°,) using Gd-BOPTA (MultiHance) one day before invasive coronary angiography. Fig. 1 shows the study protocol. Images were analysed visually. Patients with obstructive lung disease, atrial fibrillation and unstable angina were excluded. Stenosis >50% in invasive angiography was considered significant.

TABLE 1
Sensitivity and specificity of the tests

| | DE | Stress perfusion | Coronary angiography | DE or perfusion positive | DE or perfusion or CA positive |
|---|---|---|---|---|---|
| Sensitivity | 33 | 86 | 92 | 86 | 100 |
| Specificity | 93 | 92 | 38 | 93 | 50 |

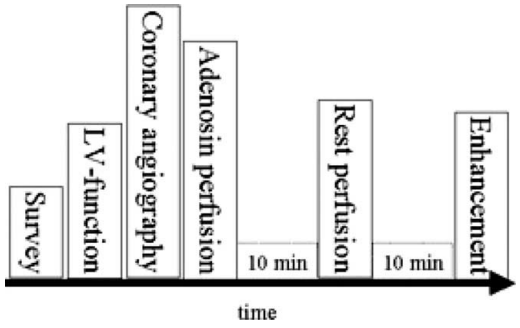


FIG. 1.

*Results:* The prevalence of CAD was 52% (24 men). In 1 patient adenosine had to be stopped before imaging due to increasing dyspnoe. Fourteen-percent of MRCAs (5/35) had non diagnostic image quality. Mean study time was 75 min (range 57–111 min). Table 1 shows the sensitivities and specificities for each test and for combined evaluation. The combination of stress PERF and DE led to the highest sensitivity and specificity. Adding the results of MRCA increased sensitivity to 100%, but decreased specificity to 50% due to a high rate of false positive readings.

*Conclusion*: The combination of stress perfusion, delayed enhancement and coronary angiography is feasible, combining stress perfusion and delayed enhancement yields the highest accuracy. The data does not demonstrate an additional value for MRCA.

## 444. IMAGING STENOSIS OF THE GREAT VESSELS: WHAT IS THE BEST STRATEGY? A COMPARATIVE STUDY OF 3D STEADY-STATE FREE PRECESSION IMAGING AND CONTRAST-ENHANCED MAGNETIC RESONANCE ANGIOGRAPHY

**Shankar Sridharan, Rod Jones, Louise Coats, Andrew M. Taylor. *UCL Insitute of Child Health & Great Ormond Street Hospital for Children, London, United Kingdom.***

*Introduction:* Contrast-enhanced magnetic resonance angiography (CE-MRA) is a routine sequence in cardiovascular MR imaging protocols, providing excellent definition of the great vessels of the thorax. However, CE-MRA has several disadvantages that may affect accurate measurement and visualisation of these vascular structures:

1. Lack of ECG-gating leads to image blurring, in particular for structures close to the heart. This may lead to an

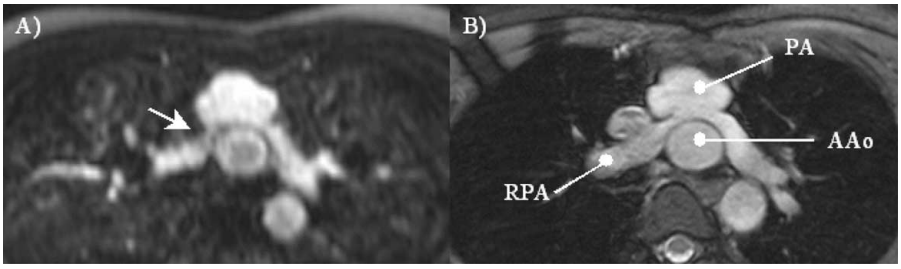


FIG. 1. Oblique axial reconstructions through the pulmonary bifurcation in a patient with transposition of the great arteries and an arterial switch operation. A) CE-MRA image and B) b-SSFP image. There is narrowing of the branch pulmonary artery origins (right (arrow) worse than left). There is overestimation of the branch pulmonary artery stenoses on the CE-MRA images, with some signal loss on the right. Furthermore, as the b-SSFP images are ECG-gated, the image quality is superior, with better definition of the adjacent structures. PA—pulmonary trunk, RPA—right pulmonary artery, Aao—ascending aorta.

underestimate of vessel dimensions (underestimate of maximum systolic diameter);
2. Use of a flow insensitive sequence leads to signal loss secondary to turbulent flow, in particular at tight stenosis. This may lead to an overestimation of stenosis severity.

ECG-gated 'black-blood' images are one method to solve these problems, but do not provide a three-dimensional data set as with CE-MRA. A new strategy is to use 3D balanced steady-state free precession (b-SSFP) imaging. This sequence has near isotropic 3D resolution and is designed to be relatively flow insensitive and thus less susceptible to image artefact from signal degradation at sites of turbulent flow. In addition, no extrinsic contrast agents are required for the assessment of vascular structures.

*Purpose:* To compare CE-MRA and 3D b-SSFP imaging of suspected stenosis of the great vessels in children and adolescents with congenital heart disease.

*Methods:* CE-MRA and 3D b-SSFP imaging was performed in 40 consecutive children, adolescents and adults with congenital heart disease (mean age = 15 ± 5.2 years). All subjects gave informed consent. Ten patients were imaged to assess aortic stenosis (coarctation, hypoplastic left heart syndrome) and 30 patients to assess branch pulmonary artery stenosis (repaired tetralogy of Fallot, arterial switch operation for transposition of the great arteries). MR imaging was performed at 1.5T (Avanto, Siemens, Erlangan, Germany). Non-contrast 3D b-SSFP imaging of the great vessel of interest was acquired initially during free breathing and navigator echo (NE) gating. Sequence parameter: TR = 3.4 ms, TE = 1.7 ms, flip angle = 90°, resolution = 0.9 × 0.9 × 1.0 mm, iPAT factor = 2, NE window 8 mm, NE correction factor = 0.6. Images were acquired in the diastolic diastasis. CE-MRA was performed during a single breath-hold following the administration of 0.4 mL/kg of Gadolinium. A gradient echo sequence was used with the following imaging parameters: TR = 3.7 ms, TE = 1.2 ms, flip angle = 25°, resolution = 0.9 × 0.9 × 1.5 mm, iPAT factor = 2. The dimensions of the stenosed segment, and dimensions 1 cm proximal to, and 1 cm distal to the stenosed region were also measured for each vessel of interest.

*Results:* Navigator-echo 3D b-SSFP imaging was successfully performed in all patients. 3D reconstruction of all of these datasets was possible. For mild to moderate stenosis (<75% luminal diameter change at site of stenosis), there was good agreement between the dimensions measured on the b-SSFP and CE-MRA images ($r = 0.9$, $p < 0.001$). However, for severe stenosis ($n = 10$), a degree of signal dropout was seen in all the CE-MRA images, but in none of the b-SSFP images (Fig. 1). Accurate measurement of the stenostic site was only possible on the b-SSFP images.

*Conclusions:* 3D b-SSFP imaging is an accurate method for assessing vascular stenosis. This sequence is less susceptible to signal dropout secondary to turbulent flow at sites of severe stenosis, allowing accurate assessment of such sites. Furthermore, as data is ECG-gated, images of great vessels in close proximity to the heart (pulmonary trunk and aortic root) are less affected the cardiac motion artefact seen on CE-MRA images.

## 445. GADOLINIUM MIXED-MICELLES AS INTRAVASCULAR MR AGENTS FOR VESSEL WALL IMAGING

**Karen C. Briley-Saebo, PhD, Fabien Hyafil, PhD, Venkatesh Mani, PhD, Juan Carlos Frias, PhD, Vardan Amirbekian,**

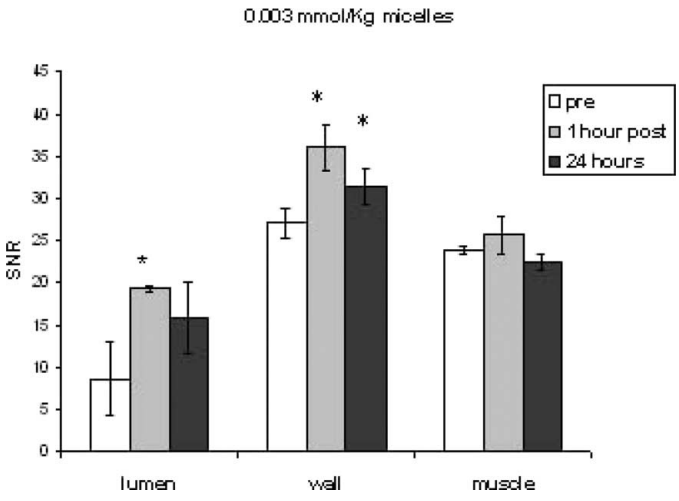


FIG. 1. SNR in rabbit aorta as a function of time after administration of 0.003 mmol Gd/Kg.

FIG. 2. MIP of aorta pre and 1-hour post micelle.

**MD, Zahi A. Fayad, PhD.** ***Mount Sinai School of Medicine, New York, NY, USA.***

*Introduction:* Although gadolinium based micelles are currently being developed for atherosclerotic plaque targeting, preliminary *ex vivo* studies have shown that these materials also cause significant signal increase in blood, relative to GdDTPA.

*Purpose:* The purpose of this study was to test the hypothesis that gadolinium micelles are effective intra-vascular agents with increased signal enhancement in blood and vessel wall, relative to GdDTPA in atherosclerotic rabbit models.

*Methods:* Gadolinium lipophylic complex (7 w/w% of GdDTPA-(C18)2) were incorporated into mixed micelles composed of surfactant (Tween 80Â®, 14 w/w%) and 79 w/w% POPC according to established methods. The micelles were characterized as follows: hydrated particle diameter = 106.5 Â ± 0.2 nm, r1 blood = 13.0 Â ± 0.5 $s^{-1}$ $mM^{-1}$ (63 MHz, RT), and Gd/micelle = 4100. Atherosclerotic New Zealand White rabbits were administered either 0.1 mmol/Kg GdDTPA or 0.003 mmol/Kg micelles. A low gadolinium micelle dose was chosen, since the safety profile of this material in rabbits has not been determined. Imaging was performed at 1.5T over a 24-hour time interval post injection. Aortic images were obtained from the level of the left renal artery to the iliac bifurcation. Thirty three contiguous axial images of the aorta were obtained using T1-w TSE sequences with TR/TE/flip = 800/5.6/180Â° and pixel size = 0.47 $mm^2$. Additionally, 2D Time-of-Flight images were obtained with TR/TE/flip = 28/7.3/50Â°. From the axial images, SNR values were obtained in the vessel lumen, vessel wall and proximal muscle tissue as a function of time post injection.

*Results:* Significant enhancement was observed in both the vessel wall and lumen for up to one-hour post injection of 0.003 mmol Gd/Kg micelles (Figs. 1 and 2). Additionally, significant enhancement of the vessel wall was also observed at 24 hours post micelle injection (Figs. 1 and 3). No significant change in the SNR of muscle was observed at any time point post injection.

*Conclusions:* The results of this study strongly suggest that gadolinium micelles may be both effective intravascular agents and may also enable visualization of the vessel wall for extended time periods post.

## 446. MR EVALUATION OF MYOCARDIAL CONTRAST KINETICS: COMPARISON OF HEALTHY VOLUNTEERS AND PATIENTS WITH SUSPECTED MYOCARDITIS

**Kai Nassenstein,[1] Frank Breuckmann,[2] Thomas Schlosser,[1] Christoph Naber,[2] Raimund Erbel,[2] Joerg Barkhausen.[1]**

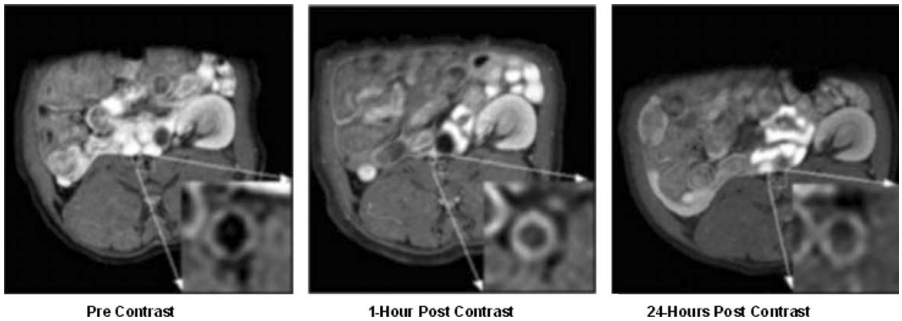


FIG. 3. T1-w TSE images of rabbit aorta as a function of time post micelle injection.

[1] *Department of Diagnostic and Interventional Radiology and Neuroradiology, University Hospital Essen, Essen, Germany,* [2] *Department of Cardiology, West German Heart Center Essen, University Hospital Essen, Essen, Germany.*

*Introduction:* The onset of acute myocardits is difficult to recognize clinically and all currently available diagnostic tools including ECG, echocardiography and myocardial biopsy are not without limitations. Therefore, several studies evaluated the diagnostic impact of cardiac magnetic resonance imaging in patients with suspected myocarditis. Cardiac MRI may show regional or global wall motion abnormalities, focal myocardial edema on T2 weighted images or areas of increased contrast enhancement. However, controversies about the pattern of contrast enhancement still exist. Whereas (1) assessed focal areas of late enhancement (2, 3), measured myocardial global relative enhancement to confirm the diagnosis of acute myocarditis.

*Purpose:* Thus, our study aimed to evaluate differences in myocardial contrast medium kinetics after injection of a low-molecular extracellular contrast agent in healthy volunteers and patients presenting with myocarditis.

*Methods:* Twenty healthy volunteers (5 female, 15 male; mean-age 51 $\pm$ 12 years) and 7 patients (2 female, 5 male; mean-age 45 $\pm$ 17 years) with clinically diagnosed acute myocarditis were examined on a 1.5 T MR scanner (Siemens Avanto). Steady state free precession cine sequences were measured in standard short and long axis views. For the assessment of myocardial edema T2-weighted inversion recovery sequences (TE 6.9 ms, TR 700 ms, TI 170 ms, FA 180°) were acquired in the same slice orientations. After injection of 0.2 mmol Gd-DTPA/kg bodyweight a steady state free precision sequence with increasing inversion times (TR 2.4 ms, TE 1.1 ms, FA 50°) was repetitively acquired in the 4-chamber view over 15 minutes. Signal intensity measurements were performed in multiple regions of interest in the left ventricular myocardium and in the skeletal muscle, to define the inversion times ($TI_{min}$) resulting in the minimum signal intensity. T1 values of all different tissues were calculated based on the standard formula $T1 = TI_{min}/\ln 2$. Finally, the relative myocardial T1-values (T1myocadium/T1skeletal-muscle) were calculated for all time points.

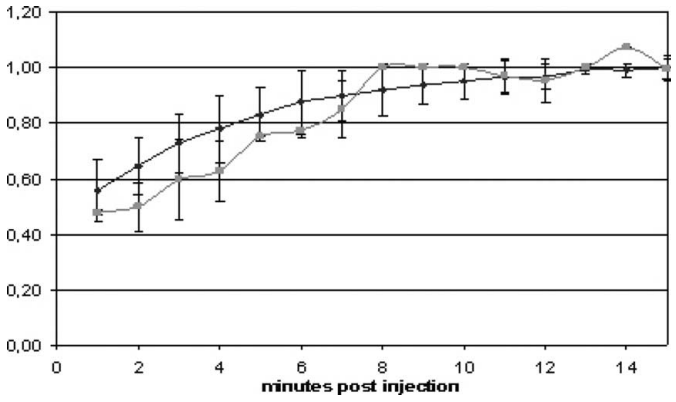


FIG. 1. Relative myocardial T1 values over 15 minutes after contrast medium injection. Blue curve: healthy volunteers; red curve: patients presenting with acute myocarditis.

*Results:* Relative myocardial T1-values increased over the time in the form of a continuous increasing curve with asymptotic approximation to the value 1.0 in the healthy volunteers as shown in Fig. 1. No statistical relevant differences between the curve in healthy volunteers and patients with acute myocarditis was found. Absolute myocardial T1-values increased in healthy volunteers and in patients presenting with myocarditis over the time, too (healthy volunteers: 201; 5 minutes.: 302; 10 minutes: 350; 15 minutes p.i. 353/myocarditis: 5 minutes: 317; 10 minutes: 336; 15 minutes: 370). Three patients with myocarditis showed a reduced left ventricular ejection fraction (<50%). Neither in healthy volunteers nor in symptomatic patients detection of relevant myocardial edema or delayed enhancement could be achieved.

*Discussion:* Recent data suggested that T1 weighted contrast enhanced MRI reveals increased relative global myocardial T1 values within the first minutes after application of low-molecular contrast agents in patients suffering from acute myocarditis. Myocardial hyperemia has been thought to contribute to this phenomenon. Even though our data demonstrated a slight deviation between the curves of patients with myocarditis and healthy volunteers within the first 2 to 3 minutes following application of contrast no statistically significant difference could be assessed.

*Conclusions:* Our preliminary data show no significant differences between the relative myoardial T1 value of patients with acute myocarditis compared to healthy volunteers. However, additional evaluation in a higher number of patients is required in order to further elucidate the relevance of myocardial contrast media kinetics in patients with suspicion of acute myocarditis.

## REFERENCES

1. Mahrholdt, et al. Circulation 2004.
2. Friedrich, et al. Circulation 1998.
3. Abdel-Aty, et al. J Am Coll Cardiol 2005.

## 447. A NOVEL BOLD-SENSITIVE SSFP SEQUENCE FOR THE DETECTION OF ISCHEMIA

**Jordin D. Green, PhD,[1] Andreas Kumar, MD,[2] Matthias G. Friedrich, MD.[2]** [1] ***Siemens Medical Solutions, Calgary, AB, Canada,*** [2] ***University of Calgary, Calgary, AB, Canada.***

*Introduction:* Non-invasive assessment of tissue ischemia is challenging. Because the BOLD (Blood Oxygen Level Dependent) effect mainly relies on endogenous contrast (deoxyhemoglobin) to differentiate ischemic from non-ischemic tissue, BOLD has the potential to directly assess tissue oxygenation. Traditionally, BOLD imaging has used T2*-weighted sequences (such as Echo Planar Imaging [EPI]), but many of these are hampered by problems with image quality and SNR. Steady-state Free Precession (SSFP) typically achieves excellent SNR

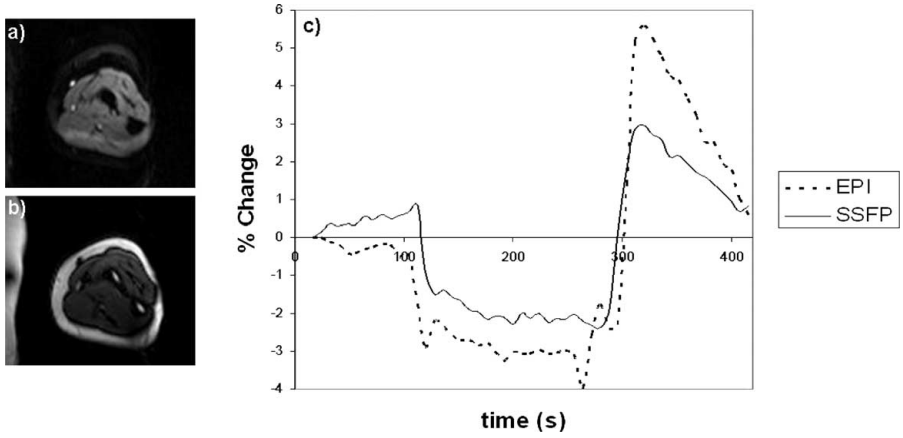


FIG. 1. Sample cross-section of the forearm before cuff inflation, scanned using a) EPI and b) SSFP. Typical EPI distortions are seen in a), c) Percent change (compared to the first measurement) vs. time for the mean of each time point for EPI (dashed line) and SSFP (solid line). The pressure cuff was inflated at 120 s, and deflated at 300 s.

and image quality. Additionally, it has been demonstrated that a steady-state SSFP sequence BOLD-sensitive (1). However, a direct implementation of steady-state BOLD-SSFP for the imaging of moving structures is complicated, because spins will be continually moving in and out of the imaging plane. Therefore modifications to steady-state BOLD-SSFP must be made before it can be applied for this type of application.

*Purpose:* To develop a novel steady-state BOLD-sensitive SSFP sequence which can image moving structures, and to compare its behavior to T2* weighted EPI.

*Methods:* A modified SSFP sequence was designed with the goal of obtaining strong T2-weighted images. Before each acquisition period, a train of SSFP dummies designed to excite a 7 cm slice (centered on the acquisition slice) were played out for 850 ms. Next, a flip back pulse was applied to "store" the transverse magnetization on the longitudinal axis. This was followed by a gradient spoiling, then slice-selective (10 mm) SSFP dummies and acquisition. All studies were performed on a 1.5T Siemens Avanto. As a model of ischemia, a pressure cuff was placed on the upper arm of 11 volunteers. Each underwent two seven minute scans of their forearm, once with T2-weighted SSFP and once with T2* weighted EPI. During each scan, the cuff was inflated to 170 mmHg for the middle three minutes to produce ischemia, followed by a period of reactive hyperemia after the cuff was deflated. To evaluate BOLD sensitivity, the mean signal for the two sequences was calculated over four data points for three time periods: 48–72 s (baseline), 240–264 s (ischemia), and 328–352 s (hyperemia). Regions-of-interest (ROI) were drawn in the arm muscle for each data set using as large an ROI as possible while excluding vessels, bone, and artifacts. The average signal was calculated for each of these periods and was used to determine the percent change from rest to ischemia and from rest to hyperemia. A matched pairs t-test was used to determine if the signal change was statistically significant ($\alpha = 0.05$). Sequence parameters for both sequences were FOV $= 263 \times 350$ mm$^2$; matrix $= 119 \times 256$; 8 s/image. Segmented acquisition was repeated once per second. Sequence parameters specific to EPI: train length = 29; echo spacing = 0.9 ms; flip angle = 90o; acquisition began 35 ms after excitation. For SSFP: TR/TE/flip angle = 5.5 ms/2.75 ms/60o; 15 lines/acquisition period.

*Results:* Mean percent signal changes ± standard error for EPI were 2.7 ± 0.7 (baseline vs. ischemia) and 4.8 ± 0.6 (baseline vs. reactive hyperemia). Mean percent signal changes for SSFP were 2.4 ± 0.4 (baseline vs. ischemia) and 2.1 ± 0.2 (baseline vs. reactive hyperemia). All signal changes were statistically significant ($p < 0.05$). Signal curves for both EPI and SSFP followed a trajectory seen previously for this type of model (Fig. 1).

*Conclusion:* The new T2-weighted SSFP sequence has sufficient BOLD sensitivity to detect signal changes at 1.5 T in an arm cuff model of ischemia/hyperemia, while maintaining a sequence structure that is potentially suitable for the imaging of moving structures. T2-weighted SSFP shows promise for identifying regions of ischemia in cardiac imaging.

## REFERENCE

1. Dharmakumar R, et al. Magn Reson Med 2004;53:574–83.

## 448. MODIFIED HARP METHOD IMPROVES TRACKING AND QUANTIFICATION OF CARDIAC MOTION IN PATIENTS

**Ayman M. Khalifa, MS,[1] Jerry Prince, PhD,[2] Nael F. Osman, PhD.[2] [1] *Cairo University, Cairo, Egypt,* [2] *Johns Hopkins University, Baltimore, MD, USA.***

*Introduction:* HARP is an image processing technique used for rapid analysis of tagged cardiac magnetic resonance imaging (1). The technique filters the specific peaks in the k-space of the tagged images to produce phase images. Based on the fact that

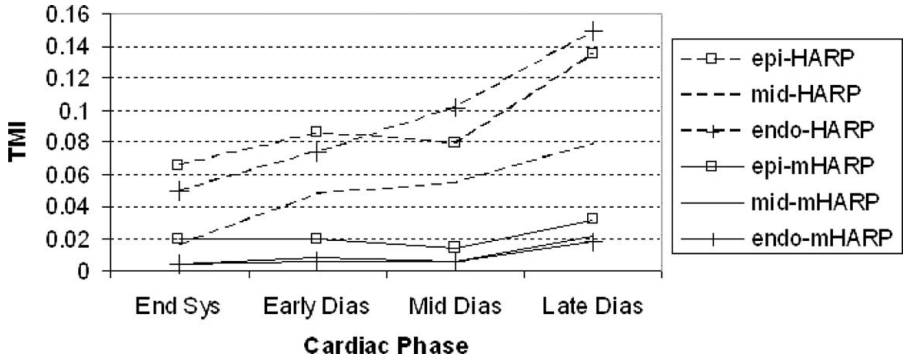


FIG. 1. The total mistracking index (TMI) at the epicardium, endocardium, and mid-wall for the original and modified HARP techniques.

the phase of any material point does not change with time, HARP can track the motion of any point through a cine of tagged images. In order to calculate the circumferential and radial strain, a circular mesh is manually built at a specific timeframe and all the points are then tracked using the HARP technique. The strains are then computed by measuring the changes in the distance between the neighboring points. However, because of regional fading of tags, rapid motion, and through-plane motion, the tracking of some individual points can fail, resulting in miscalculation of the strain, which provides the information about regional function. A modified HARP technique (2) is proposed to correct for these mistracking errors by combining the HARP technique with active contour methods (3). Correction of the mistracked points is validated using three observers and the results for the modified HARP technique show a great improvement compared to those from the original HARP technique.

*Purpose:* We propose and validate a modified HARP technique and compare the results to those of the original HARP technique.

*Methods:* Eight studies of tagged images were used to validate the modified HARP technique. A circular mesh was manually built after end diastole. This mesh consisted of three contours: epicardial; endocardial; and mid-wall. The mesh was then tracked using both the original HARP and the modified HARP techniques. Three observers evaluated the results visually and determined, for any point, whether they strongly agreed, agreed, disagreed, or strongly disagreed with the accuracy of the tracking of each technique. We defined a mistracking index (MI) for each point as 0 for strongly disagreement, 1/3 for agreement, 2/3 for disagreement, and 1 for strongly disagreement. The Total Mistracking Index (TMI) was calculated at four phases for the heart at end systole, early diastole, mid diastole, and late diastole, by taking the average MI of the points at a specific time phase for the three observers.

*Results:* Fig. 1 shows the TMI at the epicardium, endocardium, and mid-wall for the original and modified HARP techniques. This figure shows that the TMI of the modified HARP is much lower than that for the original HARP. The graph also shows that the TMI is lower in the mid-wall than in the epicardium or endocardium.

*Conclusions:* Using the modified HARP improves the tracking of cardiac motion while maintaining the fast analysis advantages of the original HARP.

## REFERENCES

1. Osman NF, et al. Magn Reson Med 1999;42:1048–60.
2. Khalifa A, et al. SCMR 2004.
3. Kass M, et al. Int J Comput Vision 1988;1:321–31.

## 449. GENERATION OF SHORT AXIS CARDIAC CONTOURS USING LONG AXIS CARDIAC MRI CONTOURS

**Gilion Hautvast[1], Marcel Breeuwer[2], Ursula Kose[2], Frans Gerritsen.[1]** [1]***University of Technology Eindhoven, Eindhoven, The Netherlands,*** [2]***Philips Medical Systems, Best, The Netherlands.***

*Introduction:* Functional cardiac MRI examinations usually contain image sequences from three orthogonal views, i.e. short axis, long axis 2 chamber and long axis 4 chamber (Fig. 1). These images are used to quantify left ventricular function, which requires the delineation of the left ventricular endocardium and epicardium. This may involve up to 1500 contours. Most cardiac MR analysis applications provide computer assistance for separate analysis of each view. A combined analysis can reduce the analysis time significantly.

*Purpose:* The purpose of our work is to develop an automatic method to generate short axis contours based on long axis segmentations. In combination with existing contour propagation methods, user interaction is reduced to manually segmenting the end diastolic phase of both long axis sequences, after which the remaining long and short axis images are segmented automatically.

*Method:* The new method faces two major problems. One is the misalignment between the three acquisitions, caused by different breath-hold positions. The other is the construction of valid myocardial contours based on only 4 intersections between the long axis contours and the short axis image planes. We

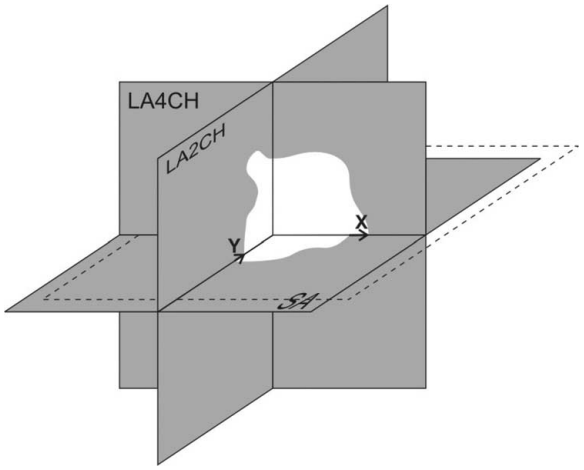


FIG. 1. The short axis image plane is translated over (X,Y) to maximize the match of the gray-values at the image plane intersection lines.

propose a two-step procedure to deal with these problems. The first step is to align the short axis images to the 2 and 4 chamber long axis images. Our method calculates in-plane translations in order to simultaneously maximize the match of gray-value profiles extracted along the intersection lines of the image planes in all phases (Fig. 1). The second step is to construct valid endocardial and epicardial contours, given only the intersection points of the long axis contours with the short axis image plane. We apply a partial elliptical interpolation scheme, in which the connecting arcs between the intersection points are reconstructed based on local estimates of the major and minor axis of an ellipse (Fig. 2). The new method is optimized and validated using 75 orthogonal image sets, acquired with the BTFE protocol using ECG-triggered cine cardiac MR. We are grateful to Eike Nagel of the Deutsches Herzzentrum, Berlin, for supplying image data. For each image, a golden standard segmentation is determined by averaging 6 expert segmentations, which had an interobserver variability of 1.01 mm.

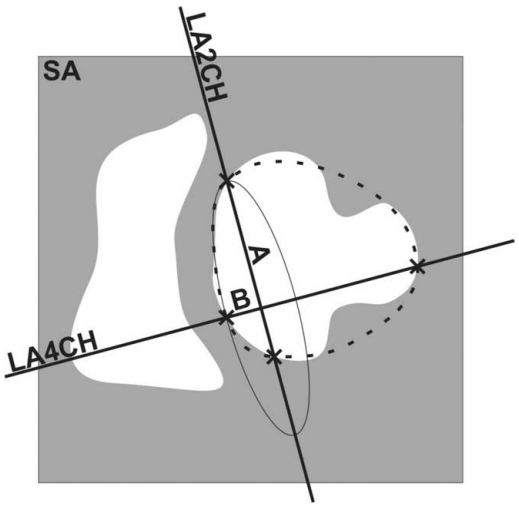


FIG. 2. Local estimates of the major axis A and minor axis B of an ellipse are used reconstruct myocardial contours.

*Results:* Each step is validated independently. The alignment reduces the distance between the intersection points of the long axis contours and the golden standard in the short axis image plane from $2.00 \pm 1.50$ mm to $1.52 \pm 0.82$ mm, which approximates the pixel dimensions. Given 4 golden standard contour points, the elliptical interpolation results in contours with average RMS positioning errors of $1.04 \pm 0.59$ mm for the endocardium and $0.90 \pm 0.39$ mm for the epicardium. The complete procedure results in contours with average RMS positioning errors of $1.99 \pm 0.66$ mm for the endocardium and $1.32 \pm 0.35$ mm for the epicardium. In combination with existing contour propagation methods, short axis contours with average RMS positioning errors of $1.77 \pm 0.62$ mm for the endocardium and $1.35 \pm 0.34$ mm for the epicardium are generated.

*Conclusions:* We have developed a two-step procedure to generate short axis myocardial contours based on long axis contours. The procedure consists of image alignment and elliptical contour interpolation. We are able to perform image alignment with pixel precision. Considering the inevitable inaccuracy of the elliptical contour interpolation, we are able to generate short axis cardiac contours of reasonable precision. A further reduction of analysis time is achieved by combining this method with existing contour propagation methods.

## 450. TOWARDS THE IMAGING OF CAROTID ARTERY AND CAROTID PLAQUE EMPLOYING PASADENA

**Pratip Bhattacharya, PhD,[1] Daniel Tofan,[1] Alexander Lin, BS,[1] Thao Tran, BS,[2] Kent Harris, PhD,[2] Valerie Norton, BS,[1] Anna Freundlich, BS,[2] Daniel P. Weitekamp, PhD,[1] Brian D. Ross, PhD, MD.[2]** [1]***California Institute of Technology, Pasadena, CA, USA,*** [2]***Huntington Medical Research Institutes, Pasadena, CA, USA.***

*Introduction:* PASADENA (1, 2) (Parahydrogen And Synthesis Allow Dramatically Enhanced Nuclear Alignment) or PHIP (ParaHydrogen Induced Polarization) method of enhancing nuclear spin polarization has recently been improved (3, 4) and demonstrated (3–8) to produce $^{13}C$ polarizations (P) of order unity for the nascent products of molecular addition by parahydrogen. A magnetic resonance spectroscopy or imaging pulse sequence initiated at this time provides a sensitivity that is $10^4$ times greater than the signal from the same population of molecules at equilibrium. This corresponds to a usable signal-to-noise ratio for a single repetition of this experiment that would otherwise require $10^8$ repetitions (at least $10^8$ s = 3 years). This approach opens up an entirely unexplored regime for real-time imaging of morphology and function characterized by radically improving the finesse of MRS and MRI for measuring localized changes in concentrations of metabolites and biomolecules *in vivo*.

*Methods:* To facilitate routine PASADENA trials, GE Healthcare, Malmo has developed a PHIP polarizer. We have installed and optimized the polarizer and parahydrogen generator in our laboratory. Employing the polarizer and novel polarization transfer sequences, we have been able to achieve high $^{13}C$ polarizations in water soluble molecules with promise for targeted MRI & MRS. To use the hyperpolarized $^{13}C$ signal efficiently and routinely in imaging, we have also developed $^{13}C$ 3D FIESTA and $^{13}C$ CSI sequences for 1.5T GE Signa LX 9.1 clinical scanner.

*Results:* High $^{13}C$ polarizations ($P > 0.3$) are observed in several water soluble molecules leading to high SNR (200–700) in $^{13}C$ imaging, previously observed by Golman et al. (3, 4).This is the basis of the development of the high resolution contrast agents as there is negligible background. We have obtained ultrafast high resolution in vivo images of carotid artery in pig and rats, following arterial injection of these molecules. Furthermore, we have incorporated the PASADENA functionality and carotid plaque binding features in a family of molecules by organic synthesis. These molecules are purified, characterized, binding abilities studied, and employed in hyperpolarization experiments to image carotid plaques *in vitro* and *in vivo*.

*Discussion:* Advancing from intravascular hyperpolarized $^{13}C$ MRI necessitates "smart" PASADENA reagents with biological functionalities. Vulnerable plaque offers such a medically valuable object for over 10,000 fold enhanced MRI based on targeted chemical synthesis.

*Conclusion:* Routine $^{13}C$ imaging with PASADENA is amenable to repetitive experimentation (~2 minutes time lapse) allowing clinical flexibility. Extension of PASADENA to real time *in vivo* MRI of carotid artery and carotid plaque is now feasible.

*Acknowledgment:* Research funded by James G. Boswell Foundation, Caltech SURF Program.

## REFERENCES

1. Bowers CR, Weitekamp DP. Phys. Rev. Lett. 1986;57:2645.
2. Bowers CR, Weitekamp DP. J. Am. Chem. Soc. 1987;109:5541.
3. Golman K, Axelsson O, Johannesson H, Mansson S, Olofsson C, Petersson JS. Magn Reson Med. 2001;46:1.
4. Golman K, Ardenkjaer-Larsen JH, Petersson SJ, Mansson S, Leunbach L. PNAS USA. 2003;100:10435.
5. Bhattacharya P, Weitekamp DP, Harris K, Lin AP, Ross BD, ESMRMB Annual Meeting, 2004;236.
6. Bhattacharya P, Weitekamp D, Harris K, Mansson M, Lin AP, Perman WH, Ross BD. Proc Int Soc Magn Reson Med 2005;13:171.
7. Bhattacharya P, Norton V, Harris K, Mansson M, Lin AP, Ross BD, Weitekamp D. Gordon Research Conference on Magnetic Resonance 2005.
8. Bhattacharya P, Harris K, Lin AP, Mansson M, Norton V, Perman W H, Weitekamp D, Ross BD. MAGMA. 2005;18:5.

## 451. EFFECT OF CARDIAC REHABILITATION ON VASODILATED MYOCARDIAL PERFUSION BY QUANTITATIVE MRI

**Jessica E. Holly, BS, Sriram Padmanabhan, MD, Li-Yueh Hsu, PhD, Richard O. Cannon, III, MD, Andrew E. Arai, MD.** ***National Institutes of Health, Bethesda, MD, USA.***

*Introduction:* Supervised exercise in patients with coronary artery disease is often prescribed as part of a cardiac rehabilitation program. Exercise-based cardiac rehabilitation has been associated with reduced mortality, nonfatal myocardial infarction, and rates of coronary revascularization.

*Purpose:* The aim of this study was to use quantitative MRI to determine if clinically indicated cardiac rehabilitation improves rest and stress myocardial perfusion (mL/min/g).

*Methods:* Twenty-three patients completed the prscribed 36 sessions of supervised and monitored exercise and completed rest and dipyridamole stress MRI scans before and after starting cardiac rehabilitation. 4 other subjects were excluded due to intervening PCI during the protocol period. A dual-bolus first pass perfusion protocol was used to image myocardial perfusion during dipyridamole (0.56 mg/kg over 4 min) and rest perfusion was performed 2 hours later. Myocardial blood flow during stress and rest were quantified with Fermi model-constrained deconvolution and reported in units of mL/min/g. Results are mean $\pm$ SD.

*Results:* Patients averaged $64 \pm 9$ years old, 21 were male and 2 were female. 48% had a history myocardial infarction, 70% had a history of PCI and 26% had CABG. Patients averaged $9.7 \pm 2.0$ mets on day 1 and increased to $15.4 \pm 4.3$, $18.0 \pm 4.3$, and $20.7 \pm 5.5$ mets by session 12, 24, and 36 respectively (all $p < 0.001$ vs day 1). As a group, stress myocardial perfusion did not change significantly from baseline $3.20 \pm 0.56$ mL/min/g to follow-up $2.97 \pm 0.87$ mL/min/g ($p = NS$). Flow reserve also did not change significantly. The methodology was able to discriminate normal vs ischemic regions of the heart ($3.67 \pm 0.59$ vs $1.77 \pm 0.62$ mL/min/g, $p < 0.001$). Stress perfusion did not change significantly in the 10 ischemic sectors ($1.77 \pm 0.62$ vs $1.68 \pm 0.74$ mL/min/g, $p = NS$). Furthermore, the study had a power of 0.996 at a p value of 0.005 to detect a 20% change in stress myocardial perfusion based on the sample size and measured standard deviations.

*Conclusions:* Although exercised-based cardiac rehabilitation achieved substantial levels of exercise, there was no significant change in stress myocardial perfusion. The study had ample power to detect a clinically relevant 20% change in stress myocardial perfusion.

## 452. THE FORGOTTEN SIDE: IN-VIVO ASSESSMENT OF INFLAMMATORY ATHEROMA BURDEN ON THE CONTRALATERAL SIDE TO SYMPTOMATIC CAROTID STENOSIS USING HIGH RESOLUTION USPIO ENHANCED MR IMAGING

**Simon P. Howarth,[1] Tjun Tang, MRCS,[1] Rikin Trivedi, MRCS,[1] Jean U-King-Im, MRCS,[1] Martin Graves, MA,[1] Peter J. Kirkpatrick, FRCS (SN),[2] Jonathan H. Gillard,**

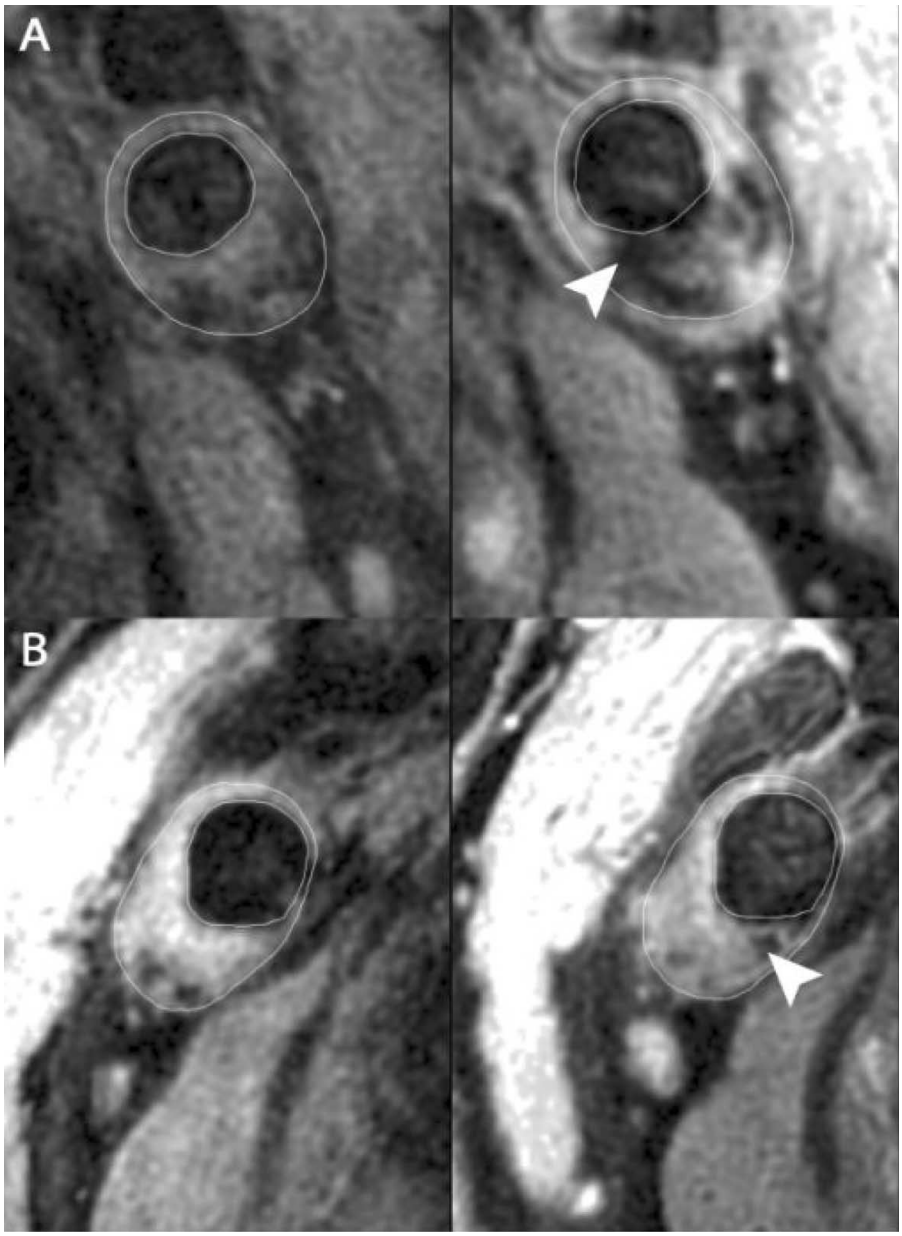


FIG. 1.

**FRCR.[1] [1]*University Department of Radiology, Cambridge, United Kingdom, [2]University Department of Neurosurgery, Cambridge, United Kingdom.***

*Background:* It is well described that "vulnerable" atheromatous plaque has a thin, fibrous cap and extensive lipid core with associated inflammation. This inflammation can be detected on high resolution MR imaging using a novel contrast medium, Sinerem, an Ultrasmall Super-Paramagnetic Iron Oxide (USPIO) (1). Studies using USPIO to quantify inflammatory burden in symptomatic carotid stenosis have thus far not reported USPIO status on the contralateral asymptomatic side.

*Methods:* Ten symptomatic patients scheduled for carotid endarterectomy were imaged at 1.5 Tesla pre and 36 hours post USPIO infusion. (Sequences included $T_1$,$T_2$,$T_2$*, FatSat and short inversion time (STIR) sequences). Images were manually segmented into quadrants (CMR Tools, Imperial College, London) and signal change in each quadrant was calculated following USPIO infusion. There were 6 males with a median age of 78 years (range 62–84). All patients had severe internal carotid artery stenosis (mean 77%) on their symptomatic side compared

to a mean of 42% on their asymptomatic side as measured by angiography.

*Results:* On the contralateral (asymptomatic) side there were 80 quadrants in total (52%) demonstrating a signal drop post USPIO infusion (symptomatic side = 114 quadrants [75%]). Only one patient with USPIO signal drop on the symptomatic side displayed no evidence of signal drop on the asymptomatic side. Mean signal drop per quadrant was higher on the asymptomatic side when compared with the symptomatic side (26 vs 18, $p < 0.05$). Fig. 1 below shows $T_1$ weighted imaging of the common carotid artery of a patient pre and post USPIO infusion (A asymptomatic side, B symptomatic side) Focal signal drop can clearly be seen on the post infusion imaging bilaterally (white arrows).

*Conclusions:* This study suggests that investigation of the contralateral side in patients with symptomatic carotid stenosis can demonstrate inflammatory activity in over 50% of plaques, even with a mean stenosis of only 42%. Thus inflammatory activity may be a significant risk factor in asymptomatic disease.

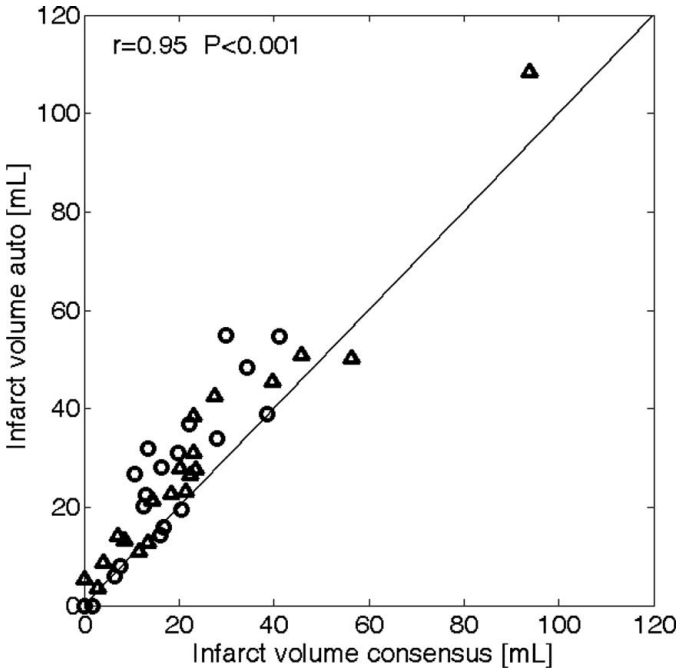


FIG. 1. Difference between automatic method and infarct volume consensus from three manual observers. Circles denote patients scanned using a Siemens scanner, and triangles denote patients scanned using a Philips scanner.

## REFERENCE

1. Trivedi RA, et al., Neurology 63(1):187–8.

## 453. AUTOMATED QUANTIFICATION OF DELAYED CONTRAST-ENHANCED MR IMAGES

**Einar Heiberg,[1] Henrik Engblom,[1] Jan Engvall,[2] Erik Hedström,[1] Martin Ugander,[1] Håkan Arheden.[1] [1]*Department of Clincial Physiology, Lund University, Lund, Sweden,* [2]*Department of Clincial Physiology, Linköping University, Linköping, Sweden.***

*Introduction:* Accurate and reproducible assessment of myocardial infarction is important for treatment planning in patients with ischemic heart disease. We describe a method to quantify myocardial infarction by automatic delineation of hyperenhanced myocardium in delayed contrast enhanced magnetic resonance images.

*Method:* The method was evaluated in 40 patients; 20 with acute infarction and 20 with chronic healed infarction using scanners from two different manufacturers (Philips and Siemens). Infarct size measured by the proposed automatic method was compared with an infarct volume consensus based on the mean of manual measurements by three experienced observers. The mean signal intensity and standard deviation was calculated in 5 sectors in each slice. The 20% most endocardial and epicardial myocardium in each sector was excluded, leaving the middle 60% of the myocardial wall as basis for the mean signal intensity calculation. The region with the lowest mean signal intensity was considered 'remote' myocardium. A slice-specific threshold was set as the mean of the remote sector plus 2.4 standard deviations. The number of standard deviations was chosen as the value that minimized the variation between the automatic method and the infarct volume consensus. A fast level set algorithm was applied and the speed term was set to the signal intensity minus the slice-specific threshold. The slice-specific threshold may be incorrect in cases with completely infarcted slices. This was adressed by comparing the mean signal intensity in the remote sector to the signal intensity in the left ventricle blood pool. The method was implemented in a cardiac image analysis software package, freely available for research purposes at http://segment.heiberg.se.

*Results:* The difference in infarct size between semi-automatic quantification and the mean of the three observers was 6.1 ± 6.6 mL (mean ± SD), and the interobserver variability (SD) was 4.2 mL. Fig. 1 shows difference between the automatic method and infarct volume consensus. The bias and variability was not statistically different (two sample t-test) with respect to the two MRI scanners ($P = 0.19$), and chronic versus acute infarcts ($P = 0.15$). Fig. 2 shows the graphical user interface.

*Conclusions:* The presented method is a highly automated method for analyzing myocardial viability from DE-MR images. The bias of the method is acceptable and the variability is in the same order of magnitude as the interobserver variability for manual delineations.

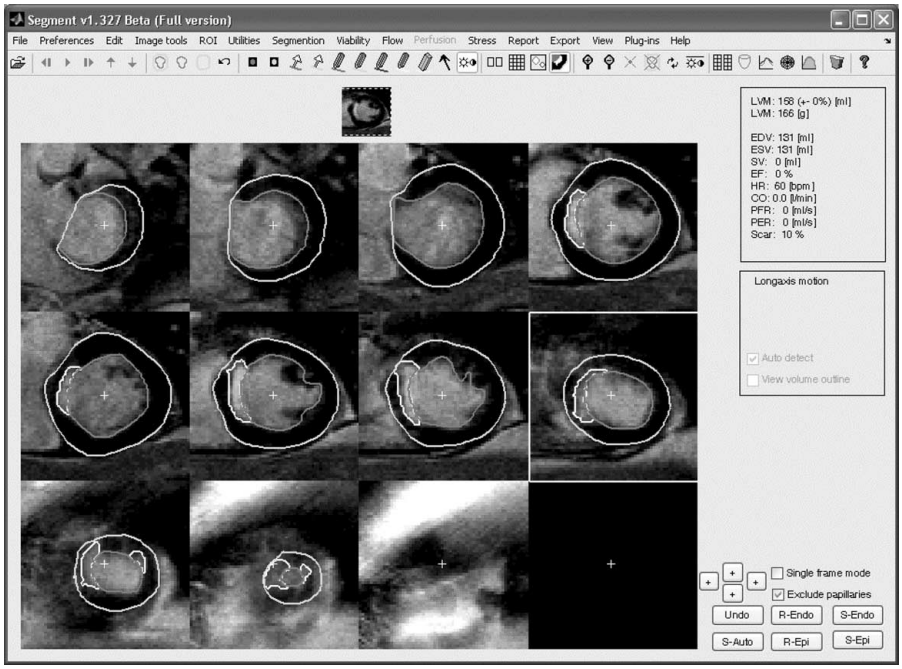


FIG. 2. Graphical user interface.

## 454. SIZE AND TRANSMURAL EXTENT OF ACUTE MYOCARDIAL INFARCTION CAN BE ESTIMATED BY ECG: COMPARISON TO DELAYED ENHANCED MAGNETIC RESONANCE IMAGING

**Henrik Engblom, MD,[1] Erik Hedstrom, PhD,[1] Einar Heiberg, PhD,[1] Galen Wagner, MD,[2] Olle Pahlm, MD, PhD,[1] Håkan Arheden, MD, PhD.[1]** [1]***Lund University Hospital, Lund, Sweden,*** [2]***Duke University Medical Center, Durham, NC, USA.***

*Introduction:* The ability to quantify size and transmural extent of myocardial infarction (MI) by 12-lead ECG is not fully explored. Q waves have historically been considered predictive of transmural MI. Recent studies have, however, indicated that this may not be the case.

*Purpose:* To test the hypotheses the size and transmural extent of acute MI can be estimated by QRS scoring from the ECG and that presence of Q waves are not predictive of transmural MI.

*Methods:* Twenty-nine patients with first-time reperfused MI were studied by delayed enhanced magnetic resonance imaging (DE-MRI) and 12-lead ECG one week after the acute event. Selvester QRS score from the ECG was compared with MI size (Spearman's correlation) and transmurality in 12 left-ventricular segments (Jonckheere-Terpstra's test for trend) assessed by DE-MRI.

*Results:* There was a good correlation ($r = 0.79$, $p < 0.001$) between MI size by QRS scoring and DE-MRI (Fig. 1). As local MI transmurality increased, as assessed by DE-MRI, the local QRS score increased progressively ($p < 0.001$). There was no significant difference in the number of Q-wave criteria met between non-transmural and transmural MI ($1.8 \pm 0.6$ vs. $2.9 \pm 0.4$, $p = 0.14$, mean $\pm$ SEM), whereas the global QRS score differed significantly ($3.1 \pm 0.8$ vs. $5.1 \pm 0.6$, $p < 0.05$, mean $\pm$ SEM).

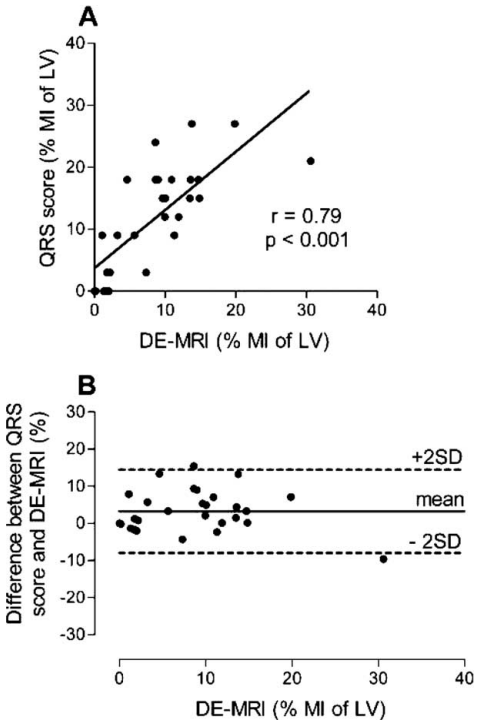


FIG. 1.

*Conclusions:* QRS score from the standard 12-lead ECG is significantly related to MI size and transmural extent by DE-MRI in patients with first-time reperfused MI. Presence of Q waves, however, is not predictive of transmural MI in this patient group.

## 455. NON-INVASIVE DETECTION OF MYOCARDIAL FIBROSIS BY CARDIAC MAGNETIC RESONANCE IN INACTIVE RHEUMATIC CARDIOPATHY: CORRELATION WITH THE SEVERITY OF THE DISEASE

**Martha Morelos.** ***Instituto Nacional de Ciencias Medicas y Nutricion Salvador Zubiran, Mexico City, Mexico.***

*Objetive:* Determine the utility of cardiac magnetic resonance (CMR) in the evaluation of myocardial fibrosis: correlation with the severity of valvular heart disease.

*Material and Methods:* Prospective, observational and transversal study. Twenty-eight patients were included with inactive rheumatic cardiopahty (IRC) diagnosed, all cases included clinical history, physical exam, electrocardiogram, transthoracic echocardiogram and CMR study. Myocardial fibrosis was determined with delay enhancement technic. Left ventricle was divides in 16 segments, evaluating the presence of fibrosis in each of them, using a scale from 0 (meaning no enhancement) to 1 in presence of ehnacement, inicating fibrosis. Statistical significance between clinical parameters and fibrosis scores observed in CMR was stablished.

*Results:* Thirteen out of 28 patients presented myocardial fibrosis (46.4%), being the most frequent location the posterolateral wall featuring a "patchy" pattern. A reduction in the ejection fraction was observed in the group with fibrosis (52%) when compared with those without fibrosis (66%), $p = 0.003$ NYHA functional class was lower in patientes with fibrosis, $p = 0.005$.

*Conclusion:* Myocardial fibrosis is presented in IRC and CMR is an ideal method for its detection. Myocardial fibrosis is associated with major severity of valvular heart disease.

## 456. MAGNETIC RESONANCE CORONARY ANGIOGRAPHY USING AN INTRAVASCULAR CONTRAST AGENT: T1 TIME COURSE OF NORMAL MYOCARDIUM AND BLOOD

**Kai-Uwe Waltering, Holger Eggebrecht, Kai Nassenstein, Thomas Schlosser, Peter Hunold, Jörg Barkhausen.** ***University Hospital Essen, Essen, Germany.***

*Introduction:* Noninvasive magnetic resonance coronary angiography (MRCA) has become feasible using either breath-hold or navigator gated sequences. However, the sensitivity and specificity of current approaches remains insufficient for broad clinical use. Contrast-enhanced MRCA may overcome some of these limitations, however extracellular contrast agents provide improved signal-to-noise und contrast-to-noise ratios only for a short period of time following injection. Recently, intravascular contrast agents have been introduced and several studies have shown that these compounds improve the diagnostic accuracy of MRCA. Due to the long plasma half-life time after a single injection, these compounds allow for multiple breath-hold or even up to three navigator scans covering the entire coronary tree. To optimize the contrast between the coronary arteries and the myocardium, inversion-recovery sequences are used with an inversion-time set to null the signal intensity of the normal myocardium. The correct setting of the inversion-time (TI) requires knowledge of the T1 times of the different tissues. To our knowledge these T1 times have not been systematically investigated so far.

*Purpose:* The purpose of our study was to measure the T1 times of normal myocardium and blood following injection of an intravascular contrast agent (Gadomer, Schering AG, Berlin, Germany) in volunteers and patients.

*Methods:* Twenty-eight healthy volunteers (17 male, 11 female, mean age 28 $\pm$ 4 years) and 6 CAD (6 male, mean age 61 $\pm$ 9 years) patients included in this study. All examinations performed on a 1.5T MR scanner (Sonata, Siemens medical solutions, Erlangen, Germany). Long axis views were collected with a segmented inversion-recovery steady state free precession sequence (TR 2.5 ms, TE 1.1 ms, FA 50°), generating images of a single slice with different inversion times 1, 5, 10, 15, 20, 25, 30, 35 and 40 minutes after injection of Gadomer (0.150 mmol Gd/kg bodyweight). Signal intensity measurements were performed in the LV cavity and the normal myocardium to define the inversion-times ($TI_{min}$) resulting in the minimum signal intensity. T1 values of myocardium and blood were calculated based on the standard formula $T1 = TI_{min}/\ln(2)$ for all time points. Additionally, breath-hold MRCA was performed using inversion-recovery fast low angle shot sequences up to 40 minutes after injection.

*Results:* Up to 15 minutes after injection, T1 times of blood were below 100 ms. Thereafter, T1 values increases over time from $125.3 \pm 9.8$ ms at 20min post injection (p.i.) to $204.1 \pm 12.3$ ms at 40 min p.i. (Fig. 1). The T1 time of normal myocardium was 240.8 $\pm$ 34.0 ms 1 minute after injection, followed by a minimum value of $190.1 \pm 19.8$ ms 10 min (p.i.). Thereafter, T1 times of myocardium continuously increased over time (40 min p.i. 281.7 $\pm$ 18.3 ms) (Fig. 1). High quality MRCA data sets could be acquired within the first 15 minutes after injection, whereas thereafter image quality slightly decreased, due to lower CNR values and blurring of the vessel walls.

*Conclusions:* The suppression of the myocardial signal is mandatory for 3D inversion-recovery gradient echo MRCA and optimizes the contrast between blood and myocardium. Therefore, the correct setting of the inversion-time is a prerequisite for excellent image quality. Our data show that a single injection of Gadomer results in a T1 time of blood below 100 ms for about 15 minutes after injection. However, the T1 time of the myocardium changes significantly within the first 15 minutes after injection. Therefore the inversion time has to be individually

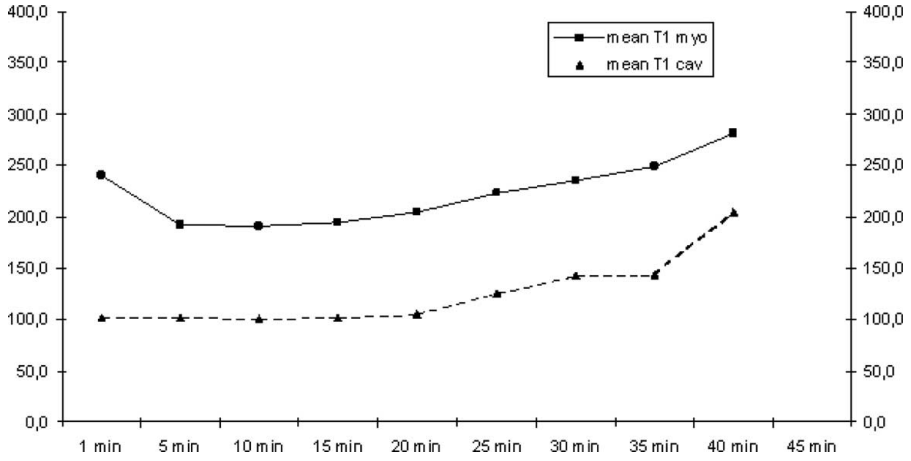


FIG. 1. T1 time course for myocardium and blood pool.

adjusted to optimize the image quality. More than 15 minutes after injection, the T1 time of blood increases due to renal excretion and blurring of the contours occurs. This may be explained by enhancement of the vessel wall or extravasation of the contrast agent. We conclude that high quality MRCA should be performed within the first 15 minutes after injection of a single dose of Gadomer.

## 457. PHASE CONTRAST MRI MEASUREMENT OF QP/QS: COMPARISON OF TWO SCAN PLANE TECHNIQUES

**Deval Mehta, MD, Himanshu Gupta, MD, Hrudaya Nath, MD, Steven Lloyd, MD, PhD.** ***University of Alabama at Birmingham, Birmingham, AL, USA.***

*Background:* Phase contrast MRI (PC-MRI) is an established technique for obtaining quantitative information on flow. It can be used to accurately measure flow across the aorta (Ao) and pulmonary artery (PA) and to calculate the ratio Qp/Qs in attempts to detect intracardiac shunts. Ideally, the imaging plane should be perpendicular to the vessel in which the flow is being measured (1). However, background velocity offsets and transient shifts in hemodynamics (including cardiac output) may affect the measured flow values and Qp/Qs ratio if the Qp and Qs measurements are obtained in different scan planes or if transient changes in cardiac output occur between the two acquisitions. Therefore, we sought to determine if a "hybrid" scan plane encompassing both arteries is more accurate for the comparison of Qp and Qs.

*Methods:* We performed 16 independent measurements of cardiac output in 6 normal subjects (with no suspicion of intracardiac shunt) across the Ao and PA; in these subjects the "true" Qp/Qs value was assumed to be 1.0, and deviation from this number was considered to be in error. Two separate methods were used to perform these measurements. In the first method separate scan planes were optimized to measure flow across the Ao and the PA. The flow was measured across these vessels using a retrospectively gated PC-MRI (Cine PC; Signa CV/i 1.5 Tesla system, GE Healthcare; scan details: 32 cardiac phases; 256x128 matrix; 34 cm FOV; 5 mm slice thickness; $v_{enc}$ 100 to 150 cm/s; TR 20 ms; TE 5.5 ms; flip angle 20 degrees, right-left frequency encoding, 2 NEX). Standard clinical software (CV Flow, v. 3.1, Medis, The Netherlands) was used to determine the flows and Qp/Qs was calculated. Then a hybrid plane was identified which revealed Ao and PA in a near-perpendicular plane, and Qp/Qs was measured by PC-MRI with the same scan parameters. The Qp/Qs estimated by the 2 methods was compared using a paired t-test and Bland-Altman analysis.

*Results:* The average of the 16 measurements of the Qp/Qs ratio by the separate-plane method was $1.03 \pm 0.1$ (range, 0.89–1.25) and by the hybrid-plane method was $1.07 \pm 0.09$ (range, 0.95–1.27). There was no difference in these measurements using either paired t-test ($p = 0.14$) or Bland-Altman analysis (Fig. 1; 95% confidence limits indicated by the dotted lines).

*Conclusions:* Use of a hybrid plane to determine the Qp/Qs value is no more accurate than use of individual planes for the

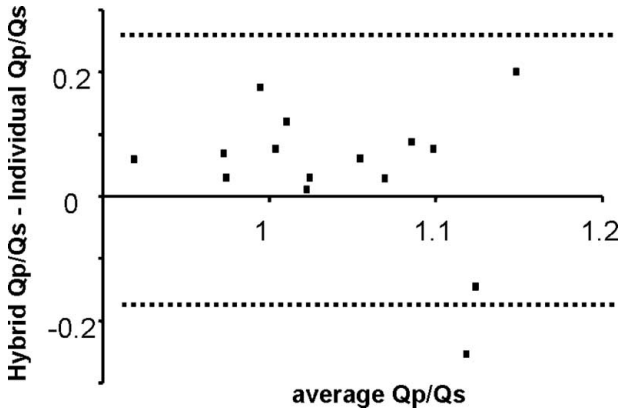


FIG. 1.

Ao and PA. However, making both measurements in a single plane does reduce the overall scan duration and might be useful in cases where minimizing the scan time is important.

## REFERENCE

1. Gatehouse PD, et al. Eur Radiol Jul 8 2005; [Epub ahead of print].

## 458. TOTAL VS EFFECTIVE EJECTION FRACTION FOR THE EVALUATION OF RIGHT VENTRICULAR FUNCTION IN POSTOPERATIVE TETRALOGY OF FALLOT COMPLICATED BY PULMONARY REGURGITATION

**Karen G. Ordovas, Mei-Han Wu, MD, Mario Morales, MD, Gautham P. Reddy, MD,MPH, Charles B. Higgins, MD.**
***UCSF, San Francisco, CA, USA.***

*Introduction:* Pulmonary regurgitation is one of the most important complications after surgical correction of tetralogy of Fallot and is one of the determinants of long term clinical outcome. Prior studies have used volumetric cine MR and phase-contrast cine MR to assess pulmonary regurgitation and right ventricular volumes and function in these patients. Traditionally, the major parameter used in evaluating right ventricular (RV) function has been ejection fraction. Pulmonary valve replacement has been shown to improve ventricular function in these patients as assessed by CMR. Consequently, it is important to determine the need for and timing of valve replacement.

*Purpose:* The purpose of this study was to assess the relationship between pulmonic regurgitation and right ventricular function using MRI volumetric and functional measurements in order to provide an indication for valve replacement. A secondary goal was to assess the relationship between MRI volumetric parameters and RV function and also to compare parameters of RV function between patients and normal volunteers.

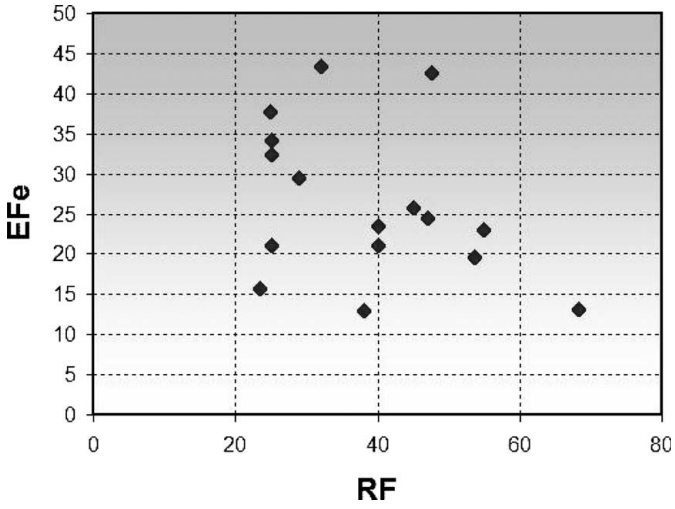


FIG. 1. Correlation between effective RVEF (EFe) and PRF (RF).

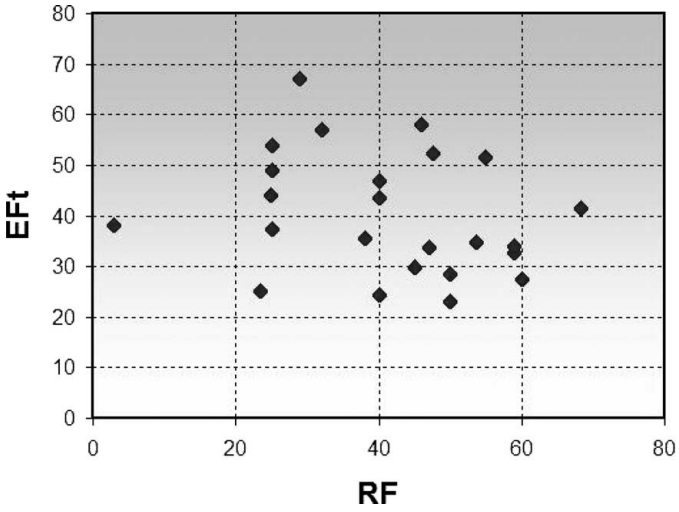


FIG. 2. Correlation between total RVEF (EFt) and PRF (RF).

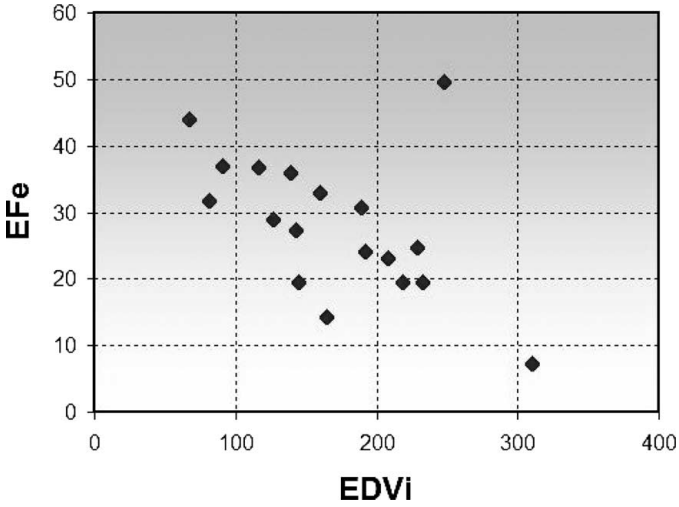


FIG. 3. Correlation between effective RVEF (EFe) and EDVi.

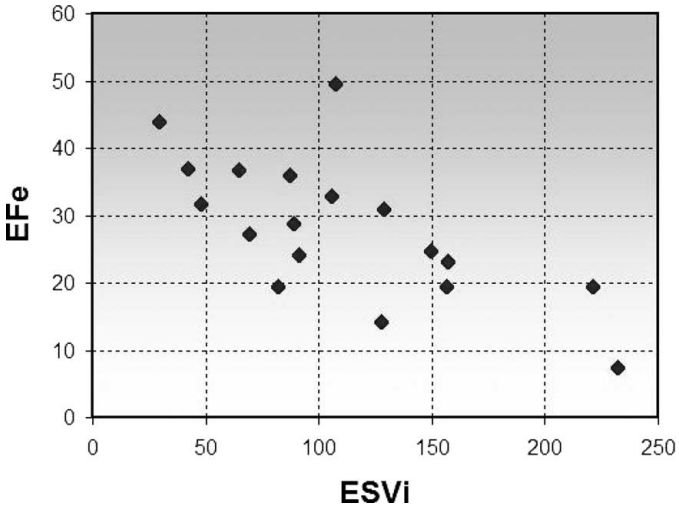


FIG. 4. Correlation between effective RVEF (EFe) and RVESVi.

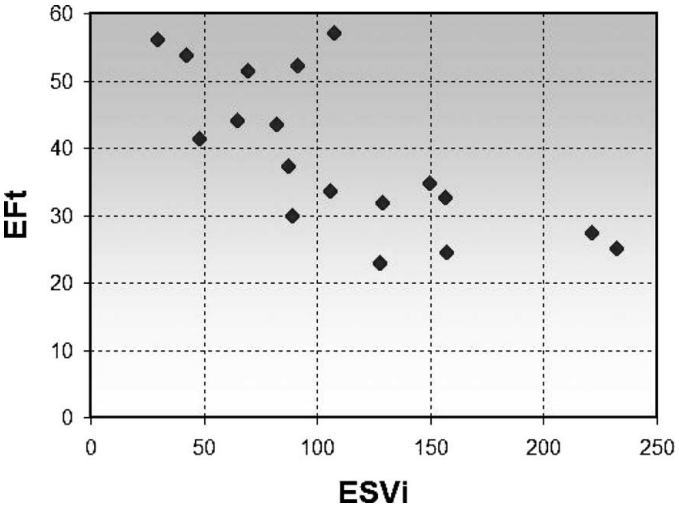


FIG. 5. Correlation between total RVEF (EFt) and RVESVi.

*Patients and methods:* Twenty-seven patients with corrected tetralogy of Fallot and pulmonary regurgitation underwent MRI studies. Cine MRI images in the short-axis plane were obtained. Pulmonary regurgitant fraction (PRF), RV end-diastolic volume (RVEDV), RV end-systolic volume (RVESV), RV stroke volume (RVSV) and RV ejection fraction (total RVEF) were calculated. In the presence of regurgitation, the use of ejection fraction to assess ventricular function is complicated by the fact that much of the stroke volume is related to regurgitant volume. As an alternative, we assessed the effective (forward) RVEF, calculated by dividing the difference between right ventricular stroke volume and pulmonary regurgitant volume by the right ventricular end-diastolic volume (RVSV- pulmonary regurgitant volume/RVEDV). End-diastolic volume and end-systolic volume indexes (EDVi, ESVi) were calculated based on the body surface area. MRI studies to calculate total RVEF and effective RVEF were also performed in 10 normal volunteers. Pearson's correlation test was used to measure the correlation of total RVEF and effective RVEF with PRF as well as with the volumetric parameters. A multivariate regression model was fitted to evaluate the determinants of total and effective RVEF. ANOVA was used to compare means of total and effective RVEF in patients and normal volunteers.

*Results:* An inverse correlation between PRF and effective RVEF ($r = -0.53$; $p = 0.03$) (Fig. 1) was detected, but not between PRF and total RVEF ($r = -0.25$; $p = 0.23$) (Fig. 2). Also found was an inverse correlation between effective RVEF and RVEDVi ($r = -0.5$; $p = 0.03$) (Fig. 3) and between effective RVEF and RVESVi ($r = -0.68$; $p = 0.002$) (Fig. 4). Only RVESVi showed a correlation with total RVEF ($r = 0.72$;$p = 0.001$) (Fig. 5). PRF, RVEDVi and RVESVi were considered independent determinants of effective RVEF, but just the volumetric parameters determined total RVEF. Mean effective RVEF was significantly higher in normal volunteers (48%) than in patients (25%) ($p < 0.001$). However, mean total RVEF was not significantly different between normal volunteers (48%) and patients (40%) ($p = 0.051$).

*Conclusions:* Effective RVEF was a better parameter than total RVEF for evaluating RV function. Calculation of total RVEF in patients with pulmonary regurgitation is probably not useful because of the confounding effect of obligatory pulmonary regurgitant volume. PRF and RVESVi were the best independent predictors of decresed RV function.

## 459. A HEAD TO HEAD COMPARISON BETWEEN CONTRAST TRANSTHORACIC TRIPLANE-ECHOCARDIOGRAPHY AND MAGNETIC RESONANCE IMAGING FOR DETERMINATION OF LEFT VENTRICULAR MASS

**Karol Miszalski-Jamka, MD, Giso von der Recke, MD, Christoph Hammerstingl, MD, David Hardung, MD, Jan Schnapauff, Bernhard Saxler, Harald Schmidt, MD, Heyder Omran, MD, PhD.** ***St.-Marien-Hospital, Bonn, Germany.***

*Introduction:* Left ventricular mass (LVM) is an independent predictor of morbidity and mortality in cardiac patients. The accuracy and reproducibility of cardiac magnetic resonance (CMR) LVM measurements has been proved in many studies. Yet, the availability of CMR is still limited. On the contrary, standard echocardiography is the imaging modality most commonly used for LVM measurement but it is based on geometrical assumptions.

*Purpose:* To compare a novel triplane-echocardiography with and without intravenous contrast injection to standard clinical two-dimensional echocardiography and CMR for determination of LVM in humans.

*Methods:* Echocardiographic imaging was performed in 85 consecutive patients referred for CMR. Digital standard parasternal, apical views and triplane apical views by means of the new triplane-transducer (GE, USA) before and after intravenous contrast injection were acquired by an experienced observer. Meticulous care was taken to avoid foreshortening. Endocardial and epicardial boundaries were traced off-line and mass was calculated by use of the area length technique, biplane method of discs and software provided by the triplane-transducer's producer. CMR multiple (10–12) short axis sections of left ventricle were performed using TurboFlash sequence with a 1.5T scanner by an independent blinded experienced observer. LVM was calculated offline by the method of discs.

*Results:* All echocardiographic methods overestimated LVM versus CMR. Bland-Altman analysis revealed clinically insignificant bias in differences between biplane method of discs, triplane-method without and with contrast agent (bias: 16.5 g; 15.8 g and 9.2 g; respectively). The area-length method was much less accurate (bias 49, 3 g). The 95% limits of agreement were the smallest for both triplane-methods and narrowed after contrast injection (area-length method: from −32.9 g to 131.5 g;

biplane method of discs: from −26.9 g to 59.9 g; triplane-method: from −14.1 g to 45.7 g; triplane-method with contrast: from −15.9 g to 34.3 g). Correlations between echocardiographic and CMR measurements were moderate for area-length method and biplane method of discs (0.63 and 0.69, respectively) but they were very good for both triplane-methods (without contrast 0.80; with contrast 0.85). In echocardiographic methods the image quality was sufficient in all but 5 patients but it was unsatisfactory in two-dimensional methods in 18/80 (22.5%) and in triplane-methods in 27/80 patients (33.7%), respectively. Image quality was sufficient in CMR for manual contour tracing in all patients.

*Conclusions:* Compared to standard techniques triplane-echocardiography significantly improves accuracy of LVM measurements and is more accurate when adding an intravenous contrast agent. Echocardiographic techniques have recently improved with new contrast agents and triplane-imaging method but are still inferior to CMR in the assessment of LVM.

## 460. LOCATION OF PORCINE CARDIAC AUTONOMIC NERVE PLEXI WITH FAT-SUPPRESSED MRI

**Ehud J. Schmidt,[1] Peter A. Noseworthy, MD,[2] J. A. Armour, MD,[3] Zachary Malchano, MS,[2] Vivek Y. Reddy, MD.[2]** ***[1]GE Medical Systems ASL East, Newton, MA, USA, [2]Cardiology, Massachusetts General Hospital, Boston, MA, USA, [3]Pharmacology, University of Montreal, Montreal, PQ, Canada.***

*Introduction:* Autonomic nerve plexi are thought to be important for the initiation and maintenance of atrial fibrillation and may represent novel targets for ablation (1). Current techniques to localize the nerves bundles *in-vivo* use surrogate markers such as bradycardic response to electrical stimulation.

*Purpose:* Develop an MRI technique to localize cardiac nerve ganglia (NG), with emphasis on ganglia surrounding the atria. NG position could eventually be superimposed on anatomic maps of the atria, and serve as roadmaps for guided navigational ablation.

*Methods:* Explanted porcine heart bases were imaged using a high spatial resolution (1.4 mm slice, 0.5 mm in-plane resolution) fat-suppressed T1-weighted 3D gradient-echo MRI sequence (n = 5). Putative NG were identified as small (0.5 mm) circular hyper-intense structures, interconnected by linear structures, on a dark background within several fat pads. Regions containing NG were then cut into thin section (n = 2) and independently examined by a pathologist. NG were identified and counted under a dissection microscope and correlated to the MRI findings. 3D reconstructions of the aortic root, atrial structures, and autonomic ganglia were created to depict the relationships of these ganglia to surrounding structures.

*Results:* Regions identified in MRI were confirmed to contain autonomic nerve ganglia (Fig. 1A, sites i-iii), which visually resemble (Fig. 1C) branches and fruits of "cherry tomatoes". These sites were concentrated in fat pads at the base of the aortic root and at the origin of the pulmonary artery. The porcine NG locations were similar to those anatomically described (2). The porcine NG are similar in size to those found in humans (3). Further preliminary data (n = 1) suggests that the porcine ganglia may be observed *in vivo* using 1.4–1.6 mm slice-width respiratory-motion-navigated- and cardiac-gated fat-suppressed 3D- gradient-echo scans.

*Conclusion:* This study demonstrates the ability of MRI to identify the shape and position of cardiac nerve ganglia in the

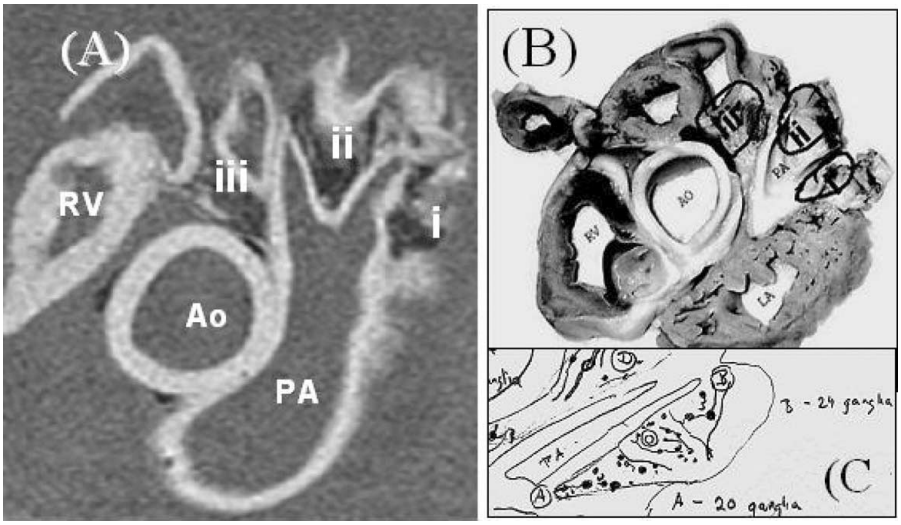


FIG. 1. Explanted porcine heart, imaged at the level of the roof of the left atrium. (A) 1.4 mm slice fat-suppressed 3D T1-weighted MRI slice. (B) 5 mm cut from the heart, sliced at the same level as (A), showing the physical appearance of the region. (C) Histological drawing of zone i of (A) and (B), showing the actual shape of the NG. "Cherry-tomato" shaped (small bright dots interconnected by straight lines) hyper-intensities (A) were identified within the fat pads (i,ii,iii). All fat-pads were confirmed by histology to contain multiple nerve ganglia.

explanted porcine heart. Further investigation is required to determine the repeatability of the technique in living subjects, including in non-intubated, free-breathing, humans. MRI mapping of the NG could potentially shorten and enhance the efficacy of atrial catheter ablation procedures.

## REFERENCES

1. Nakagawa H, et al. Circulation 2004;110;7, III-543.
2. Armour JA, et al. Anatomic Record 2003;271A:249–58.
3. Armour JA, et al. Anatomic Record 1997;247:289–298.

## 461. CAROTID ARTERY PULSE WAVE VELOCITY MEASUREMENT BY CARDIOVASCULAR MAGNETIC RESONANCE

**Niall Keenan, MB BCh MRCP, Peter Gatehouse, PhD, Raad H. Mohiaddin, MD PhD, David Firmin, PhD, Dudley J. Pennell, MD FACC.** ***Royal Brompton Hospital, London, United Kingdom.***

*Introduction:* Pulse wave velocity (PWV) is the rate at which a pressure and flow wave moves along a blood vessel. PWV has not previously been measured in the carotid artery by cardiovascular magnetic resonance (CMR). Arterial stiffness increases with age and disease such as atherosclerosis (1, 2). PWV can be measured non-invasively by aplanation tomometry, ultrasound and more recently by CMR. CMR has several advantages over ultrasound in that full 3D visualisation of the vessel is possible enabling the imaging plane to placed perpendicular to the vessel in a reproducible location. Velocity data can be acquired virtually simultaneously in two imaging planes and the path length (distance between the two imaging planes) can be measured precisely. CMR has previously been limited by poor temporal resolution which is a crucial factor, given the short path length involved. However we have developed a new interleaved sequence using maximal gradient and RF performance which has enabled us to reach a temporal resolution of 3.8 ms.

*Method:* We recruited 7 healthy volunteers (3 female, 4 male, age range 28–35). We performed CMR imaging of the carotid arteries using a Siemens Sonata 1.5-T scanner with purpose-built two element phased-array surface coils. Non-segmented through-plane phase velocity mapping (at 85 cm/s VENC) was applied to two planes transecting the common carotid and the internal carotid arteries (Fig. 1). We aimed to maximise path length while keeping both planes within the area of optimal coil response. In the first three subjects we used geometric transverse planes; subsequently we imaged each side separately using planes perpendicular to the vessel to maximise through plane velocity. Data acquisition for the two slices was interleaved for 80 cine frames per slice within each cardiac cycle, and repeated with velocity encoding on the subsequent cycle. Velocity images were reconstructed by subtraction of the phase images, with a further subtraction of background velocity errors (measured by imaging the same planes in a stationary phantom). Using maximum gradient and RF performance, and inverting the slice-selection gradient for velocity-encoding, TR 1.9 ms was achieved, giving TR 3.8 ms for each imaging plane. Voxel size was FE 1.8 mm by PE 2.4 mm by SLT 8 mm, echo time 1.1 ms and flip angle 15°. The mean arterial velocity for each phase was calculated. Mean velocities were plotted against time (Fig. 2). A best fit straight line was fitted to the velocity points between 25% and 75% of the maximum. The pulse arrival time was defined as the point where a line drawn back from these two points intersected with

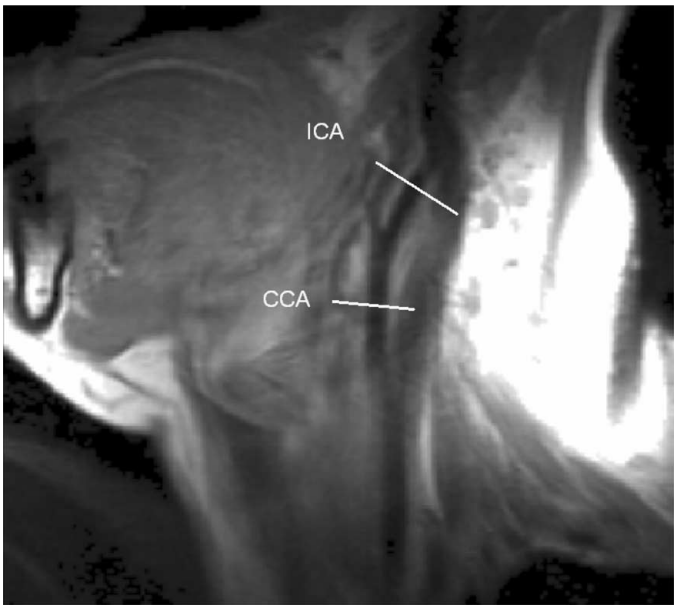


FIG. 1. T1-weighted turbo spin echo image of the carotid bifurcation showing two imaging planes transecting the common carotid (CCA) and internal carotid (ICA) arteries.

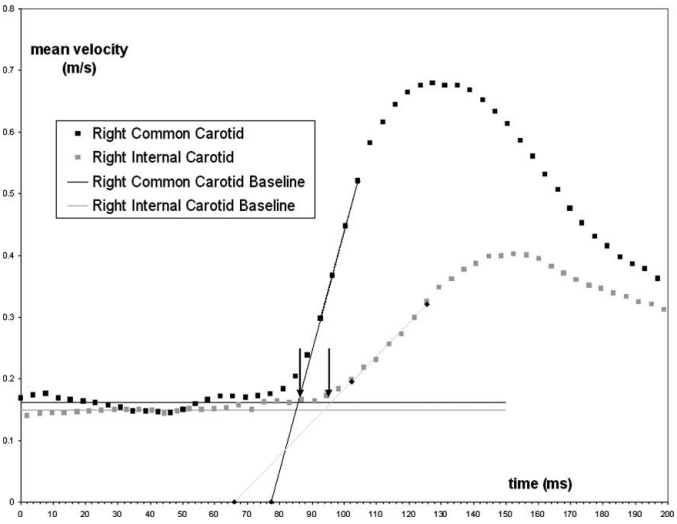


FIG. 2. Pulse waves sampled at common and internal carotid arteries. Black arrows indicate intercept points of tangent to curve with baseline. Delay time is the difference between two arrows.

the baseline. The pulse arrival time was determined for both planes. PWV was calculated from the path length divided by the difference in arrival times (PWV = distance/ time). To determine intra-scan reproducibility, data was acquired twice for each vessel.

*Results:* Mean PWV was 5.1 m/s with a range of 3.3 to 8.5 m/s. A Chronbach alpha value for intra-scan reproducibility was 0.77. This suggests a high degree of consistency between the image acquisitions. The mean path length was 54 mm (range 39–60 mm).

*Conclusion:* We have demonstrated in this preliminary study that PWV can be measured in the carotid arteries by CMR over very short path lengths. Intra-study reproducibility is good. The wide range of PWVs found requires further investigation and explanation. This may be physiological; however a major source of error is in determining the pulse arrival time from the velocity-time curves, and other methods such as peak-second-derivative are being investigated.

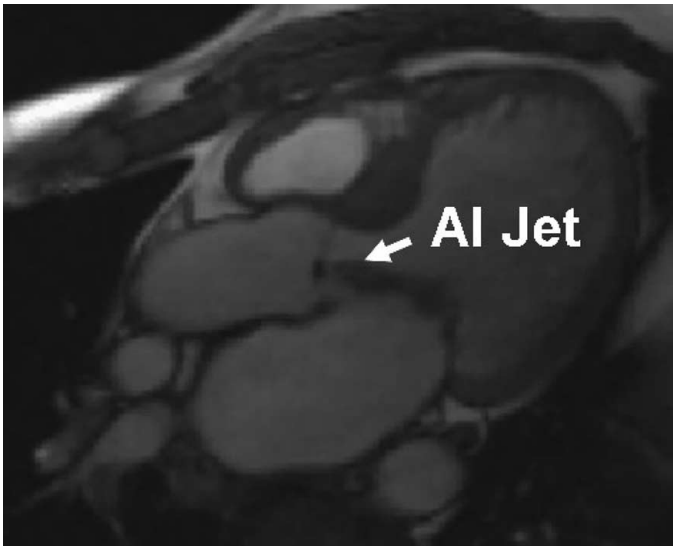


FIG. 1.

## REFERENCES

1. Lehmann E. Clinical value of aortic pulse-wave velocity measurement. Lancet 1999;354:528–529.
2. Mohiaddin RH. Assessment of the mechanical properties of the arterial wall. In: Cardiovascular MR (Manning W and Pennell DJ eds. Churchill Livingstone 2001;272–279.

## 462. THE EFFECT OF BACKGROUND VELOCITY ERROR IN THE PHASE CONTRAST MRI MEASUREMENT OF FLOW: PROPAGATION-OF-ERROR THEORY APPLIED TO REGURGITANT VALVULAR DISEASE

**Steven G. Lloyd, MD, PhD, Himanshu Gupta, MD.** ***University of Alabama at Birmingham, Birmingham, AL, USA.***

*Background:* The severity of valvular regurgitation may be graded by regurgitant volume $V_{reg}$ or regurgitant fraction RF, where $RF = V_{reg}/V_{for}$, with $V_{for}$ the forward stroke volume. Flow-based methods for measuring $V_{reg}$ and RF such as phase-contrast MRI (PC-MRI) are attractive for this purpose. However, PC-MRI suffers from stationary offsets due to nonzero background velocity $v_{BG}$. The magnitude of $v_{BG}$ depends on the scan plane and spatial position; the errors $v_{BG}$ are commonly $\pm$ 2 cm/s and may reach $\pm$ 4 to 6 cm/s (1). $v_{BG}$ is usually small compared to the dynamic range $v_{enc}$, so has a negligible effect on the measured systolic blood flow velocities. However, a small error (even $\pm$ 1 to 2 cm/s) has a large impact on the calculation of $V_{reg}$ or RF (2). The impact of this on $V_{reg}$ and RF has not been analyzed. Thus, we performed a theoretical propagation-of-error analysis of the impact of $v_{BG}$ on $V_{reg}$ and RF.

*Methods and calculations:* The error in $RF = (E_1^2 + E_2^2)^{1/2}$ with $E_1 = (\partial RF/\partial V_{for})\Delta V_{for} = -(V_{reg}/V_{for}^2)\Delta V_{for}$ and $E_2 = (\partial RF/\partial V_{reg})\Delta V_{reg} = \Delta V_{reg}/V_{for}$ (Eq. 1), where $\Delta V_{for}$ and $\Delta V_{reg}$ are the measurement errors in $V_{for}$ and $V_{reg}$.

*Results:* The total errors are: $\Delta V_{reg} = v_{BG}\, T_D$ ; $\Delta RF = (v_{BG}/[v_{for}]_{mean})(T_D/T_S)(1 + RF^2)^{1/2}$ (Eq. 2) with $[v_{for}]_{mean}$ the time-averaged mean measured systolic flow velocity in the ROI and $T_D$ and $T_S$ the diastolic and systolic durations. $\Delta V_{reg}$ is increased with slow heart rates (HR), while HR has a lesser effect on $\Delta RF$.The measured estimate of RF has minimal effect on $\Delta RF$ and is neglected. With typical values for $[v_{for}]_{mean}$ ($\approx$25 cm/s), and with the ratio $T_D/T_S \approx 2$, $\Delta RF$ is $\pm$ 16% for the realistic value $v_{BG} = 2$ cm/s and $\pm$ 8% for the very small value $v_{BG} =$ 1 cm/s. Long axis MRI (diastolic frame) of a patient with qualitatively moderate to severe aortic insufficiency (AI) is shown in Fig. 1. The impact of $v_{BG}$ on the measured $V_{for}$ and $V_{reg}$ in this

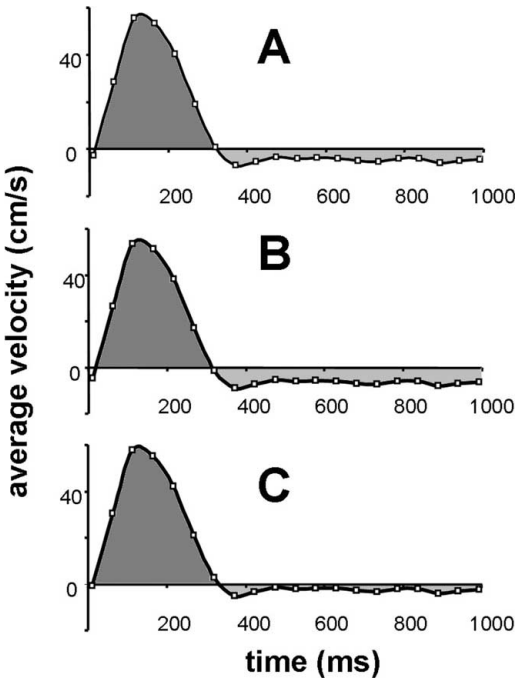


FIG. 2.

patient is shown in Fig. 2, which depicts the aortic flow velocity data. The raw measured data (Fig. 2A) yielded $V_{reg} = 28$ mL and RF = 32%, consistent with moderate AI. To illustrate the impact of $v_{BG}$ on $V_{reg}$ and RF, a shift in the position of the zero-velocity $v_{BG} = \pm 2$ cm/s was considered. This results in $V_{reg} = 40$ ml and RF = 49% (for $v_{BG} = 2$ cm/s in the direction of systolic flow, Fig. 2B) to $V_{reg} = 16$ mL and RF = 17% (for $v_{BG} = 2$ cm/s in the opposite direction, Fig. 2C). Despite a small assumed $v_{BG}$, its effect on the $\Delta$RF is severe (52% relative effect), with the resulting RF values being consistent with anywhere from mild (for $v_{BG} = 2$ cm/s opposite ascending aorta flow) to severe AI (for $v_{BG} = 2$ cm/s in the direction of systolic flow). The effect on $\Delta V_{reg}$ is less severe (43% relative effect) but still sizeable.

*Conclusions:* Small offset errors occur in PC-MRI measurement of velocity. Though the magnitude is small, it results in a large uncertainty in $V_{reg}$ and RF. $V_{reg}$ is somewhat less impacted by this, with better theoretical accuracy particularly at higher heart rates, and thus may be more reliable than RF in estimating severity of valvular regurgitation.

## REFERENCES

1. Lloyd SG, et al. Proc Intl Soc Mag Reson Med. 2005;13:1729.
2. Gatehouse PD, et al. Eur Radiol. Jul 8 2005; Epub ahead of print.

## 463. THE BIOMECHANICS OF PLAQUE RUPTURE IN CAROTID ATHEROMA: UTILITY OF *IN VIVO* HIGH RESOLUTION MRI

**Zhi-Yong Li, Jonathan Gillard.** ***University of Cambridge, Cambridge, United Kingdom.***

*Background:* Atheromatous carotid plaque rupture is responsible for the majority of ischemic strokes in the developed world. Plaque rupture has been associated with plaque morphology, plaque components' properties, inflammation and local stress concentration. Whilst the biological and biochemical processes within have been widely investigated, the biomechanics underlying plaque rupture is still not well understood. High resolution multi-spectral magnetic resonance imaging (MRI) has allowed these plaque components to be visualized in vivo. This study combines the recent advances in finite element analysis (FEA) and MRI, and performed stress analysis of ruptured and unruptured vulnerable carotid plaques based on the geometry derived from in vivo MRI.

*Methods and results:* Five symptomatic patients underwent high-resolution multi-sequence in vivo MR imaging of the carotid bifurcation. Each axial MR slice was segmented based on multi-spectral MRI and co-registered against histology for plaque characterisation. Contours of lipid core, fibrous cap, vessel lumen and wall were traced to generate boundaries for finite element analysis. Plaque fibrous cap, lipid pool and vessel wall were modelled as isotropic, incompressible hyperelastic materials performing large deformation under pulse pressure. High stress concentrations were predicted at the shoulders and the thinnest fibrous cap regions of the plaque, and maximal stresses were found to be higher in the ruptured plaques than in the unruptured plaques ($983.3 \pm 3.94$ versus $226.9 \pm 1.15$, $p < 0.01$). The effect of the relative stiffness of fibrous cap to lipid pool on stress within the cap itself was studied. It was shown that larger relative stiffness of fibrous cap to lipid pool resulted in higher stress within the cap.

*Conclusion:* It may be when local stresses exceed the strength limit of the plaque that leads to plaque rupture and acute ischaemic sequelae. A combination of in vivo high resolution MRI and FEA could potentially act as a useful tool to assess plaque vulnerability and risk stratify patients with carotid atheroma.

## 464. CENTRAL ARTERIAL STIFFNESS ASSESSED BY MRI OF THE FEMORAL ARTERY

**Harry A. Silber, MD, PhD, David A. Bluemke, MD, PhD, Pamela Ouyang, MD, Joao A. C. Lima, MD.** ***Johns Hopkins University School of Medicine, Baltimore, MD, USA.***

*Introduction:* Central arterial stiffness is a powerful predictor of atherosclerosis and cardiovascular events, and is associated with cardiovascular risk factors. One of the most important ways of measuring arterial stiffness is by measuring pulse wave velocity—pulse waves travel faster in stiffer vessels. Most MRI applications of pulse wave velocity to assess central arterial stiffness consist of measuring the difference in pulse wave arrival time between two sites in the aorta. However, the pulse wave arrives at the femoral artery just after traversing the central arteries, and the femoral artery is easily accessible by MRI. We hypothesized that central arterial stiffness could be assessed by imaging just one location in the femoral artery.

*Purpose:* To compare pulse wave arrival time at the femoral artery between two groups - one group with and the other group without cardiovascular risk factors.

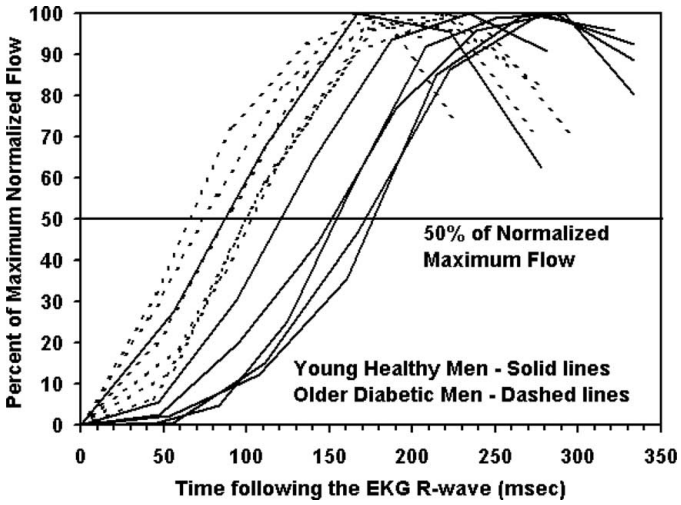


FIG. 1.

*Methods:* We studied 12 men - 6 men 40 years of age or younger, with no cardiovascular risk factors; and 6 men over 50 years of age with type 2 diabetes. A four-element phased-array receiver coil was placed above and below the thigh, and later a 3-inch coil was placed at the medial surface of the right upper arm. An ECG-gated, phase-contrast MR pulse sequence was used with the following parameters: Matrix size $256 \times 128$, field-of-view 10 by 10 cm for the femoral artery and 8 by 8 cm for the brachial artery, 16 signal averages (NEX), slice thickness 3 mm, flip angle 25 degrees, bandwidth 31.2 kHz, repetition time (TR) 11.43 msec, echo time (TE) 5.25 msec, 8 views per segment, first order flow compensation, no phase-wrap, and no magnitude weighting. View-sharing was used to obtain 20 images per cardiac cycle. A user-independent algorithm was used to calculate instantaneous flow in the cross-section. Arrival time in an artery was calculated as the elapsed time after the R-wave trigger that it took for the instantaneous flow in the cross-section to reach 50% of its peak systolic value. The arrival time was normalized to path length by dividing by a normalized height ratio: the subject's height divided by 72 inches. The one-location method of assessing stiffness at the femoral artery was compared with a two-location method commonly used with tonometry - the difference between arrival times in the brachial and femoral arteries was also calculated for each subject. The difference was then normalized to path length by dividing by the normalized height ratio.

*Results:* Heart rate and height were not different between the two groups. Pulse wave arrival time was shorter in the older diabetic men compared with the young healthy men, whether measured in the femoral artery alone ($88 \pm 15$ vs.$146 \pm 33$ msec, $p = .003$), or by the difference in arrival times between the femoral and brachial arteries ($36 \pm 21$ vs. $89 \pm 37$ msec, $p = .008$). Pulse arrival time assessed at the brachial artery alone did not differ between older diabetic men and young healthy men ($52 \pm 18$ vs. $56 \pm 10$ msec, $p = .37$).

*Conclusions:* Pulse wave arrival time at the femoral artery was shorter in older diabetic men than young healthy men, indicating stiffer central arteries. Using a single femoral site provided the same information as the more commonly used tonometric technique measuring the difference in arrival times between the femoral and brachial arteries. However, using a single accessible artery significantly simplifies the technique. Femoral artery MRI may be a novel and useful technique to measure central arterial stiffness.

## 465. SINGLE BREATH-HOLD 3D EVALUATION OF LEFT VENTRICULAR FUNCTION AT 1.5 AND 3T

**Brett R. Cowan, BE MbCHb,[1] Alistair A. Young, BE ME PhD,[1] Berndt J. Wintersperger,[2] M F. Reiser,[2] K Sprung,[2] Ben Wen,[1] S O. Schoenburg[2]. [1]*University of Auckland, Auckland, New Zealand,* [2]*Klinikum der Universitat Munchen-Grosshadern, Munchen, Germany.***

*Introduction:* Approaches such as TSENSE (1) can accelerate cardiac studies by acquiring multiple slices within a single breath-hold. This study sought to compare left ventricular volumetric, mass and ejection fraction results at 1.5 and 3T, both with and without TSENSE acceleration. It was hypothesized that analysis of single breath-hold TSENSE studies with reduced slices using 3D software would provide accurate functional information.

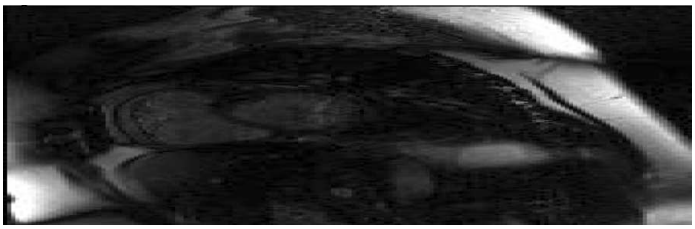

(a)

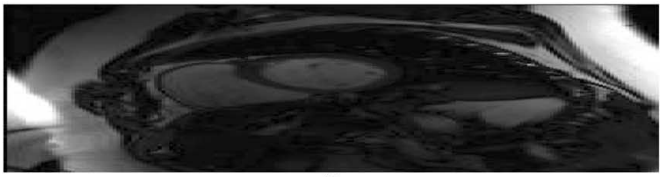

(b)

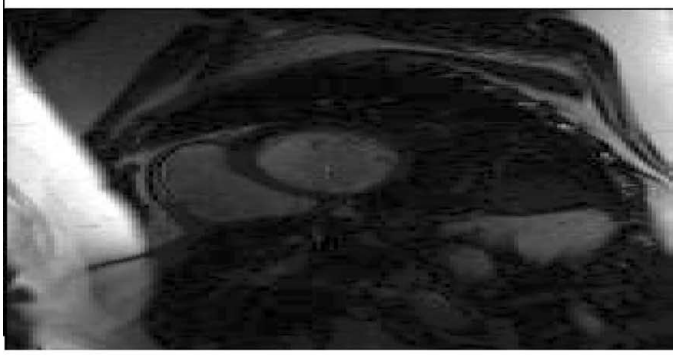

(c)

(d)

FIG. 1. Typical short axis images from the same subject (a) 1.5T TSENSE, (b) 3T standard, (c) 3T TSENSE and (d) 3D CIM model of the endocardial and epicardial surfaces.

TABLE 1
Functional parameters for each method

| | EDV (mL) | ESV (mL) | SV (mL) | EF (%) | LVM (g) | Epi ED (mL) | Epi ES (mL) |
|---|---|---|---|---|---|---|---|
| 1.5T Standard | 155.9 | 71.7 | 84.1 | 55.0 | 137.4 | 287.3 | 203.9 |
| 1.5T TSENSE | 146.0* | 71.5 | 74.4* | 51.7 | 158.5+ | 298.8 | 224.6+ |
| 3.0T Standard | 166.6 | 75.4 | 91.2 | 55.5 | 155.7* | 316.1* | 224.1* |
| 3.0T TSENSE | 159.7 | 75.6 | 84.0 | 53.1 | 161.8+ | 314.2* | 232.2+ |

EDV = end-diastolic volume, ESV = end-systolic volume, SV = stroke volume, EF = ejection fraction, LVM = left ventricular mass, Epi ED = volume of the epicardium at end-diastole, and Epi ES = volume of epicardium at end-systole. Statistically significant differences from the 1.5T gold standard shown as $^{*}p < 0.05$ and $^{+}p < 0.01$.

*Purpose:* To report the differences in left ventricular mass (LVM), volumes (EDV, ESV and SV) and ejection fraction (EF) between i) standard cine acquisitions at 1.5 and 3T and ii) single breath-hold TSENSE acquisitions at 1.5 and 3T with reduced slices and 3D modeling.

*Methods:* Ten individuals (8 male, 28–63 years, mean 49), comprising 9 patients with a history of myocardial infarction and one healthy volunteer, were recruited and imaged on a 1.5T Avanto and 3T Trio with Tim (Total Imaging Matrix) technology (Siemens, Erlangen). Written informed consent was obtained from all subjects and the regulatory authorities approved the study protocol. Standard SSFP (true-FISP) cine acquisitions were obtained in 1 long and 10 short axis slices. TSENSE scans acquired 2 long and 4 short axis slices within a single breath-hold using an acceleration factor of $R = 4$. Typical 3T parameters were TR/TE/FOV 51.7 ms/1.52 ms/360 mm and 1.5T 42.3 ms/1.42 ms/360 mm (Fig. 1). All 40 studies were blinded randomly and analyzed by a single observer blinded using guidepoint modeling (CIM version 4.6). This calculates a moving curved surface representing the endocardial and epicardial boarders of the left ventricle and is able to fully correct for through plane motion of the mitral valve (2). All volumes were calculated by numerical integration of these surfaces and were therefore not dependent on the limitations of slice summation. LVM was calculated for every phase and then averaged. In order to determine intra-observer reproducibility all studies were re-randomized and re-analyzed by the same observer. The standard acquisition at 1.5T was considered to be the gold standard for the purposes of comparison.

*Results:* (a) LV functional parameters—Table 1 shows the results for each of the methods. Endocardial volumes (EDV, ESV, SV, EF) were mainly not significantly different from the gold standard, due to the excellent blood to myocardial contrast produced by SSFP sequences. However, with TSENSE and standard acquisition at 3T, LVM was overestimated, due primarily to the increased volume of the epicardial contour (shown in the table at ED and ES). (b) Reproducibility - there were no significant differences between the first and second analyses in any of the parameters for any of the acquisitions (all $p > 0.33$).

*Conclusion:* Lower SNR, reduced slice data sets acquired in a single breath-hold with TSENSE at 1.5 and 3T produced accurate estimates of left ventricular endocardial volumes (EDV, ESV, SV and EF) when analyzed with the 3D CIM software. Epicardial TSENSE contours were more difficult to place accurately due to reduced SNR and image quality, resulting in an overestimation of LVM. Further work is required to determine the reason for epicardial volume overestimation using standard acquisitions at 3T.

## REFERENCES

1. Kellman P, et al. MRM 2001;45:846–52.
2. Young AA, et al. Radiology 2000;216:597–602.

## 466. A STUDY OF POSSIBLE INVERSION-RECOVERY ARTEFACTS IN "LATE-GD" MYOCARDIAL CONTRAST ENHANCEMENT IMAGING

**Peter Gatehouse, Saed O. Al-Shalabi, David Firmin.** ***Royal Brompton Hospital, London, United Kingdom.***

*Aim:* To examine whether artefacts at the subendocardial border could arise from the continuing magnetisation recovery during the segmented acquisition.

*Introduction:* "Late-Gad" (late-enhancement, viability, MCE ...) imaging usually employs inversion-recovery with segmented imaging over several cardiac cycles. The inversion-recovery delay (TI) is adjusted so that normal myocardium with typical CA-concentrations is "nulled", so that infarcts which contain higher [Gd] have strong image contrast to normal myocardium (1). The "null" occurs as myocardial magnetisation recovers through zero at the time of ky = 0 acquisition. In cases where a thin or obscure subendocardial abnormality is seen, the slice is often re-acquired for confirmation, with "swapped" phase-encode direction. This abstract investigates the consequences of the continuing magnetization recovery during the segmented data acquisition, which causes a changing signal strength from the first to the last segment acquired, leading to artefacts along the phase-encode direction.

*Method:* We studied alternate cardiac-cycle inversion-recovery segmented-FLASH (1) (non-sel IR, IR delay, then 23 segments at TR 6ms, FA 20, BW 230Hz/pixel). The point-spread-functions (PSFs) along the phase-encode direction were

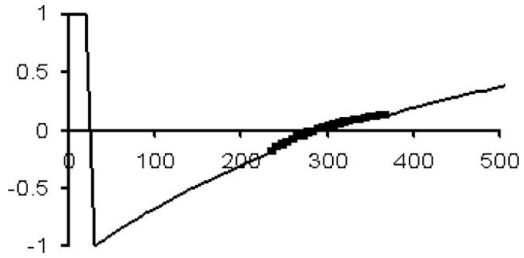


FIG. 1. Mz variation after inversion and during segmented acquisition (points).

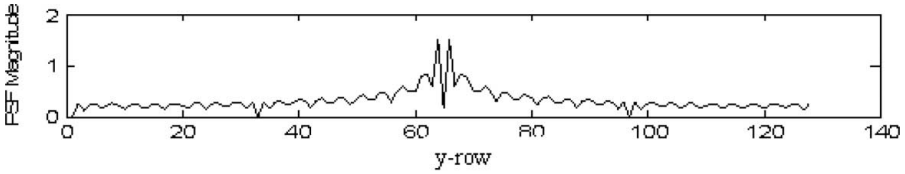


(a)

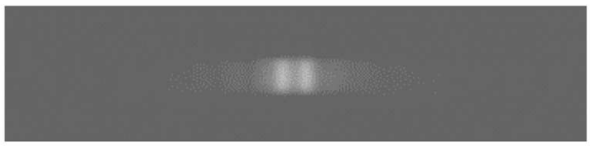

(b)

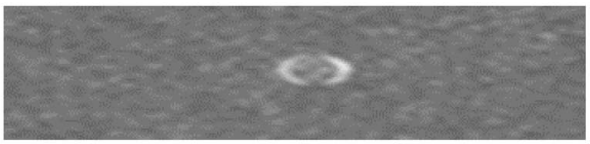

(c)

FIG. 2. (a) PSF simulation. (b) PSF along image phase-encode direction (horizontal). (c) Effect of phase-encode PSF on nulled small circle of normal myocardium.

calculated for T1 values 240, 320, 400 ms, modeling infarct, blood and normal myocardium 10–20 mins after 0.1 mmol/kg Gd-DTPA injection, using inversion-recovery TI delays nulling normal myocardium (≈290 ms). The calculation modeled Mz-recovery including the saturating effect of segmented-FLASH, and took the Mxy amplitudes and phases as input to a 1D-FFT. The 1D-FFT output represented the phase-encode PSF magnitude and phase. The phase-encode distortion was imaged using 1 cm diameter diluted Gd-DTPA cylindrical phantoms, with the phase-encoding gradient switched off, with T1s and TI as above. Images with the phase-encode gradient on were obtained for comparison. The simulations and images were repeated without inversion, to separate Gibbs artifact from recovery-related artifact.

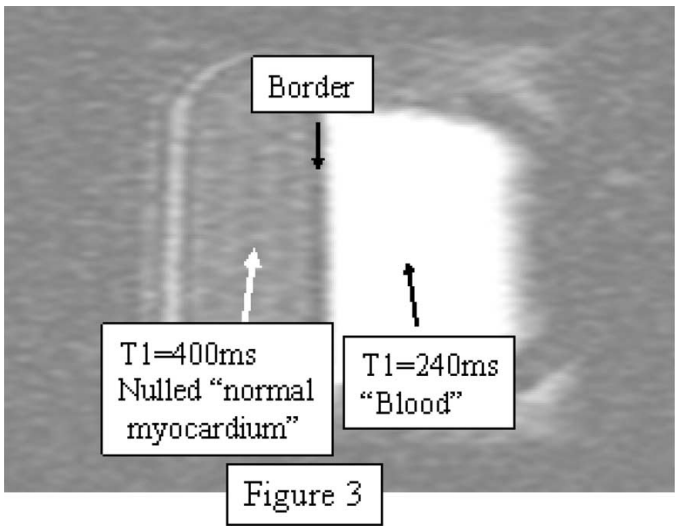


FIG. 3.

A model of the normal myocardium-blood border was imaged, using the T1 = 400 ms and T1 = 240 ms Gd mixtures separated by thin plastic film perpendicular to the slice. Short-axis and long-axis late-enhancement patient images were reviewed for artifacts at the subendocardial border.

*Results and Discussion:* Fig. 1 shows the magnetization of normal myocardium in each cycle when "nulled" by TI adjustment (assuming full recovery between alternate cycles). The zero-crossing "split" the phase-encode PSF in simulations (Fig. 2A), in PSF imaging (B) and appears PE-convolved with the small circular tube in (C). The split peaks' opposing phases may have complex effects at tissue borders. Although the PSF has small amplitude at the null time, larger PSF amplitude with some broadening occurred at ±30 ms. In the endocardial border model (Fig. 3) the PSF distortion was concealed by other artifacts (Gibbs, partial volume) at the endocardial border. A thin bright line due to the PSF distortion occurs at the left "epicardial" edge. In patient images, no examples were found, whereas ringing effects occurred across the endocardial border due to Gibbs artifact and probably also myocardial motion (2). Signal amplitude variation during the segmented readout crossing zero from "nulled" tissue is the principal cause of PSF distortion, and it is weak compared to the bright infarct. The effect may be stronger in high-dose 0.2 mmol/kg and also in blood-suppressed late-enhancement techniques (3).

*Conclusion:* Zero-crossing magnetization recovery during IR-segmented FLASH causes phase-encode distortion, but is insignificant in-vivo, probably concealed by low SNR and artifacts such as R-R variations, Gibbs, motion and partial-volume effects.

## REFERENCES

1. Simonetti OP, et al. Radiol 2001;218:215–23.
2. Storey P, et al. MRMed 2002;48:1028–36.
3. Foo TK, et al. MRMed 2005;53:1484–9.


## 467. MODEL-BASED GRAPH CUT METHOD FOR SEGMENTATION OF THE LEFT VENTRICLE


**Xiang Lin, BSc, Brett R. Cowan, BE MbCHb, Alistair A. Young, BE ME PhD.** ***University of Auckland, Auckland, New Zealand.***


*Introduction:* Model-based cardiac image analysis methods are useful for fast, accurate analysis of cardiac function (1). However, many methods optimize a cost function using local gradient-based minimization procedures, which are sensitive to the initial location of the model (2). Graph cut methods have been widely used in image segmentation due to their ability to compute globally optimal solutions. However, they can be applied only to a limited set of energy functions (3), commonly including boundary and regional terms. It has been difficult to include high level information into the graph cut formulation. We propose a method for integrating model-based a priori information into the graph cut formulation.

*Purpose:* i) To incorporate high-level information to guide the graph cut process, thereby producing a model-based globally optimal segmentation. ii) To validate this method against standard techniques.

*Methods:* A 4D model prior of the left ventricle was calculated from an average of historically analyzed cases, and then scaled and rotated to fit the given case. A 2D spatial prior was calculated for each image by intersecting the model with each image plane. The spatial prior was then combined with pixel intensity and edge information in the graph cut optimization. Both epicardial and endocardial contours could be found using variations of this procedure. The proposed method was applied to 17 cases, 11 normal cases and 6 cases from patients with heart disease. Each case used true FISP cine imaging, had at least 6 short axis slices, and 28 phases on average.

*Results:* Fig. 1 show the algorithm for segmentation of the blood pool, and Fig. 2 shows the algorithm for segmentation of the epicardial surface. In all cases the algorithm provided a good initial approximation, with an average Hausdorff distance of 4 pixels between automatic contours and guide-point modelling contours.

*Conclusion:* The method demonstrates the ability of the graph cut to provide a global optimum for the entire image, while incorporating high-level spatial prior information. This feature is particularly important when the low-level information is unable to determine the correct segmentation, for example, in distinguishing between the RV myocardium and the LV myocardium.


## REFERENCES

1. Young A, Cowan B, Thrupp S, Hedley W, Dell'Italia L. Left Ventricular Mass and Volume: Fast Calculation with Guide-Point Modeling on MR Images. Radiology, 2000;216:597–602.
2. Frangi A, Niessen W, Viergever M. Three-dimensional modeling for functional analysis of cardiac images: A review. IEEE Transactions on Medical Imaging. 2001;1:2–25.
3. Kolmogorov V. Graph Based Algorithms for Scene Reconstruction from Two or More Views, PHD Thesis, Cornell University, 2004.


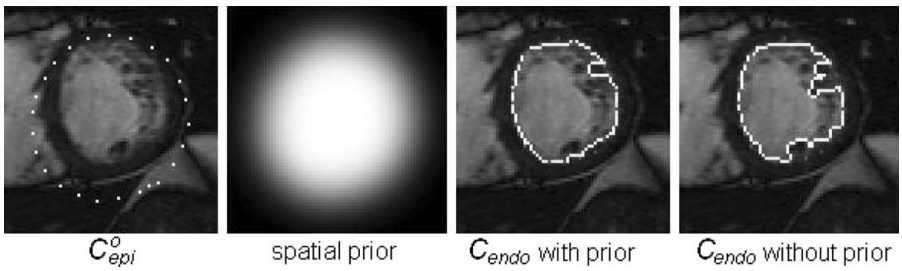


FIG. 1.

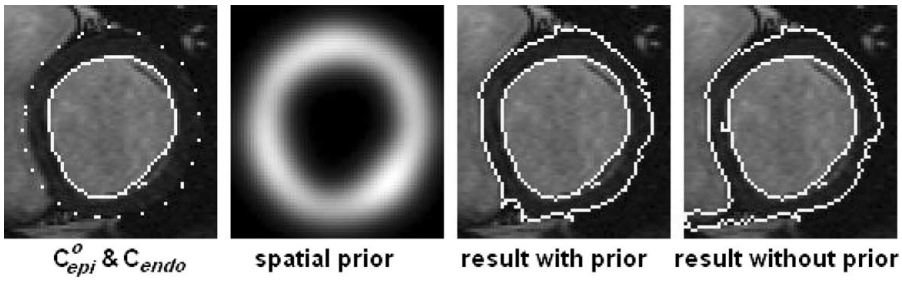


FIG. 2.

## 468. FIRST-PASS MRI PERFUSION AND DELAYED IMAGING CAN BOTH PROVIDE ACCURATE CHARACTERIZATION OF CORONARY MICROVASCULAR OBSTRUCTION IN ACUTE MYOCARDIAL INFARCTION

**Andrew Yan, MD,[1] Eric Larose, MD,[1] Carmen Chan, MBBS,[1] Adolphe Shayne, MD,[1] Tuan Luu,[1] H. Glenn Reynolds, MSc,[2] Raymond Y. Kwong, MD.[1]** [1]***Brigham and Women's Hospital, Boston, MA, USA,*** [2]***General Electric Healthcare, Boston, MA, USA.***

*Background:* Microvascular obstruction (MO) portends adverse ventricular remodeling and patient outcome after acute myocardial infarction (AMI) despite patency of the infarct-related artery. We assessed whether first-pass MRI perfusion and delayed imaging can characterize angiographic quantitation of MO in the infarct-related artery, and examined their respective relationship with post-infarct prognostic markers.

*Methods:* We performed cardiac MRI in 25 consecutive patients (84% men, age 58 $\pm$ 10) in the initial 72 hours of a first reperfused AMI. Patients with previous bypass surgery or hemodynamic instability were excluded. We estimated the severity of MO by the myocardial extents of the first-pass perfusion defect (%PD) and of the hypoenhanced core region within delayed enhancement (%$MDE_{core}$) using an automated algorithm. We adjusted %PD and %$MDE_{core}$ to the myocardial mass subtended by the infarct-related artery. %PD, %$MDE_{core}$, and corrected TIMI frame count of the revascularized infarct-related artery were independently analyzed with blinding to clinical data.

*Results:* Average LV infarct size was 17 $\pm$ 14% and LVEF was 51 $\pm$ 12%. %PD demonstrated strong correlation to TIMI frame count ($\rho = 0.62$, $P < 0.001$), infarct size ($\rho = 0.64$, $P < 0.001$), and LVEF ($\rho = -0.39$, $P = 0.05$). %$MDE_{core}$ demonstrated correlation to TIMI frame count ($\rho = 0.54$, $P = 0.005$) and infarct size ($\rho = 0.52$, $P < 0.01$) but not to LVEF (P = NS). First-pass perfusion defect was seen in more patients (84% vs. 36%, $P < 0.002$) and involved a larger myocardial extent (23.5 $\pm$ 17.5% vs. 3.5 $\pm$ 7.7%, $P < 0.001$) than the hypoenhanced core region on delayed imaging.

*Conclusions:* Both %PD and %$MDE_{core}$ correlate with angiographic measures of MO in the reperfused infarct-related artery. However, %PD correlates with more post-MI prognostic markers than %$MDE_{core}$. First-pass MRI perfusion can be used as a noninvasive technique to quantify MO for novel post-infarct therapies targeting coronary microvasculature.

## 469. QUANTIFYING THE PROGRESSION OF MECHANICAL DYSSYNCHRONY DURING POST-INFARCT LV REMODELING IN MICE WITH MYOCARDIAL TAGGING

**Patrick A. Helm, PhD,[1] Brent A. French, PhD,[1] Zequan Yang, MD, PhD,[1] Alistair A. Young, PhD,[2] Christopher M. Kramer, MD,[1] Frederick H. Epstein, PhD.[1]** [1]***University of Virginia, Charlottesville, VA, USA,*** [2]***University of Auckland, Auckland, New Zealand.***

*Introduction:* In heart failure (HF) patients, cardiac resynchronization therapy (CRT) has been shown to enhance left ventricular (LV) systolic and diastolic function and promote reverse remodeling (1). Increasing evidence suggest that mechanical synchrony is a better predictor of response to CRT than the presence of a conduction defect (2). Global mechanical synchrony is a direct function of regional wall stress, dysfunction, and adaptive remodeling. The CURE metric (3), which is based on circumferential (E11) strain, measures the uniformity of mechanical synchrony of the LV and is currently the most effective technique for assessing mechanical synchrony (4). Experimental myocardial infarction has been shown to induce global LV remodeling in mice, which provides a unique opportunity to study the function of genes in the development of post-infarct LV remodeling and mechanical dyssynchrony. Using contemporary MR imaging techniques, we studied the relationship between post-infarct LV remodeling and mechanical dyssynchrony.

*Methods:* Myocardial infarction (MI) was induced in five C57BL/6 mice by 60 min occlusion of the left anterior descending coronary artery followed by reperfusion. Myocardial function was assessed using magnetic resonance (MR) imaging at baseline, 1, 7, and 28 days after MI. 3D strain was computed from multi-slice tagged MR images. The CURE metric was used to quantify synchrony in the mice from baseline to 28 days post-MI. CURE was studied in three short axis regions: base, mid-ventricle, and apex. LV volumes were computed from MR images using guide point modeling (5).

*Results:* Unlike prior studies of mechanical dyssynchrony that focused only on post-infarct assessment, we observed changes in synchrony pre- and post-infarct. All mice showed a significant ($p < 0.01$) reduction in uniformity of circumferential strain post-infarct in the apical and mid-ventricular regions (Panel A). No statistical difference was noted in the base. Furthermore, despite pronounced global LV remodeling ($\sim$40% and 60% changes in EDV and ESV, respectively) between 1 and 28 days post-MI (Panel B), no significant recovery or deterioration of synchrony was observed during that same period.

*Conclusions:* Thus, infarction alone leads to significant dyssynchrony, independent of bundle branch block or QRS widening. Our results agree with recent studies in patients with ischemic HF, where infarct location was found to affect the degree of CURE more than the width of QRS (6). In the current study, the mid to apical regions exhibited the most dyssynchrony after infarction due to the the location of the infarct. The CURE values for the mouse model are significantly less than that reported in human hearts($\sim$0.78). The difference in heart size across these two species and the fact that some patients in the human studies had conduction defects may account for higher CURE values. In conclusion, this murine model of

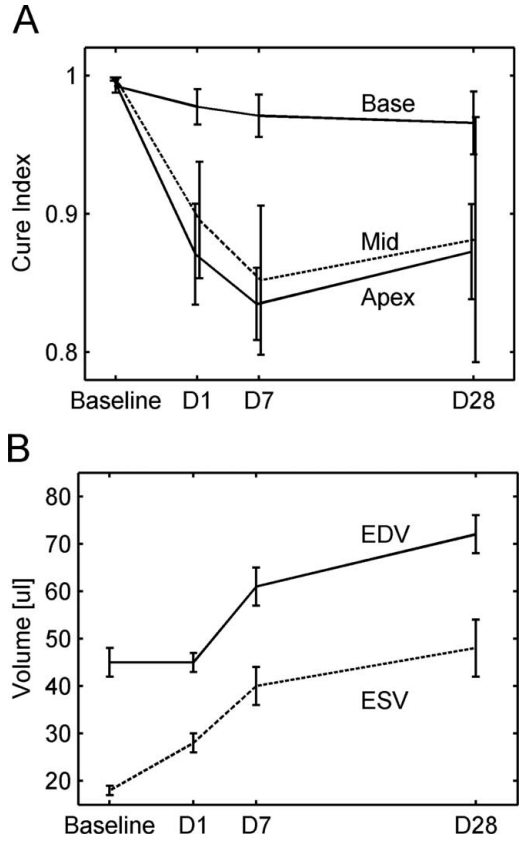


FIG. 1.

post-infarct LV remodeling mimics many of the phenotypes found in human HF, and specifically shows that CURE values are significantly decreased as early as one day post-MI and remain depressed during the LV remodeling process. The use of genetically-manipulated mice in this model coupled with functional imaging will provide new tools in the study of post-infarct LV remodeling and dyssynchrony.

## REFERENCES

1. Sutton MG, et al. Circulation. 2003;107:1985–1900.
2. Bleeker GB, et al. J Cardiovas Electrophysiol. 2004;15: 544–549.
3. Leclercq C, et al. Circulation. 2002;106:1760–1763.
4. Helm RH, et al. Circulation. 2005;31:111:2760–7.
5. Young AA, et al. Radiology, 2000;216:597–602.
6. Helm RH, et al. Proceeding AHA. Nov. 13–16, 2005, Dallas, Texas.

## 470. MICROVASCULAR OBSTRUCTION IN PATIENTS WITH ACUTE MYOCARDIAL INFARCTION PREDICTS PATTERN OF LEFT VENTRICULAR REMODELING

**Stijntje D. Roes, MD, Theodorus A. M. Kaandorp, MD, Jeroen J. Bax, MD, PhD, Eric P. Viergever, MD, Ernst E. van der Wall, MD, PhD, Hildo J. Lamb, MD, PhD, Albert de Roos, MD, PhD.** ***Leiden University Medical Center, Leiden, The Netherlands.***

*Introduction:* Microvascular obstruction (MO) occurs in patients after acute myocardial infarction and can be assessed by constrast enhanced first- pass perfusion using MRI. It is demonstrated that MO is related with adverse clinical outcome and impaired cardiac function. However, the exact relationship between microvascular obstruction and left ventricular remodeling has not yet been elucidated.

*Purpose:* To evaluate the influence of MO on left ventricular remodeling in patients after acute myocardial infarction.

*Methods:* Twenty-nine patients underwent MRI on a 1.5 T system (Philips Medical Systems, Best, the Netherlands) within 10 days after acute myocardial infarction. Cine MRI and (delayed) contrast enhanced MRI with 0.15 mmol/kg Gadolinium was performed to assess ventricular function and infarct tissue. First-pass perfusion was assessed with TFE/EPI sequence with sense technique. MO was defined as hypoenhancement within the infarct region (assessed with delayed enhancement) during first passage of contrast. These first pass perfusion images were visually scored and two groups were defined; patients with MO and patients without MO. A second MRI scan was performed $8.6 \pm 5.5$ months later in order to assess changes in left ventricular volumes and function. Left ventricular volumes and function were measured by manually tracing end-diastolic and end-systolic endocardial borders. The Paired-Samples T-test was used to evaluate data within one group and data between the two groups were compared using the independent samples T-test.

*Results:* Of the 29 consecutive patients who were included, 1 patient was excluded because images were lost, and in 1 patient the second MRI scan was not performed. MO was present in 18 patients and 10 patients did not have signs of MO. There was no significant difference in baseline patient characteristics and baseline left ventricular ejection fraction (EF) and volumes between the two groups. After $8.6 \pm 5.5$ months, left ventricular end-diastolic volume (EDV) had increased significantly from $205.48 \pm 27.13$ ml to $215.10 \pm 32.02$ ml ($p = 0.001$) in patients with MO whereas in patients without MO EDV remained the same; $184.65 \pm 27.63$ ml and $183.39 \pm 28.10$ ml ($p =$ NS). Left ventricular end-systolic volume (ESV) and EF did not differ significantly between the two groups after 8.6 months. Both groups showed the same pattern in decrease of ESV and improvement of EF. ESV in patients with MO decreased from $111.05 \pm 28.33$ ml to $104.02 \pm 31.30$ ml ($p = 0.001$) and EF improved from $46.51 \pm 8.00$ % to $52.42 \pm 8.71$% ($p < 0.001$). In patients without MO ESV decreased from $90.25 \pm 18.08$ ml to $79.21 \pm 18.10$ ml ($p < 0.001$) and EF increased from $50.83 \pm 9.22$ % ($p < 0.001$).

*Conclusion:* In patients with MO, the LV dilates during follow-up whereas LV-EDV remains the same in patients without MO. This finding suggests that MO adversely affects LV myocardium and that LV-remodeling, not only by hypertrophy, but also by increase of LV-EDV is necessary to improve LV function after myocardial infarction.

## 471. QUANTIFICATION OF MYOCARDIAL LIPID USING A BREATH HOLD MULTIECHO TECHNIQUE AT 3.0 TESLA

**Declan P. O'Regan, MBBS, Stephan Schmitz, PhD, Martina Callaghan, PhD, Rossi Naoumova, MD, Julie Fitzpatrick, DCR(R), Joanna Allsop, DCR(R), Jo Hajnal, PhD.** ***Imperial College, London, United Kingdom.***

*Introduction:* Animal and human studies of cardiac lipotoxicity show that accumulation of triglycerides within cardiomyocytes is associated with systolic and diastolic dysfunction. Cardiorespiratory gated proton spectroscopy has been attempted to measure myocardial lipid but presents a number of technical challenges for routine clinical use.

*Purpose:* Our aim was to develop a spatially-resolved breath hold sequence to quantify myocardial lipid content.

*Method:* We optimized a multiecho cardiac-triggered gradient echo sequence on a Philips Intera 3.0 tesla MRI system using a 6-element phased array cardiac coil. A dual inversion black blood prepulse was used to suppress flow artifacts. The echo times (TE) were chosen so that the signals from fat and water were either in-phase or out-of-phase with respect to each other. The TEs ranged between 1.15 and 5.75 ms yielding 5 data points. Phantom studies using a lipid emulsion were performed with cardiac simulation to test the sensitivity of the technique to low fat fractions. In vivo imaging was performed in normal volunteers and in patients with obesity, hyperlipidaemia or diabetes. A set of 10 mm mid-ventricular short axis slices at end diastole were acquired. Signal intensities were measured within regions of interest drawn over the myocardial septum and liver parenchyma. A curve fitting model derived the fat fraction, global T2* decay and the difference in precessional frequency between fat and water protons.

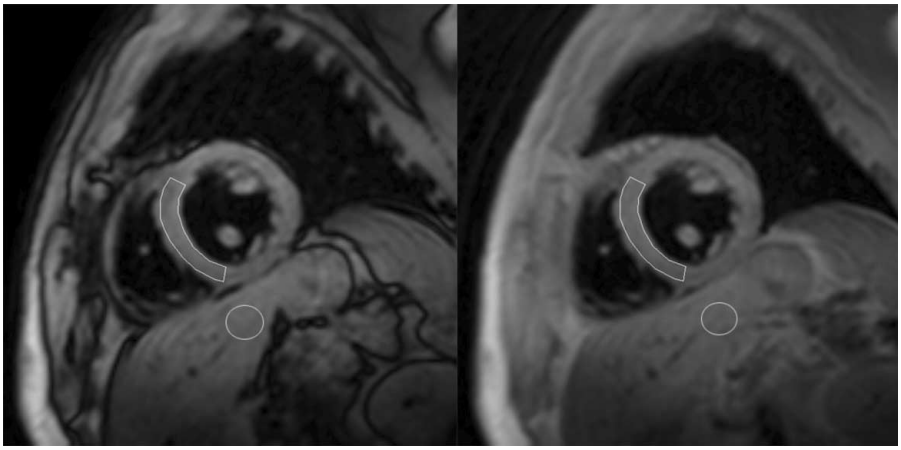

FIG. 1. Examples of the black-blood gradient echo sequence with regions of interest placed over the myocardial septum and liver parenchyma. Left image out-of-phase echo time (TE 1.15 ms), right image in-phase echo time (TE 2.3 ms).

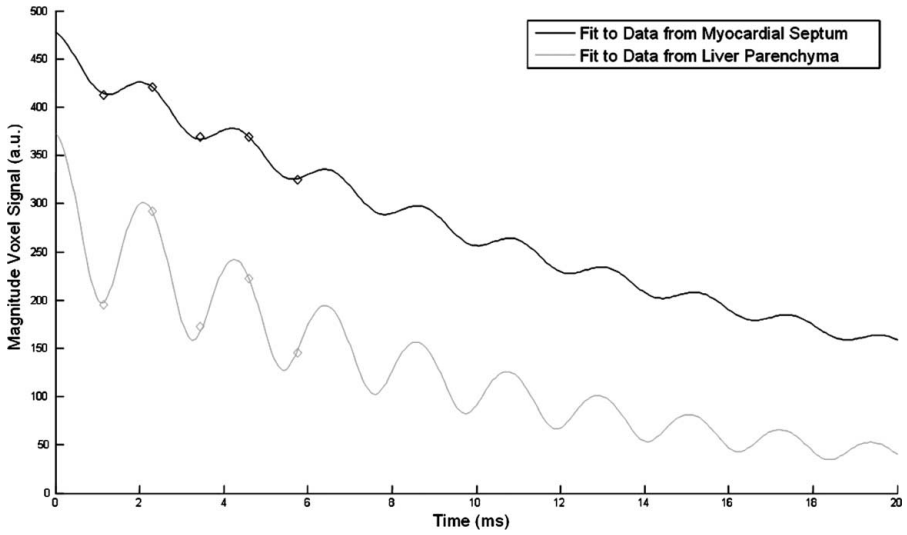


FIG. 2. Curve fitting for the signal intensities of myocardial and liver tissue at five echo times. The curves demonstrate T2* decay, with the signal amplitude of the oscillation reflecting the fat fraction.

*Results:* Phantom studies using concentrations of 10 and 20% lipid emulsified in water demonstrated a characteristic oscillating signal intensity with increasing echo time. Proton spectroscopy was performed on the samples at 11.7T and the fat fraction and fat/water frequency shift were in good agreement with the multiecho technique. The imaging protocol was well-tolerated and a complete cardiac study could be performed within an hour. In vivo studies demonstrated satisfactory image quality for TEs of up to 5.75 ms and breath hold times did not exceed 20 seconds (Fig. 1). Flow artifacts were adequately suppressed by the black blood prepulse and only minor susceptibility artifact was apparent adjacent to the left ventricle posterior wall. Preliminary in vivo imaging amongst high-risk patients demonstrated an oscillating signal decay in myocardial tissue corresponding to fat fractions of up to 5% (Fig. 2). Liver parenchyma typically contained greater levels of lipid with fat fractions of up to 25%. Normal volunteers demonstrated no significant fat within the myocardium.

*Conclusion:* Our preliminary phantom and patient data shows—as a proof of concept—that breath hold in-phase and opposed-phased imaging is a promising technique for assessing myocardial fat content. Further work is required to validate the technique and explore its clinical value.

## 472. CHARACTERIZATION OF REGIONAL FUNCTION FOLLOWING MYOCARDIAL INFARCTION: COMPARISON BETWEEN MULTIDETECTOR COMPUTED TOMOGRAPHY AND QUANTITATIVE MAGNETIC RESONANCE MYOCARDIAL TAGGING

**Caterina Silva, Luciano C. Amado, Karl H. Schuleri, Anastasios P. Saliaris, Marco A. S. Cordeiro, Nael Osman, Richard T. George, Joao A. C. Lima, Albert C. Lardo.** ***Johns Hopkins University, Baltimore, MD, USA.***

*Background:* Assessment of regional left ventricular (LV) function has important prognostic implications after acute myocardial infarction (MI). We aimed to determine the ability of multidetector computed tomography (MDCT) to quantify regional LV function following myocardial infarction relative to quantitative magnetic resonance imaging (MRI) tagging strain analysis.

*Methods:* Six pigs were studied 2 ± 1 months after an experimental MI (infarct size 12 ± 9% LVmass). MDCT was performed using a 32 slice (Toshiba Inc) detector, using a retrospective ECG-gating after a bolus injection of Visipaque. Short axis reconstructions were analyzed to calculate regional function parameters: wall motion (WM), wall thickening (WT), regional ejection fraction (REF), in a 16-sector model. WM (mm) was quantified from the end-diastolic epicardial wall diameter—end-systolic epicardial wall diameter; WT (%) from the end-diastolic wall thickness—end-systolic wall thickness/end-diastolic wall thickness X 100%; REF (%) from the end-diastolic endocardial diameter—end-systolic endocardial diameter)$^2$/end-diastolic endocardial diameter$^2$ X 100%. Circumferential strain (Ecc) was calculated by harmonic phase analysis from tagged MRI, using a 16-sector model, as the average of the peak systolic value in the endocardium, midwall and epicardium walls. Regions of interest were defined based on delayed enhancement MRI.

*Results:* Transmural Ecc showed significant differences between infarct and adjacent ($p = 0.025$) and remote ($p = 0.012$) regions of interest (infarct: $-6.94 \pm 5.60$; adjacent: $-12.97 \pm 5.12$; remote: $-12.25 \pm 3.99$). Similarly, WM was able to differentiate infarct to adjacent ($p = 0.048$) and remote ($p = 0.036$) regions of interest (infarct: $1.23 \pm 1.27$ mm, adjacent: $1.58 \pm 1.30$ mm, remote: $2.52 \pm 1.33$ mm). However, REF and WT didn't distinguish among infarct, adjacent and remote regions of interest.

*Conclusions:* After a chronic experimental MI, MDCT based wall motion analysis is able to distinguish between infarct and adjacent or remote regions and compared well with quantitative MRI tagging analysis. These data may have important implications for patients with implantable devices who are not candidates for MRI.

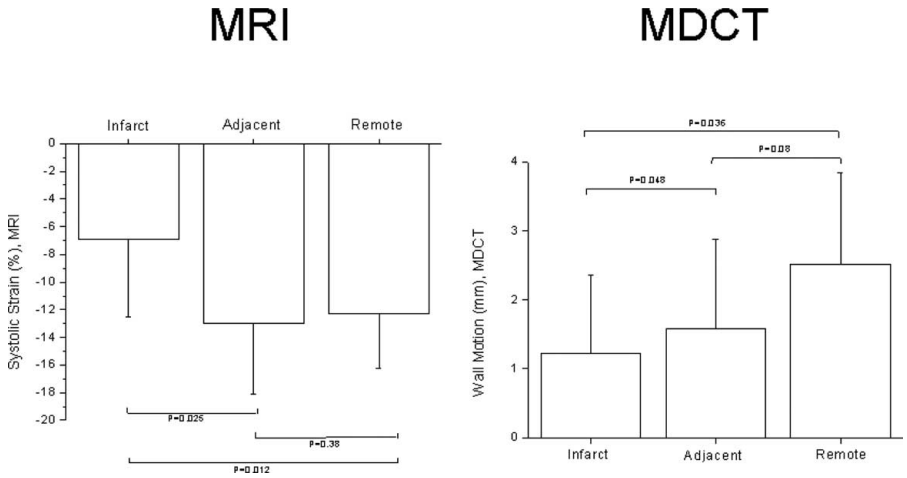


FIG. 1.

## 473. OBSTRUCTIVE SLEEP APNEA IS ASSOCIATED WITH SMALLER PULMONARY VEIN SIZE AND LESS CARDIAC CYCLE VARIATION

**Thomas H. Hauser, MD, MMSc, Vidal Essebag, MD, PhD, Seth McClennen, MD, Susan Yeon, MD, JD, Mark E. Josephson, MD, Warren J. Manning, MD.** ***Beth Israel Deaconess Medical Center, Boston, MA, USA.***

*Introduction:* Atrial fibrillation (AF) is the most common sustained cardiac arrhythmia and is a major cause of stroke. Both OSA and changes in PV anatomy have been implicated in the pathophysiology of AF, but their relationship to each other has not been investigated.

*Purpose:* The goal of this study was to define the relationship between obstructive sleep apnea (OSA) and pulmonary vein (PV) size and variability over the cardiac cycle.

*Methods:* We prospectively evaluated a consecutive series of 71 patients with AF who were referred for evaluation prior to an AF ablation procedure. Breath-hold PV magnetic resonance angiography (MRA) was obtained using a spoiled 3D gradient echo sequence. The maximal diameter, perimeter and cross-sectional area (CSA) were determined using a standard method (1). For each patient, the PV measures were summed to determine the patient total diameter, total perimeter and total CSA. Gated steady-state free-precession breath-hold gradient echo cine CMR of the left and right proximal PV was performed in a subset of 14 patients. The maximal and minimal PV sizes during the cardiac cycle were measured. For each patient, the average PV variability was calculated. The relationship of PV size and variation to clinical and anatomic factors were also evaluated to assess for confounding. Statistical analysis was performed using standard correlation and Student's t-test.

*Results:* The study cohort was comprised of 71 subjects (55 men, age $52 \pm 11$, 33 with mitral regurgitation, 32 with systemic hypertension, 19 with OSA, 10 with diabetes, 7 with coronary artery disease, 4 with heart failure, 3 with obstructive lung disease). AF was paroxysmal in 40, persistent in 25 and permanent in 6. OSA was significantly associated with smaller total PV diameter, perimeter and CSA (Table). Men had significantly larger PV size compared to women ($p < 0.05$ for all measures). No other clinical or anatomic factors were significantly associated with PV size. OSA was also significantly associated with decreased PV variability over the cardiac cycle (Table).

Relationship of OSA to PV size and variation

| | OSA | No OSA | p |
|---|---|---|---|
| PV Size (N = 71) | | | |
| Total Diameter (cm) | $6.1 \pm 1.8$ | $7.1 \pm 1.6$ | 0.031 |
| Total Perimeter (cm) | $17.6 \pm 5.1$ | $20.9 \pm 3.6$ | 0.004 |
| Total CSA ($cm^2$) | $7.1 \pm 2.6$ | $8.5 \pm 2.0$ | 0.028 |
| PV Variation (N = 14) | | | |
| Diameter (%) | $10 \pm 2$ | $16 \pm 4$ | 0.036 |
| Perimeter (%) | $10 \pm 4$ | $16 \pm 4$ | 0.014 |
| CSA (%) | $18 \pm 6$ | $29 \pm 6$ | 0.014 |

*Conclusions:* OSA is associated with significantly smaller PV size and less variation over the cardiac cycle. These anatomic data suggest a different underlying pathophysiology may promote AF in patients with OSA.

### REFERENCE

1. Hauser TH, Yeon SB, McClennen S, et al. A method for the determination of proximal pulmonary vein size using contrast-enhanced magnetic resonance angiography. J Cardiovasc Magn Reson 2004;6:927–36.

## 474. LEFT VENTRICULAR VOLUME-MASS RATIO IS SUPERIOR TO LEFT VENTRICULAR MASS FOR IDENTIFYING PATIENTS WITH AMYLOID CARDIOMYOPATHY

**Frederick L. Ruberg, MD,[1] Martha Skinner, MD,[1] Kraig V. Kissinger, RT(R)(MR),[2] Warren J. Manning, MD.[2]** ***[1]Boston University School of Medicine, Boston, MA, USA, [2]Beth Israel Deaconess Medical Center, Boston, MA, USA.***

*Introduction:* Amyloid cardiomyopathy (AC) has been characterized echocardiographically by increased biventricular wall thickness and reduced left ventricular (LV) end-diastolic volume (EDV) (1). Hypertrophy of the LV as a response to chronic hypertension may also be characterized by similar findings, making differentiation between these two entities challenging (2). Volumetric cardiovascular magnetic resonance (CMR) affords accurate assessment of LV volumes, LV mass, and the capacity to identify tissue specific abnormalities through delayed enhancement (DE) CMR. DE has previously been reported in AC as a function of increasing LV mass (3).

*Purpose:* We hypothesized that a volume-mass ratio (VMR = LVEDV/LV mass) might better characterize the geometric abnormalities of AC in a gender and body size neutral manner, thereby affording a means to identify disease and better correlate with DE.

*Methods:* Eleven subjects (9 male, 2 female) with systemic AL amyloidosis and cardiac involvement (AC) as well as a cohort of eleven age, gender, and BSA matched control subjects with hypertension and normal ventricular function (HTN) underwent functional and DE CMR.

*Results:* Among patients with AC vs. HTN controls, LV mass was significantly increased ($95 \pm 38$ vs. $74 \pm 15$ g/$m^2$, $p = 0.05$) while LV EDV ($146 \pm 147$ mL vs. $181 \pm 35$ mL, $p = 0.03$) was significantly reduced. VMR was markedly reduced in AC subjects ($0.8 \pm 0.2$ mL/g) as compared to HTN controls ($1.2 \pm 0.2$ mL/g, $p < 0.0001$). DE was noted in 8 of 11 (73%) subjects with AC and none (0%) with HTN. Among subjects with AC, VMR permitted differentiation between subjects with and without DE ($0.7 \pm 0.2$ vs. $1.0 \pm 0.1$ ml/g, $p = 0.02$) while LV mass between these groups was similar ($101 \pm 41$ vs. $81 \pm 31$ g/$m^2$, $p = 0.24$).

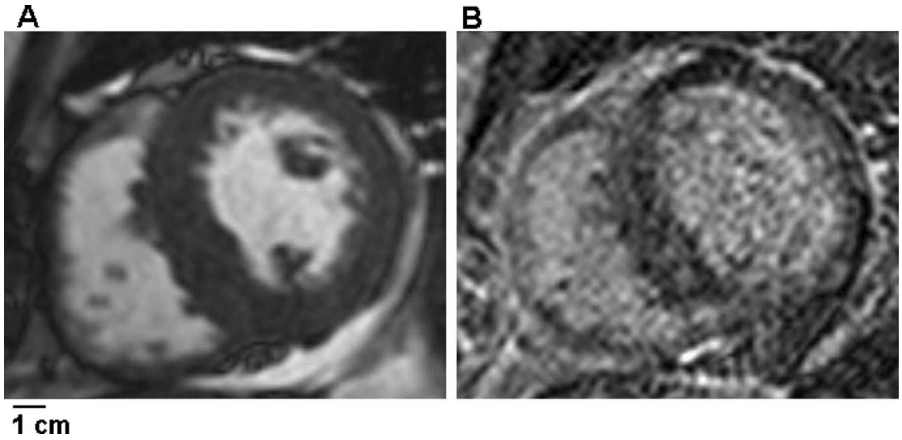


FIG. 1 Mid-LV short axis matched images of a patient with AC by SSFP (A) and DE (B) CMR techniques illustrating the small cavity and heterogenous enhancement patterns observed.

*Conclusions:* CMR and specifically volume-mass ratio may provide a means by which amyloid cardiomyopathy may be differentiated from hypertensive LV remodelling and better characterize the geometric distortion associated with AC than LV mass alone. VMR also appears superior to LV mass for identifying patients with amyloid cardiomyopathy and DE.

## REFERENCES

1. Rahman JE, et al. Noninvasive diagnosis of biopsy-proven cardiac amyloidosis. J Am Coll Cardiol 2004;43:410–415.
2. Devereux RB, and Roman MJ. Left ventricular hypertrophy in hypertension: stimuli, patterns, and consequences. Hypertens Res 1999;22:1–9.
3. Maceira AM, et al. Cardiovascular magnetic resonance in cardiac amyloidosis. Circulation 2005;111:186–193.

## 475. THE REMOTE MYOCARDIUM IS DYSFUNCTIONAL IN THE EARLY PHASE AFTER TRANSMURAL INFERIOR MYOCARDIAL INFARCTION: A TISSUE MRI STUDY

**Bernard P. Paelinck,[1] Christiaan J. Vrints,[1] Johan M. Bosmans,[1] Jeroen J. Bax,[2] Albert de Roos,[2] Hildo J. Lamb.[2]**
***[1]University Hospital Antwerp, Edegem, Belgium, [2]Leiden University Medical Center, Leiden, The Netherlands.***

*Introduction:* Impairment of longitudinal left ventricular (LV) shortening and expansion in the remote myocardium contributes to global LV dysfunction early after transmural anterior myocardial infarction. The impact of the remote myocardium on global LV function remains unresolved in transmural inferior myocardial infarction.

*Purpose:* The study was aimed to assess longitudinal function in the remote myocardium in recent transmural inferior infarction.

*Methods:* Longitudinal systolic (Sa) and early diastolic (Ea) velocities of the infarcted, adjacent and remote myocardium were measured using tissue MR imaging in 12 consecutive patients with a recent ($6 \pm 3$ days) first reperfused transmural inferior myocardial infarction (single vessel disease of the right coronary artery). The results were compared with 12 age and LV-mass index matched control subjects.

*Results:* Myocardial scar extent was $28 \pm 9\%$, LV systolic function (ejection fraction $47 \pm 8\%$ vs $57 \pm 4\%$, $P < 0.01$) and global LV diastolic function impaired (peak filling rate $312 \pm 105$ vs $424 \pm 68$ ml/s, $P < 0.01$). Velocities in the infarcted myocardium (Sa: $5.5 \pm 1.5$ cm/s vs $7.7 \pm 1.9$ cm/s, $P < 0.01$, and Ea: $5.9 \pm 1.5$ cm/s vs $9.4 \pm 2.8$ cm/s, $P < 0.01$) and diastolic velocities in the remote myocardium were lower in patients (Ea $7.4 \pm 2.6$ cm/s vs $10.7 \pm 2.5$ cm/s, $P < 0.01$).

*Conclusions:* In transmural inferior myocardial infarction early longitudinal diastolic motion of both the remote and infarcted myocardium is impaired. This supports the hypothesis that impairment of long-axis LV motion in the remote myocardium contributes to global LV diastolic dysfunction.

## 476. A DARK BLOOD T2* IMAGING TECHNIQUE FOR IMAGING IRON OVERLOAD

**Yiu-Cho Chung,[1] Bernd Kuehn, PhD,[2] Orlando P. Simonetti, PhD.[3] [1]*Siemens Medical Solutions USA, Inc., Chicago, IL, USA,* [2]*Siemens Medical Solutions, Erlangen, Germany,* [3]*The Ohio State University, Columbus, OH, USA.***

*Introduction:* Myocardial iron overload in patients with thalassaemia and sickle cell disease can be assessed by T2* imaging (1). The myocardial iron content reduces T2*. The values can be calculated from images acquired with a multi-echo gradient echo (gre_me) technique. However, such images are prone to flow artifacts which can degrade image quality, compromising the accuracy of derived T2* maps. We propose here a dark blood gre_me that will improve T2* map accuracy, and hence the accuracy of estimating myocardial iron deposition.

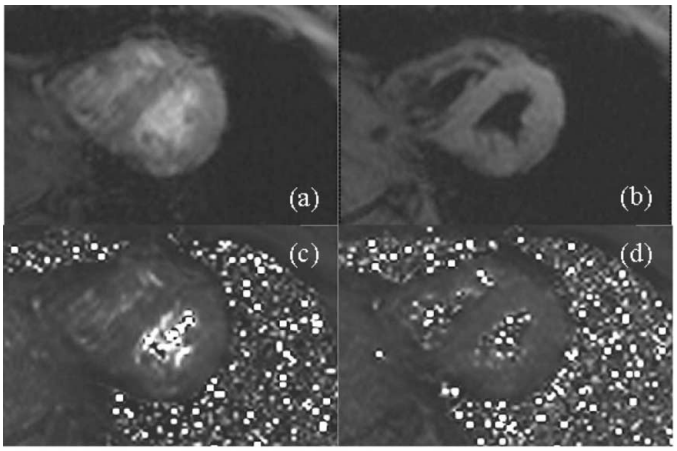


FIG. 1 (a) Bright blood image TE = 22 ms, note the flow artifact. (b) Dark blood image @ TE = 22 ms, windowed at the same level as (a). Myocardium is more uniform. (c) T2* map from the bright blood images. (d) T2* map from the dark blood images, with identical windowing as (c). The T2* values here are more uniform than those in (c).

*Purpose:* To design a dark blood gre_me sequence and show that it reduces the standard deviation (SD) of T2* maps in healthy volunteers.

*Methods:* The dark blood gre_me was designed and implemented on a 1.5T scanner (Avanto, Siemens, Germany). It differs from (1) in that: dark blood pulse is applied immediately following the R-wave and image data are acquired at diastole (similar to Li et al. (2) in timing). Data acquisition is skipped every other heart beat. GRAPPA (3) is used to reduce scan time (acceleration factor = 2, 27 reference lines) and a water excitation (WE) pulse is used to suppress fat. Six echoes were acquired following each RF pulse. The longer duration of the WE pulse led to slightly longer echo times that that reported in (1). Lower readout bandwidths were used to compensate for SNR loss in later echoes. The sequence is motion compensated, and monopolar readout was used. Other imaging parameters are: 192 matrix, ~80–90 lines, 8 mm thick slice, flip angle = 15 deg, TR = 29 ms, 7–9 segments per heart beat (depending on heart rate), TEs/BWs = 2.9 ms/400 Hz, 5.8 ms/400 Hz, 8.8 ms/400 Hz, 12.2 ms/250 Hz, 17.3 ms/230 Hz, 22 ms/200 Hz. The technique was tested on 5 volunteers with bright blood (bb) and dark blood (db) preparation with GRAPPA. Both techniques acquire images at identical times in the cardiac cycle. Shimming conditions were kept identical. Nine measurements were made (measurements were made at 2 slice positions in 4 volunteers). For each measurement, a T2* map was generated from the 6 short axis images with varying TEs using the exponential curve-fitting tool on the MRI console. The ROI was drawn on the septum (least influenced by susceptibility artifacts). The mean T2* and SD at the ROI were measured.

Table 1. Comparison of T2* values and their SDs as obtained from the images using two different methods.

| | | | | | | | | | |
|---|---|---|---|---|---|---|---|---|---|
| | T2* values from BRIGHT blood images | | | | | | | | |
| Mean | 36.8 | 37.4 | 34.5 | 39.5 | 45.9 | 36.9 | 34.5 | 36.6 | 33.6 |
| SD | 12 | 6.7 | 5.9 | 6 | 5.8 | 6.9 | 4.2 | 6.8 | 12.7 |
| | T2* values from DARK blood images | | | | | | | | |
| Mean | 35.2 | 36.5 | 36 | 32.9 | 38.9 | 35.6 | 34.5 | 35.9 | 32.1 |
| SD | 5.7 | 7.5 | 4.5 | 4.7 | 5.7 | 3.5 | 2.5 | 4.4 | 4.1 |

Note the generally lower SDs for T2* obtained from dark blood images.

*Results:* Table 1 tabulated the T2* of the septum from the two techniques in the 9 measurements. The mean and standard deviation of the 9 measurements in Table 1 were 37.2 ms and 3.7 ms in the bright blood case and 35.3 ms and 2 ms in the dark blood case. These values were close to those reported in (1). SDs from bright blood images are higher than those from dark blood technique despite the use of GRAPPA in the later case (which adds noise, and hence randomness to images). Fig. 1 shows the images of the last echo from the two techniques and the corresponding T2* maps windowed to the same contrast in the same study. The bright spots in (c), originating from the blood flow in the ventricle, are mostly cleaned up in (d) because of the dark blood pulse. They may be the main reason for the higher variability in the T2* values from the maps.

*Conclusions:* The results showed that dark blood T2* imaging of myocardium improves image quality and hence the accuracy of the resulting T2* maps. With iPAT, the breathhold time was only slightly increased. The technique may also be used to measure BOLD induced T2* changes in the diagnosis of ischemic heart diseases.

## REFERENCES

1. Westwood M, et al. JMRI 2003;18:33–39.
2. Li D, et al. AJR 1999;172:141–145.
3. Griswold MA, et al. MRM 2002;47:1202–1210.

## 477. SOFTWARE CHANNEL COMPRESSION FOR DYNAMIC MYOCARDIAL PERFUSION MRI

**Sathya Vijayakumar,[1] Feng Huang,[1] James H. Akao,[1] Edward V.R. DiBella,[2] Mark K. Limkeman.[1]** [1]***Invivo Diagnostic Imaging, Gainesville, FL, USA,*** [2]***UCAIR, University of Utah, Salt Lake City, UT, USA.***

*Motivation:* The use of multiple channel phased array coils benefits MRI studies with increased signal to noise ratio (SNR), but it also leads to increased memory requirements and reconstruction times. With the increase in efficient partially parallel imaging (PPI) techniques (1, 2), the need for greater number of channels has increased owing to the higher reduction factors in more than one dimension so achievable. PPI techniques reduce acquisition time, but memory requirement and reconstruction time increase faster. Hence the need to reduce the data obtained without loss in SNR.

*Methods:* An example of efficient hardware channel reduction is the 8 channel neuro-vascular EIGENCOIL® array

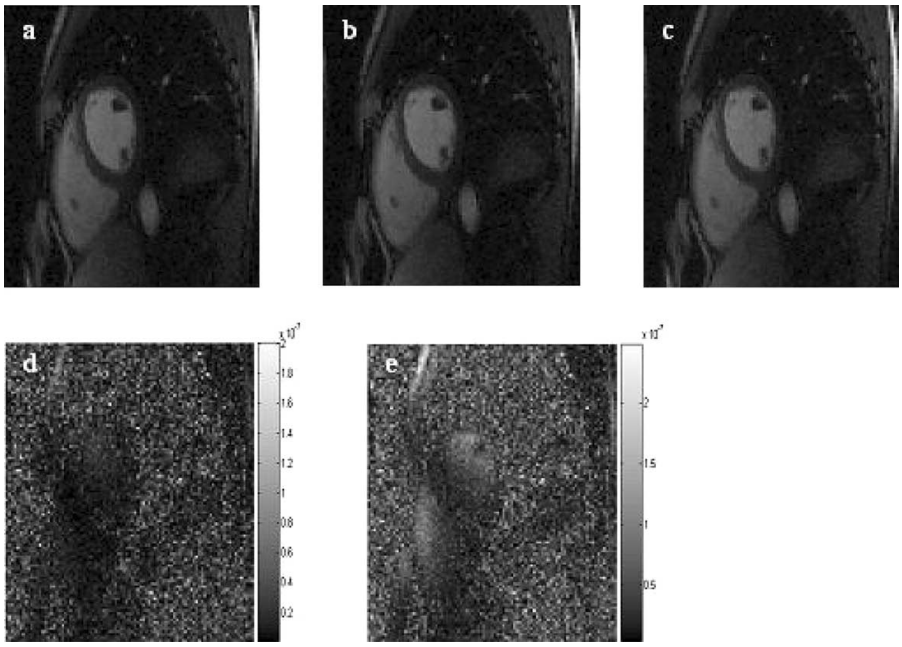


FIG. 1. (a) Original 8-channel dataset (b) Compressed to 6-channels (c) Compressed to 4-channels (d) Difference image between (b) and (a) (e) between (c) and (a).

(Invivo Corporation) (3, 4). In this work, we focus on a software channel compression technique. Principle component analysis (PCA) has been widely used in data analysis compression (5). PCA maximizes the variance in each combined channel, maximizing the energy information in fewer channels. This implies the reduced number of channels can still achieve high SNR. Also, PCA generates orthogonal combined channels, which is crucial for PPI techniques. In (6), details of the algorithm are described and it was shown that the software data compression technique worked efficiently for 32 channel data with PPI. Here, we apply the PCA method of channel compression to dynamic myocardial perfusion MRI data to verify that no critical information in the temporal dimension is lost. Data was acquired on a 3T Trio Siemens scanner (Siemens Medical Solutions, Erlangen, Germany) using a standard perfusion turbo flash saturation recovery sequence with the Siemens 8 channel cardiac array. (Matrix size: 256 × 128 × 70, TI:100 TE:1.27 TR:2.05, FA 12). The center 40 phase encode lines of k-space were used to compute the compression matrix, averaged over the time dimension for all 8 channels. For a particular slice, all 70 time frames were compressed with the same compression matrix. Contrast agent Gd-DTPA was administered at a rate of 6 cc/sec with a dose of 0.05 mmol/kg. Full k-space data was acquired. The 8-channel raw data was compressed to 6 and 4 channels. The three datasets were processed identically and the myocardium was segmented using the same set of contours before fitting to a two-compartment model (7) to estimate the contrast washin parameter that is representative of flow.

Table 1. Estimated washin parameters

| Region | 8-channels | 6-channels | 4-channels | % Diff 1 | % Diff 2 |
|---|---|---|---|---|---|
| 1 | 1.23 | 1.18 | 1.15 | 4.07% | 6.50% |
| 2 | 1.02 | 1.10 | 1.17 | 7.80% | 14.70% |
| 3 | 0.59 | 0.65 | 0.77 | 10.10% | 30.51% |
| 4 | 0.52 | 0.62 | 0.65 | 19.20% | 25.00% |
| 5 | 0.58 | 0.65 | 0.62 | 12.07% | 6.90% |
| 6 | 1.07 | 1.00 | 0.67 | 6.54% | 37.38% |

*Results:* Figure 1 illustrates time frame 16 of the same slice of all three datasets. Table 1 shows the washin parameters obtained in all 3 cases from one slice of the dataset, and also shows the percentage difference between the original and the compressed datasets. From the paired student's t-test, it was found that the two datasets obtained from the compressed channels, are not significantly different ($p > 0.3$, $p > 0.6$) for the 6-channel and 4-channel compression respectively. Similar results were seen on other slices as well. The data compressed to 4 channels didn't perform as well as that compressed to 6 channels indicating that there is an optimum level to which one can suitably compress data. From [6], it can be expected that a larger starting number of channels will offer a greater compression ratio than that shown in this initial study. More work is being done on channel compression of 32 channel cardiac data.

## REFERENCES

1. Pruessman, et al. MRM 1999;42:952–962.
2. Griswold, et al. MRM 2002;47:1202–1210.
3. King SB, et al. Proc. 11th Annual Meeting of ISMRM, 2003;712.
4. Gotshal U, et al. Proc. 12th Annual Meeting of ISMRM, 2004;2389.
5. Gonzalez RC, Woods RE, Digital Image Processing, Addison Wessley Publishing Company; 1992.

6. Huang F, et al. Proc. 27th Annual International Conference of the IEEE-EMBC, 2005.
7. Vijayakumar S, et al. Proc. 12th Annual Meeting of ISMRM, 2004;1847.

## 478. INFLUENCE OF DIETARY FAT ON TRIGLYCERIDE ACCUMULATION IN THE HUMAN HEART ASSESSED BY $^1$H-MRS

**Rutger vd Meer, MD,[1] Jan W. A. Smit, MD, PhD,[1] Sebastiaan Hammer,[1] Sebastian Kozerke, PhD,[2] Michael Schär, PhD,[2] Albert de Roos, MD, PhD,[1] Johannes A. Romijn, MD, PhD,[1] Hildo J. Lamb, MD, PhD.[1]** [1]***Leiden University Medical Center, Leiden, The Netherlands,*** [2]***University of Zurich, Zurich, Switzerland.***

*Introduction:* In type 2 diabetic subjects, plasma levels of free fatty acids and triglycerides (TG) are elevated because of unsuppressed lipolysis in adipose tissue and hepatic overproduction of TG-rich particles. This long-term excessive lipid exposure, in the presence of impaired glucose utilization, results in accumulation of triglycerides in non-adipose tissues, including the myocardium. However, recent data suggest that short-term variation in dietary fat content may influence myocardial fat as well, even in healthy subjects. To assess TG accumulation in non-adipose tissue, proton magnetic resonance spectroscopy ($^1$H-MRS) has proven to be a useful tool.

*Purpose:* To determine the short-term effect of dietary fat content on TG accumulation in the human heart as assessed by $^1$H-MRS.

*Materials and Methods:* In this pilot study, $^1$H-MRS of the myocardium was performed at 1.5T (Gyroscan ACS/NT15; Philips, Best, the Netherlands) in 4 healthy non-obese men (Mean (SD) age: 22.5 (3.1), BMI 23.1 (1.7)), to determine TG content at baseline and after two 3-day periods of either a low-caloric, low-fat diet or a high-fat diet. A spectrum with water suppression was acquired to detect weak lipid signals. The single-voxel spectra ($2 \times 4 \times 1$ cm) were recorded by using a point resolved spectroscopy sequence with an echo time of 26 ms and a repetition time of 3 s. 1024 data points were collected over a 1000 Hz spectral width and averaged over 128 acquisitions. Spectra without water suppression with a repetition time of 10 s and with 4 averages were also recorded to be used as an internal standard. $^1$H-MRS of the heart was performed with the use of respiratory motion compensation based on navigator echo's to minimize breathing influences. Chemical shifts were measured relative to water at 4.7 ppm. TG signals at 1.3 and 0.9 ppm of the suppressed spectrum and the water signal of the unsuppressed spectrum were quantified using the MRUI/AMARES package. Finally the percentage of TG was calculated ($100 \times$ TG/(water + TG)).

*Results:* The mean (SD) percentage of myocardial TG at baseline was 0.42%. It increased to 0.76% during the low-fat diet and to 0.59% during the high-fat diet. In all patients, myocardial TG content was increased after both a low-caloric, low-fat diet and a high-fat diet as compared to baseline myocardial TG. Friedman testing of these data showed borderline significance ($p = 0.05$) between the 3 feeding conditions.

*Conclusion:* Our data suggest that dietary fat content influences TG accumulation in the healthy human heart. This observation is of importance for the understanding of pathophysiological myocardial TG accumulation in patients with diabetes mellitus type 2. The number of study participants needs expansion.

## 479. LEFT VENTRICULAR EJECTION FRACTION CALCULATION: INFLUENCE OF THE PAPILLARY MUSCLES

**Elena Montalvo Martin,[1] Maria Jose Olivera,[1] Teresa Presa,[1] Paloma Caballero Sanchez-Robles,[1] Raul Hernandez,[2] David Tagarro,[1] Luis Martinez Elbal,[1] Luis J. Jimenez-Borreguero[1]** [1]***University Hospital La Princesa, Madrid, Spain,*** [2]***Clinica Ruber, Madrid, Spain.***

*Introduction:* CMR is considered as the gold standard method for left ventricular (LV) volumes and ejection fraction (EF) assessment. For this purpose, the Simpson's rule method in the LV-short axis is applied. Theoretically, the subtraction of papillary muscle and trabeculations from the LV cavity should provide identical stroke volume (SV) but different LVEF, and different end-systolic (LVESV) and end-diastolic volumes (LVEDV), as well.

*Purpose:* To test the hypothesis that LVSV and LVEF measured by the Simpson's rule method including and excluding papillary muscles and trabeculations, are different.

*Methods:* Nineteen patients with an EF ranging 40%–76% by echocardiography were included. Subjects were imaged on a 1.5T MR system (Signa CV/i, GE Healthcare) with a ECG-triggered breath-hold steady-state free precession technique (FIESTA). LV end-diastolic and end-systolic volumes and EF were calculated from a set of short-axis cine images using a semiautomatic contour detection algorithm and Simpson's rule method (MRI-MASS software; MEDIS, Netherlands). All datasets were analyzed including (group A), and excluding (group B) the papillary muscles in the ventricular cavity.

*Results:* Measurement of LVESV in both groups showed a significant difference ($66.6 \pm 27.9$ vs. $57.8 \pm 25.0$, respectively; $p < 0{,}001$; 95% CI: 6.7–11.1 ml). There were no significant differences in the quantification of LVEDV ($161.2 \pm 52.1$ vs. $158.1 \pm 50.7$, $p = 0{,}57$) due to the difficulties in segmentation of the trabeculae in enddiastolic images. LVEF was significantly larger in group A than in group B ($63.6 \pm 7.1\%$ vs. $60.0 \pm 7.3\%$, $p < 0.001$; 95% CI: 2.8–4.5%). There were no statistically significant differences in the LVSV between group A and group B ($100.1 \pm 30.9$ mL vs. $99.2 \pm 31.1$ mL, $p = 0.38$; 95% CI: 1.2–3.0 mL).

*Conclusions:* In our series, the inclusion or exclusion of papillary muscles and trabeculations in the LVEF calculation can provide a variation up to 4.5%, which can be considered clinically

relevant. The absence of significant differences in the LVSV calculation demonstrates the high precision of this measurement technique.

## 480. INFARCT LOCATION DETERMINES EARLY LV REMODELING IN REPERFUSED ST-SEGMENT ELEVATION MYOCARDIAL INFARCTION

**Jan Bogaert, Maria Kalantzi, Steven Dymarkowski, Frank E. Rademakers, Frans Van de Werf, Stefan Janssens.** ***Gasthuisberg University Hospital, Leuven, Belgium.***

*Introduction and Purpose:* Infarct location determines postinfarct cardiac dysfunction, with more infarct expansion and LV remodeling in anterior myocardial infarctions (MI) compared to non-anterior MI's. We assessed the relationship between infarct location and early LV remodeling in patients with a reperfused acute ST-segment elevation MI using serial MRI analysis.

*Methods:* Fifty-two patients with an ST-segment elevation MI (27 anterior, 25 non-anterior [inferior 23, lateral 2]), who underwent successful revascularization within 2–12 h after symptom onset were studied 1week (1W) and 4 months (4M) postinfarction.

*Results:* Time from symptom onset to revascularization, pre-PCI TIMI flow, and maximal cardiac enzymes were comparable between groups. At 1W, MRI showed no differences in infarct size or transmurality, or in size or transmurality of microvascular vascular obstruction, but a significantly larger area at risk in anterior MI's ($p < 0.0001$). No differences in LV volumes or mass were found albeit a trend toward lower EF in anterior MI's ($p = 0.08$). At 4M, global and regional function exclusively improved with time in anterior MI's (LV-EF: $+3.6 \pm 6.5\%$, $p < 0.01$; systolic wall thickening infarct area: $+11.8 \pm 21.5\%$, $p = 0.03$; peri-infarct area: $+15.1 \pm 20.5\%$, $p = 0.0022$), while non-anterior MI's showed an evolution toward adverse remodeling evidenced by an increased LV sphericity ($p = 0.04$). In anterior MI's morphological wall thinning was not limited to the infarct area but involved the peri-infarct area too, resulting in a significant reduction of LV mass ($-14.6 \pm 16$ g, $p < 0.0001$) at 4M.

*Conclusions:* Timely reperfusion has a greater beneficial effect in anterior MI's with better functional recovery and less adverse LV remodeling than in non-anterior MI's.

## 481. CORONARY ARTERY AND VIABILITY EVALUATION USING MAGNETIC RESONANCE IMAGING IN PATIENTS WITH NECROTIZING VASCULITIS

**Sophie Mavrogeni,[1] Theodora Karagiorga,[2] Menelaos Manousakis,[2] Marouso Douskou,[3] Haralambos Moutsopoulos,[2] Dennis V. Cokkinos.[1]** [1]***Onassis Cardiac Surgery Center, Athens, Greece,*** [2]***Department of Pathophysiology, University of Athens, Athens, Greece,*** [3]***Bioiatriki MRI Unit, Athens, Greece.***

Table 1. Coronary vessel diameter in patients with necrotizing vasculitis.

| Coronary vessel | MPA+PAN | WG | Controls |
|---|---|---|---|
| LAD (mm) | $4.67 \pm 1.37$ | $3.54 \pm 0.30$ | $2.56 \pm 0.27$ |
| RCA (mm) | $4.68 \pm 1.00$ | $3.18 \pm 0.94$ | $2.43 \pm 0.30$ |
| LCx (mm) | $4.01 \pm 1.16$ | $3.14 \pm 0.43$ | $2.53 \pm 0.23$ |

*Introduction:* Polyarteritis Nodosa (PAN), Microscopic Polyangiitis (MPA) and Wegener Granulomatosis (WG) are forms of necrotizing vasculitis. Coronary arteries can be occasionally affected in all forms.

*Purpose:* We evaluated the coronary arteries of these patients non-invasively using magnetic resonance angiography (MRA), and performed viability study using contrast enhanced MRI (CE-MRI).

*Methods:* Eleven patients with MPA, 2 with PAN and 5 with WG, without any cardiac symptoms, were studied and compared with 15 age- and sex-matched controls, in whom the absence of stenotic coronary artery disease was proven by X-ray angiography. The maximal diameter of the proximal 1/3 of each coronary vessel was recorded. Ectasia was defined as dilatation of an arterial segment to a diameter at least 1.5 times that of the adjacent normal artery. MRA was performed using a Philips Intera 1.5 T system. Data acquisition was performed with ECG gating in mid-diastole. All scans were carried out with the patient free breathing. CE-MRI images were acquired 15 minutes after the IV injection of 0.1 mmol/kg Gd-DTPA using an inversion recovery gradient echo pulse sequence.

*Results:* Coronary artery diameter was found significantly increased in all vasculitis patients compared to controls ($p < 0.001$) (Table 1). Criteria for ectasia were fullfiled by MPA+PAN, but not WG patients. The comparison of coronary vessel diameters between MPA+PAN vs WG group had revealed significant difference only for RCA ($p < 0.01$). Previous myocardial infarction was documented in 1 patient with MPA.

*Conclusions:* Coronary ectasia appears a quite common finding in asymptomatic vasculitis patients, while necrosis is rare. Magnetic resonance evaluation is feasible in these forms of vasculitis and may prove of value for treatment guidance.

## 482. CARDIOVASCULAR MRI ADDS HIGH SPECIFICITY TO CHARACTERIZATION OF CARDIAC MASSES INITIALLY IDENTIFIED BY ECHOCARDIOGRAPHY

**Tarun Tewatia, MD, Mark Doyle, PhD, Vikas K. Rathi, MD, June Yamrozik, Ronald Williams, Robert W. W. Biederman, MD.** ***Allegheny General Hospital, Pittsburgh, PA, USA.***

*Introduction:* The vast majority of cardiac masses are initially detected using TTE but cannot be unequivocally identified due to lack of differentiation of the echocardiograpic signal. Yet, accurate mass identification is mandatory prior to therapy. In the majority of centers, mass characterization is performed using a combination of TEE, biopsy, catheterization and CT. Cardiovascular MRI (CMR) has tissue contrast properties and flexible view selection that permit mass identification.

*Hypothesis:* We hypothesize that CMR can provide noninvasive diagnosis of cardiovascular masses seen by echocardiography, providing the necessary specificity required for patient management.

*Methods:* From Auggust 2002 through March 2005, CMR was performed in 76 patients referred for evaluation of unknown cardiac masses detected by echocardiography. Contrast mechanisms exploiting intrinsic T1, T2, tissue relaxation properties, uptake kinetics of exogenous contrast agent, delayed hyperenhancement and inversion contrast to identify fat and water signals were performed in multiple views characterizing cardiac and paracardiac masses.

*Results:* Of 76 patients imaged, CMR characterized 100% of masses: 91% non-neoplastic; 9% with high suspicion for malignancy. Of the total, CMR diagnosed 43% as benign fat deposits, including lipomatous hypertrophy and epicardial fat; 7% were not masses but normal variants, e.g. prominent crista terminalis (100% of these were referred as "echogenic material with a suspicion of either thrombus, fat or malignancy"); 8% were diagnosed as myxoma and 7% thrombus. Of those masses diagnosed as malignant by CMR, verification was obtained by histopathology, where 6 of 7 (86%) were shown to be malignant and 1 (14%) benign. In masses defined as non-malignant, the clinical sequelae were consistent with the CMR diagnosis.

*Conclusion:* In patients with suspicious cardiac masses by echocardiography, the wide range of contrast mechanisms available to CMR permits noninvasive characterization, differentiating with high degree of specificity non-neoplastic vs. malignant lesions. These results suggest that CMR can be and should be utilized following identification of cardiac masses by echocardiography to provide the necessary specificity for optimal patient management.

## 483. ASSESSMENT OF CARDIAC COMORBIDITY IN HIV+ INDIVIDUALS WITH INCREASED BNP LEVELS BY CARDIAC CINE MRI

**Frank Breuckmann, MD,[1] Kai Nassenstein, MD,[2] Till Neumann, MD,[1] Jana Kondratieva, MD,[1] Lena Schaefer,[2] Raimund Erbel, MD,[1] Joerg Barkhausen, MD.[2] [1]*West German Heart Center Essen, Department of Cardiology, University Duisburg-Essen, Essen, Germany,* [2]*West German Heart Center Essen, Department of Diagnostic and Interventional Radiology and Neuroradiology, University Duisburg-Essen, Essen, Germany.***

*Introduction:* Human immunodeficiency virus (HIV) and acute immunodeficiency syndrome are known to be associated with cardiac involvement. Highly active antiretroviral therapy (HAART) has substantially improved the survival of patients with HIV disease what resulted in a significant reduction in mortality of HIV + patients and prolonged survival of HIV + individuals associated with an increase of severe cardiac comorbidity. However, HAART may independently contribute to cardiac impairment.

*Purpose:* A subsectional program of the German heart failure network currently analyzes the primary prevalence of heart failure in HIV + patients. Standardized examination included patient history, clinical examination, ECG, x-ray of the chest, 6-minutes-walk-test, BNP measurement and transthoracic echocardiography. In this study we report contrast enhanced cardiac MRI in HIV + individuals with an increased serum brain natiuretic peptide (BNP) levels in order to determine different reasons for cardiac failure.

*Methods:* Sixteen of 132 HIV + patients met the inclusion criteria of significantly elevated BNP levels. Of these 16 individuals 3 patients refused to participate in the study and 1 patient died before the scheduled examination. Therefore, 12 patients (male/female 8/4, age 25–75 years, status CDC/WHO A2-C3) were included in this study in accordance with the regulations of the local ethics committee. In all patients therapy consisted of a combination of nucleoside reverse transcriptase inhibitor and protease inhibitor resulting in a stable immunologic and virologic outcome. All examinations were performed on a 1.5T MR scanner equipped with high performance gradients (Magnetom Sonata, Siemens Medical Solutions, Erlangen, Germany). The MRI protocol included a steady state free precession cine sequence (TrueFISP, TR 3 ms, TE 1.5 ms, FA60°) for the assessment of the myocardial function in all patients. Based on contiguous short axis scans volumetric measurements were performed using the manufacturer provided software (ARGUS). For assessment of myocardial edema a fat-suppressed T2-weighted turbo spin echo (TR 2 heart beats, TE 4 ms, FA180°) sequence was performed. Additionally, an inversion recovery fast low angle shot sequence (IR-turboFLASH: TR 8.0 ms, TE 4.0 ms, TI 180–240 ms, FA20°) was acquired in short and long axis views 10 min after injection of a 0. 2 mmol/kg bodyweight of Gd-DTPA (Schering AG, Berlin, Germany).

*Results:* Patients exhibited a median serum BNP level of 188 pg/mL. Adequate image acquisition could be achieved in all but one patient. A reduction of the ejection fraction (EF) was detected in 4 patients resulting in a left ventricular EF of 45%. One patient showed isolated right ventricular dilatation. Regional hypo- or akinetic areas were detected in 3 patients, left ventricular myocardial hypertrophy in 3 subjects. Transmural enhancement indicating myocardial scar tissue was detected in 1 patient, whereas delayed enhancement with spotted, streaky or subepicardial distribution was found in 2 of our 12 patients. Myocardial edema was detected in none of our patients. Based on the MR findings the diagnosis of hypertrophic cardiomyopathy

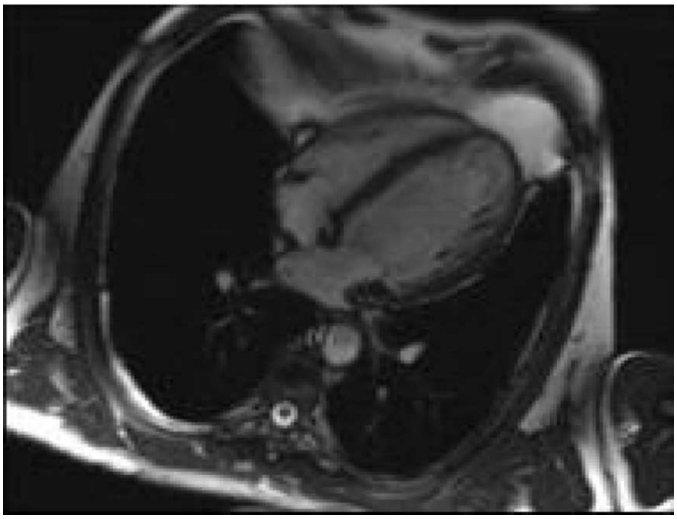

FIG. 1.

(n = 3), myocarditis and perimyocarditis (n = 2), chronic myocardial infarction (n = 2), dilated cardiomyopathy (n = 1, Fig. 1) and isolated right ventricular failure (n = 1) was made. Only two patients showed no pathologic abnormalities.

*Conclusions:* However, a coexistence of direct HIV-induced myocardial changes, HIV-related cardiomyopathy and coronary artery disease as well as HAART-associated intracellular myocardial abnormalities including mitochondrial dysfunction has been proposed in the pathogenesis of secondary heart failure. In this study an elevated BNP level was used to screen for cardiac failure in HIV+individuals. In this patient cohort 9 of 12 showed different cardiac abnormalities on contrast enhanced cardiac MRI. However, due to the coexistence of an eminent HIV infection and ongoing HAART regimen, a direct HIV-related heart failure or therapy-induced cardiac impairment cannot be discriminated. Although no specific pattern of functional abnormalities or contrast enhancement was found, our study demonstrates that contrast enhanced MRI allows characterizing different underlying diseases in HIV+individuals with elevated serum BNP levels.

## 484. FIRST PASS PERFUSION AND LATE ENHANCEMENT MRI IMAGING IN TAKO-TSUBO CARDIOMYOPATHY

**Kobayashi Yasuyuki.** ***St. Marianna University School of Medicine, Kawasaki, KANAGAWA, Japan.***

*Purpose:* Tako-tsubo cardiomyopathy is an enigmatic disease characterized by transient left ventricular dysfunction of a broad area with a hyperkinetic area around the cardiac base. There is ST-segment elevation with no coronary stenosis. The exact mechanism remains unknown. First pass perfusion and late enhancement is used in MRI as a diagnostic tool in various myocardial pathologies such as infarction, fibrosis, edema and inflammation. The purpose of our study was to evaluate myocardial perfusion and late enhancement in Tako-tsubo cardiomyopathy.

*Method and Materials:* The subjects were 8 patients with Tako-tsubo cardiomyopathy who underwent stressed and/or rest perfusion (both in 6 and only rest in 2) and late enhancement MRI. In 2 cases, follow-up examination was performed between 2 and 3 weeks after onset. All patients underwent Echocardiography and CAG within 10 days of MRI study. Echocardiography and CAG revealed that characteristic wall motion (extensive left ventricular apical ballooning and over-contraction of the basis) and coronary arteries are normal. Consequently, Tako-tsubo cardiomyopathy was diagnosed from the clinical course. The MRI system used was a 1.5T MR imager (EXCELART; Toshiba Corporation, Tokyo). FFE-EPI sequence for perfusion during and without pharmacological stress was below; TR = 7.1–8.3 ms TE = 2.1 ms TI = 10 ms FA = 30 NAQ = 1 FOV = 25–28 × 36 cm MX = 64–96 × 128 ST = 8 mm NS = 4–8 Number of Shots = 20–24 Dynamic = 25–30 times Time = about 1min. And Inversion Recovery sequence for late enhancement was acquired.

*Results:* 1) In all cases, early defect (ED) was observed in apical ventricular wall on both stress and rest perfusion MRI. ED observed in the apical ventricular wall with low contraction capability in rest perfusion indicates that severe microcirculation failure exists. In 2 cases that was performed follow-up MRI examination, ED in apical ventricular wall remained. 2) In 5 cases out of 8, late enhancement (LE) was observed in the apical ventricular wall, which indicates linear (in 3 cases) or patchy (in 2 cases) pattern.

*Conclusions:* It is considered that ED can be observed in the apical ventricular wall with low contraction capability, and myocardial ischemia is concerned with the causes of Tako-tsubo cardiomyopathy. First pass perfusion and late enhancement is very useful for diagnosis and clinical course observation.

## 485. FREE-BREATHING TIME-RESOLVED PARALLEL 3D MRA OF CONGENITAL HEART DISEASE IN INFANTS AND SMALL CHILDREN: A VALIDATION STUDY

**Joachim G. Eichhorn, MD,[1] Christian Fink, MD,[2] Raoul R. Arnold, MD,[1] Sebastian Ley, MD,[2] Herbert E. Ulmer, MD,[1] Hans-Ulrich Kauczor, MD.[2]** ***[1]University Children's Hospital II, Pediatric Cardiology, Heidelberg, Germany, [2]Deutsches Krebsforschungszentrum (DKFZ), Department of Radiology, Heidelberg, Germany.***

*Introduction:* Until now, contrast-enhanced MR angiography (MRA) could only be considered an alternative modality to conventional catheter angiography (CCA) in older and cooperative children, since a breathhold acquisition was required to

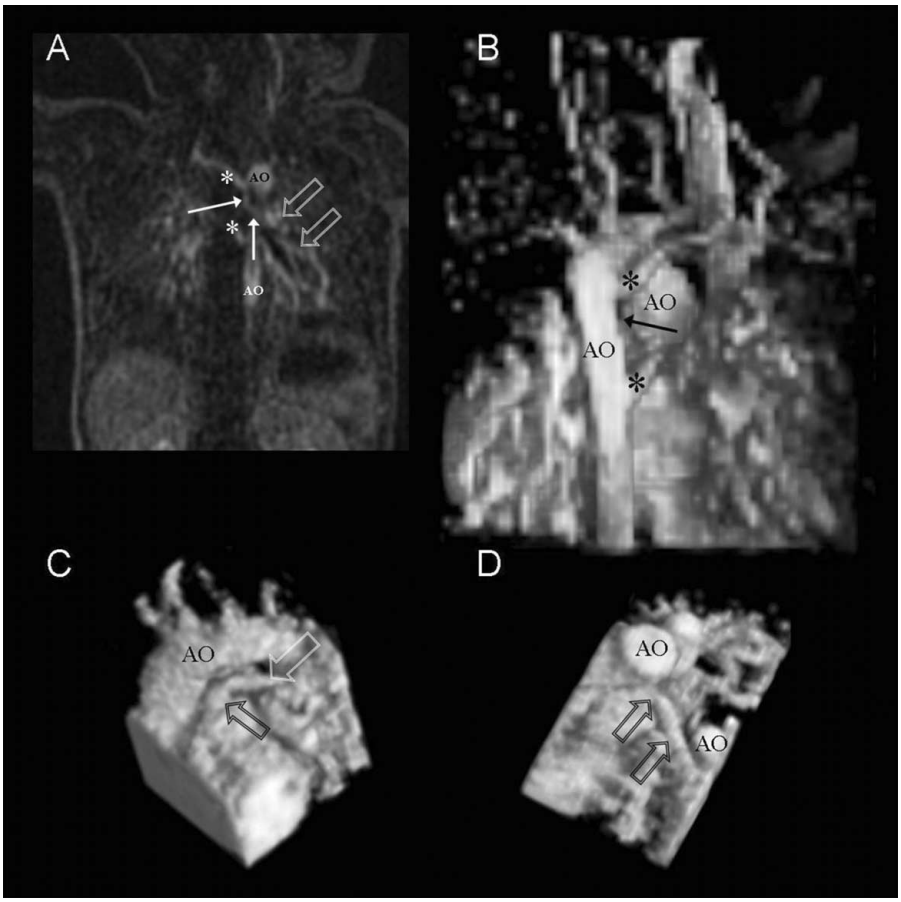


FIG. 1. A newborn (7 days old) with TOF+PA: A, Coronal targeted MIP shows 3 aortopulm. collaterals, two to the right sight (*), one to left pulm. system (arrows). B-C, Volume rendering with posterior (B), left-lateral (C) and cranial views (D). Aorta (AO). The type of pulmonary blood supply could be evaluated completely, and the presence of a native main and a left-sided pulmonary artery system was demonstrated preoperatively (arrows).

reduce motion artifacts from breathing. With parallel imaging the acquisition time of MRA can be significantly shortened without reducing the spatial resolution. The aim of this study was to assess the feasibility of free-breathing time-resolved parallel 3D MRA in the preoperative evaluation of congenital heart disease in infants and small children.

*Methods:* During a period of 2 years, 22 infants and small children (mean age 2.3, SD 1,8 years [median 1 year, range: 1 week to 6 years) with suspected vascular anomalies were examined: tetralogy of Fallot with pulmonary atresia (TOF+PA, n = 10), pulmonary stenosis (n = 4), vascular ring (n = 6), aortic coarctation (n = 2). MRA was performed at 1.5 T (Magnetom Symphony, Siemens, Erlangen, Germany) using a combination of body and spine phased array coils. All exams were performed during free breathing. The children received an adequate intravenous sedation (Chloralhydrat and/or Phenobarbital). Time-resolved 3D MRA was performed with a 3D FLASH pulse sequence with parallel imaging: TR/TE/$\alpha$ = 2.4 ms/0.9/60°, GRAPPA, acceleration factor 2, 24 reference lines, FOV: 300 mm, matrix: 192, spatial resolution: $\sim$1.4 $\times$ 1.4 $\times$ 2.0 mm$^3$, TA: $\sim$2.8 s, 0.2 mmol Gd-DTPA/kg b.w. i.v. @ 1–2 mL/s. Image data was post-processed using multiplanar reconstruction and volume-rendering and compared to CCA (n = 19).

*Results:* In all patients, the image quality was of diagnostic value. Despite the free-breathing acquisition of time-resolved MRA no relevant motion artifacts were observed. The diagnostic information of MRA regarding the visualization of vascular anomalies was nearly equivalent to CCA. This included the visualization of smallest aberrant vessels such as multiple aortopulmonary collateral arteries (MAPCA). Only in 2 patients CCA showed one/two further MAPCA (diameter < 1.5 mm). In addition to the visualization of vascular morphology, the high temporal resolution of the MRA technique facilitated the functional characterization of the vascular anomalies. This included the definition of pulmonary venous drainage and pulmonary perfusion in patients with TOF+PA (MAPCA n = 7; PDA n = 3). Due to the 3D information, MRA offered valuable complementary information to CCA and facilitated surgical planning of vascular anomalies.

*Discussion:* Our results indicate the feasibility of free-breathing time-resolved parallel 3D MRA as a non-invasive and non-ionizing imaging tool also in infants and small children. While the accuracy for the visualization and charaterization of vascular anomalies appears equivalent to CCA, it seems to be more valuable than CCA regarding the visualization of complex morphology.

*Conclusion:* Parallel imaging allows for a significant reduction of the acquisition time of MR angiography without reducing the spatial resolution. In this study the feasibility of free-breathing time-resolved parallel 3D MRA was assessed in 22 infants and small children in the preoperative evaluation of congenital heart disease. Despite the free-breathing acquisition, no relevant motion artifacts were observed. As a consequence the diagnostic information of MRA was equivalent to conventional catheter angiography.

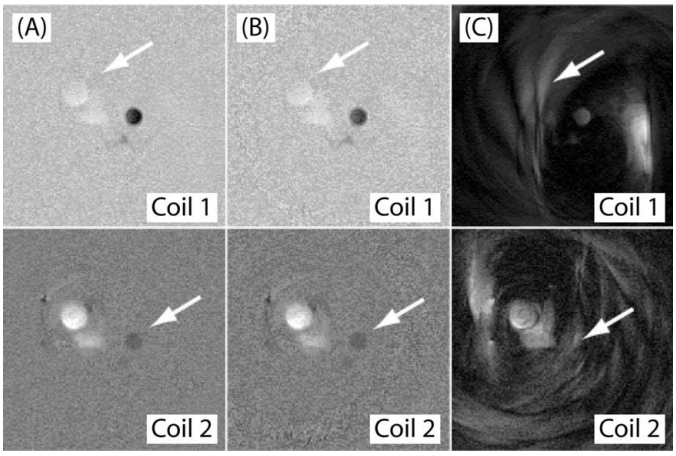


FIG. 1. Example full FOV and pFOV complex difference processing.

## 486. RAPID BLOOD FLOW QUANTIFICATION USING PARTIAL FIELD OF VIEW SPIRAL PHASE CONTRAST IMAGING

**Reza Nezafat,[1] Richard Thompson,[2] Elliot McVeigh.[1]**
***[1]National Heart, Lung and Blood Institute, NIH, Bethesda, MD, USA, [2]Department of Biomedical Engineering,University of Alberta, Edmonton, AB, Canada.***

*Introduction:* Blood flow within the cardiovascular system can be measured non-invasively using phase contrast MRI . In many applications, fractional k-space acquisitions can be used to reduce the duration of image acquisition or to increase the temporal resolution, but image-phase information is lost during the reconstruction rendering these techniques incompatible with phase-contrast. In this study, the image information lost by undersampling is not synthesized, but rather, the effects of undersampling are eliminated by subtracting out the aliased signals. A partial field of view (pFOV) complex difference technique is introduced and used to reduce the acquisition time by factor of at least two while maintaining the spatial and temporal resolution.

*Methods:* The raw MR signals in a spiral phase contrast acquisition consist of signals from moving and non-moving spins. The complex signals from the moving spins will change in two consecutive steps of the phase contrast acquisition, while the signals from non-moving spins will be constant. Therefore, if the k-space is undersampled by a factor R such that only the non-moving spins alias, they can still be removed by subtracting the two complex MR signals from two bipolar gradient steps, resulting in an un-aliased flow weighted image with the temporal resolution improved by R. A modified through-plane spiral phase contrast sequence was developed by time-shifting the bipolar gradient to achieve a first moment difference between two steps while minimizing the background phase due to gradient changes. Images were acquired on a GE Excite 1.5T MR imaging system with an 8-channel cardiac phased array coil. In vitro experiments were performed with a constant flow phantom. In vivo through-plane flow images were acquired in an axial slice superior to the aortic valve with a fully sampled k-space in normal volunteers. The imaging parameters were as follow: TR = 23.6 ms, Venc = 150 cm/s, $\theta$=30°, FOV = 30 cm, BW = ±125 kHz, slice thickness = 6 mm, spiral interleaves = 16. Statistical analysis using Bland-Altman method was performed on flow velocity measurement from an ROI within the ascending aorta. In addition to this analysis, SNR measurement was performed using the non-calibrated complex difference data to quantify the signal to noise loss using the pFOV reconstruction.

*Results:* In vitro: For phantom studies, the correlation analysis of average flow velocity of full FOV and pFOV complex difference processing yielded an $r > 0.998$ and a slope of 0.992.

In vivo: Fig. 1A shows the flow maps reconstructed using all sixteen spiral interleaves processed with complex difference for two coil elements, and Fig. 1B shows flow maps reconstructed using only eight spiral interleaves. The corresponding magnitude image is in Fig. 1C. Significant aliasing artifacts in the magnitude images are visible which are totally removed in the flow map. Fig. 2A shows the blood flow velocity within an ROI in the ascending aorta for the full FOV and pFOV acquisitions. Fig. 2B shows the Bland-Altman plot of flow measurements which shows a majority of the data points (>96%) lie in the mean ± 1.96 STD of the differences, which means the two techniques could be used interchangeably. The SNR analysis shows 30% decrease in the pFOV reconstruction.

*Conclusions:* We proposed a novel technique for imaging and reconstruction of pFOV phase contrast MRI. The results show that the flow estimates using pFOV technique are in good agreement with the full FOV estimates.

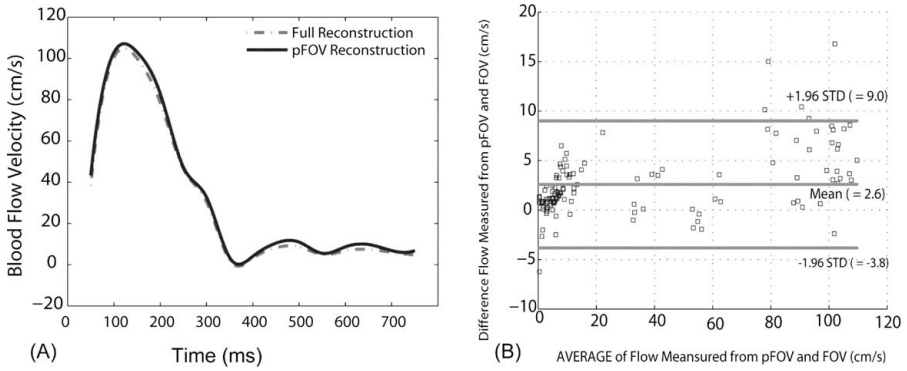


FIG. 2. Blood flow velocity through ascending aorta and the corresponding Bland-Altman plot.

## 487. MYOCARDIAL PERFUSION IN THE INFARCT CORE AND PERIPHERY IN ACUTE MYOCARDIAL INFARCTION

**Sven Plein, PhD,[1] John P. Greenwood, PhD,[1] John P. Ridgway, PhD,[1] Mohan U. Sivananthan, MD,[1] Stephen G. Ball, PhD.[2]** [1]***Leeds General Infirmary, Leeds, United Kingdom,*** [2]***University of Leeds, Leeds, United Kingdom.***

*Introduction:* Following reperfused acute myocardial infarction, microvascular obstruction (MO) can lead to reduced blood flow to the infarct core ("no-reflow"). MO has been demonstrated using CMR, echocardiography and nuclear scintigraphy. By CMR, MO is most often assessed by delayed contrast enhanced imaging. In animal studies first pass CMR perfusion has been used to show that flow rates in MO are significantly lower than in remote segments. At present, only limited patient studies have assessed first pass perfusion imaging of MO and no data exist on rest and stress perfusion imaging of MO in man.

*Purpose:* To obtain semiquantitative measurements of rest and stress myocardial perfusion in patients with evidence of MO early after acute myocardial infarction.

*Methods:* Ten patients were selected from a cohort of 92 patients who underwent CMR as part of a separate research protocol. All were admitted with a first acute myocardial infarction treated with thrombolysis. They underwent CMR imaging between days 3 and 6 after AMI on a 1.5T Intera CV system (Philips Medical Systems, The Netherlands). Rest and Adenosine-stress perfusion images were acquired with a T1-weighted saturation recovery segmented k-space gradient echo pulse sequence combined with Sensitivity Encoding (TE 1.6 msec; TR 3.3 msec; flip angle 15°, four parallel short axis slices acquired at every heart beat for 40 seconds, bolus of 0.05 mmol/kg Dimeglumine gadopentetate). A further contrast bolus of 0.1 mmol/kg was given immediately after the second (stress) perfusion acquisition. Delayed contrast-enhanced images were obtained in 10 contiguous short-axis slices using a segmented inversion-recovery gradient-echo pulse sequence 10–15 minutes after the stress perfusion acquisition. Patients were selected for the current analysis if delayed enhancement imaging showed an area of hypoenhancement in the infarct core in a slice spatially corresponding to the perfusion data. Analysis was performed on an offline workstation running MASS software (Medis, Leiden, The Netherlands). On the late-enhancement image regions of interest were placed in the MO core, the hyperenhancing periphery of the infarct, in a remote myocardial segment and in the LV cavity. These contours were then copied to the rest and stress perfusion studies at an equivalent slice position and adjusted as necessary to consider differences in cardiac phase and FOV. Finally, the contours were propagated to all dynamic images of the two perfusion series and their position manually corrected to account for respiratory motion. SI curves were generated for all ROIs at rest and stress. Maximal upslopes of the SI curves (7 point linear fit), amplitude and T0 of signal upslope were calculated. All myocardial measurements were normalised to the baseline signal intensity and LV input function. A myocardial perfusion reserve index between stress and rest perfusion slopes was calculated. Comparison between results was made using multiple paired t-tests.

Table 1.

| | REST | | | STRESS | | | STRES/REST |
|---|---|---|---|---|---|---|---|
| | Slope | Amplitude | T0 | Slope | Amplitude | T0 | MPRI |
| MO | 4.2* | 10.5*§ | 14.4 | 4.6* § | 10.3* | 15.3 | 1.2* |
| Infarct periphery | 5.1* | 12.6* | 9.9 | 6.5 * | 13.8* | 7.2 | 1.4 |
| Remote | 14.0 | 27.8 | 8.2 | 23.9 | 37.1 | 6.9 | 1.7 |

*Denotes significance to Remote.
§denotes significance to Infarct periphery.

*Results:* The main results are listed in Table 1. SI uplsopes and amplitudes in the MO core were lower and T0 occurred later compared with the periphery of the infarct and the remote myocardium (not significant for slope between MO and periphery). All differences between MO, periphery and remote myocardium were larger at stress than at rest. The MPRI was lower in the MO core than in both the periphery (not significant) and remote myocardium (significant).

*Conclusions:* Hypoenhanced cores of AMI show reduced signal uptake during first pass CMR perfusion imaging when compared with both the periphery of the infarct and remote myocardium. These differences are more marked during vasodilator stress than at rest. Consequently, the MPRI in the MO is lower than in the periphery of the infarct. These results are in concordance with previous animal studies.

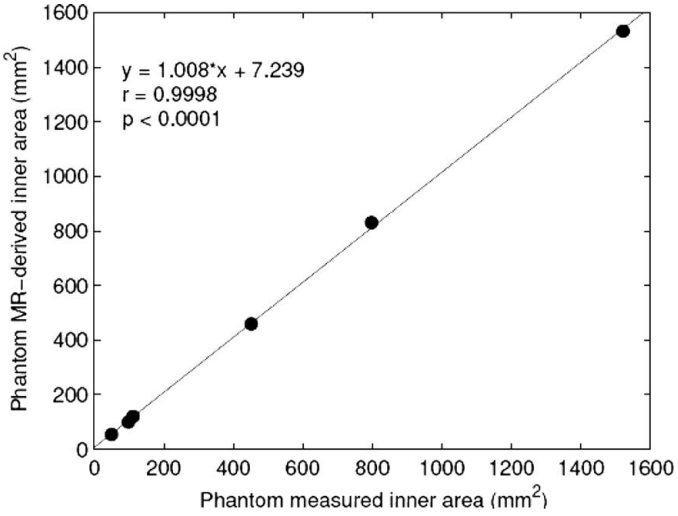


FIG. 1. Comparison of results of automatic method with actual phantom dimensions.

## 488. ACCURATE AUTOMATED MEASUREMENT OF DYNAMIC ARTERIAL LUMEN AREA BY CMR

**Clare E. Jackson, PhD, Cheerag C. Shirodaria, MRCP, Justin M. S. Lee, MRCP, Robin P. Choudhury, DM, MRCP, Keith M. Channon, MD, FRCP, Stefan Neubauer, MD, FRCP, Matthew D. Robson, PhD.** ***University of Oxford Centre for Clinical Magnetic Resonance Research, Oxford, United Kingdom.***

*Introduction:* Magnetic resonance imaging is uniquely suited to study the pathophysiology of arteriosclerosis. By studying the dynamic changes in the lumen and relating this to the observed pulse pressure, it is possible to derive a measure of arterial compliance (a mechano-elastic property of the arterial wall that reflects stiffness and endothelial dysfunction and is an important indicator of vascular function). MR measurements of vessel dimensions generally use manual tracing of the vessel lumen. However, these studies tend to generate very large datasets so such data post-processing is very time-consuming and has limited accuracy and objectivity.

*Purpose:* To develop and validate an automated method to measure the dynamic changes in the arterial lumen.

*Methods:* All studies were performed on a 1.5T clinical MR scanner (Siemens Sonata, Erlangen, Germany). Bright blood SSFP cine MR images were acquired of 33 newly diagnosed coronary artery disease patients, who were each imaged on two separate occasions. The method was used to automatically characterise the ascending, proximal descending and distal descending aorta on each of the 66 examinations An automated measurement method was implemented under Matlab (Version 6.5, The Mathworks, Inc, Natick, MA). This method was based upon a semi-automated method for the measurement of vessel wall thickness that was validated in (1). The data analysis method was based upon: (1) vessel wall unwrapping, followed by (2) a gradient detection algorithm for MR data post-processing and (3) automated tracking of the maximum gradient. All the cine MR images were analysed using this method, with the only user input being to outline the vessel on the first image. Analysis by manual tracing was also performed for each of these vessels and the results were compared with those from the automated method. Plexiglass tubes of known varying diameters were also imaged and analysed using both the automatic and manual methods.

*Results:* There was a close correlation between the results of the automated method and the true dimensions of the plexiglass tubes ($r = 0.9998$, MR-derived tube area $= 1.008 *$ true tube area $+ 7.239$ mm$^2$, $p < 0.0001$) (Fig. 1).

Correlation coefficients (r) were calculated for each of the 198 area-time curves. Example curves from the automated and manual methods are shown in Fig. 2. A close correlation ($r > 0.7$) between the manual and automated methods was found for

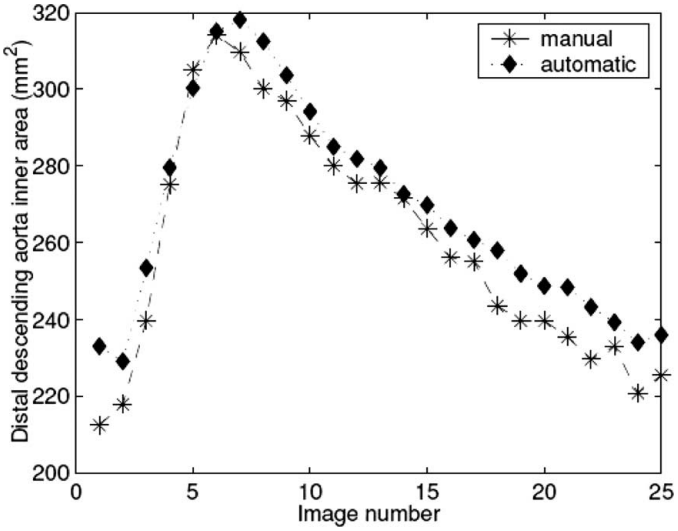


FIG. 2. Change in lumen area over a sequence of cine-MR images for an example vessel.

184 of the 198 lumen area curves (93%). As the individual measurements through the cardiac cycle are independent, we have used a measure of temporal smoothness to determine an upper limit on the measurement errors of each approach. The average Coefficient of Variation in the manual method was found to be 1.21% and the error in the automated method was 0.58% and corresponds to sub-pixel accuracy. This error is small when compared to peak fluctuations of area of around 15.7% and shows that the automatic method is more reproducible. A poor correlation was found for 14 of the 198 lumen area curves. 6 of these cases had obvious artefacts in the images. Another 8 failed on the ascending aorta, where the slice plane chosen resulted in the movement of the aorta in and out of the image plane which had a large effect on the observed vessel area.

*Conclusions:* Automated dynamic lumen area (DLA) segmentation of bright blood SSFP images yields reliable and accurate measurements. Further work on this project will involve integration pulse wave velocity (PWV) calculation into the same software package and investigating the functional form of both the PWV and the DLA.

## REFERENCE

1. Qian W, Robson MD, et al. Accuracy of Quantitative MR Vessel Wall Imaging Applying a Semi-Automated Gradient Detection Algorithm-A Validation Study. JCMR 2004;6:895–907.

## 489. INTRA AND INTEROBSERVER REPRODUCIBILITY OF RIGHT VENTRICLE VOLUMES AND FUNCTION BY CARDIAC MAGNETIC RESONANCE

**Oronzo Catalano, Guido Moro, Serena Antonaci, Maria Mussida, Mauro Frascaroli, Giuseppe Calsamiglia, Mariarosa Perotti, Franco Cobelli.** ***Fondazione Salvatore Maugeri, Pavia, Italy.***

*Introduction:* Right ventricle (RV) assessment has independent diagnostic and prognostic value in many congenital and acquired heart diseases. Cardiac magnetic resonance (CMR) allows quick and non-invasive evaluation of RV volumes and function, with established good accuracy and interstudy reproducibility.

*Purpose:* We evaluated if also intra and interobserver reproducibility are adequate in variable conditions of RV dimension and function.

*Methods:* We analysed CMR exams of 10 healthy volunteers and of 30 pts with healed myocardial infarction, dilated cardiomyopathy or primary arrhythmic disorders and RV enlargement. Cine gradient-echo and steady-state free procession dynamic gradient-echo sequences were used, both with a 1.0 Tesla scanner (Magneton Harmony, Siemens, Erlangen, Germany) and a phased-array cardiac coil. The whole RV, from the tricuspidal valve ring to the apex, was scanned by 8–10 mm thick, 6–10 contiguous short-axis slices. RV end-diastolic and end-systolic volumes (EDV, ESV) were evaluated, by semi-automatic tracing of endocardial border and disk-area summation method. Ejection fraction was then derived (EF = 100*(EDV-ESV)/EDV). The outflow tract and the trabeculae were included in the RV cavity. All cases were blindly evaluated by two operators (twice by one operator). The mean difference and the absolute difference in percent of the mean between repeated measures (variability), by the same investigator or two investigators, were used to assess intra and interobserver reproducibility.

*Results:* Tracing and calculation procedures required 7 minutes on the average. The study population showed a wide range of age (8–83 years) and body surface (0.89–2.34 $m^2$). Female gender was sufficiently represented (30%). Accordingly, there was a large variability of EDV (range: 46–239 mL), ESV (20–129 mL) and EF (6–64%). The mean intraobserver difference was −5.5 mL for EDV, −1.6 mL for ESV and −1.3% for EF, with a variability of 11%, 15% and 15%, respectively. The mean interobserver difference was 4.3 mL for EDV, 0.3 mL for ESV and 2.4% for EF with a variability of 12%, 15% and 17%, respectively.

*Conclusions:* Intra and interobserver reproducibility of RV volumes and function assessed by CMR seems to be adequate in a wide range of RV dimensions and function.

## 490. THREE-DIMENSIONAL MYOCARDIAL TISSUE MOTION—QUANTITATIVE REGIONAL WALL MOTION ANALYSIS IN HEALTHY VOLUNTEERS USING CINE PHASE CONTRAST VELOCITY MAGNETIC RESONANCE IMAGING

**Steffen E. Petersen,[1] Bernd A. Jung, PhD,[2] Frank Wiesmann, MD,[1] Joseph B. Selvanayagam, MBBS, FRACP, DPhil,[1] Jane M. Francis, DCRR, DNM,[1] Helen A. Doll, Dphil,[1] Juergen Hennig, PhD,[2] Stefan Neubauer, MD, FRCP,[1] Matthew D. Robson, PhD[1]** [1]***University of Oxford, Oxford, United Kingdom,*** [2]***University of Freiburg, Freiburg, Germany.***

*Introduction:* Assessment of myocardial regional wall motion plays a key role in many diagnostic and therapeutic decisions in current clinical practice. Semi-quantitative grading or regional wall motion is the most frequently applied technique, but is highly subjective with limited reproducibility. Despite dramatic improvements in echocardiography and cardiovascular magnetic resonance technology, permitting quantitative and objective regional wall motion analysis, none has yet been widely applied in clinical practice.

*Purpose:* We aimed to establish prospectively a database of normal, three-dimensional, systolic and diastolic, endo- and epicardial velocities of all myocardial segments in healthy volunteers using cine phase contrast velocity magnetic resonance imaging ('tissue phase mapping' or TPM).

*Methods:* 96 healthy volunteers (mean ± SD age = 38 ± 12 years, 57 [59%] men) underwent cardiac phase contrast imaging

Table 1. Mean ± SD segmental and myocardial layer distribution of radial and longitudinal velocity parameters

| | Basal | Mid | Apical | Basal | Mid | Apical |
|---|---|---|---|---|---|---|
| | Systolic peak radial velocity [cm/s] | | | Diastolic peak radial velocity [cm/s] | | |
| Epicardium | 2.97 ± 1.22 | 3.09 ± 1.27 | 2.57 ± 0.96 | −3.52 ± 1.71 | −3.72 ± 1.54 | −3.36 ± 1.37 |
| Endocardium | 3.92 ± 1.26 | 3.83 ± 1.12 | 3.22 ± 0.94 | −4.62 ± 2.13 | −5.05 ± 1.80 | −4.61 ± 1.56 |
| Transmural | 3.44 ± 1.33 | 3.46 ± 1.25 | 2.90 ± 1.00 | −4.07 ± 2.01 | −4.38 ± 1.80 | −3.98 ± 1.60 |
| | Systolic time to peak radial velocity [%ES] | | | Diastolic time to peak radial velocity [%ED] | | |
| Epicardium | 47.8 ± 29.9 | 48.0 ± 25.3 | 46.0 ± 20.8 | 21.7 ± 11.2 | 23.1 ± 11.1 | 26.0 ± 11.5 |
| Endocardium | 48.3 ± 25.6 | 47.4 ± 18.5 | 47.4 ± 16.1 | 21.5 ± 10.5 | 21.4 ± 11.7 | 25.6 ± 9.56 |
| Transmural | 48.1 ± 27.8 | 47.7 ± 22.1 | 46.7 ± 18.6 | 21.6 ± 10.8 | 22.2 ± 11.4 | 25.8 ± 10.6 |
| | Systolic peak longitudinal velocity [cm/s] | | | Diastolic peak longitudinal velocity [cm/s] | | |
| Epicardium | −5.59 ± 2.73 | −4.14 ± 3.01 | −2.66 ± 2.71 | 9.25 ± 3.04 | 6.94 ± 2.80 | 4.27 ± 2.49 |
| Endocardium | −5.65 ± 2.61 | −4.11 ± 2.82 | −2.71 ± 2.65 | 9.59 ± 3.18 | 7.28 ± 2.80 | 4.35 ± 2.45 |
| Transmural | −5.62 ± 2.67 | −4.12 ± 2.92 | −2.68 ± 2.68 | 9.42 ± 3.11 | 7.11 ± 2.80 | 4.31 ± 2.47 |
| | Systolic time to peak longitudinal velocity [%ES] | | | Diastolic time to peak longitudinal velocity [%ED] | | |
| Epicardium | 37.3 ± 38.8 | 50.6 ± 61.0 | 64.4 ± 67.4 | 21.7 ± 7.36 | 22.7 ± 8.19 | 15.2 ± 17.7 |
| Endocardium | 38.4 ± 41.8 | 54.4 ± 62.8 | 65.5 ± 67.2 | 21.5 ± 7.54 | 22.2 ± 8.90 | 11.7 ± 19.4 |
| Transmural | 37.9 ± 40.3 | 52.5 ± 61.9 | 65.0 ± 67.3 | 21.6 ± 7.45 | 22.4 ± 8.55 | 13.4 ± 18.7 |

using a black blood k-space segmented gradient echo sequence for the analysis of three-dimensional myocardial velocities with high spatial resolution at 1.5 Tesla in basal, mid-ventricular and apical short axis views. Eighteen consecutive volunteers were scanned twice for inter-study reproducibility and were analysed for intra- and inter-observer variability. Systolic and diastolic velocity curves were analyzed for peak velocities and time to peak velocities in the radial, circumferential and longitudinal direction as well as torsion-rate and longitudinal strain-rate. Mixed effects models with a random intercept for volunteer were used to test for differences between the three ventricular slices and transmural endo- and epicardial parameters.

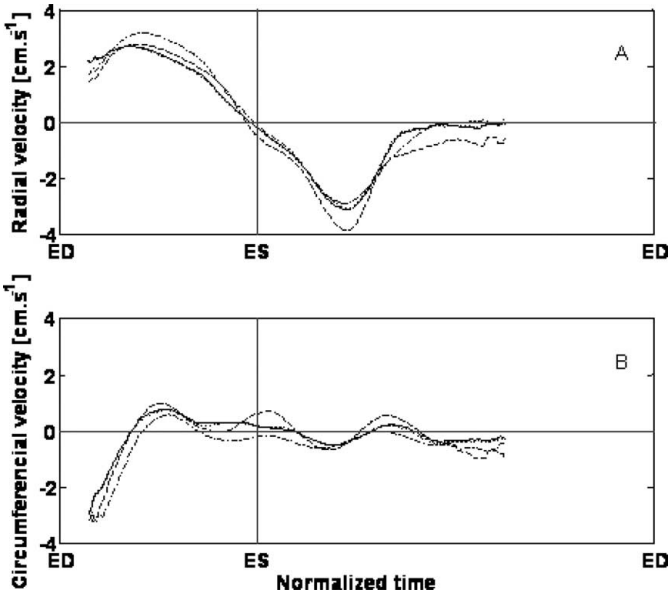


FIG. 1. Intra- and inter-observer variability and inter-study reproducibility for radial and circumferential velocities during the cardiac cycle at mid-ventricular level shown as the mean for the first 18 consecutive healthy volunteers. Observer 1, measurement 1 (solid line), observer 1, measurement 2 (dashed-dotted line), observer 2 (dashed line) and second scan (dotted line). Note the small variation in systolic and diastolic peak velocities and systolic and diastolic time to peak velocities. ED = end-diastole, ES = end-systole.

*Results:* TPM enabled a reproducible assessment of myocardial velocities with small intra- and inter-observer variability (Fig. 1). Systolic peak radial velocity was lowest at apical level ($p < 0.001$), diastolic peak radial velocity was similar at all three myocardial levels ($p = 0.73$, Table 1). As viewed from the apex, a relative counter-clockwise rotation during systole was followed by a relative clockwise rotation of the apex against the base. Diastolic and systolic peak longitudinal velocities decreased from base to apex ($p < 0.001$). A gradient between endo- and epicardium could be observed for radial velocities with greater endocardial velocities ($p < 0.001$).

*Conclusions:* Tissue phase mapping is a reproducible, comprehensive modality to assess regional wall motion, and intra- and inter-observer and inter-study variabilities are low.

## 491. MAGNETIC RESONANCE IMAGING DEMONSTRATES INCREASED BURDEN OF ATHEROSCLEROTIC DISEASE IN DIABETES WHEN ASSOCIATED WITH HYPERTENSION

**Silvia H. Aguiar, MD,[1] Venkatesh Mani, MD,[1] Hiroaki Taniguchi, MD,[1] Daniel D. Samber, PE,[1] John E. Postley, MD,[2] Karen B. Weinshelbaum,[1] R. J. van der Geest, MD, PhD,[3] J. H. Reiber, MD, PhD,[3] Valentin Fuster, MD, PhD,[1] Zahi A. Fayad, PhD.[1]** [1]***Mount Sinai School of Medicine, New York, NY, USA,*** [2]***Columbia University Medical Center, New York, NY, USA,*** [3]***Leiden University Medical Center, Leiden, The Netherlands.***

*Introduction:* Hypertension is two-fold more prevalent in diabetic than in non-diabetic patients. Overwhelming evidence

shows that the association of hypertension and diabetes accelerates the progression of macrovascular disease.

*Purpose:*The aim of this study is to use Magnetic Resonance Imaging to evaluate Burden of Atherosclerotic Disease (as direct subclinical atherosclerosis quantification) in patients with Diabetes associated with hypertension versus diabetes alone.

*Methods:* A total of 33 subjects (63.2 ± 14.27 years, age 19 to 83 years, 36.36% females) underwent Rapid EXtended Coverage (REX) black-blood turbo spin echo MRI of the aorta and common carotid arteries and were distributed as following: DM with hypertension (n = 21) and patients with DM alone (n = 12). Patients with overt renal insufiency were excluded. All hypertensive patients were treated with anti-hypertensive therapy. Cross-sectional images of the aorta (n = 36 to 48) and carotids (n = 12 to 24) were analyzed. Average arterial wall area (AWA) and Plaque Index, AWA normalized with lumen diameter, were measured in each resulting image. Average imaging time was 50 minutes. Interobserver variation was 4.7%.

*Results:* Average Wall Area of carotid and aorta was not significantly different between the two groups. However, when normalized for lumen diameter, Plaque Index of Thoracic Aorta was increased in Diabetics with hypertension (5.77 ± 1.33) as compared to Diabetes alone (4.83 ± 1.02, p = 0.015). Carotid Plaque Index was not different between the groups.

*Conclusions:* Burden of atherosclerotic disease is increased in Thoracic Aorta of patients with both Diabetes and hypertension. MRI may be used to monitor affected diabetic population to facilitate initiation of aggressive anti-hypertensive therapy and to prevent end-organ complications.

## 492. BURDEN OF ATHEROSCLEROTIC DISEASE BY MAGNETIC RESONANCE IMAGING IN YOUNG ADULTS AND PEDIATRIC POPULATION WITH METABOLIC SYNDROME

**Silvia Aguiar, MD,[1] Venkatesh Mani, PhD.,[1] Hiroaki Taniguchi, MD,[1] Svetlana Ten, MD,[2] Amrit Bhangoo, MD,[2] Daniel D. Samber, PE,[1] Karen B. Weinshelbaum,[1] Donald G. Mitchell, MD,[3] Jeffrey Saland, MD,[1] T. J. Starc, MD,[4] Christine L. Williams, MD,[4] Peter Belamarich, MD,[5] Lisa C. Hudgins, MD,[6] R. J. van der Geest, PhD.,[7] J. H. Reiber, PhD.,[7] Valentin Fuster, MD, PhD.,[1] Samuel S. Gidding, MD,[8] Zahi A. Fayad, PhD.[1] [1]*Mount Sinai School of Medicine, New York, NY, USA,* [2]*Maimonides Medical Center, Brooklyn, NY, USA,* [3]*Thomas Jefferson University, Philadelphia, PA, USA,* [4]*Columbia University Medical Center, New York, NY, USA,* [5]*The Children's Hospital at Montefiore, Bronx, NY, USA,* [6]*Rockefeller University, New York, NY, USA,* [7]*Leiden University Medical Center, Leiden, The Netherlands,* [8]*Alfred I. duPont Hospital for Children/Nemours Cardiac Center, Wilmington, DE, USA.***

*Introduction:* Metabolic Syndrome (MetS) is a risk factor for Coronary Heart Disease (CHD) and is increasingly prevalent among young individuals. Data is limited regarding the premature development of atherosclerosis in this high-risk group.

*Purpose:* The aim of this study is to test the hypothesis that Magnetic Resonance Imaging (MRI) may be used to evaluate burden of atherosclerotic disease (as direct subclinical atherosclerosis quantification) in young patients with MetS and in a high-risk group distribution for CHD.

*Methods:* A total of 31 subjects (13 MetS, mean age 16.61 ± 6.19, age 9 to 35 years, 11 females and 18 controls) underwent high-resolution black-blood MRI of aorta and extracranial carotid arteries. MetS was defined according to NCEPIII guidelines. Controls were age-matched patients in the high cardiovascular risk distribution from causes other than MetS. For each subject, cross-sectional images of aorta (n = 36 to 48) and carotids (n = 12 to 24) were analyzed. Average arterial wall area (AWAr), average and maximal wall thickness and Plaque Index (AWAr normalized to average lumen diameter) were calculated from each resulting image. Average imaging time was 50 minutes. Arterial wall tracings interobserver variation was 4.7%.

*Results:* It was found that atherosclerotic disease was more prevalent in MetS (46.15%) than in high-risk controls (27.78%, $p < 0.05$). Thoracic aorta AWAr was higher in MetS (0.689 $mm^2$ ± 0.19) than high-risk controls (0.55 $mm^2$ ± 0.12, p = 0.017). The remaining arterial wall measurements were not significantly different in these two groups.

*Conclusions:* Early atherosclerotic disease is more prevalent in MetS than in other CHD high-risk groups. Burden of Atherosclerotic Disease in MetS as measured by MRI is increased in thoracic aorta than in the high-risk group counterpart. MRI is a fast, easy, and highly reproducible method for the detection and quantification of subclinical atherosclerotic disease in MetS Patients.

## 493. HYPERTENSION IS ASSOCIATED WITH INCREASED ATHEROSCLEROTIC PLAQUE BURDEN AS QUANTIFIED BY MRI

**Venkatesh Mani, PhD,[1] Silvia Aguiar, MD,[1] Karen B. Weinshelbaum, BA,[1] Hiroaki Taniguchi, MD,[1] Daniel D. Samber,[1] John E. Postley, MD,[2] Robert J. van der Geest, PhD,[3] J. H. Reiber, MD,[3] Zahi A. Fayad, PhD.[1] [1]*Mount Sinai School of Medicine, New York, NY, USA,* [2]*Columbia University, New York, NY, USA,* [3]*Leiden University Medical Center, Leiden, The Netherlands.***

*Introduction:* Hypertension (HTN) is a known risk factor for cardiovascular disease. The purpose of this study was to determine if atherosclerotic plaque burden as measured by MRI in patients with HTN was different than in patients without HTN.

*Methods:* Thirty patients with HTN and 35 control patients matched by Framingham score and 10-year risk but without HTN were imaged using a 1.5T scanner. Using a rapid extended coverage black blood turbo spin echo sequence (REX, 12–24 transverse images 3 mm thick centered on the carotid bifurcation

Table 1. Comparison of MR measures in patients with and without Hypertension

| | Patients without hypertension (Mean ± SD) n = 30 | Patients with Hypertension (Mean ± SD) n = 38 | p value |
|---|---|---|---|
| Framingham Score | 6.5 ± 3.74 | 9.1 ± 4.2 | 0.11 |
| 10 year risk (%) | 10 ± 6 | 16 ± 9 | 0.09 |
| Wall Area Thoracic Aorta ($mm^2$) | 0.99 ± 0.32 | 1.18 ± 0.35 | 0.034 |
| Plaque Index Thoracic Aorta ($mm^2$) | 4.72 ± 1.05 | 5.49 ± 1.32 | 0.011 |
| Plaque Index carotid artery | 3.64 ± 0.76 | 4.1 ± 1.08 | 0.043 |

and 32–48 images 5 mm thick of the aorta from the aortic arch to the level of the iliac bifurcation were obtained from all subjects. Total examination time was <1 hour. Inner, outer vessel wall and diameter of lumen on two axes were measured by manually tracing the vessel wall contours on all MR images. Average wall area of carotids and thoracic aorta and plaque index (vessel wall area normalized to average lumen diameter) for aorta and carotids were also calculated for all images of all patients. All patients with HTN were on anti-hypertension medication.

*Results:* The MRI plaque indices showed that patients with HTN had significantly higher thoracic aorta wall area, thoracic aorta plaque index and carotid plaque index as compared to matched patients without HTN despite the fact that all patients with HTN were on anti-hypertension medication. The results are shown in Table 1.

*Conclusions:* Changes in atherosclerotic plaque burden as a result of HTN can be successfully measured by MRI. MRI may be used to non-invasively detect vascular pathology in hypertensive patients. MRI based measures may be also used to screen patients especially at risk for cardiovascular diseases and as an adjunct to cardiovascular assessment.

## 494. A FAST METHOD FOR MOTION TRACKING OF TAGGED MR IMAGES USING MODIfiED HARP

**Ayman M. Khalifa, MS,[1] Jerry Prince, PhD.,[2] Nael F. Osman, PhD.[2]** [1]***Cairo University, Cairo, Egypt,*** [2]***Johns Hopkins University, Baltimore, MD, USA.***

*Introduction:* HARP is an image processing technique used for rapid analysis of tagged cardiac magnetic resonance imaging

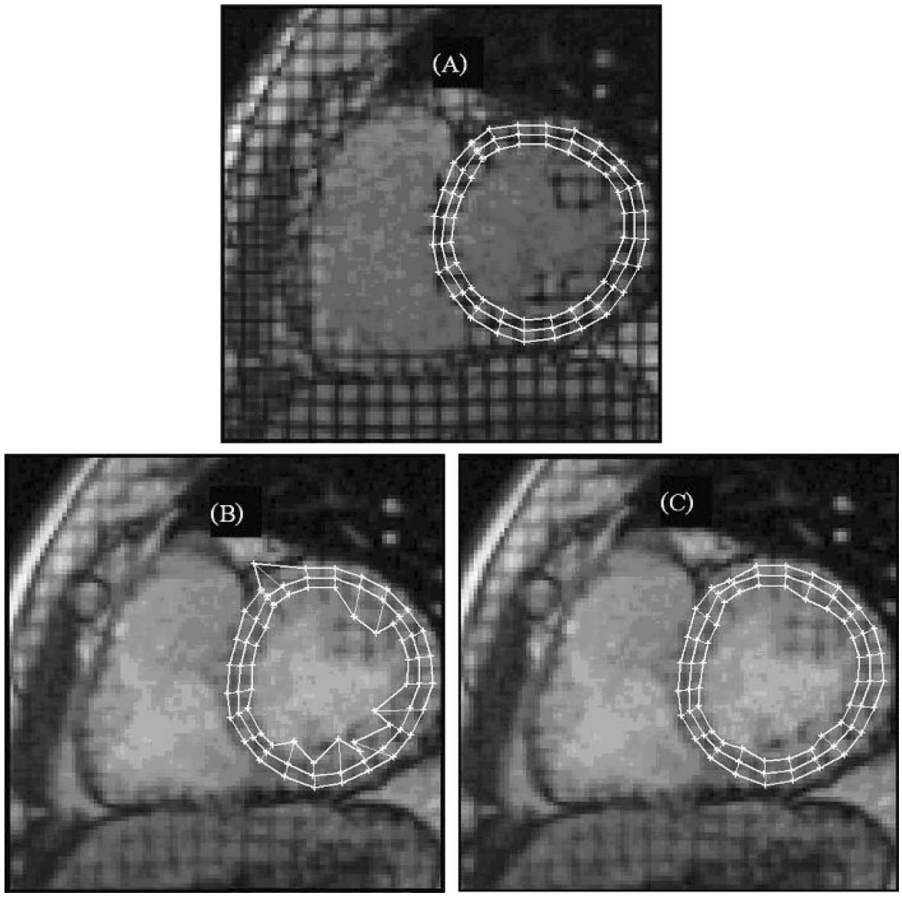


FIG. 1. (A) Manually drawn contour at the first time frame. (B) The contour after HARP tracking at mid diastole. (C) The contour after modified HARP tracking at mid diastole.

(1). HARP can track the motion of any point through a cine of tagged images. Because of regional fading of tags, too-rapid motion, and through plane motion the tracking of some individual points could fail resulting in miscalculation of strain. A modified HARP technique (2) was proposed to correct for these mistracking errors by combining HARP with active contour methods (ACM) (3). However, the technique suffered from long computation time; hence further speed is needed.

*Purpose:* We propose detecting mistracked points and working only on them using the ACM to speed the correction of mistracking. We also propose a new energy function that improves the ability to reach the correct shape of the contour.

*Methods:* We assume that the general geometrical features of the contour are time-invariant. For example, if the shape of a given contour is circular and smooth then it should be the same for subsequent timeframes. Because mistracking disrupts the smoothness of the contour, mistracked points can be detected using the theory of outliers (4). Specifically, we calculate the strain and the second derivative at each point on the contour and compare these values by the values at the previous timeframe. If any of these values is detected for a point as an outlier then this point is considered mistracked. To correct the mistracked points, we define an energy function on the contour that is the summation of the external and internal energies. The external energy at any point is computed from the difference in phase between the current and initial timeframe (phase/time invariance) while the internal energy is calculated from the difference in the internal energy between the current and the previous timeframe (shape/time invariance). The new algorithm was tested by tracking a contour using HARP on good-quality images where no mistracking occurred. The position of one point is changed manually to simulate the mistracking, and the modified HARP is used to identify a mistracked point and correct it. We repeat this for each mistracked point on the contour. The mean and standard deviation of the distance between the correct positions achieved using HAPR and the new positions achieved by the modified HARP after mistracking is calculated.

*Results:* Figure 1A shows the initial contour drawn manually on the first time frame. Fig. 1B shows the contour after tracking using HARP at the mid-diastole. Some mistracked points are observed. Fig. 1C shows the same contour after tracking using the modified HARP. It is obvious that the mistracked points were corrected. The mean and standard deviation in error correction were 0.0657 mm and 0.1929 $mm^2$, respectively.

*Conclusions:* The modified HARP is a robust technique against mistracking of motion using tagged MR images. This will consequently improve the calculations of regional Lagrangian strain.

## REFERENCES

1. Osman NF, et al., Magn Reson Med 1999;42:1048–1060.
2. Khalifa A, et al., SCMR 2004.
3. Kass M, et al., Int J Comput Vision 1988;1(4):321–331.
4. JL. Devore. Probability and Statistics for Engineering and the Sciences. Duxbury Pr.

## 495. TRICUSPID ANNULUS SYSTOLIC PLANE EXCURSION IN ARRHYTHMOGENIC RIGHT VENTRICULAR DYSPLASIA PATIENTS: A FUNCTIONAL MARKER FOR DISEASE PRESENCE

**Robson Macedo, Harikrishna Tandri, MD, Prakasa Kalpana, MD, Joao A. C. Lima, MD, Hugh Calkins, MD, David A. Bluemke, MD, PhD.** ***Johns Hopkins Hospital, Baltimore, MD, USA.***

*Introduction:* Increased right ventricular (RV) volume and reduced RV ejection fraction are hallmarks of arrhythmogenic right ventricular dysplasia (ARVD). RV volume determination, however, is more subjective and complex and less frequently performed compared to left ventricle evaluation.

*Purpose:* The purpose of this study was to evaluate tricuspid annulus systolic plane excursion (TASPE) measured by MRI as a potentially useful marker of ARVD presence/severity.

*Methods:* The study included 18 patients with ARVD meeting Task Force criteria (independently of MRI results) and 20 normal volunteers. All studies were performed with the same 1.5-T MRI system (Signa LX, General Electric Medical Systems, Waukesha, WI, USA) using ECG gating with fiberoptic leads and a thoracic phased-array surface coil for radiofrequency signal

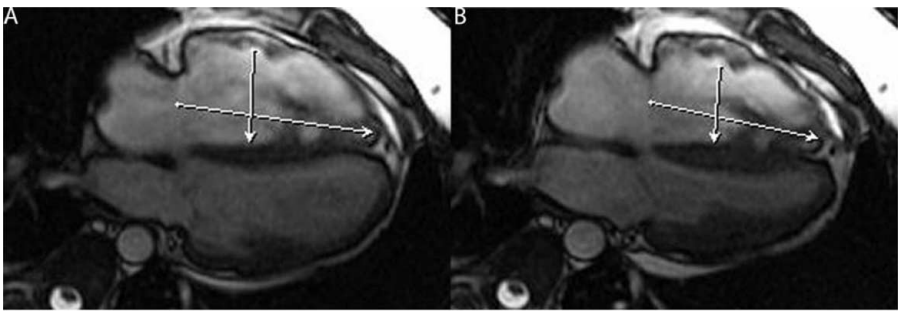


FIG. 1. (A) Bright blood four chamber view image of the heart showing the distance between the tricuspid annulus plane/apex and RV wall/septum in diastole. (B) Bright blood four chamber view image of the heart showing the distance between the tricuspid annulus plane/apex and RV wall/septum in systole.

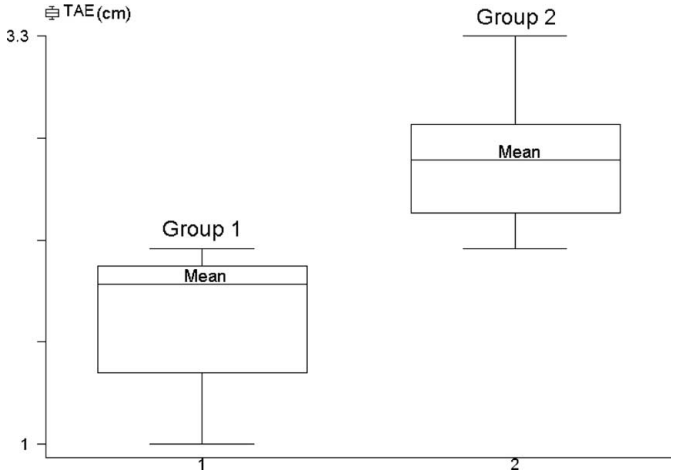


FIG. 2. Tricuspid annulus systolic plane excursion for the ARVD patients (group 1) compared to the normal volunteers (group 2) ($p < 0.0001$).

detection. All MR images were obtained using breath-hold techniques to reduce respiratory motion. For the ARVD group ECG gated black blood images of the myocardium were acquired in the transaxial and/or short axis plane using either double inversion recovery fast/turbo spin echo technique. ECG gated bright blood cine images were obtained using steady state free precession images (FIESTA), in the four chamber and two chambers views for the ARVD and the normal groups. On the four chamber view, the distance between the tricuspid annulus plane and the apex of the heart in both end diastolic and end systolic period of the cine images was determined (Fig. 1). RV shortening was measured as the distance connecting a midpoint at the RV free wall between the moderate band and the tricuspid annulus plane to the septum. RV function and volumes for the ARVD group and for the normal volunteers were determined with the software program MASS (version 6.1, Medis, The Netherlands). Two observers analyzed the MRI images separately in a blinded fashion.

*Results:* The mean TASPE for ARVD patients was 1.7 cm (SD 0.35 cm) and 2.5 cm (SD 0.52 cm) for the normal volunteers (Fig. 2). The decrease in TASPE and RV fractional shortening in ARVD patients compared to normal volunteers was 31.3% and 47.7%, respectively. The sensitivity and specificity for TASPE were 77% and 80%, respectively. TASPE, RV fractional shortening, RV end diastolic volume (RVEDV) and RV ejection fraction (RVEF) were significantly different between the two groups ($p < 0.05$). In 04 patients, there was overlap of TASPE in ARVD with that of the control group (Fig. 3). There was good correlation between the observers for the TASPE measurement.

*Conclusion:* Analysis of TASPE by MRI rather than RVEDV or RVEF is a rapid and reproducible technique that may distinguish ARVD patients from normal patients. This measument has the potencial to be reliable applied for determining the presence/severity of ARVD.

*Acknowledgement:* This work was supported by The Johns Hopkins ARVD program, the Bogle Foundation and the National Institutes of Health Research Grant 1 UO1 HL65594-01A1.

## 496. PULMONARY ARTERY CROSS SECTIONAL AREA AND DISTENSION BY CARDIOVACULAR MAGNETIC RESONANCE IN HEALTHY VOLUNTEERS

**Elisabeth D. Burman, MSc, Philip J. Kilner, MD PhD.** ***Royal Brompton Hospital, London, United Kingdom.***

*Introduction:* Cardiovascular magnetic resonance (CMR) gives unobstructed, non-invasive access to the pulmonary arteries. Abnormalities of pulmonary artery size and distensibility can be of clinical importance in congenital heart disease and pulmonary hypertension, but there is a need to establish standardised

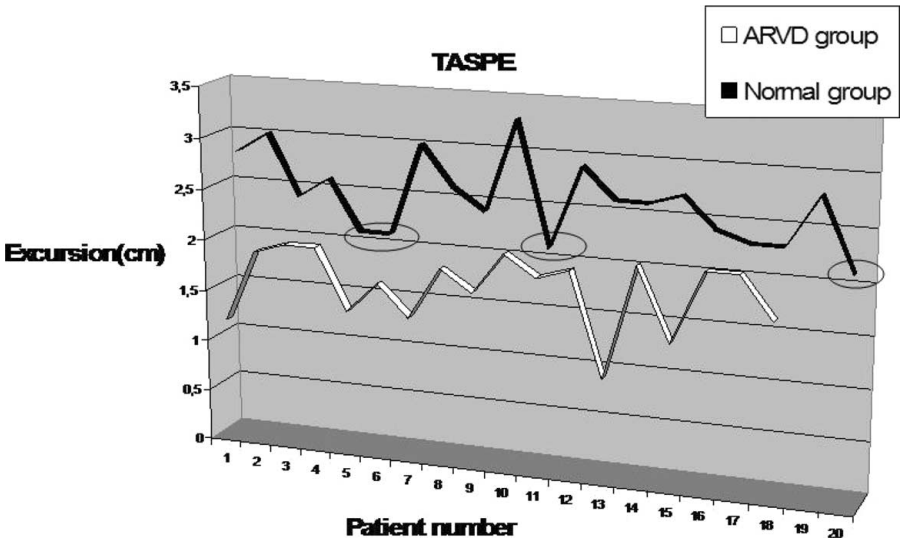


FIG. 3. Tricuspid annulus systolic plane excursion of the ARVD group and the normal group. Overlap of two groups was present in 4 cases (circles).

Pulmonary artery area and % distension

| Age | MPA Diastole | MPA Systole | MPA % | RPA Diastole | RPA Systole | RPA % | LPA Diastole | LPA Systole | LPA % |
|---|---|---|---|---|---|---|---|---|---|
| Male | | | | | | | | | |
| 20–40 | 3.5 ± 0.9 | 5.4 ± 1.0 | 54 | 1.4 ± 0.2 | 2.2 ± 0.4 | 57 | 1.6 ± 0.3 | 2.2 ± 0.5 | 38 |
| 40–60 | 3.8 ± 1.1 | 5.0 ± 1.2 | 32 | 1.7 ± 0.3 | 2.5 ± 0.4 | 47 | 1.9 ± 0.4 | 2.6 ± 0.6 | 37 |
| 60–80 | 3.8 ± 1.4 | 4.9 ± 1.4 | 29 | 2.1 ± 0.7 | 3.0 ± 1.0 | 43 | 2.5 ± 0.6 | 3.3 ± 0.7 | 32 |
| Female | | | | | | | | | |
| 20–40 | 3.6 ± 0.5 | 5.4 ± 0.9 | 50 | 1.6 ± 0.4 | 2.5 ± 0.5 | 60 | 2.1 ± 0.3 | 2.7 ± 0.2 | 29 |
| 40–60 | 3.4 ± 0.6 | 5.0 ± 0.9 | 47 | 1.4 ± 0.3 | 2.1 ± 0.5 | 50 | 1.8 ± 0.2 | 2.4 ± 0.3 | 33 |
| 60–80 | 3.2 ± 0.5 | 4.2 ± 0.8 | 31 | 1.7 ± 0.4 | 2.4 ± 0.5 | 41 | 2.1 ± 0.6 | 2.8 ± 0.7 | 33 |

methods for acquisition and measurement, and to provide the corresponding ranges of normal values with respect to gender and age.

*Purpose:* To measure minimum diastolic and maximum systolic cross sectional areas, and hence systolic distension, of the main, right and left pulmonary arteries (MPA, RPA, LPA) by a defined CMR protocol in healthy men and women in three age ranges.

*Methods:* Sixty healthy normotensive volunteers were recruited (30M, 30F, age range 20–79, average age 48M, 47F). They comprised three age groups, 20–40, 40–60, and 60–80 years, with ten men and ten women in each. CMR was performed using a 1.5T Siemens Sonata scanner. Multislice HASTE transaxial scans and steady state free precession cine imaging in an oblique sagittal RVOT slice, an oblique coronal RPA view, and an oblique sagittal LPA view were used to align cine acquisitions, voxels 6 × 1.4 × 1.6 mm, transecting orthogonally the MPA, RPA and LPA. These 3 cines were used to measure minimum end diastolic and maximum systolic diameters and cross sectional areas, and hence % systolic distension ([maximum area—minimum area] × 100 ÷ minimum area).

*Results:* The measurements are shown in the tables.

*Conclusions:* From the volunteers studied, we provide ranges of normal pulmonary artery area and distension values with respect to gender and age.

## 497. USE OF THE TEICHHOLZ FORMULA IS ASSOCIATED WITH UNDERESTIMATION AND LOWER REPRODUCIBILITY AS COMPARED WITH LEFT VENTRICULAR EJECTION FRACTION DETERMINED BY VOLUMETRIC IMAGING

**Michael L. Chuang, MD,[1] Carol J. Salton, BA,[2] Mark G. Hibberd, MD, PhD,[2] Ahsanuddin Ahmad, MD,[1] Nathan J. Foster, MD,[1] Warren J. Manning, MD.[2]** [1]***Unviersity of Michigan, Ann Arbor, MI, USA,*** [2]***Beth Israel Deaconess Medical Center, Boston, MA, USA.***

*Introduction:* Accurate measurement of ejection fraction (EF) is important for risk stratification and selection of therapy for patients. The Teichholz formula, LVVol = $7D^3/(2.4 + D)$, allows rapid calculation of left ventricular (LV) volume using a single measurement of LV diameter (D), which greatly simplifies data acquisition and analysis. The formula makes allowance for increased LV sphericity as D increases, which may be advantageous compared to other commonly used geometric formulas that assume a constant relationship between long and short-axes despite nonisotropic ventricular dilatation (as seen in, eg, most dilated cardiomyopathy) but nonetheless the Teichholz formula still requires that LV shape conform to its underlying geometric assumptions, which may not be universally valid.

*Purpose:* To determine the accuracy and reproducibility of the Teichholz method in calculation of LV EF, as compared with the reference standard of volumetric cardiovascular magnetic resonance imaging (CMR).

*Methods:* Forty adults (11 women, 29 men, ages 23–76) with left ventricles free of aneurysmal dilatation underwent multislice breathhold cine CMR on a 1.5-T scanner. For volumetric imaging, endocardial contours were manually segmented and LV volumes at end-systole and end-diastole were determined using a summation of disks method; volumetric EF (volEF) was the ratio of stroke volume to end-diastolic volume. Volumes and EF were also calculated using the Teichholz formula (tEF), where D was determined at end-diastole and end-systole from a CMR LV short-axis image plane immediately basal to the papillary muscle tips. We have previously shown that end-diastolic volume is overestimated by the Teichholz method and developed a "corrected Teichholz" formula (cLVVol = $4.06^*D^3/(D+2.4) + 8.6$ (1), so EFs were also calculated using this corrected formula for LV volumes. Finally, 20 subjects underwent 2 serial CMR studies to assess reproducibility of volumetric and Teichholz measures of LV EF. Continuous variables are summarized as mean ± standard deviation (SD) and Student's t test was used to compare means, with $p < 0.05$ considered significant. Reproducibility for volumetric and Teichholz EFs was assessed using the Bland-Altman method.

*Results:* volEF = 0.595 ± 0.149 (range 0.183 to 0.756) was significantly greater than tEF = 0.514 ± 0.155 (range 0.031 to 0.694), $p < 0.001$. Linear regression revealed volEF $= 0.88^*$tEF$+0.143$, $r = 0.916$. Use of the "corrected Teichholz" formula for converting Teichholz to equivalent volumetric LV volume still resulted in systematic underestimation of EF by the

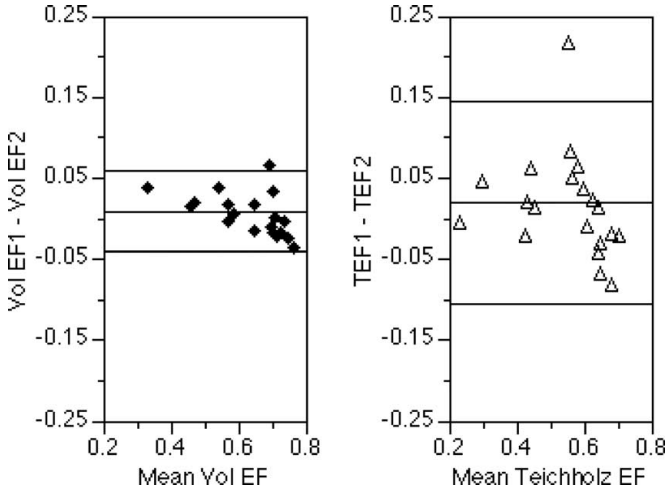


corrected Teichholz formula, $p < 0.001$. Limits of agreement (mean bias $\pm$ 2SD) between repeat studies were $0.009 \pm 0.052$ (volEF) and $0.020 \pm 0.128$ (tEF), as shown in the Figure, where the left panel (closed diamonds) represents volumetric EF and the right panel (open triangles) represents Teichholz EF.

*Conclusions:* The Teichholz formula continues to be used in clinical and research settings as it allows rapid estimation of LV volume and EF. However, volumetric and Teichholz EFs are not interchangeable. Teichholz EF significantly underestimates volumetric ("true") EF in both clinical and statistical terms. Further, volumetric measures of LV EF are substantially more reproducible than Teichholz EF which is determined using linear measurements combined with a geometric formula. Thus volumetric measures of EF are preferred as their use would allow detection of smaller changes in EF between serial studies as compared with the Teichholz method.

## REFERENCE

1. Salton, et al. SCRM 2005.

## 498. NORMAL HUMAN LEFT AND RIGHT VENTRICULAR AND LEFT ATRIAL DIMENSIONS USING STEADY STATE FREE PRECESSION MAGNETIC RESONANCE IMAGING

**Lucy E. Hudsmith, MRCP MA BM BCh, Steffen E. Petersen, MD, Jane M. Francis, DCCR, DNM, Matthew D. Robson, PhD, Stefan Neubauer, MD FRCP.** ***Oxford University, Oxford, United Kingdom.***

*Introduction:* Cardiovascular magnetic resonance imaging (CMR) has become the gold standard method for the characterisation of cardiac anatomy, function and mass. It is an accurate and reliable technique for the serial monitoring of patients, particularly in response to therapeutic intervention. CMR is a well-tolerated, non-invasive technique with no known side-effects and is becoming increasingly available to the clinician. However, most current published databases for normal values are based on outdated fast low angle shot (FLASH) sequences.

*Purpose:* The aim of this project was to establish normal values for left and right ventricular and left atrial volumes, mass and function, using steady-state free precession cardiac magnetic resonance imaging, the clinical technique of choice, across a wide age range and to investigate the effect of age and sex on these parameters in healthy volunteers.

*Methods:* One hundred eight healthy volunteers (63 male; mean age $38 \pm 12$ years, range 21–68 years) were recruited with no history of cardiac disease, hypertension or cardiac risk factors and a normal electrocardiogram (ECG) and underwent cardiac magnetic resonance (CMR) imaging using steady-state free precession sequences. All CMR examinations were performed on a 1.5 Tesla MR scanner (Sonata, Siemens Medical Solutions, Erlangen, Germany) with integrated spine coil and phased array surface coil, prospective electrocardiographic gating and the patient in the supine position. After piloting, a horizontal long-axis, vertical long-axis and short-axis pilots, steady-state free precession cine images (TE/TR 1.5/3.0 ms, flip angle 60°, slice thickness 7 mm, 3 mm inter-slice gap, in-plane resolution $1.5 \times 1.5$ $mm^2$, temporal resolution 45 ms, breath-hold duration of 14–17 heartbeats per breath-hold) were acquired in the horizontal and vertical long axis views during breath holding in end-expiration. The short axis stack was then obtained, parallel to the atrioventricular groove, covering the entire left and right ventricle. The left atrial volumes, ejection fraction and stroke volume were measured using the biplane area-length method in the horizontal and vertical long axes. Manual analysis was performed by

Reproducibility of measurements

| | Intraobserver | | Interobserver | | Interstudy | |
|---|---|---|---|---|---|---|
| | Bias (95% Limits of Agreement) | CoV | Bias (95% Limits of Agreement) | CoV | Bias (95% Limits of Agreement) | CoV |
| LV ejection fraction | 0.5 (−2.6 to 3.5) | 2.3 | 1.6 (−2.8 to 6.0) | 3.3 | 0.5 (−9.1 to 10.1) | 7.5 |
| LV end-diastolic volume index | 4.6 (−4.4 to 13.7) | 5.6 | 0.4 (−3.8 to 4.6) | 2.7 | −1.4 (−9.7 to 6.9) | 5.2 |
| LV mass | 5.4 (−6.8 to 17.5) | 6.1 | 5.8 (−4.4 to 16.0) | 5.2 | 1.8 (−17.9 to 21.6) | 9.4 |
| RV ejection fraction | 0.1 (−6.2 to 6.4) | 5.3 | −2.8 (−15.2 to 9.1) | 10.7 | 1.9 (−11.48 to 15.2) | 11.4 |
| RV end-diastolic volume index | −3.2 (−18.8 to 12.5 | 9.0 | −0.1 (−16.7 to 16.5) | 9.6 | 0.7 ( − 21 to 4.3) | 7.4 |
| LA ejection Fraction | −1 ( − 18 to 17) | 16.4 | 4.4 ( − 6 to 15) | 9.6 | −3 ( − 19 to 12) | 14.7 |

CoV = Coefficient of Variability.

2 experienced observers with Argus software (Version 2002B, Siemens). Interobserver, interstudy and intraobserver variability was assessed.

*Results:* Left and right ventricular volumes and left ventricular mass were larger in males than females: LV end-diastolic volume 160 ± 29 mL versus 135 ± 26 mL, LV end-systolic volume 50 ± 16 mL versus 42 ± 12 mL; RV end-diastolic volume 190 ± 33 mL versus 148 ± 35 mL, RV end-systolic volume 78 ± 20 mL versus 56 ± 18 mL ($p < 0.05$ for all). Normalisation of values to body surface area removed the statistical differences for LV volumes, but not for LV mass or RV volumes. With increased age, males showed a significant decrease in volume and mass indices for both ventricles, while female values remained unchanged. Compared to females, males had significantly larger maximal left atrial volumes (103 ± 30 mL versus 89 ± 21 mL, $p = 0.01$) and left atrial stroke volumes (58 ± 23 mL versus 48 ± 15 mL, $p = 0.01$). There was no difference in left atrial ejection fraction between the sexes. Variability is shown in the Table.

*Conclusions:* We have shown significantly different volumes with gender, and significant differences in age-specific left and right ventricular volumes, mass and ejection fraction in males but not in females. We have produced a large database for left and right ventricular and left atrial volumes of healthy volunteers using SSFP images at 1.5 T which will be of particular use for reference in both clinical and research studies. We have also demonstrated the use and limitations of the biplane area-length method to acquire left atrial volumes and ejection fraction.

## 499. INITIAL EXPERIENCE WITH CARDIAC IMAGING USING A SHORT, WIDE BORE 1.5T SYSTEM

**Peter Kellman, PhD, Christine Mancini, W. Patricia Bandettini, MD, Elliot R. McVeigh, PhD, Andrew E. Arai, MD.**
***National Institute of Health, Bethesda, MD, USA.***

*Introduction:* We present our initial experience with cardiac MR on a short, wide bore system. The wide bore 1.5T MR system provides a new capability for imaging large and claustrophobic patients but also presents unique challenges for cardiac MR due to a reduction in FOV in the z-direction. The image quality, imaging speed, and FOV are characterized for the short, wide bore system as compared to the standard bore 1.5T systems.

*Purpose:* To demonstrate the feasibility of cardiac MR imaging using a short, wide bore 1.5T system.

*Methods:* A cardiac MR protocol consisting of localization (trueFISP), cine function (trueFISP), 1st pass perfusion (GRE-EPI or turboFLASH), and delayed enhancement (turboFLASH) was used to image patients (weighing up to 404 lbs) using the Siemens Magnetom Espree 1.5T system (70 cm bore, 125 mm length, 33 mT/m, SR 100T/m/s). A total of 51 patients were scanned (5 patients > 300 lbs). Parallel imaging (rate = 2) was used for localization and cine (GRAPPA), as well as perfusion (TSENSE). Siemens product spine and body array coils (12 elements) were used. The reduction in imaging speed due to reduced gradient performance of the wide bore system was measured for each protocol and compared with equivalent protocols on the Avanto with higher performance gradients (45 mT/m, SR 200 T/m/s). The z-FOV was measured using the sagittal localizer as the region clear of banding artifacts since the trueFISP sequence is highly sensitive to off-resonance caused by field inhomogeneity. Myocardial SNR was measured for cine images, and artifacts due to off-resonance effects were noted.

FIG. 1. Sagittal TrueFISP localizer for patient weighing 404 lbs.

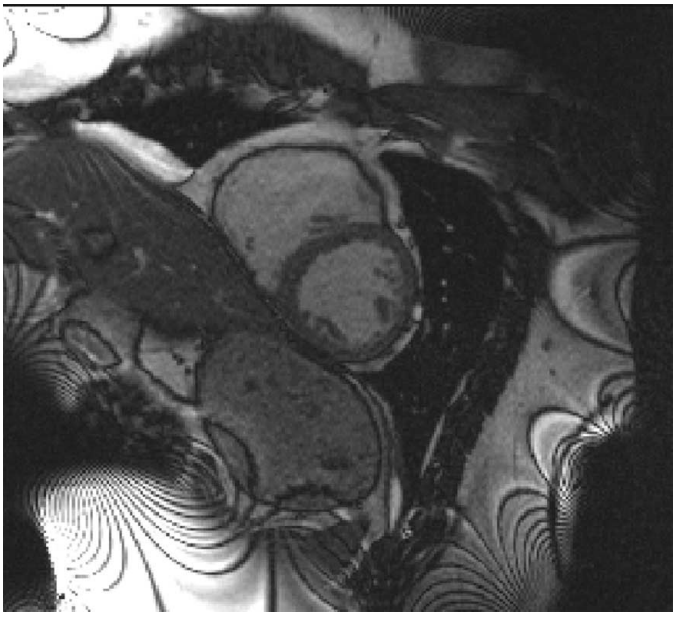

FIG. 2. TrueFISP retrogated cine image for patient weighing 404 lbs.

*Results:* The trueFISP FOV was shortest in the z-direction, and was measured to be 22.6 ± 0.9 cm (m ± sd, N = 51). An example sagittal localizer is shown in Fig. 1 illustrating the banding artifacts due to field inhomogeneity. TrueFISP cine artifacts due to blood flow (predominantly LAX views) were minimized by moving the table position such that the aortic arch was not outside the usable trueFISP FOV. Table positioning and re-positioning was straightforward. Banding artifacts for cine images are outside the heart region (Fig. 2). The worst case myocardial SNR for large patients was >10 for cine imaging using parallel imaging (SENSE g-factor was less than 1.2). Protocols optimized to achieve equivalent spatial and temporal resolution to standard bore systems with high performance gradients had reduced speed: 9 vs 8 heartbeats breath-hold duration for retrocine (256 × 160, temporal resolution = 43 ms), 125 vs 111 ms/slice including SR prep (75 vs 61 ms imaging duration) for GRE-EPI perfusion (128 × 80), 8.7 vs 8.4 ms TR for delayed enhancement. The temporal resolution of the most demanding highly accelerated (rate = 4) real-time, trueFISP sequence used for patients with arrhythmia was increased, 53 vs 42 ms (128 × 72). Parallel imaging artifacts (phase encode wrap) were observed in several cases due to high field inhomogeneity at the edge of the FOV for trueFISP and GRE-EPI sequences. In the k-space methods (GRAPPA), the effective non-linear gradient in the banding region caused artifacts, where as in image domain methods (TSENSE) artifacts resulted from GRE-EPI off-resonance ghosting. There were no parallel imaging artifacts observed using turboFLASH perfusion with TSENSE.

*Conclusions*: Cardiac MR imaging with the short, wide bore 1.5T system is feasible and it was possible to image subjects that were previously too large for standard bore systems (up to 404 lbs to date). Temporal resolution equivalent to that achieved with higher performance gradients was possible within reasonable breath-hold durations. Artifacts due to field inhomogeneity were generally outside the heart region. All studies were diagnostic quality.

## 500. MYOCARDIAL TAGGING AT 3.0T: IMPROVED TAG PERSISTENCE AND CONTRAST-TO-NOISE RATIO IN COMPARISON TO 1.5 T

**Ulrich Kramer, MD,[1] Vibhas Desphande, PhD,[2] Michael Fenchel, MD,[1] Gerhard Laub, PhD,[2] Paul J. Finn, MD,[2] Claus D. Claussen, MD,[1] Stephan Miller, MD[1]** [1]***Universiy of Tuebingen, Tuebingen, Germany,*** [2]***Universiy of Los Angeles, Los Angeles, CA, USA.***

*Introduction:* Using gradient echo (GRE) sequences, tag persistence is largely dependent on T1 times of the myocardium and flip angle. With longer myocardial T1 at 3T, tag persistence is expected to be better than at 1.5T.

*Purpose:* Therefore aim of this prospective study was the optimization of a GRE MR tagging sequence at 3.0T in comparison to 1.5T in order to get best image contrast between myocardium, tag lines and blood signal. Second, calculations of theoretically expected improvements of signal-to-noise (SNR) and contrast-to-noise (CNR) ratios were performed.

*Methods:* Seventeen consecutive healthy subjects (mean age 43.2 years) and 3 patients were scanned at a 1.5T and a 3T whole body scanner (Siemens) to evaluate image quality and tag persistence. The first 6 volunteers were imaged at only one field strength to optimize the protocol with respect to slice thickness, tag thickness and readout bandwidth. After optimization, these parameters were kept constant for the remaining volunteers (n = 11) as well as the patients (n = 3). Since one of the major factors determining tag persistence is the flip angle, it was varied from 6 to 16 deg (increments of 2 deg) at both field strengths. For each flip angle, the SNR, CNR and relative contrast myocardium-to-tag (RCMT) were evaluated. RCMT was calculated as: (Signal of untagged myocardium - Signal of tag)/(Signal of untagged myocardium). A prospectively triggered gradient-echo sequence was used. Sequence parameters were as follows: TR/TE = 5.2 ms/3.7 ms, slice thickness 6 mm, tag thickness 8 mm (grid tags), temporal resolution 46 ms.

*Results:*While the conspicuity of the tags is greatly reduced in the diastolic phase in the images acquired at 1.5T, tags are clearly visible in the myocardium in all phases at 3T. From the first 6 volunteers used for optimizing the imaging parameters, a slice thickness of 6 mm and a tag thickness of 8 mm were found to be suitable. The choice of the flip angle for the patients was based on the data acquired in consecutive 11 volunteers. At 1.5T, the optimal flip angle was found to be 12 deg while that at 3T was found to be 8 deg based on overall image quality, SNR and tag conspicuity (RCMT). Blood SNR was higher at 3T despite the lower flip angle. RCMT was also found to be higher at 3T than at 1.5T significantly.

*Conclusions:* Myocardial tagging at 3.0T has shown a superior image quality in comparison to 1.5T due to a higher baseline SNR and an improved CNR as well as RCMT. As a consequence of suppressed fading of the tags, the accessibility to the diastolic phase of the cardiac cycle becomes possible.

## 501. REPRODUCIBILITY OF MYOCARDIAL TISSUE VELOCITIES MEASURED WITH MRI AND TDI

**Jana G. Delfino,[1] Mohit Bhasin,[2] Robert Cole,[2] Angel R. Leon,[2] Robert L. Eisner,[2] John Merlino,[2] John N. Oshinski[1]** [1]***Georgia Insitute of Technology/Emory University, Atlanta, GA, USA,*** [2]***Emory University, Atlanta, GA, USA.***

*Introduction:* Patients are diagnosed with ventricular dyssynchrony based on prolonged QRS duration on a surface electrocardiogram or by velocity and timing parameters from Tissue Doppler imaging (TDI). TDI is an echocardiographic method that measures longitudinal (apex-to-base) velocity of the myocardial wall. Magnetic Resonance Phase Velocity Mapping

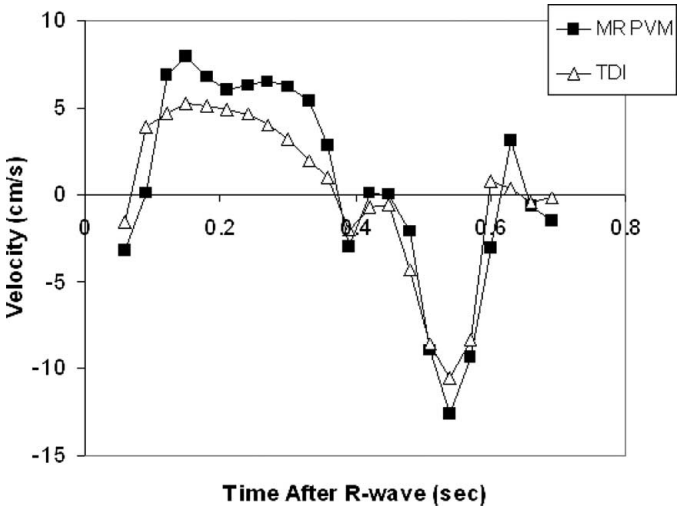


FIG. 1.

(MR PVM) can also measure myocardial wall velocities and has some potential advantages over TDI, including the abiltity to measure 3- velocity directions throughout the myocardium. However, MR PVM has not been evaluated in dyssynchrony patients, has not been rigorously compared to TDI, and the repeatability of both techniques has not been evaluated in the same set of subjects.

*Purpose:* The purpose of this study is to compare measurements of longitudinal myocardial velocities by MR PVM and TDI in normal volunteers and patients with ventricular dyssynchrony, and to assess the repeatability of both techniques in normal volunteers.

*Methods:* Ten normal volunteers (age 28.6 $\pm$ 7.72) and ten patients (age 61.8 $\pm$ 15.63) diagnosed with asynchrony (QRS $>$120 msec and LVEF $<$ 35%) participated in the study. Apex-to-base velocities in the septal and lateral myocardial walls were examined in the 4-chamber view by digital color-coded TDI using a General Electric Vivid 7 system. Regions of interest (8 $\times$ 8 mm) were placed in the myocardial wall at 70% of the distance from apex to base. Values of velocity vs. time were digitized and exported to a spreadsheet. MRI scans were performed on a Philips Medical Systems Intera CV MRI scanner on the same day as TDI. A segmented, navigator-echo and ECG-gated sequence acquired velocity in the thru-plane (apex-to-base) direction on a short axis slice positioned at 70% of total LV length. Regions of interest (8 $\times$ 8 mm) corresponding to the locations measured by TDI were selected in the septal and lateral walls. The imaging protocol was repeated on a subsequent day in normal subjects to assess reproducibility. MR-TDI velocity values were compared using a linear regression analysis. Peak velocities (systolic and diastolic) measured by TDI and MRI were compared using a two-tailed t-test. Agreement between MRPVM and TDI was assessed using Bland-Altman analysis. Reproducibility of MR and TDI data was calculated by comparing peak velocities and time to peak velocities between repeated scans by the coefficient of variation (CV = standard deviation of repeated measurements divided by their mean).

*Results:* Velocities measured with MR PVM correlated well with velocities measured by TDI in both normal subjects and dyssynchrony patients (r = 0.86). The correlation coefficient was greater for normal subjects (0.88 in the septal wall, 0.88 in the lateral wall) than for dyssynchrony patients (0.78 in the septal wall, 0.72 in the lateral wall). Time to peak velocities measured by MR and TDI correlated strongly (r = 0.97). Fig. 1 shows velocity curves in the septal wall of a normal volunteer. Excellent reproducibility was observed in repeated MR PVM and TDI measurements. The coefficient of variation (CV) between repeated measurements of peak velocity was 11.0% for MR and 13.1% for TDI, p = NS. Bland-Altman analysis showed a mean difference of 0.12 $\pm$ 1.9 cm/s for repeated TDI measurements and-0.51 $\pm$ 2.1 cm/s for repeated MRI measurements, Fig. 2. The CV for repeated time to peak velocity measurements was 5.7% by MR and 9.1% by TDI, p = NS.

*Conclusions:* MR and TDI correlate strongly in measuring myocardial tissue velocity and time to peak velocity in both

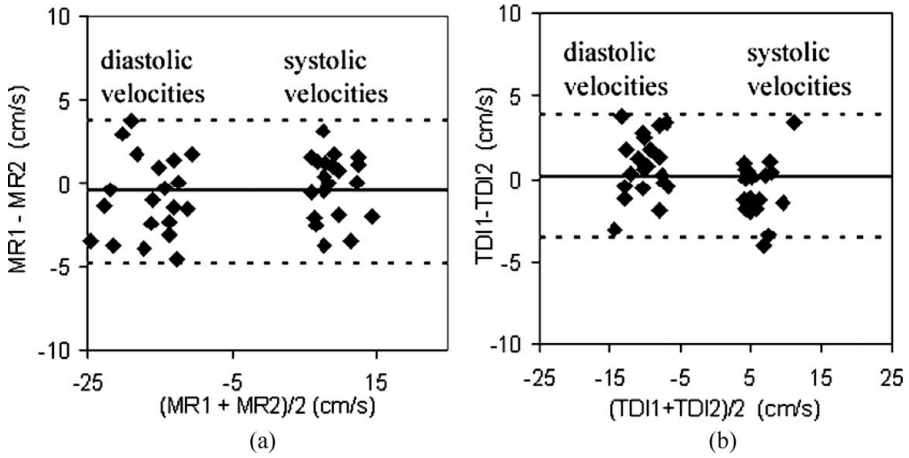


FIG. 2.

normal subjects and patients with dyssynchrony. Reproducibility was comparable for MR PVM and TDI for measuring both peak longitudinal myocardial tissue velocity and time to peak velocity. MR may provide an alternative method for detecting cardiac dyssynchrony.

## 502. EVALUATION OF THE MYOCARDIAL SCARS PATTERN OF LATE GADOLINIUM-ENHANCED CMR IN THE DIAGNOSIS OF NON-ISCHAEMIC CARDIOMYOPATHIES; COMPARED WITH ISCHAEMIC CARDIOMYOPATHIES

**Shintaro Kiuchi, MD, Kunihiko Teraoka, MD, Kuniomi Ooi, MD, Masanobu Yoshida, MD, Mineko Kino, MD, Hiroshi Kobayashi, MD, Kenji Takazawa, MD, Akira Yamashina, MD.** ***Tokyo Medical University Hatioji Medical Center, Tokyo, Japan.***

*Purpose:* We investigated the pattern of hyperenhancement detected by DE-CMR to distinguish ischaemic cardiomyopathy (ICM) from non-ischaemic cardiomyopathy (NICM).

*Methods & Results:* We performed DE-CMR in 87 patients with ICM (n = 67) or NICM (n = 20) with less than 35% LVEF. The systolic dysfunction in both groups were quite severe (mean LVEF 27 ± 6% in ICM and 22 ± 8% in NICM). Hyperenhancement was found in 100% of patients with ICM in 55% with NICM ($P < 0.0001$). The hyperenhancement pattern in all ICMs involved the subendocardium and grew towards the epicardium (transmural). In twenty patients with NICM, 12 patients were diagnosed with DCM, four patients were dilated-HCM, three patients were cardiac sarcoidosis and one was mitral regurgitation (MR). Fifty percent (6 patients) of patients with DCM had hyperenhancement, the pattern of hyperenhancement occurred in 5 patients with DCM was linear hyperenhancement limited to the midmyocardium of the ventricular wall and one patient with DCM was found only subendocardial hyperenhancement. All patients with dilated-HCM had hyperenhancement involving at the junctions of the interventricular septum and the right ventricular free wall. All cardiac sarcoidosis had hyperenhancement was found mid-myocardial wall, subendocardium or epicardium. A patient with MR had no hyperenhancement.

*Conclusions:* The pattern of hyperenhancement demonstrated by DE-CMR is useful non-invasive imaging modality to distinguish ICM from NICM.

## 503. T2-WEIGHTED CARDIAC MAGNETIC RESONANCE IMAGING DELINEATES AREA AT RISK IN THE ABSENCE OF REPERFUSION INJURY 2 DAYS POST-INFARCTION

**Gauri S. Tilak, Li-Yueh Hsu, Andrew E. Arai, Anthony H. Aletras.** ***National Institutes of Health, Bethesda, MD, USA.***

*Purpose:* The aim of this paper was to determine whether edema imaging by T2-weighted CMR could be used as an 'ischemic memory' imaging tool for retrospectively delineating the hypoperfused area at risk in non-reperfused myocardial infarction i.e. in the absence of reperfusion injury. We hypothesized that the area at risk by MR perfusion during a permanent occlusion would be of similar size to the T2 abnormality observed two days later, and that the T2-weighted hyperintense region would exhibit myocardial hypokinesis.

*Methods and Results:* Fourteen dogs underwent permanent coronary artery occlusion. The area at risk, as measured with MR perfusion, was comparable to the size of the hyperintense zone on T2-weighted images 2 days later (36.3% ± 3.3% vs. 38.9% ± 3.0%, p = NS) but was significantly larger than the infarcted zone as measured by triphenyl tetrazolium chloride (TTC) staining (28.7% ± 3.0%; p-value < 0.01). The hyperintense myocardium on T2-weighted images exhibited depressed systolic strain as demonstrated with DENSE (displacement encoding with stimulated echoes), circumferential shortening (CS) = 2.6% ± 1.0%, radial thickening (RT) = 1.0% ± 1.3%) compared to the remote zone (CS = 16.6% ± 0.8%, RT = 25.5% ± 0.5%, p < 0.001 for both).

*Conclusions:* T2-weighted imaging satisfies the definition of "ischemic memory" in the absence of reperfusion injury since the hyperintense region of edema 2 days after non-reperfused myocardial infarction corresponds to the ischemic area at risk.

## 504. DELAYED ENHANCED MYOCARDIUM EVALUATED IN ACUTE PHASE AFTER AMI IS A BETTER PREDICTOR OF REMODELLING COMPARED WITH FOLLOW-UP

**Giovanni Donato Aquaro, Alessandro Pingitore, Elisabetta Strata, Gianluca Di Bella, Daniele De Marchi, Vincenzo Positano, Massimo Lombardi.** ***Institute of Clinical Physiology, MRILab, pisa, Italy.***

*Introduction* : In acute myocardial infarction Delayed Enhanced Magnetic Resonance (DMR) is an useful tool to evaluate and measure the extent of damaged myocardium (necrosis, microvascular obstruction and oedema) in acute phase and scar in chronic phase.

*Purpose*: To evaluate the role of Delayed Enhancement (DE) as a predictor of remodelling in acute and chronic phase following AMI.

*Method*: Twenty patients (17 males; mean age 61 years) with AMI treated with primary PTCA with stenting were enrolled. All the patients underwent to a first MRI examination after a mean of 6 ± 3 (range 3–9 days) days following admission and a follow-up examination after a mean of 160 ± 35 days (range 103–230 days). Study protocol included a contrast-enhanced MR evaluation of DE using a T1 weighted inversion recovery sequence with a prepulse delay to null signal from normal myocardium.

Images from 10 to 15 short axis and horizontal and vertical long axis views were acquired ten minutes after contrast injection. LV volumes and mass were obtained with FIESTA sequence from 10 to 15 short axis slices from mitral plane valve to apex. A software tool was used to detect endocardial and epicardial contours and to quantify the global (GDE) and the transmural (TDE) extent of DE. The same protocol was used in the follow-up examination. The ratio between mass and EDV (LVM/EDV) was chosen as remodelling index using a cut off value of less than 0.7.

*Results*: All the patients completed both the MR exam without complication. Mean GDE was 20.5 ± 10.2% at the first MR exam (GDE1), 10.7 ± 6.4% at the follow-up (GDE2) with a mean reduction of 54.7 ± 28.4%. Mean TDE was 22.5 ± 11.4%. Mean improvement in ejection fraction (EF) at the follow-up was 8.9 ± 6.9. Mean LVM/EDV was 0.89 ± 0.22. Seven patients (35%) had a LVM/EDV less than 0.7 showing also a significant lower EF (49.4 vs 57.4% $p < 0.05$). At the ROC analysis GDE1 (cut-off 21.16%) had a 100% of sensitivity and 84.6% of specificity to predict a Mass/EDV ratio less than 0.7 while GDE2 (cut-off 10.6%) showed 80% sensitivity and 83% of specificity; TDE showed a 100% sensitivity and 76.9% specificity to predict remodelling (cut off 22.29%). The product between GDE1 and TDE (PDE) as a combined index (cut-off 636) had 100% sensitivity and 92.3% specificity to predict remodelling.

*Conclusion*: In acute myocardial infarction global and transmural extent of DE evaluated in acute phase is a good predictor of remodelling with higher sensitivity and specificity if compared with global DE at follow-up. The combined index can improve specificity.

## 505. A NOVEL CORONARY ARTERY SEGMENTATION ALGORITHM OPTIMIZED FOR MR: THE SIGNIFICANCE OF PRE-PROCESSING FILTERS

**Allen J. Keel, Noah Lee, David Lesage, Shmuel Aharon, PhD, Matthias Rasch, PhD, Christine Lorenz, PhD.** ***Siemens Corporate Research Inc, Princeton, NJ, USA.***

*Introduction:* CT has recently dominated the area of noninvasive coronary imaging, in part due to the ability to segment and visualize the coronaries automatically from high resolution, high contrast-to-noise CT data. However, an equivalent segmentation in MR datasets is very difficult due to the inherent qualities of MR images:lower contrast, lower spatial resolution, and more noise, including motion.

*Purpose:* We hypothesized that an optimized pre-processing algorithm could alleviate some of the shortcomings of MR, and provide a basis for semi-automatic segmentation of the coronary tree in MR. Keeping user interaction to a minimum (ie, least number of seedpoints) was one of the specific aims. Another key objective was to eliminate boundary leakage into surrounding tissue, while avoiding undersegmentation.


FIG. 1. Segmentation of entire coronary tree RCA (green), LCA/LCX.

*Methods:* The segmentation algorithm as a whole can be divided into two aspects: pre-processing and post-processing. For post-processing, which is the actual segmentation process, a multi-layered fast-marching algorithm is employed. At the voxel level, a multiscale "vesselness" measure, which represents the geometric similarity to a tubular shape, is calculated according to the second-order variations of the Hessian matrix. A gray-level statistics score is calculated, based on an adaptive estimation of the intensity distribution in the vessel. After multiplication by the weights, these two scores are summed up, and a final score s(p) (0–1) is computed. If the final score is above a threshold T, then the voxel is accepted into the segmentation. After experimenting with different weight parameters, the ones yielding the optimal segmentation results for MR were found. The pre-processing pipeline consists of (in following order): supersampling, an unsharp masking filter, and a de-noising filter. In MRI, the diameter of the coronary vessel can be as low as 2 pixels in basal slices. Supersampling consists of upsampling to a higher resolution, lowpass filtering, multiplying by the Fourier gain, and taking the inverse Fourier transform. This procedure adds more pixels and therefore facilitates front propagation throughout the entire artery. This procedure was followed by unsharp masking, which enhances the edges of the vessel to prevent leaking. De-noising was performed by using a 3D anisotropic diffusion filter (1), and this removes the noise surrounding the vessel. Nonlinear diffusion makes the diffusivity parameter a function of the concentration gradient, which decreases for high gradients. Image

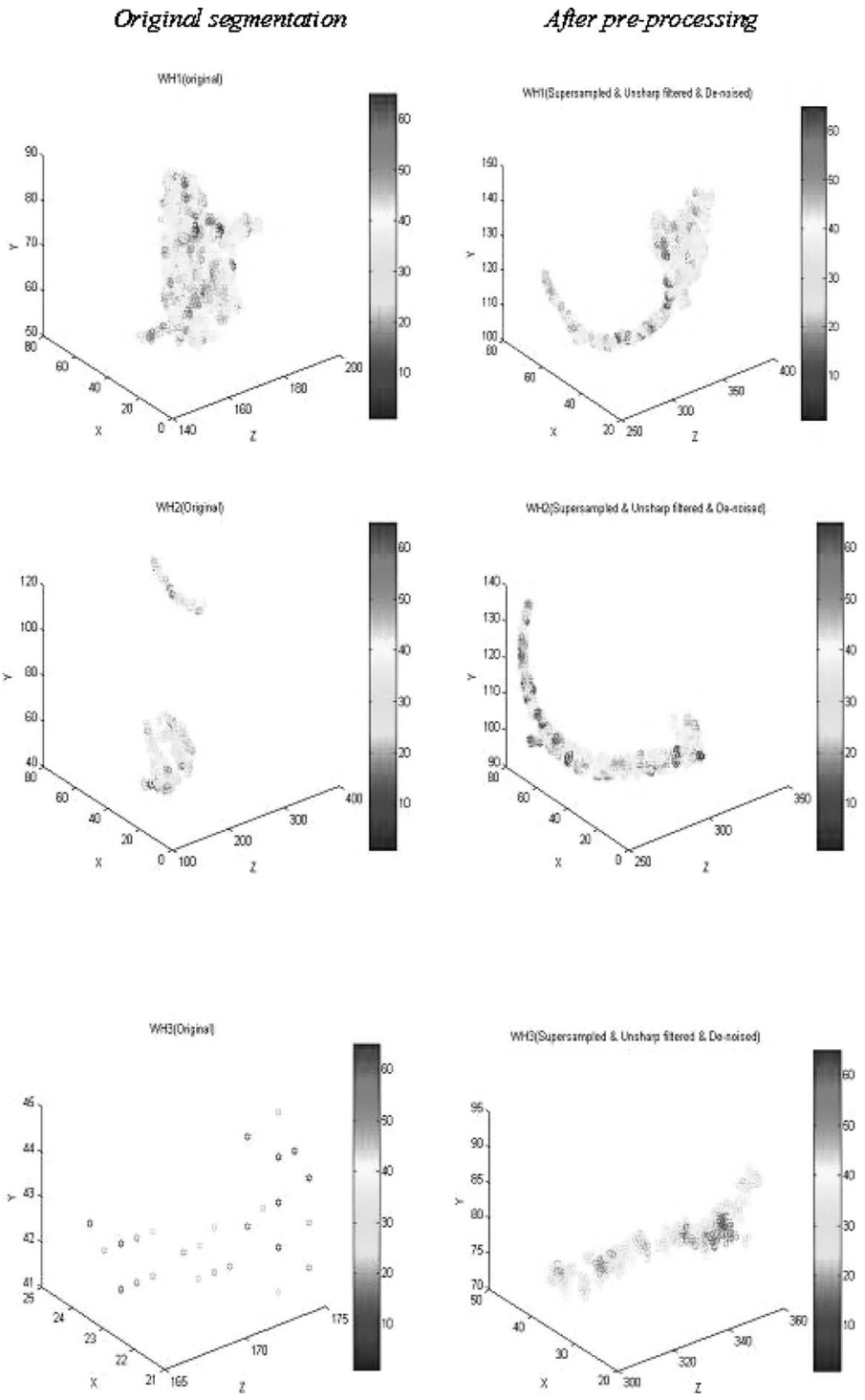


FIG. 2. Segmentaion of RCA only (single seedpoint).

borders are therefore not affected. The resulting image can then be processed by the segmentation algorithm, which includes a vessel centerline that can then be used to navigate the original data. The studied datasets (n = 5) were navigator gated, axial whole-heart coronary MR scans acquired using a True-FISP pulse sequence, using T2-preparation, on a Siemens 1.5 T Avanto scanner (FOV/Matrix = 190 × 320, TR/TE = 3.9/1.5 ms, Flip angle = 90°, 120 slices, 1 mm thick, TA = 10:10 min).

*Results:* For each dataset, the centerline coordinates of the vessel were overlaid on a volume-rendered image (examples shown below). In addition to virtually eliminating boundary leakage out of the vessel, the pre-process series increased the

through-plane (apex-to-base) RCA propagation by an average of ~400%, all with just a single seedpoint. Although the LCA and LCX required roughly a combined 5 to 7 seedpoints to track through all the branching, the segmentation error was minimal.

*Conclusions:* Preprocessing the MR images prior to segmentation improved the results significantly. In each of the five datasets, the RCA was successfully segmented with only one user-defined seedpoint. Overall, the pre-processing increased the CNR and the spatial resolution of the MR volumes, as a positive step toward fully satisfying the challenge of coronary segmentation in MR.

*Acknowledgment:* The authors thank Vibhas Deshpande and Gerhard Laub, Siemens, UCLA for use of the images.

## REFERENCE

1. Perona P, et al. IEEE 1990;12;1–11.

## 506. IDENTIFICATION OF PEAK BIOCHEMICAL MARKERS IN ACUTELY REPERFUSED PATIENTS PROVIDES ACCURATE ESTIMATION OF MYOCARDIAL INFARCT SIZE AS DETERMINED BY DELAYED CONTRAST-ENHANCED MAGNETIC RESONANCE IMAGING

**Erik Hedström, PhD,[1] Karin Astrom-Olsson, MD,[1] Hans Ohlin, MD, PhD,[1] Fredrik Frogner, MD,[1] Marcus Carlsson, MD,[1] Therese Billgren, MD,[1] Stefan Jovinge, MD, PhD,[1] Peter Cain, MD, PhD,[1] Galen S. Wagner, MD,[2] Hakan Arheden, MD, PhD[1]** [1]***Lund University, Lund, Sweden,*** [2]***Duke University, Durham, NC, USA.***

*Introduction:* Sample timing is of importance for determination of myocardial infarct size by peak biochemical markers.

*Purpose:* We sought to: 1) find the time-to-peak for creatine kinase MB (CKMB) and cardiac troponin T (cTnT) after acute revascularization; 2) test if the peak value is as accurate as cumulative value for determination of infarct size; 3) evaluate how accurately clinical routine biochemical markers assess infarct size.

*Methods:* Primary percutaneous coronary intervention (PCI) was performed in patients presenting with first time infarction. Serial samples were acquired before PCI and at 1.5, 3, 6, 12, 18, 24, and 48 hours thereafter in 21 patients with an occluded coronary artery. In 17 other patients, clinical routine samples were acquired. Infarct size was assessed by delayed contrast-enhanced magnetic resonance imaging (DE-MRI) one week after the acute event.

*Results:* Time-to-peak in the serial sampling group was $7.6 \pm 3.6$ h for CKMB and $8.1 \pm 3.4$ h for cTnT. Peak value from serial sampling correlated to cumulative release of CKMB ($r_s = 0.98$, $p < 0.001$) and cTnT ($r = 0.97$, $p < 0.001$). Peak and cumulative values both correlated to MR infarct size (peak CKMB: $r_s = 0.82$, $p < 0.001$; peak cTnT: $r_s = 0.80$, $p < 0.001$; cumulative CKMB: $r_s = 0.85$, $p < 0.001$; cumulative cTnT: $r_s = 0.83$, $p < 0.001$). Clinical routine samples showed weaker relationships to MR infarct size (CKMB: $r_s = 0.47$, $p = 0.06$; cTnT: $r_s = 0.60$, $p = 0.01$).

*Conclusions:* The peak value of CKMB or cTnT, assessed at 3, 6, and 12 hours after acute revascularization of an occluded coronary artery, constituted good estimates of cumulative values and correlated well with MR infarct size, and may therefore be used to estimate myocardial infarct size.

## 507. MAGNETIC RESONANCE ANGIOGRAPHY EVALUATION OF COMMPLEX CONGENITAL HEART DISEASE IN EARLY INFANCY

**Ashwin Prakash,[1] Beth F. Printz, MD, PhD,[1] Welton M. Gersony, MD,[1] James C. Nielsen, MD,[2]** [1]***Columbia University College of Physicians and Surgeons, New York, NY, USA,*** [2]***Mount Sinai School of Medicine, New York, NY, USA.***

*Background:* Echocardiography is often sufficient in evaluating congenital heart disease (CHD) in young infants. However, cardiac catheterization is needed in some instances to evaluate the pulmonary arteries (PA) and other extracardiac thoracic vessels. Magnetic resonance angiography (MRA) is accurate in the evaluation of extracardiac thoracic vessels in adults and older children. However, MRA imaging quality in small infants may be limited by technical factors. This study evaluated the quality of visualization of PAs and other extracardiac thoracic vessels by MRA in young infants with CHD.

*Methods:* Twenty-nine contrast-enhanced MRA scans were performed at a single institution on 28 infants < 3 months of age (median age 6, range 1 to 90 days), in whom delineation of either PAs, pulmonary veins, aortic arch or aortopulmonary collaterals was inconclusive by echocardiography. A blinded observer at a different institution graded the quality of visualization of the main, branch, lobar and second generation PAs, lobar pulmonary veins, aortopulmonary collaterals, vena cavae, thoracic aorta and its branches, patent ductus arteriosus, and visceral sidedness as follows: *A*-structure absent; 0-not seen due to poor image quality; 1-indistinct margins insufficient for diagnosis; 2-indistinct margins sufficient for diagnosis but not measurement; 3-distinct margins sufficient for diagnosis and measurement.

*Results:* Diagnoses were single ventricle (n = 10), pulmonary vein anomaly (n = 4), scimitar syndrome (n = 4), tetralogy of Fallot with pulmonary atresia (n = 5), left PA sling (n = 2), situs inversus with coarctation (n = 1), truncus arteriosus (n = 1) and absent pulmonary valve (n = 1). Median image quality grade was 3/3 for all structures except second-generation PA branches, for which it was 2/3. Imaging grade was ≥2 for every structure in every subject. Median total scan duration was 9 (3–46) minutes. Findings were concordant with surgical inspection (n = 25) and cardiac catheterization (n = 8) in all subjects. There were no complications of the MRA.

*Conclusion:* MRA is excellent for the visualization of PAs and other extracardiac thoracic vessels in young infants with CHD and can be used as an alternative to cardiac catheterization when echocardiography is inconclusive.

## 508. HIGH-ENERGY PHOSPHATE METABOLISM IN PATIENTS WITH UNILATERAL, SYMPTOMATIC PERIPHERAL ARTERIAL DISEASE DURING PROGRESSIVE CALF EXERCISE COMPARED TO RUN-OFF SCORE MEASURED BY MAGNETIC RESONANCE ANGIOGRAP

**Andreas Greiner, MD, Regina Esterhammer, MD, Hannes Muehlthaler, MD, Werner Jaschke, MD, Gustav Fraedrich, MD, Michael Schocke.** ***Innsbruck Medical University, Innsbruck, Austria.***

*Introduction:* Patients with peripheral arterial disease (PAD) show an impaired regeneration of high-energy phosphates in the affected limb during exercise. However, investigations of high-energy phosphate changes in asymptomatic limbs of PAD patients have not been done up to now.

*Purpose:* The purpose of this study was to investigate the high energy phosphate metabolism of the exercising calf muscle in patients with unilateral PAD compared to healthy volunteers using 31 Phosphor magnetic resonance spectroscopy (31P MRS). In addition, the high energy phosphate metabolism was correlated with the ankle brachial pressure index (ABPI) and the arterial run-off score.

*Methods:* Using a 1.5 Tesla MR scanner, serial 31P MRS were separately carried out in each leg of all included patients ($n = 15$, 30 legs) and the volunteers ($n = 10$, 20 legs) during 4 increments of progressive calf exercise (2, 3, 4 and 5 Watt) with a time resolution of 10s. The run-off score was determined with the help of magnetic resonance angiography of both legs. For each exercise increment the time constant of phosphocreatine (PCr) hydrolysis $\tau$ ($\tau$2W-$\tau$5W) was calculated as well as the pH (pH2W-pH5W). For the regeneration period the time constant of PCr recovery ($\tau$rec) as well as pH after 1, 2, 3 and 10 minutes (pHr1,2,3,10) was evaluated.

*Results:* All patients had a fontaine's stage II with one symptomatic and one asymptomatic leg. There was a significant difference in $\tau$rec between the symptomatic and the asymptomatic legs ($p < 0.01$). The symptomatic legs of the patient group differed significantly from the legs of the healthy group in $\tau$2W, $\tau$3W, $\tau$5W and $\tau$rec ($p < 0.01$). A significant negative correlation was detected between ABPI as well as run-off score and $\tau$2W, $\tau$3W, $\tau$5W and $\tau$rec. In the symptomatic legs, pHr1 and pHr2 were significantly decreased.

*Conclusions:* Our study shows that the symptomatic legs of PAD patients exhibit prolonged PCr time constants at the onset of calf exercise with increasing workload and during the recovery time, which is associated with lower pH values compared to the asymptomatic legs and the legs of healthy controls. The prolongation in PCr time constants is correlated with ABPI and run-off score. Our findings indicate that 31P MRS can be used as a non invasive and objective method, to investigate the influence of arterial occluding lesions on muscle metabolism and consequently on muscle function in patients suffering from PAD.

## 509. NO-REFLOW PHENOMENON ASSESSED BY DE-MRI AS A PREDICTOR OF CHRONIC SCAR AND REMODELLING AFTER ACUTE MYOCARDIAL INFARCTION

**Giovanni Donato Aquaro,[1] Alessandro Pingitore,[1] Elisabetta Strata,[1] Daniele De Marchi,[1] Anna Sonia Petronio[2]** ***[1]Institute of Clinical Physiology, MRiLab, pisa, Italy, [2]Dipartimento Cardiotoracico, pisa, Italy.***

*Introduction:* Early assessment of late enhancement by MRI in acute myocardial infarction (AMI) with no-reflow phenomenon (NR) quantification could be a predictor of chronic scar and remodelling.

*Purpose:* To assess the relation between the presence and the extent of NR with the extent and hemodynamic correlates of chronic scar and remodelling in patients with AMI.

*Method:* Twenty-eight patients (22 males; mean age 61y) with AMI treated with primary or rescue PTCA with stenting were enrolled. All the patients underwent to a first MRI examination after a mean of $6 \pm 3$ (range 3-9 days) days following admission and a follow-up examination after a mean of $160 \pm 35$ days (range 103-230 days). Study protocol included a contrast-enhanced MR evaluation of HE and NR and MR study of function to assess left ventricular end-diastolic (EDV), end-systolic (ESV) volumes, ejection fraction (EF) and mass. A software tool was used to detect endocardial and epicardial contours and to quantify the extent of HE and NR in grams. The same protocol was used in the follow-up examination. As a remodelling index was chosen the ratio between mass and EDV (LVM/EDV). Result: NR was present in 16 (57%) patients (mean extent 5.6 $\pm$ 3.9%). Mean LVM/EDV was $0.90 \pm 0.22$). The presence of NR in acute MRI was related to the extent of HE ($p < 0.01$), to the EDV ($p < 0.05$) and ESV ($p < 0.05$) at the follow-up. The extent of NR was related to the extent of HE ($p < 0.01$) in the follow-up and to the HE-ratio ($p < 0.05$). The transmural extent of HE on the first examination was significantly related to the extent of HE ($p < 0.01$), the LVM/EDV ratio ($p < 0.05$) and the EDV ($p < 0.05$) and ESV ($p < 0.05$) at the follow-up. The extent of HE at the follow-up was related to LVM/EDV ratio.

*Conclusion:* NR was related to left ventricular dilatation and chronic scar assessed at follow up of patients with AMI. The extent of DE at the follow-up was related to unfavorable remodelling.

## 510. THE NO-REFLOW PHENOMENON IN PATIENTS WITH ACUTE MYOCARDIAL INFARCTION AND CLINICAL, ELETTROCARDIOGRAPHIC AND

## BIOUMORAL CORRELATES: A STUDY WITH DELAYED ENHANCEMENT MR

**Giovanni Donato Aquaro,[1] Alessandro Pingitore,[1] Gianluca Di Bella,[1] Elisabetta Strata,[1] Daniele Rovai,[1] Fabrizio Paoli,[2] Massimo Lombardi[1] [1]*Institute of Clinical Physiology, MRiLab, pisa, Italy,* [2]*Institute of Clinical Physiology, Massa, Italy.***

*Introduction:* No-reflow phenomenon (NR) is a markers of worse outcome during acute myocardial infarction (AMI). Contrast enhanced Magnetic Resonance imaging (CE-MRI) can detect NR in acute phase following AMI providing also a three-dimensional quantification.

*Purpose:* To evaluate the clinical and instrumental correlates to the presence and extent of NR in patient with AMI.

*Method:* Fifty-two patients with AMI (42 males, mean age 64.7 ± 12 years) treated with primary or rescue PTCA and stenting within 6 h after admission. All the patients underwent CE-MRI 6 ± 3 days (range 3–10) after the AMI. NR was defined as a hypoenhanced area surrounded by hyperenhanced area (HE). A software tool allowed semi-automatic endocardial and epicardial contours detection and 3-dimensional quantification of HE and NR extent. A Wall motion Score Index (WMSI, from 1 = normal to 4 = dyskinetic in a 17 segment model of LV) was evaluated. Global ST-elevation was defined as the sum of ST-tract elevation in millimeters in each leads on 12-lead electrocardiograms.

*Result:* NR was present in 17 (33%) patients (mean extent 5.9 ± 4.7%). The extent of NR was related to reported family hystory of CAD ($p < 0.05$) and Diabetes ($p < 0.05$). Patient with NR had higher extent of HE (mean extent 27.2 ± 10.5% vs 10.7 ± 6.6%, $p < 0.0001$), higher transmurality of HE (32.1 ± 2.5% vs 13.2 ± 1.9%, $p < 0.0001$) than patient without NR. The extent of NR was significantly correlated with enzyme elevation (CPK $p < 0.005$; Troponine I $p < 0.05$), global extent of HE ($p < 0.0001$), number of segments with HE ($p < 0.0005$), transmural extent of HE ($p < 0.0001$) and WMSI ($p < 0.0005$). At admission the global ST-elevation was higher in patient with NR (18.1 ± 1.9 vs 9.1 ± 1.5 mm $p < 0.001$) and correlated with the extent of NR ($p < 0.005$). At discharge the number of Q-waves was related to the extent of NR ($p < 0.05$). At multivariate analysis only the global extent of HE was a predictor of NR.

*Conclusion:* No-reflow phenomenon and mostly its three-dimensional extent was associated to higher extent of infarction, left ventricular dysfunction, biohumoral and electrocardiographic changes.

| n. | No-Reflow 17 | Reflow 35 | |
|---|---|---|---|
| HE(%) | 27.2 ± 105 | 10.7 ± 6.6 | $p < 0.0001$ |
| Tranmural extent (%) | 30.5 ± 12.7 | 14.2 ± 8.5 | $p < 0.0001$ |
| Num. segments | 9.3 ± 0.77 | 6.04 ± 3.24 | $p < 0.005$ |
| SigmaST (mm) | 17.2 ± 9.5 | 9.0 ± 5.8 | $p < 0.002$ |
| CPK (U/I) | 3406 ± 2477 | 1653 ± 1617 | $p < 0.01$ |
| troponine (ng/dl) | 225.9 ± 236.9 | 155.6 ± 178.6 | $p < 0.27$ |
| EF MR (%) | 43.01 ± 10.7 | 52.2 ± 11.1 | $p < 0.03$ |
| WMSI MR | 1.79 ± 0.32 | 1.36 ± 0.22 | $p < 0.0001$ |

## 511. IMAGING CARDIAC FUNCTION IN THE RODENT AT 1.5T WITH A CLINICAL MRI SCANNER

**Karin Abou-Montet, Jean-Luc Daire, Jean-Noel Hyacinthe, Denis Morel, Jean-Paul Vallée. *Geneva University Hospital, Geneva-14, Switzerland.***

*Introduction:* The use of Magnetic Resonance Imaging (MRI) is increasing in cardiac investigation and there is a need to develop MR protocol dedicated to heart function of small animal.

*Purpose:* The aim of this work is to demonstrate the feasability in rats of cardiac function imaging and characterization on a 1.5T clinical MR system.

*Methods:* Five adult male rats (OFA(SD), Charles River Laboratory, France) (360–410 g) were imaged on a 1.5T MR system (Intera, Philips Medical Systems, Best, The Netherlands) using a surface coil (47 mm diameter). Four ECG-triggered field echo sequences were systematically realized in a long axis and two short axis views (at the mid-ventricle and at the apex of the heart): a spiral fast field echo (FFE) sequence and three cartesian Turbo Field Echo (TFE) sequences with different parameter settings: two conventional TFE sequences with different in-plane resolution and a TFE sequence with flow compensation and complex conjugate reconstruction (half scan) (TFE-hs-flowcomp). Physiological parameters (ECG, body temperature, breathing rate) of the rats were monitored in real time during the whole experiment.

*Results:* All cine protocols were successfully performed in every rat even at high heart rate (371 bpm ± 57 bpm). A high contrast between the blood and the myocardium was observed in all the sequences as shown in the figure (Spiral-FFE (a), TFE-flowcomp (b), TFE (c), and TFE-lowres (d)). From the consensus reading, the best sequence was the cartesian TFE with flow compensation and complex conjugate reconstruction. This sequence, showing robustness and reproducibility at 1.5T, provides a high temporal resolution (14 phases/beat) and spatial resolution (voxel size: 0.31 × 0.31 × 2 mm). Using the modified Simpson method, end-diastolic (EDV) and end-systolic (ESV) volumes as well as the ejection fraction (EF) were consistent with literature values (EDV(cm3) = 0.571 ± 0.052; ESV(cm3) = 0.162 ± 0.024; EF = 71.1 ± 6.9%).

*Conclusions:* This study demonstrates the feasibility of cardiac imaging of the rat on a 1.5T clinical MR scanner. Due to the large base of such systems installed in cardiac research center, this will boost the cardiovascular research on small animal.

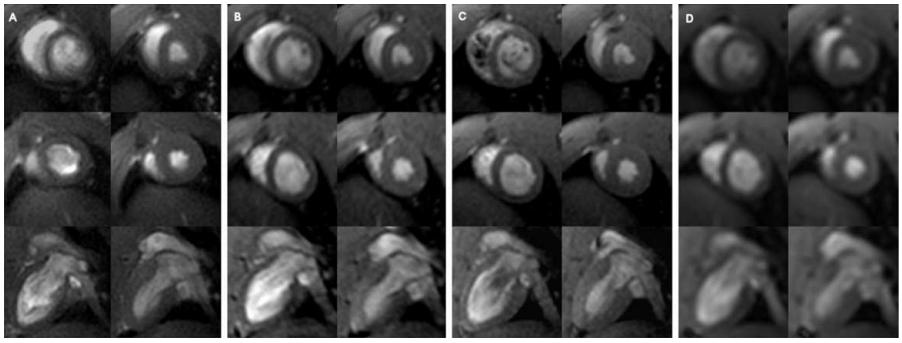

## 512. QUANTITATIVE 3D REGIONAL ANALYSIS OF LEFT VENTRICULAR FUNCTION

**Brett R. Cowan, BE MbChb, Alistair A. Young, PhD.** ***University of Auckland, Auckland, New Zealand.***

*Introduction:* Cardiac disease often affects the left ventricle in a regional rather than global manner. In particular, myocardial infarction causes functional impairment in specific regions perfused by the occluded coronary arterial supply. Overall cardiac function is typically quantified by global parameters such as left ventricular mass (LVM), end-diastolic volume (EDV), end-systolic volume (ESV) and ejection fraction (EF), whereas regional dysfunction is usually reported qualitatively based on visual inspection. The use of a 3D model of the left ventricle allows the automatic quantitative determination of regional cardiac function.

*Purpose:* i) To develop and validate an automated regional analysis for LV cardiac function, and ii) to determine reference ranges for a group of normal subjects.

*Methods:* Twenty individuals (10 male, age range 30–55 years) with normal ECG and echcocardiographic scans, without history of cardiac disease and not taking cardio-active medications, were imaged on a 1.5T MRI scanner (Siemens, Erlangen). Six equally spaced short axis and three radially spaced long axis scans were acquired using SSFP (true-FISP). Written informed consent was obtained from all subjects and the institutional ethic committee approved the study protocol. All studies were analyzed by a single observer using guide-point modeling (CIM version 4.6) (1). This calculates moving curved surfaces representing the endocardial and epicardial boarders and is able to fully correct for through plane motion of the mitral valve (1). Volumes were calculated by numerical integration of these surfaces and were therefore not dependent on the limitations of slice summation or Simpson's rule. LVM was calculated for every phase and then averaged. Each heart model was divided into equal thirds from the mitral valve to the apex, (apex, mid and base) at each phase of the cardiac cycle. The insertion of the right ventricle was marked at end-diastole and used to define the septum at each level. The septum was further divided into two equal segments (anterior and posterior) and the remainder of the wall into four equal segments (inferior, infero-lateral, antero-lateral and anterior) to create a 16 segment model. Volume was then calculated for every segment from the endocardial or epicardial surface to the central axis of the LV. In order to determine inter-observer reproducibility all studies were independently analyzed by a second observer. Statistical testing was conducted using the paired students t-test with significance defined as $p < 0.05$. A water filled perspex phantom was constructed to contain a movable plastic sectors of similar size to ventricular regional volumes. This was scanned using the same protocol and analyzed for the purposes of validation.

*Results:* (a) Table 1 shows the results for each region. (b) There were no significant differences between the two analyses performed. (c) The average error in regions similar in size to the human heart in the phantom experiment was 0.2 mL.

Table 1. Regional functional parameters averaged between both observers.

| EDV (mL) | ESV (mL) | SV (mL) | EF (%) | LVM (g) | |
|---|---|---|---|---|---|
| | | BASE | | | |
| Postero-septal | 9.21 | 4.86 | 4.30 | 47.84 | 6.44 |
| Inferior | 9.47 | 4.11 | 5.31 | 56.54 | 7.84 |
| Infero-lateral | 10.08 | 3.55 | 6.49 | 63.64 | 9.17 |
| Antero-lateral | 12.25 | 3.65 | 8.55 | 69.74 | 9.40 |
| Anterior | 13.63 | 4.48 | 9.09 | 67.61 | 9.17 |
| Antero-septal | 11.74 | 5.55 | 6.13 | 52.61 | 8.41 |
| | | MID | | | |
| Postero-septal | 7.74 | 2.27 | 5.42 | 71.53 | 7.08 |
| Inferior | 9.08 | 2.13 | 6.90 | 77.50 | 6.80 |
| Infero-lateral | 12.18 | 2.82 | 9.32 | 77.18 | 7.93 |
| Antero-lateral | 14.82 | 4.28 | 10.49 | 71.05 | 9.22 |
| Anterior | 16.54 | 6.09 | 10.40 | 63.38 | 9.52 |
| Antero-septal | 11.04 | 3.88 | 7.11 | 64.77 | 8.65 |
| | | APEX | | | |
| Septal | 5.10 | 1.44 | 3.60 | 71.20 | 6.03 |
| Inferior | 5.22 | 0.92 | 4.40 | 82.60 | 5.20 |
| Lateral | 5.41 | 1.21 | 4.17 | 77.36 | 5.60 |
| Anterior | 5.89 | 2.11 | 3.73 | 63.23 | 6.00 |
| OVERALL | 159.4 | 53.3 | 105.4 | 66.5 | 122.5 |

EDV = end-diastolic volume, ESV = end-systolic volume, SV = stroke volume, EF = ejection fraction, LVM = left ventricular mass.

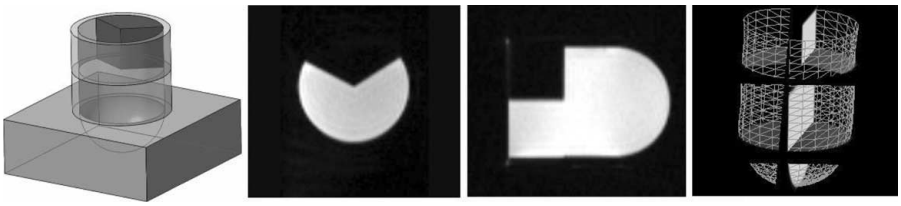

FIG. 1. Regional volume phantom. a) 3D schematic; b) short axis view; c) long axis view; d) 3D view.

*Conclusion:* A 3D model of the heart allows the automated calculation of accurate regional volumes and standard functional parameters on a regional basis.

## REFERENCE

1. Young AA, et al. Radiology 2000;216:597–602.

## 513. CORRECTION OF TEMPORAL MISREGISTRATION ARTIFACTS FOR JET FLOW

**Mark Doyle, PhD,[1] Geetha Rayarao,[1] Eduardo Kortright, PhD,[2] Andreas Anayiotos, PhD,[3] Longchuan Li, PhD,[3] Ketheswaram Caruppannan, MD,[1] Vikas K. Rathi, MD,[1] Robert W. W. Biederman, MD[1]** [1] ***Allegheny General Hospital, Pittsburgh, PA, USA,*** [2] ***University of New Orleans, New Orleans, LA, USA,*** [3] ***University of Alabama at Birmingham, Birmingham, AL, USA.***

*Introduction:* Quantitative velocity measurement of jet flow using phase sensitive methods can suffer from severe distortions. Errors result from the relatively low temporal resolution of acquisition, limiting bandwidth, and resulting in "blunting" of the jet flow waveform. However, we show that velocities may be overestimated by greater than 200% even for moderately severe jets. The origin and remedy of this phenomenon is demonstrated.

*Hypothesis:* We hypothesize that temporally distributed data, used to determine relative phase in assigning velocity can result in errors in jet flow, where high propagation velocities ($Vel_{prop}$) are present. Effects introduced by temporally distributed data have potential to be addressed by post processing temporal alignment of data.

*Methods:* Jet flow data was generated in a cylindrical phantom (10 cm diameter) using blood mimicking fluid (60% glycerin, 40% water) passing through a circular orifice (1 cm diameter) with a reproducible cyclic waveform (Shelly, Vancouver, Canada). A gradient echo phase velocity scan was used (TR/TE/Flip 7.7/2.5/20°) to acquire conventional temporally distributed scans using 2 views per segment (GE 1.5T CV/i, Milwaukee, WI). For each phase, a velocity compensated, followed by 1, 2 or 3 velocity-encoded scans were acquired. Velocity-encoded sensitivities (VENC) of 2.5 and 5.0 m/s were used (scan time 2 min 15 s). A reference scan was acquired using a single view per segment with the flow compensated and flow encoded data sets acquired in separate cycles to realize temporal alignment (16 min scan). Conventional data sets were post-processed in two ways: 1) without temporal alignment (non-aligned) and 2) by temporally aligning velocity compensated and velocity encoded data using spline interpolation (aligned) (The Mathworks, Natick, MA). Using automatically applied criteria, jet properties were measured: maximal velocity, jet length, $Vel_{prop}$, and correlation of velocity-time curves for 5 points along the central jet at 1 cm intervals.

*Results:* Using the reference scan, maximal jet velocity was 1.42 m/s, maximal jet length was 42 mm, and $Vel_{prop}$ was 0.78 m/s. The average maximal velocity of non-aligned data was

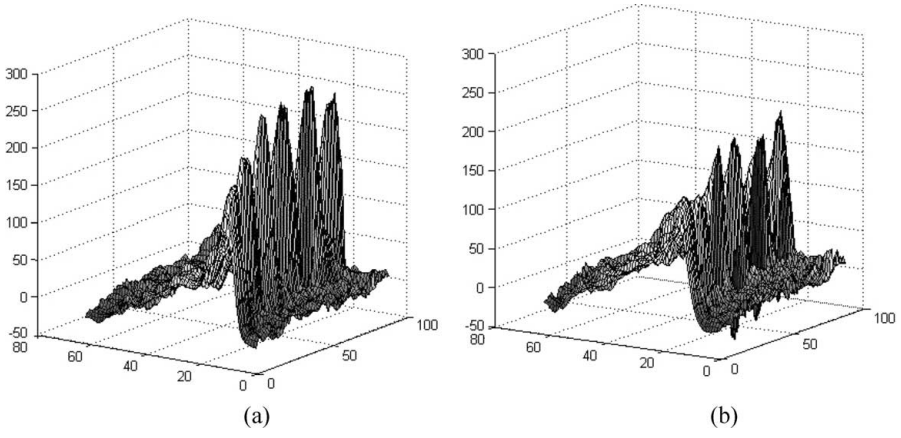


FIG. 1. Jet-velocity-space-time plot A) non-aligned and B) corresponding aligned data.

higher than aligned data (1.91 ± 0.37 m/s vs. 1.38 ± 0.04 m/s, $p < 0.01$), whereas the jet length and $Vel_{prop}$ were not different between non-aligned and aligned (41 ± 4 mm vs. 38 ± 5 mm; 67 ± 7 m/s vs. 68 ± 5 m/s, respectively). For non-aligned data, Fig. 1A, the measured average velocity tended to be higher for VENC 5 m/s vs. 2.5 m/s (1.6 ± 0.18 m/s vs. 2.21 ± 0.18 m/s, $p = 0.06$), whereas aligned data showed no systematic difference (1.37 ± 0.04 m/s vs. 1.38 ± 0.04 m/s), Fig. 1B. The correlation with the reference scan for velocity-time curves was higher for aligned vs. non-aligned data sets ($r = 0.93 \pm 0.08$ vs. 0.83 ± 0.18, $p < 0.001$).

*Conclusion:* Temporal misregistration of phase velocity data can result in overestimating average jet flow velocities in excess of 200%, with locally higher readings >350% (representing a difference of 8 vs. >100 mmHg if based on peak velocity) and leading to widespread signal aliasing. The origin of the problem is that relative phase changes are derived from temporally interleaved data, and while the temporal misregistration is only slight, the phase mismatch is large when $Vel_{prop}$ is high. In the data presented here, the $Vel_{prop}$ was 0.78 m/s, but in vivo, it ranges from 0.5 m/s to 4 m/s. Thus, the effects of temporal interleaving are expected to result in even greater inaccuracies compared to the moderate jets studied here. The exact form of the distortion cannot in general be predicted because the acquisition details are machine dependent, which may be different between manufacturers. Correction for the temporal distribution can be accomplished at the post processing stage by performing temporal alignment, effectively removing accuracy dependency on the selected VENC.

## 514. THE PHYSIOLOGY OF ISOLATED PARTIAL ANOMALOUS PULMONARY VENOUS CONNECTION OF A SINGLE PULMONARY VEIN AS DETERMINED BY CARDIAC MAGNETIC RESONANCE IMAGING

**Joshua L. Dyme, MD,[1] Ashwin Prakash, MD,[1] Beth F. Printz, MD,[1] Ira A. Parness, MD,[2] James C. Nielsen, MD.[2]**
***[1]Columbia Univerisity College of Physians and Surgeons, New York, NY, USA, [2]Mount Sinai, New York, NY, USA.***

*Introduction:* Isolated partial anomalous pulmonary venous connection (PAPVC) of a single pulmonary vein is rare. The physiology of this defect, including the magnitude of the shunt and the degree of right ventricular volume load, has yet to be fully characterized. Blood flow rate and right ventricular (RV) volume measured by cardiac magnetic resonance (CMR) has been shown to be accurate and reproducible. This study assessed the magnitude of the left to right shunt and RV dilation caused by a single anomalous pulmonary vein using CMR.

*Methods:* CMR data from 6 subjects with isolated PAPVC at two institutions were retrospectively reviewed. Subjects with >1 anomalous pulmonary vein, associated lesions including atrial and ventricular septal defects and significant tricuspid or pulmonary regurgitation were excluded. Pulmonary to systemic flow ratio (Qp:Qs) and RV end-diastolic volume indexed to body surface area (RVEDVi) were determined by phase contrast and steady-state free precession sequences, respectively. Normal RVEDVi was defined by comparing study subjects to published normative pediatric and adult data as well as to a reference cohort (N = 19) free of RV disease.

*Results:* In 4 subjects the left upper pulmonary vein connected to the innominate vein and in 2 subjects the right upper pulmonary vein connected to the right superior vena cava. The median age was 14.5 (13–38) years for the study group and 16 (1-26) years for the reference cohort. The median Qp:Qs is 1.55 (1.3–1.6). Mean RVEDVi in subjects was significantly larger than the reference cohort (108 ± 16 cc/m$^2$ versus 77.7 ± 18 cc/m$^2$, $p = 0.0009$. RVEDVi was greater than the published upper limit of normal in all subjects. Older age did not correlate with increasing magnitude of the shunt ($r = 0.3$, $p = 0.5$), however increasing age did correlate with RVEDVi, ($r = 0.9$, $p = 0.01$).

*Conclusions:* This small series is the first report of the physiology of isolated PAPVC as determined by CMR. Isolated PAPVC with only one vein connecting anomalously results in a modest left-to-right shunt and mild RV dilation. RV size is significantly larger than normal subjects and correlates with increasing age.

## 515. CARDIAC MR STRESS PERFUSION AS A PROGNOSTIC INDICATOR IN PATIENTS WITH LOW EF

**Bryant H. Nguyen, MD,[1] Anthon R. Fuisz, MD.[2]**
***[1]Georgetown University Medical Center, Washington, DC, USA, [2]Washington Hospital Center, Washington, DC, USA.***

*Introduction:* Cardiac MR adenosine stress perfusion imaging (CMRSP) has been shown to predict cardiac events in patients with ejection fraction (EF) >25%. It is not known if CMRSP can predict cardiac events in patients with EF of 25% or less.

*Hypothesis:* We hypothesized that a positive CMRSP result would predict the occurrence of cardiac events in patients with EF of 25% or less. Furthermore, we expected a positive CMRSP with perfusion abnormalities found in viable territories would have a higher cardiac event rate.

*Methods:* Twenty-four patients who met the entry criteria and underwent CMRSP at Washington Hospital Center between February, 2001 and September, 2004, were selected for follow-up. This group was excluded from a larger CMRSP outcomes study group due to EF less than 25%. All studies were performed on a Phillips Intera CV 1.5T MRI system. Follow-up was obtained for patients an average of 2.4 years (range 1.2–3.7) after CMRSP imaging. Follow-up consisted of a chart review and phone interviews with patient, patient's primary physician or family as available. A cardiac event was defined as the occurrence of any one of the following: fatal or non-fatal MI occurring any point after the procedure, fatal arrhythmia after the procedure, or revascularization performed more than 60 days after CMRSP. A positive CMRSP result was defined as any

perfusion defect found on CMRSP. The presence of a perfusion abnormality in a viable territory, identified by lack of delayed hyperenhancement in the ischemic segment, was also noted.

*Results:* Average patient age at CMRSP imaging was 68 years old (range 49–91), with 17/24 males, and an average EF of 18% (range 11–25%). The results of CMRSP were that 5/24 (21%) patients had a negative CMRSP, 19/24 (79%) patients had a positive CMRSP result (10 of those with positive CMRSP had perfusion abnormalities in a viable territory). The all-cause mortality rate in the study was high, at 10/24 (42%), and did not differ significantly between groups. The mortality rate for the group with positive CMRSP was 8/19 (42%) and the group with negative CMRSP was 2/5 (40%). Overall, 3 cardiac events occurred during the study period (1 late revascularization, 1 fatal arrhythmia, and 1 fatal MI): 3/19 (16%) in patients with positive CMRSP, and 0/5 (0%) in patients with a negative CMRSP. In addition to a positive CMRSP, all 3 patients who suffered cardiac events demonstrated ischemia in at least one viable territory. No endpoints occurred in patients with ischemia isolated to areas of delayed hyperenhancement.

*Conclusions:* A positive CMRSP, especially when the abnormality occurs in viable segments, appears to convey the poorest prognosis in patients with EF $< 25\%$. In conclusion, CMRSP may be able to predict cardiac events in patients with EF of 25% or less, especially in those demonstrating ischemia in viable territories.

## 516. DECLINE IN LEFT VENTRICULAR MASS WITHIN 3 MONTHS FOLLOWING SURGERY FOR SEVERE MITRAL REGURGITATION: IS THERE A GENDER DIFFERENCE

**Eli V. Gelfand, MD, Thomas H. Hauser, MD, M MSc, Lois Goepfert, R. N., Kraig K. Kissinger, R. T., Susan B. Yeon, MD, J. R., Ralph de la Torre, MD, Warren J. Manning, MD.** ***Beth Israel Deaconess Medical Center, Boston, MA, USA.***

*Background:* In patients with chronic severe mitral regurgitation (MR), the left ventricle (LV) may adapt to increased preload with eccentric hypertrophy. We hypothesized that following mitral valve repair/replacement (MVR) for chronic severe MR, there would be a decline in LV mass and utilized quantitative cardiovascular magnetic resonance (CMR) to test this hypothesis.

*Purpose and Methods:* Twelve patients (50% F; age 51 $\pm$ 11 yrs; 9 valve repair/3 replacement) with chronic, severe mitral regurgitation who underwent quantitative CMR with assessment of LV mass and LV mass index prior to and 3 months following MVR.

*Results:* For the entire group, pre-operative LV mass and LVMI were 140 $\pm$ 33 g and 75 $\pm$ 14 g/m$^2$, respectively. MVR was associated with a reduction in the LV mass and LVMI of 28 $\pm$ 19 g and 15 $\pm$ 10 g/m$^2$, respectively (20% relative reduction, $p < 0.01$ for both; Fig.). Postoperative LVMI was reduced in both men and women (Table), and the magnitude of LVMI reduction was similar in both groups ($p = 0.16$ for difference between men and women).

*Conclusions:* In both men and women with chronic severe MR undergoing valve surgery, there is a 20% relative reduction in LV mass within 3 months of MVR. The magnitude of LV mass index regression is comparable between both genders.

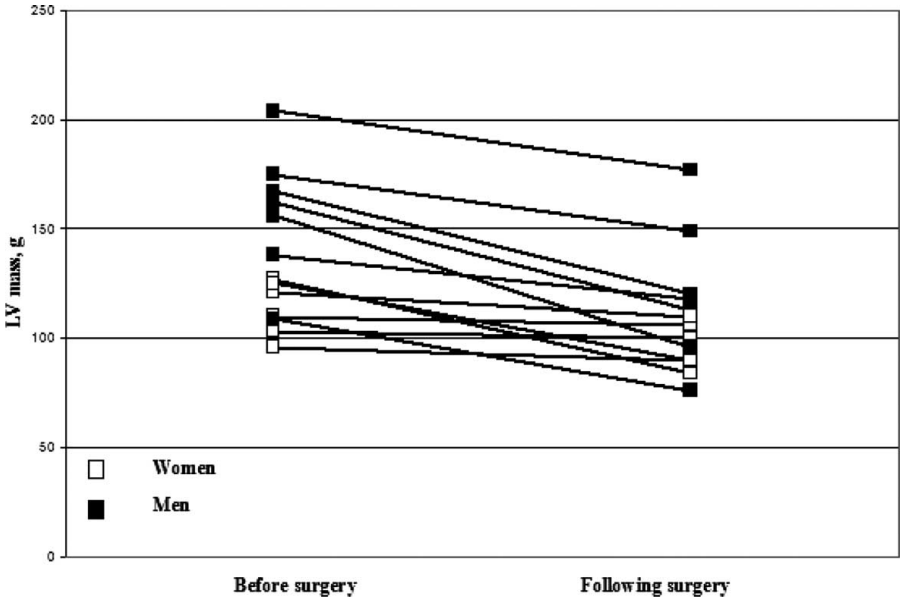


FIG. 1. Perioperative change in LV Mass.

## 517. MYOCARDIUM AT RISK IDENTIFIED WITH CONTRAST ENHANCED ADENOSINE MR

**Susan Ghods,[1] Jens Bremerich,[1] Michael Zellwerger,[2] Claudia Bösch,[2] Georg Bongartz,[1] Peter Buser.[2]** [1]***Departement of Radiology, Basel, Switzerland,*** [2]***Departement of Cardiology, Basel, Switzerland.***

*Purpose:* To identify myocardium at risk in patients with suspected coronary artery disease.

*Methods:* Twelve patients with suspected or established diagnosis of coronary artery disease were subjected to adenosine stress MR (1.5 Tesla, Avanto, Siemens Medical Solutions, Germany). Goldstandard was invasive coronary angiography. The MR imaging protocol was designed as follows: Cine TrueFisp in 3 planes for wall motion analysis. Pharmacological stress induced by adenosine infusion (140 $\mu$g kg/min for 3 min) followed by bolus injection of Gd-DTPA (Gadovist, Schering, Berlin, Germany; 0.05 mmol/kg @ 4 mL/s). First pass images were acquired in 3 short axis planes (SR-turboFLASH, TR/TE = 176 ms/1 ms). Ten min later perfusion imaging was repeated to evaluate perfusion at rest. Another 10 min later delayed enhancement imaging was performed with phase sensitive inversion recovery (PSIR) turboFLASH. Images were reviewed by two physicians experienced in cardiac MR. Perfusion images at stress and rest were compared in a semiquantitative fashion to identify stress induced hypoperfusion. Infarction was identified as positive late enhancement on PSIR images. Myocardium at risk was defined as myocardium with stress induced hypoperfusion but without evidence of infarction and related to vascular territories of right, left, or circumflex coronary arteries on goldstandard catheter angiography.

*Results:* Adenosine stress was well tolerated in all patients. A total of 36 vascular territories (3 coronary arteries in 12 patients) were assessed. Myocardium at risk was correctly identified in 5 patients in 10 territories (true positive MR). Two myocardial territories supplied by arteries with significant stenoses on catheter angiography were not identified on MR (false negative). Normally perfused myocardium supplied by normal coronary arteries was identified in 24 territories (true negative). No false positive territory was found. Sensitivity und specificity of MR for myocardium at risk as compared to catheter angiography were 83% and 92%, respectively.

*Conclusions:* Contrast enhanced adenosine stress perfusion MR identifies myocardium at risk with high sensitivity and is an excellent tool for non-invasive assessment of patients with suspected or established diagnosis of coronary artery disease.

## 518. T2* MAPPING IN PATIENTS FOLLOWING REPERFUSED MYOCARDIAL INFARCTION

**Timothy Christian,[1] Annie Fuh,[2] Karl Vigan.[2]** [1]***University of Vermont, Burlington, VT, USA,*** [2]***University of Wisconsin, Madison, WI, USA.***

*Introduction:* MRI Blood oxygen level dependent (BOLD) imaging can reflect changes in hemoglobin saturation, thus providing physiologic information regarding tissue oxygen extraction. This effect (T2*) can be measured by assessing changes in signal intensity for an ROI as a function of the TE on a gradient echo sequence.

*Purpose:* As a first step in assessing the ability of T2* mapping to provide metabolic information in patients with ischemic heart disease, this study sought to determine whether T2* effects will be significnantly less in reperfused but infarcted tissue (where oxygen concentration is high) than in perfused viable tissue (where oxygen concentration should be low) during a multigradient echo sequence.

*Methods:* The study group consisted of 9 patients imaged 5-90 days from index myocardial infarction (MI) who had restored patency of the infarct vessel. MRI consisted of; (1). Fast interleaved multi-gradient echo sequence with five TE readouts varying from 4.3 to 25 ms to generate T2* curves, (2). T2-weighted imaging to assess for significant residual edema, (3). T1-weighted inversion recovery following 0.2 mmol/Kg

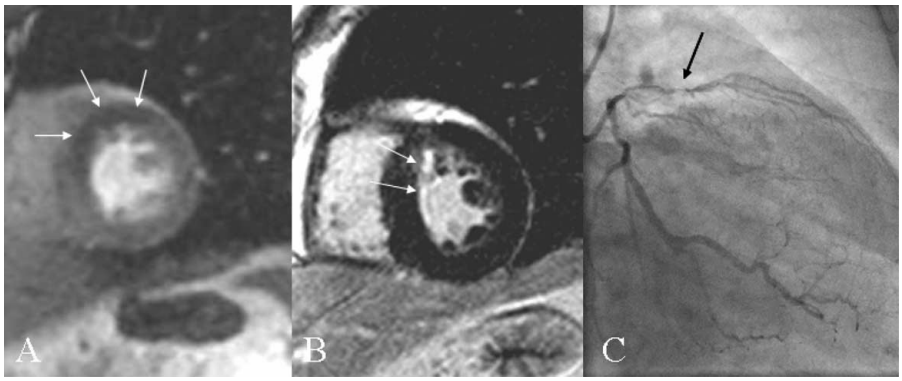


FIG. 1. (A) The stress perfusion image shows a full-thickness perfusion defect (arrow) in LAD territory. (B) The delayed contrast enhancement in the subendocardial layer of the anteroseptal wall. (C) Corresponding angiogram shows a stenotic lesion (arrow) in the proximal segment of LAD.

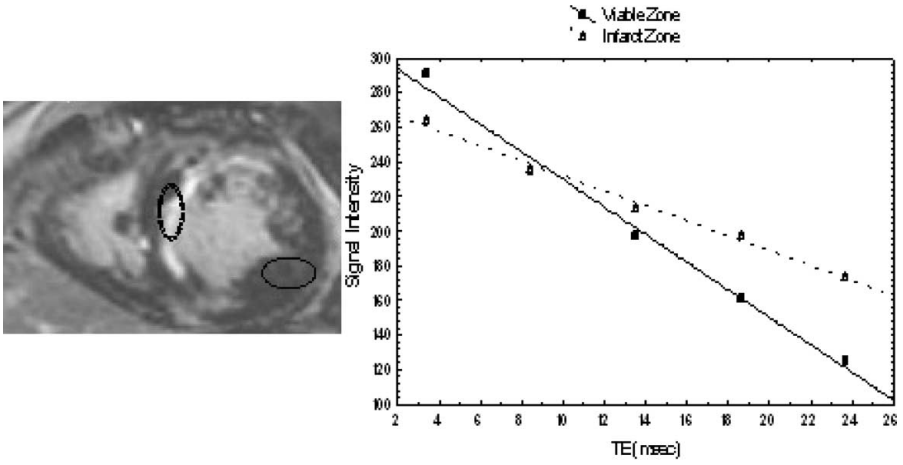


(a) (b)

Gd-DTPA IV injection for delayed viability imaging. The viability images were used to determine the infarct territory so that ROIs could be placed in an infarct zone and a viable zone for analysis. Mean signal intensity (SI) was calculated for each ROI. T2* and R2* curve fits were generated from these SI values. Infarct size was planimetered by threshold criteria from the viability images and expressed as a percent of the myocardial mass.

*Results:* Mean infarct size was 14.0 ± 9.3% LV. Results for T2* decay, R2* (1/T2*) and T2 weighted (edema) scans are shown in the Table. The Fig. compares the slope of the R2* curves in infarcted and normal myocardium in a single patient.

| Zone | T2* | R2* | T2 weighted SI |
|---|---|---|---|
| Infarct | 53.2 ± 17.7 | 20.9 ± 7.5 | 119.7 ± 62.3 |
| Control | 35.9 ± 4.4 | 28.3 ± 4.0 | 123.4 ± 60.0 |
| p (Inf vs Con) | < 0.01 | < 0.01 | NS |

*Conclusions:* Many factors contribute to T2* decay; however, T2* decay time is prolonged in reperfused but nonviable myocardium, possibly from low oxygen extraction.

## 519. SCAR TISSUE IS SMALLER IN OBESE PATIENTS: A CONTRAST-ENHANCED MAGNETIC RESONANCE STUDY IN PATIENTS WITH PREVIOUS MYOCARDIAL INFARCTION

**Gianluca Di Bella, Daniele Rovai, Massimo Lombardi, Giorgio Iervasi, Elisabetta Strata, Giovanni Donato Aquaro, Vincenzo Positano, Antonio L'Abbate, Alessandro Pingitore.** ***Institute of Clinical Physiology, Pisa, Italy.***

*Introduction:* Obesity is associated with an increased risk of death, MI and heart failure; however, its effects on infarct size are unknown.

*Purpose:* The aim of this study was to evaluate the effect of obesity and major cardiovascular risk factors on the size and transmural extent of myocardial infarction (MI).

*Methods:* In 89 patients (62 ± 11 years old, 80 males) the size and transmural extent of a previous MI (Q-wave in 72 patients) were measured by contrast-enhanced magnetic resonance imaging. Patients were categorized according to the body mass index (BMI) as in the normal range (BMI between 18.5 and 24.9), overweight (BMI 25–29,9) or obese (BMI ≥ 30 kg/m$^2$).

*Results:* Areas of delayed contrast enhancement (that reflects MI) were present in 15 ± 9% of left ventricular myocardium and were extended transmurally to 31 ± 11% of the wall thickness. Infarct size was not influenced by patient's age, gender, arterial hypertension, hypercholesterolemia, hypertriglyceridemia nor tobacco smoking (categorical variables). However, MI size and transmural extent were larger in insulin-dependent diabetic patients ($p < 0.05$). MI was smaller in obese patients (11 ± 4%) than in overweight patients (16 ± 9%) and in those with normal BMI (18 ± 10%) ($p < 0.05$). The transmural extent of MI was not affected by BMI. Insulin-dependent diabetes, family history of premature coronary artery disease and obesity were the only independent predictors of infarct size at multivariate linear regression analysis.

*Conclusions:* In patients with previous MI obesity is paradoxically associated with a smaller infarct size.

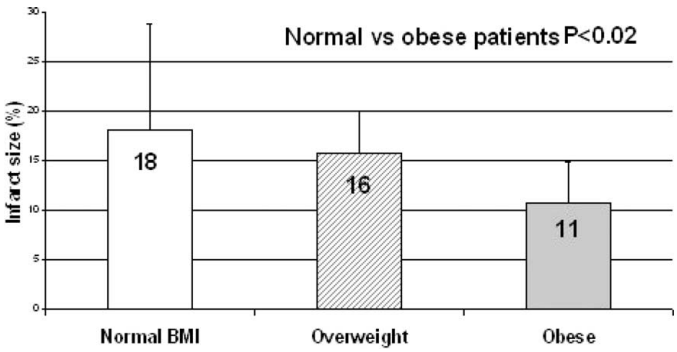

## 520. PARADOXICAL INFLUENCE OF TIME-TO-PTCA ON INFARCT-SIZE IN PATIENT WITH MYOCARDIAL INFARCTION: A DELAYED-CONTRAST-ENHANCED MAGNETIC RESONANCE STUDY

**Giovanni Donato Aquaro,[1] Alessandro Pingitore,[1] Anna Sonia Petronio,[2] Gianluca Di Bella,[1] Elisabetta Strata,[1] Mariolina Deiana,[1] Daniele Rovai,[1] Marco De Carlo,[2] Cataldo Palmieri,[1] Massimo Lombardi.[1]** [1] ***Institute of Clinical Phisiology, Pisa, Italy,*** [2] ***Dipartimento Cardio-toracico, Pisa, Italy.***

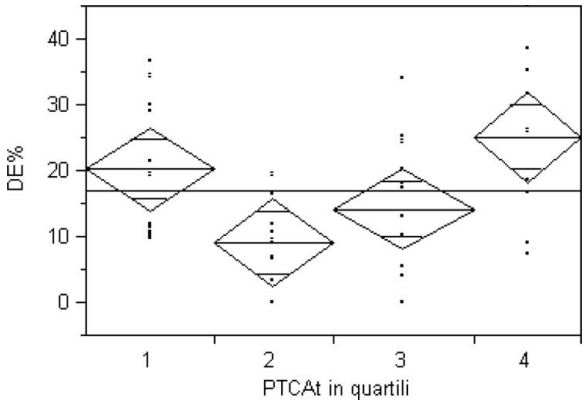


*Introduction:* Previous studies demonstrated that infarct size was significantly lower in patient with acute myocardial infarction (AMI) treated with primary stenting (PTCA) than with thrombolysis. In patient treated with PTCA no significant influence of time-to-treatment has been shown on infarct size as assessed by scintigraphy. Delayed-Contrast-Enhancement Magnetic Resonance (DCEMR) allows accurate evaluation and quantification of the damaged myocardium (necrotic area and oedema) in acute phase and the scar in chronic phase following AMI.

*Purpose:* To evaluate the influence of the PTCA-time (PTCAt) on infarct size assessed by DCEMR.

*Methods:* Fifty-two consecutive patient (42 males, mean age 64.7 ± 12 years) with ST-elevation AMI and no previous infarction or cardiomyopathy were scheduled for primary PTCA in seven peripheral Emergency Department and then transferred in one of two central cath-lab. All the patient were treated with PTCA with Drug Eluting Stent and up-to-date medical therapy. PTCAt was defined as the time between onset of chest pain and percutaneous revascularization procedure. Patients were subdivided in quartiles by PTCAt: first quartile (qI) less than166 minutes, second quartile (qII) 166–225 minutes, third quartile (qIII) 226–300 minutes and forth quartile (qIV) more than 300 minutes. Study protocol included a DCEMR study within 10 days after PTCA and a follow-up examination after 3 months. Cine short-axes images from mitral valve plane to apex were obtained for the measurement of LV volumes and mass. A custom software tool was used for the measurement of global extent (GE) and transmural extent (TRE) of delayed enhancement (DE). Twelve-leads EKG was obtained at admission and on the day of first CMR. Sigma ST-elevation (SST) was defined as the sum of the ST-elevation in millimeters in each leads.

*Results:* Fifty-one patient completed first CMR examination within 6.4 ± 3.12 days after PTCA (range 3–10); twenty-one patient (42%) underwent the follow-up examination after 160 ± 35 days (range 103-230 days). On the first DCEMR study qI group showed a significant higher extent of GE-DE compared with qII (20.3 ± 10.4% vs 11.1 ± 8.2% $p < 0.005$), and a non-significant difference with qIII and qIV. Group qI showed also higher TRE ($p < 0.005$), higher SST ($p < 0.005$), higher peak of CPK ($p < 0.0005$) and troponine ($p < 0.02$), higher echocardiographic WMSI than group qII (Table). Age and culprit vessel were not significantly different between each group. At follow-up examination group qI showed higher DE than qII (15.9 ± 6.7 vs 5.8 ± 2.3% $p < 0.01$), higher end-diastolic volume (EDV, 187.1 ± 30.2 vs 132.1 ± 48 mL) ($p < 0.05$), and a lower Mass/EDV ratio (0.74 ± 0.13 vs 1.05 ± 0.22 g/ml $p < 0.01$), assumed as a remodeling index.

*Conclusions:* Patients with ST-elevation AMI treated early with PTCA had paradoxically higher extent of global and

| | Quartile I | Quartile II | Quartile III | Quartile IV |
|---|---|---|---|---|
| n. | 13 | 13 | 16 | 10 |
| Mean Age | 56,80 | 66,5 | 64,7 | 69,6 |
| LAD(%) | 60 | 20 | 25 | 50 |
| RCA or CX(%) | 40 | 80 | 75 | 50 |
| GE-DE(%) | 20.3 ± 10.4 | 9.3 ± 5.7 | 14.3 ± 10.7 | 25.2 ± 13.2 |
| TRE-DE(%) | 24.4 ± 10.4 | 11.1 ± 8.2 | 18.2 ± 11.1 | 27.8 ± 16.4 |
| SST (mm) | 14.5 ± 8.9 | 12.7 ± 7.9 | 10.9 ± 8.9 | 11.3 ± 8.5 |
| WMSI | 1.67 ± 0.29 | 1.4 ± 0.35 | 1.48 ± 0.45 | 1.58 ± 0.35 |
| CPK (U) | 3168 ± 1695 | 1316 ± 826 | 1741 ± 2091 | 2907 ± 2999 |
| Troponine (ng/dl) | 300 ± 217 | 156 ± 165 | 111.5 ± 152 | 137 ± 225 |
| EDV follow-up (ml) | 182.1 ± 31.3 | 147.8 ± 36.7 | 120.9 ± 29.9 | 165 ± 29.9 |
| Mass follow-up (g) | 135.9 ± 14.2 | 136.5 ± 14.8 | 125.5 ± 28.8 | 129 ± 14.1 |
| Mass/EDV Follow-up (g/r) | 0.76 ± 0.13 | 0.95 ± 0.15 | 1.04 ± 0.15 | 0.8 ± 0.21 |
| EF follow-up (%) | 50.9 ± 5.7 | 57.39 ± 8.1 | 59.9 ± 8.2 | 54.5 ± 3.67 |

transmural DE in comparison with those treated later. Severity of clinical presentation may influence a more aggressive therapeutical decision making in favor of revascularization procedure. Also a reperfusion injury could not be excluded as a potential cause of this phenomenon.

## 521. DEMONSTRATION OF FLOW PATTERNS AT PATIENTS WITH CHRONIC AORTIC DISSECTION WITH PHASE-CONTRAST SEQUENCES AND TIME RESOLVED ANGIOGRAPHY: A NEW ERA FOR THE CLASSIFICATION OF CHRONIC AORTIC DISSECTION

**George Spanos,[1] Constantine Giavroglou,[2] Constantine Papazoglou,[3] Panagiotis Spanos,[4] Marianthi Arnaoutoglou.[5]** [1]***Eurodiadiagnosis-Diagnostic Center, Thessaloniki, Greece,*** [2]***Radiological Department, Aristotle University, Thessaloniki, Greece,*** [3]***5th Surgical Department, Aristotle University, Thessaloniki, Greece,*** [4]***Cardiovascular Department, Aristotle University, Thessaloniki, Greece,*** [5]***1st Neurological Department, Aristotle University, Thessaloniki, Greece.***

*Introduction:* Innovative MR techinques, like Time Resolved Angiography and Phase Contrast Sequences, allowed us to study blood flow in vessels.

*Purpose:* Our objective was to establish the flow patterns both in true and false lumen, for assessment and planning of intervention in patients with chronic aortic dissection.

*Methods:* During the last 18 months, 23 patients with chronic aortic dissection (6 with dissection type A and 15 with type B according to Stanford classification respectively) were scanned at 1.5T (Philips Intera and GE Infinity with EXCITE). Bright-blood sequences at three axis and contrast-enhanced 3D MR angiography were performed in all patients. For the assessment of flow patterns, especially in the false lumen, phase contrast sequences and Contrast Enhanced Time Resolved Techniques (2-D, 3-D and 4-D techniques) were used.

*Results:* Entry sites were easily depicted with the use of 3D MR angiography. Flow studies at patients with type B dissection according to Stanford classification demonstrated that flow in both lumens were of the same direction (from the descending to the abdominal aorta) at the region of the descending aorta. On the contrary, only in 2 out of 6 patients with type A dissection, according to Stanford classification, the flow at both lumens was of the same direction (from the descending to the abdominal aorta). Whereas, in the remaining 4 cases, the entry point was after the left subclavian artery and the flow in the false lumen was reverse to that of the true lumen at the region of the aortic arch and ascending aorta, allowing the false lumen at those regions to receive blood supply from the entry point which was positioned after the left sublavian artery. Demonstration of this reverse flow changed the interventional strategy in 2 out of these 4 patients. These patients were treated by closing the intimal tear with a stent-graft placed at the level of the left sublavian artery instead of surgical treatment.

*Conclusions:* Stanford and DeBakey classifications of aortic dissection are based on surgical treatment of patients with aortic dissection. The use of endovascular stent grafts created a new era in the treatment of patients with chronic aortic dissection. The goal of endovascular intervention is to close the intimal tear which can prevent the expansion of the aneurysm by facilitating complete thrombosis of the aortic false lumen. Thus, demonstration of reverse flow at the ascending aorta and the aortic arch might change the planning of intervention at patients with chronic aortic dissection type A, leading to stent-graft placement instead of surgical treatement.

## 522. AHA TYPE 6 ATHEROSCLEROTIC PLAQUE IDENTIFIED BY MRI IS ASSOCIATED WITH IPSILATERAL ACUTE AND HYPERACUTE TIA/IS

**Jaywant P. Parmar, MD, Christopher Kramer, MD, John Mugler, III, PhD, Erol Baskurt, MD, C. Douglas Phillips, MD, Walter J. Rogers, PhD.** ***University of Virginia, Charlottesville, VA, USA.***

*Introduction:* Atherosclerotic plaque rupture is thought to cause TIA and ischemic stroke (IS).

*Purpose:* Our aim was to examine the relationship between acute or hyperacute TIA/IS and AHA type VI atherosclerotic plaque.

*Methods:* Seventy-three consecutive patients referred for acute stroke protocol MRI/MRA examination underwent additional T1- and T2-weighted carotid bifurcation imaging using 3D variable excitation turbo spin echo black blood MRI imaging. Two blinded reviewers performed plaque gradings according to the MRI modified AHA system. Clinical outcome and brain MR results were obtained via chart review.

*Results:* Image quality for MR plaque characterization was adequate in 56/73 (77%) patients (30 male, mean age 64.3, SD 16.0). 26 patients had IS with acute/hyperacute brain MR diffusion abnormality, 14 patients had TIA diagnosis, and, 30 patients had no cerebral ischemia. Four TIA/IS patients had non carotid etiology for TIA/IS, yielding 52 patients: 104 paired watershed vessel/cerebral hemisphere observations. 16/104 (15%) demonstrated type VI plaque with ipsilateral TIA/IS. 66/104 (63%) demonstrated lesions other than type VI and had no ipsilateral TIA/IS. Positive predictive value of 59% and negative predictive value of 86% were observed. The association between plaque type VI and ipsilateral TIA/IS was significant, $p < 0.001$. No statistically significant association was observed between severe stenosis and outcome.

*Conclusions:* Type 6 carotid bifurcation region plaque identified by MRI was associated with ipsilateral acute TIA/IS, while stenosis was not. These findings suggest that TIA/IS etiology is more commonly associated with the type of underlying plaque rather than severe stenosis.

## 523. MYOCARDIAL VIABILITY: COMPARISON OF 2D AND 3D IR-TURBOFLASH AND IR-TRUEFISP SEQUENCES

**Efe Ozkan, MD, Tuncay Hazirolan, MD, Mahmut Erol, MD, Kudret Aytemir, MD, Aytekin Besim, MD.** ***Hacettepe University Hospitals, Ankara, Turkey.***

*Introduction:* Delayed contrast magnetic resonance imaging has become an accepted modality for assessment of myocardial viability in patients with acute and chronic myocardial infarction. 2D and 3D IR-turboFLASH is the most common used sequence for tissue characterization. 2D and 3D IR-trueFISP is also used for delayed enhancement studies.

*Purpose:* To compare 2D and 3D IR-turboFLASH and IR-trueFISP sequences in the detection of myocardial infarction.

*Methods:* Twenty patients with clinically proven subacute (n = 8) and chronic (n = 12) myocardial infarction were evaluated. Breath-hold, ECG gated, multisegmented 2D and 3D IR-turboFLASH and IR-trueFISP sequences were acquired after intravenous administration of 1.5 mmol/kg gadodiamide-DTPA. The presence of myocardial infarction, the transmural thickness percentage and the image quality were determined semi-quantitatively in the scale of 1–4. Infarct volume was measured. Contrast-to-noise, signal-to-noise, and signal intensity ratios were calculated for the infarct area and normal myocardium respectively.

*Results:* All of the sequences demonstrated the infarct successfully. There was intraobserver agreement in determining the transmural infarct thickness between the sequences. However the infarct volume measured in 3D IR-trueFISP sequence was overestimated. Contrast-to-noise, signal-to-noise, and signal intensity ratios were the highest in 3D IR-trueFISP. The image quality score of 2D IR-turboFLASH and 3D IR-turboFLASH was higher.

*Conclusions:* 2D and 3D IR-turboFLASH sequences are reliable compared to 2D and 3D IR-trueFISP sequences in tissue characterization.

## 524. INTRA- AND INTER-PLATFORM REPRODUCIBILITY OF 1.5T SIEMENS, GE AND PHILLIPS SCANNERS FOR QUANTITATIVE ASSESSMENT OF CAROTID ATHEROSCLEROTIC PLAQUE

**Tobias Saam,[1] Thomas S. Hatsukami, MD,[3] Hunter Underhill, MD,[1] Baocheng Chu, MD/PhD,[1] Norihide Takaya, MD/PhD,[1] Jianming Cai, MD/PhD,[1] Vasily L. Yarnykh, PhD,[1] William S. Kerwin, PhD,[1] Dongxiang Xu, PhD,[1] Nayak L. Polissar, PhD,[4] Wendy K. Hamar, BS,[1] Jeffrey Maki, MD/PhD,[1,2] Dennis W. Shaw, MD,[1] Robert Buck, PhD,[5] Phil Wastall, BSc,[5] Marika Mychajluk, BSN,[5] Brad Wyman, PhD,[5] Chun Yuan, PhD.[1]** ***[1]Department of Radiology, University of Washington, Seattle, WA, USA, [2]VA Puget Sound Health Care System & Department of Surgery, University of Washington, Seattle, WA, USA, [4]The Mountain-Whisper-Light Statistical Consulting, Seattle, WA, USA, [5]Pfizer Global Research & Development, Ann Arbor, MI, USA.***

*Introduction:* Magnetic resonance imaging (MRI) can quantify carotid atherosclerotic plaque burden with high intra-platform reproducibility on 1.5T GE MRI scanners.

*Purpose:* The goal of this study was to compare the intra-platform (Siemens vs. Siemens and Philips vs. Philips) and inter-platform (GE vs. Siemens and GE vs. Philips) reproducibility of quantitative plaque measurements.

*Methods:* Thirty two individuals with ≥15% carotid stenosis by duplex ultrasound were each imaged three times on 1.5T scanners within two weeks. All patients were imaged once by a 1.5T GE whole body scanner (Signa Horizon EchoSpeed). Half of the patients were imaged twice by a 1.5T Philips scanner (Philips Intera) and the other half were imaged twice by a 1.5T Siemens scanner (Siemens Symphony). A standardized multi-contrast protocol with TOF-/T1-/PD- and T2-weighted images and identical phased-array carotid coils were used. Expert readers, blinded to subject information, scanner type, and time point used the same image processing software (CASCADE) to measure the lumen and wall areas on the cross-sectional images. The measurement error was calculated as 100%*$\sqrt{}$ (within-patient variance)/Mean (all measurements).

*Results:* Compared to the GE scanner the mean wall area was significantly larger on both the Philips and the Siemens scanner while the mean lumen area was significantly smaller on the Philips scanner and statistically equal on the Siemens scanner (Table 1). Intra-platform measurement error for mean lumen and mean wall areas were 4.1% and 5.7% for Philips and 4.9% and 6.1% on Siemens scanner, respectively. Inter-platform measurement error for mean lumen and mean wall areas were 6.2% and 14.7% for GE vs. Philips and 4.6% and 8.4% for GE vs. Siemens.

*Conclusions:* This in vivo study achieved an intra-platform reproducibility on Siemens and Philips comparable to those in previous studies on 1.5T GE scanners. However, the use of different scan manufacturers significantly influenced quantitative measurements of carotid atherosclerotic plaque. We therefore recommend to using the same platform for individual patients that undergo serial assessment of carotid atherosclerosis.

Table 1. Quantitative Measurements

| Scan Manufacturer | Mean Lumen Area | Mean Wall Area |
|---|---|---|
| GE vs. Philips | 35.9 ± 8.6 vs. 34.0 ± 8.1 *p = 0.009 | 40.3 ± 11.0 vs. 46.9 ± 14.3 *p = 0.001 |
| GE vs. Siemens | 34.5 ± 13.0 vs. 34.7 ± 13.3 *p = 0.7 | 39.0 ± 6.6 vs. 41.6 ± 9.0 *p = 0.026 |

*paired t-test.

## 525. SIMULATION OF TAGGED MRI USING AN ELECTROMECHANICAL MODEL OF THE MYOCARDIUM FOR PATHOLOGY TESTING AND CARDIAC FUNCTION ESTIMATION

**Maxime Sermesant,[1] Oscar Camara,[2] Rado Andriantsimiavona,[1] Kawal S. Rhode,[1] Derek L. G. Hill,[2] Reza Razavi.[1]** [1]***King's College London, London, United Kingdom,*** [2]***University College London, London, United Kingdom.***

*Introduction:* Tagged magnetic resonance imaging of the heart is an accurate and non-invasive technique to obtain quantitative information on myocardial deformation. However, the inherent image acquisition limitations, such as temporal and spatial resolutions, and the difficulty to automatically extract the displacement information from the images are still limiting the use of tagged MRI for routine clinical use. Moreover, the lengthy acquisition makes it difficult to apply to arrhythmias. The aim of this work is twofold: to provide a tool to simulate tagged MR sequences, and to help in the adjustment of an electromechanical model to patient data. Simulated images can be helpful to study deformation in presence of different electrical and mechanical pathologies, and can offer an error estimation for data assimilation, which by adjusting the parameters of the model to the clinical data, not only makes it possible to extract displacement but also hidden parameters like local contractility.

*Method:* We use an electromechanical model of the myocardium based on the FitzHugh-Nagumo monodomain electrophysiology model, and a passive linear elastic constitutive law coupled with a non-linear active component, relating the contraction stress with the action potential. These models are integrated using the Finite Element Method on a tetrahedral mesh of the myocardium adjusted to a given anatomy. We can create an image of the model myocardium through rasterization, which is the process of finding the voxels corresponding to a given tetrahedron of the mesh. Then we add tag planes to this image. Finally we compute the deformed image from the simulated motion by using rasterization and linear interpolation inside each tetrahedron. Validation of such electromechanical models is very challenging, given the different parameters involved and the complexity of cardiac motion. XMR suites, which combine an x-ray and a MR scanner, provide a way to integrate anatomy, motion and electrophysiology during interventions, thus proving very useful for this validation task. The model can be initialised with these interventional measures and the simulated motion can be compared with the tagged MR images. Finally, different pathologies can be introduced in the model, such as ectopic foci, branch blocks, or modifications in the conductivity and contractility of some parts of the myocardium. Then the simulated motion can be used to create a tagged sequence of the simulated pathology. This can be particularly interesting in the frequent cases of intermittent arrhythmias, as tagged images are then difficult to acquire.

*Results:* Fig. 1 shows the process of tag simulation, starting from anatomical MRI and using the electromechanical model of the myocardium adjusted to patient anatomy. Visual comparison to acquired tagged images seems promising, the simulated image presents many of the deformation characteristics observed in the acquired image. Quantitative comparison in normal and pathological cases is under progress.

*Conclusion:* We have proposed a method to use anatomical data and an electromechanical model to simulate tagged MRI sequences. We have presented our initial simulation results for normal deformation. We are currently applying this technique to patient data to simulate pathological myocardial contraction and compare it to the acquired tagged MR images. This method can help in understanding tagged MR images in some pathological cases, as well as in estimating cardiac function parameters using MRI and an electromechanical model of the myocardium with data assimilation.

## 526. THE OPTIMISATION AND VALIDATION OF CARDIAC MASS AND FUNCTION AT 3 TESLA

**Damian J. Tyler, PhD,[2] Lucy E. Hudsmith, MA, MRCP, BM, BCh,[2] Steffen E. Petersen, MD,[2] Jane M. Francis, DCCR, DNM,[2] Peter Weale, DCCR, MSc,[3] Kieran Clarke, PhD,[4] Stefan Neubauer, MD, FRCP,[2] Matthew D. Robson,**

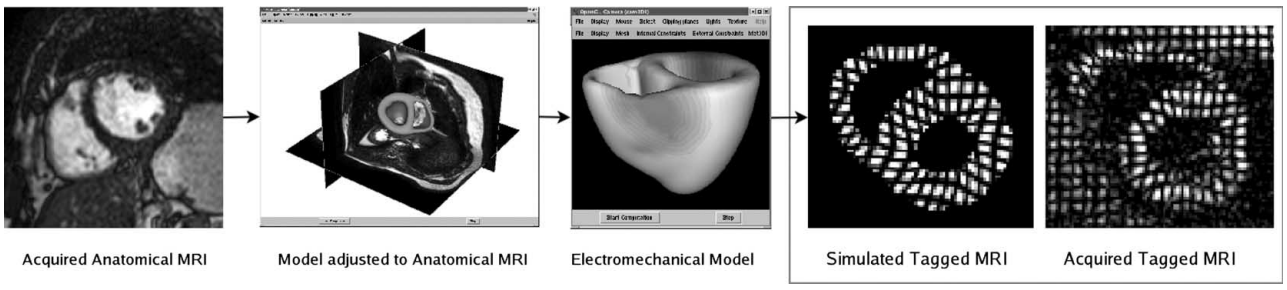


FIG. 1. The anatomical MR is used to adjust the model to patient anatomy. Then the electromechanical model is computed, initialised from electrophysiology measurements if available. Finally the computed motion is used to create a simulated tagged sequence that can be compared to the actual sequence, if available. We present here the end-systolic simulated and acquired images.

**PhD.[2] [1]*Department of Physiology, Oxford, United Kingdom, [2]OCMR, Oxford University, Oxford, United Kingdom, [3]Siemens Medical Solutions, Bracknell, Berkshire, United Kingdom.***

*Introduction:* The technical and regulatory problems of 3 Tesla clinical imagers have been solved. Neuroimaging has been demonstrated across a range of applications to be generally improved at 3T. It is unknown whether 3T provides a better field strength than 1.5T for cardiac imaging. The measurement of cardiac mass and function is a key cardiac evaluation. 1.5T MRI using SSFP provides the gold-standard approach for this evaluation, and 3T is as yet unproven. Existing studies of SSFP at 3T have shown SNR increases from 20% to 150% (1, 2) and have raised concerns over ECG triggering and SSFP artefacts.

*Methods:* Images were acquired on a 1.5T (∼63 MHz) Siemens Sonata and a 3T (∼123 MHz) Siemens Trio, 25A software, and were equipped with identical high performance gradients, and equivalent cardiac array coils. Image contrast parameters (i.e. excitation flip angle) were optimised on 5 healthy volunteers using SSFP and FLASH methods, using parameters optimised for 1.5T exams. A further 10 healthy volunteers in a normal age range were evaluated at 1.5T and 3T with both FLASH and SSFP methods. Careful ECG position, slice positioning, and frequency piloting was followed by the acquisition of a short-axis stack of images using each of the 4 methods (1.5T SSFP, 3T SSFP, FLASH 3T, FLASH 1.5T). Images were evaluated using a grading system. Images were analysed (Argus, Siemens) to assess the clinically required cardiac parameters of the right and left ventricle.

*Results:* Maximising the flip angle subject to SAR limits improves the SNR of SSFP sequences at both field strengths (Fig. 1). Flip angles of 20° and 60° were used for the FLASH and SSFP sequences respectively at both field strengths. In some cases, the excitation angle was limited by SAR, with the lowest excitation angle being 54° in the smallest volunteer. SNR increases were shown at 3T for SSFP (48% myocardium, 30% blood) (Fig. 1) and FLASH (19% myocardium, 13% blood). Scoring of image quality showed 1.5T SSFP to be the best, followed by 3T SSFP, 3T FLASH, and 1.5T FLASH was graded the worst, with the improvements in SNR of SSFP being counteracted by small amounts of image artefact. No image artefact prevented volume or function analysis, and there were no significant differences between 3T SSFP and 1.5T SSFP. Similarly, FLASH measurements agreed between the two field strengths. SSFP and FLASH gave systematic differences at both field strengths. ECG waveforms were affected by the increased field strength but triggering presented no problems in this study.

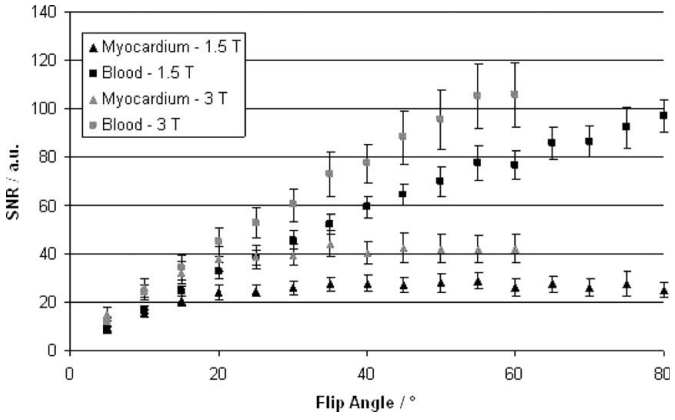


FIG. 1. Variation of SNR in the myocardium and blood and CNR at 1.5T and 3 T for the SSFP sequence.

*Conclusions:* Cardiac imaging at 3T can reliably be used for function and mass assessment, but currently does not provide results superior to the gold standard of 1.5T. 3T FLASH methods are superior to FLASH methods at 1.5T and showed no increase in artefact levels. Therefore, patients who are unable to be imaged with SSFP, 3T provides a small improvement in FLASH sequences. 3T cardiac images may be further improved by continued sequence and parameter optimisation using additional SNR to directly address image quality. The cardiac function examination at 3T provides neither a reason to purchase a 3T system (over 1.5T) nor a reason not to purchase a 3T. Imaging at 3T can perform a functional cardiac examination accurately, with errors that are not dominated by those relating to image quality.

## REFERENCES

1. Hinton DP, Wald LL, et al. Invest Radiol 2003;38:436–42.
2. Gutberlet, M. et al. Rofo 2004;176:801–8.

## 527. CAROTID PLAQUE ECHOLUCENCY RELATES TO DIFFERENT ENTITIES BASED ON MAGNETIC RESONANCE IMAGING MORPHOLOGY

**Ralf Wassmuth, Steffen Bohl, MD, Heike Olthoff, MD, Rainer Dietz, MD, Jeanette Schulz-Menger. *Franz-Volhard-Clinic Charite University Berlin, Berlin, Germany.***

*Background:* Echolucent plaque morphology on ultrasound relates to an increased risk of stroke. It might represent large necrotic cores. The purpose of our study was to compare Magnetic Resonance Imaging (MRI) plaque morphology with ultrasound echogenicity.

*Methods:* We scanned 75 patients (median age 68 years, 23 women, 8 symptomatic) with stenotic carotid plaques as defined by ultrasound in a 1.5 T MRI scanner with a bilateral phased array coil. We acquired axial 3 mm slices starting in the common carotid artery just below the bifurcation with an in-plane resolution of 0.3 mm/pixel. Cardiac gated double inversion fast spin echo images were obtained in protondensity- (PD), T1- and T2-weighting. Scan parameters were TR = 2RR for PDW and T2, TR = 1RR for T1; matrix size 256 × 256, FOV 130 mm, bandwidth 20 kHz, number of acquisitions = 2. Two independent

readers evaluated MRI plaque signal qualitatively compared to adjacent muscle in all the contrast weightings as hyperintense, isointense or hypointense. Conventional B-mode ultrasound was done within 7 days of MRI and graded qualitatively as echo-rich or echolucent. Quantification of gray scale median confirmed qualitative ultrasound assessment in a subgroup of 21 patients.

*Results:* Image quality was sufficient for evaluation in 66 patients (88%). In our low-risk patients 68% of plaques were described as echolucent, whereas 32% appeared echogenic. The echogenic plaques were predominantly isointense in MRI (62%), meaning isointense in all MRI images (24%) or isointense in PD and T1, while hyperintense in T2 (38%). Hyperintensity in all weightings was found in 18% only. However, in the echolucent group, plaques were hyperintense in all weightings in 51%. Echolucent plaques did not represent a homogenous group but were isointense in 33% and showed a mixed pattern in 16%.

*Conclusion:* Echogenic carotid plaques are predominantly isointense in MRI most likely representing fibrous tissue. Echolucent plaques in ultrasound represent different entities of hyperintense and isointense MRI morphology further questioning the unique histologic and clinical correlate of plaque echolucency.

## 528. ASSESSMENT OF THE THORACIC AORTA BY FREE BREATHING 3D BALANCED STEADY STATE FREE PRECESSION (BSSFP) VERSUS MULTIPLE SLICES 2D BSSFP (M2D BSSFP) AND CONTRAST ENHANCED MAGNETIC RESONANCE ANGIOGRAPHY (CE-MRA)

**O. L. Gomaa, R. Gebker, B. Schnackenburg, T. Kokocinski, T. Tangcharoen, E. Fleck, E. Nagel.** ***German Heart Institute, Berlin, Germany.***

*Introduction:* The accuracy for the assessment of thoracic aortic pathology by multi sequence MRI consisting of black blood TSE and CE-MRA has been reported to be almost 100%. However the need of contrast injection prolongs preparation time, attendance of physician, adds to costs and patient discomfort and limits MRI to chronic stable patients.

*Purpose:* To assess the clinical ability of free breathing navigator corrected 3D BSSFP images alone without contrast agent in comparison to M2D BSSFP and CE-MRA.

*Patients and Methods:* Twenty-seven patients (16 male, 61 $\pm$ 13 years, 6 with aortic valve replacement) and 6 controls (5 male, 48 $\pm$ 18 years) were examined with M2D, 3D BSSFP and CE-MRA (20-25 ml of Gd-DTPA) using a Philips Intera CV 1.5 T scanner. Efficiency of each sequence was calculated as covered volume in Feet head (FH) direction divided by time and normalized to CE-MRA. Luminal signal versus noise and muscle ratio (SNR and SMR), aortic annulus visualization, aortic diameters (aortic annulus, sinus of valsalva, ascending aorta, aortic arch and descending aorta), wall thickness, supra aortic arch branch involvement and artifacts (signal void artifact due to susceptibility, flow turbulence or motion) were noted.

*Results:* Significant correlations were found for the determination of diameters using the 3 techniques (P value $< 0.001$) by Bland Altman test. The accuracy for the detection of aneurysms and dissections was identical in all techniques. 4 additional pathologies (1 thrombus, 2 intramural haematoma and periaortic haematoma) were diagnosed with both BSSFP but missed by CE-MRA.

*Conclusion:* 3D BSSFP provides more diagnostic information than CE-MRA. In addition, it is superior to M2D BSSFP due to higher SNR and SMR and fewer artifacts. The need to combine 3D BSSFP with TSE need to be evaluated.

| Imaging Parameters | CE-MRA | M2D BSSFP | 3D BSSFP |
|---|---|---|---|
| Methods | | | |
| TR [ms] | 3.8 | 3.1 | 3.7 |
| TE [ms] | 1.3 | 1.5 | 1.83 |
| Flip angel [*] | 30 | 65 | 90 |
| Matrix size | $368 \times 368$ | $208 \times 208$ | $176 \times 176$ |
| Voxel size [mm] | $1 \times 1 \times 2.8$ | $1.9 \times 1.6 \times 8$ | $2.1 \times 2.1 \times 6$ |
| ECG-triggering | No | No | Yes |
| Number of stacks | 1 | 1 | 2(Aligned with overlap) |
| Respiration | Breathholding | Triggered (End expiratory) | Navigator |
| Imaging plane | Sagittal oblique | Transverse $\pm$ Sagittal oblique | Transverse |
| Average scan duration (min) | $8 \pm 2$ | $4 \pm 1$ | $6 \pm 2$ |
| Sequence efficiency | 1 | 1.8 | 0.7 |
| Results | | | |
| SNR | Not performed | 49* | 64.3* |
| SMR | Not performed | 1.9* | 2.5* |
| Aortic valve annulus visualization | 0(21) | 12(21)* | 19(21)* |
| Severe signal void artifacts (%) | 0 | 6 | 1 |
| Severe motion artifacts (%) | 0 | 23 | 0 |

* $P < 0.05$.

## 529. IN-VIVO T2* EFFECTS IN THE DUAL-SEQUENCE METHOD FOR FIRST-PASS MYOCARDIAL PERFUSION

**Peter Gatehouse, Jonathan Lyne, Dudley Pennell, David Firmin.** ***Royal Brompton Hospital, London, United Kingdom.***

*Aim:* To examine whether T2* effects in large pixels reduce the accuracy of arterial input function measurement in the left ventricle, which would distort myocardial perfusion measurement by the "dual sequence" method.

*Introduction:* Measuring myocardial perfusion requires accurate arterial input function (AIF) and myocardial tissue response function measurements, ideally during the same first-pass of Gd-based contrast agent. The "dual-sequence" method (1) obtains high T1-sensitivity high-resolution myocardial images and a low T1-sensitivity (and low-resolution, so very quick) left-ventricular blood image in the same cardiac cycle. The method aims to maximize myocardial CNR and eliminate AIF peak distortion (due to full T1-recovery) for improved perfusion accuracy (2,3). The larger voxels ($10 \times 6 \times 6$ mm) of the fast AIF sequence are more subject to T2* effects, compared to a typical myocardial imaging voxel size (e.g. $8 \times 2 \times 2$ mm). Large voxels have a greater distance over which B0-inhomogeneity can dephase the signal. (Conversely, the shorter echo-time and faster echo-sampling of the AIF sequence reduce its sensitivity to dephasing). The bolus of paramagnetic CA may significantly distort B0 at the peak LV blood concentration, even though well below 10 mM from a fast antecubital 0.1 mmol/kg injection at 0.5 M. It was therefore necessary to test for T2* effects in-vivo.

*Method:* In 10 patients with varying degrees of coronary artery disease, 140 ug/kg/min adenosine stress first-pass short-axis imaging was performed (0.5 M Magnevist, 0.1 mmol/kg, 7 mL/s, 10 mL saline flush) repeated >20 mins later at rest. The dual sequence method used FLASH for the AIF image (TR1, TE0.5 ms, FA10, $6 \times 6$ mm, $64 \times 48$ raw, 3900 Hz/pixel) in the same plane as the middle of the three TSENSE (R2 avg 8) 4-ETL kyentre-out hybrid-EPI myocardial slices (TR5.8, TE1.2, FA30, $8 \times 2.7 \times 2.7$ mm, 1860 Hz/pixel, 116 ms/image starting after 50 ms SR delay) acquired in each cycle. To minimise T1-weighting in the AIF image, its non-selective saturation pulse was disabled and the FLASH ky-ordering was centre-out. Magnitude images were reconstructed without filtering, ensuring constant receiver gains and reconstruction scaling factor for all 50 cardiac cycles. Each EPI-image was preceded by non-selective saturation so that myocardial perfusion abnormalities were reported clinically as usual. A circular ROI-mean in the LV of the AIF image was measured, of maximum diameter avoiding papillary muscles etc, moving the ROI to track in-plane components of respiratory motion. For each patient's rest and stress studies separately, the highest ROI-mean value found during bolus transit was compared with the value in the first image.

*Results and Discussion:* With no T2* loss and negligible T1 and T2-sensitivity, the ROI value at the high CA concentration (bolus peak) should be 100% of the ROI value obtained without CA, ie, before bolus arrival. In the patients, this bolus-peak-to-initial ratio was 98% ± 3% (mean ± stdev). The ROI-mean plotted against cardiac-cycle (Fig. 1) was complicated by the saturation pulses for the myocardial slices, and by the varying delay before the next cycle's AIF image due to RR-interval variations. For the relevant data, this did not matter: the first AIF image ran before any saturation pulses, and for the bolus peak, the short blood T1 caused full-recovery before the AIF image.

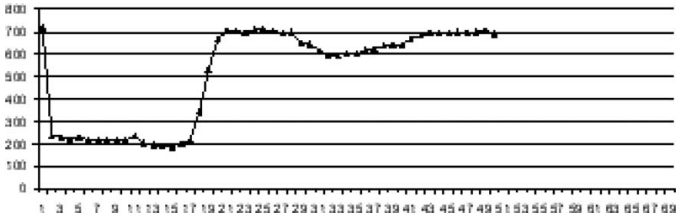

FIG. 1. First-pass LV ROI mean magnitude vs. cardiac cycle. Bolus peak has same level as first unsaturated image.

*Conclusion:* The dual-sequence AIF image has no measurable attenuation of the LV bolus peak blood signal at high-dose with fast injection, which indicates that T2* would affect only a significantly more sensitive combination of large voxel size, long TE and slow ADC-sampling.

### REFERENCES

1. Gatehouse P, Elkington AG, Pennell DJ, Firmin DN. JMRI 2004;20:39–45.
2. Christian TF, Aletras AH, Balaban RS, Arai AE. Radiol 2004;232:677–84.
3. Köstler H, Ritter C, Lipp M, Beer M, Hahn D, Sandstede J. MRM 2004;52:296–9.

## 530. STRESS MAGNETIC RESONANCE FIRST PASS PERFUSION IMAGING IN CHEST PAIN PATIENTS

**Christopher Klassen, MD, PHD, Minh Nguyen, MD, Hugo Montes, MD, Kuran Kareti, MD, Norbert Wilke, MD.** ***University of Florida/Shands Jacksonville, Jacksonville, FL, USA.***

*Introduction:* Magnetic resonance first pass perfusion (MRFPP) imaging with adenosine can be used to identify perfusion defects in certain patients with chest pain. This information can then be used for further clinical decision making regarding the need for either coronary intervention or possibly coronary computed tomography angiography.

*Purpose:* The purpose of this study was to use MRFPP imaging to detect perfusion and viability defects in patients with chest pain and report on its utilization in a tertiary hospital setting. This data will then be used in the larger setting of developing chest pain protocols and algorithms.

*Methods:* All patients evaluated for chest pain at the University of Florida/Shands Jacksonville with a cardiac MRI

extending from 05/03 to 03/05 were included. After informed consent patients were placed in a Siemens Sonata 1.5 Tesla magnet. Localizer images were acquired initially followed by a rest perfusion sequence using TurboFlash. Gadolinium contrast (Magnevist 9 mL, 0.03 mmol/kg) was injected with a power injector and serial images were obtained to capture the first pass of contrast through the myocardium. Adenosine was then infused (140 mcg/kg/min). for 4 minutes and another dose of contrast administered. After 10 minutes, a delayed enhancement scan was acquired. Exams were interpreted qualitatively and reviewed for wall motion abnormalities, perfusion and viability defects to determine the presence and distribution of ischemia and infarction. A retrospective review of patient reports was performed covering the two year period.

*Results:* Three hundred fifty-seven patient exams were acquired and reviewed (age was 60 ± 13 years with 53% female). Forty-six percent of these exams were normal with no evidence of ischemia or infarction. Ischemia was detected in 65 patients (18%) and acute or chronic infarction in 68 patients (19%) additionally of these, 14 patients had both ischemia and infarction. Twenty-two (6%) patients had evidence of hypoperfusion in a circumferential subendocardial distribution indicating microvascular disease. Of these 22 patients, 19 were female (86%) and 5 had left ventricular hypertrophy (23%), additionally, 7 had subsequent coronary angiography, 3 of these were normal, 1 non-diagnostic, 2 with mild disease (no intervention) and one had coronary stent placement.

*Conclusions:* This study demonstrates the application of MRFPP imaging in the evaluation of patients with chest pain. It demonstrates the potential utility of MR in diverting some patients from unnecessary coronary catheterization (with 46% being normal) as well as detecting microvascular disease that would evade detection by angiogram (6%). Additionally, ischemia was detected in 18% that could be referred for further diagnostic studies including computed tomography angiography or diagnostic catheterization.

## 531. IMPROVED TURBO-SPIN ECHO IMAGING OF THE HEART WITH MOTION-TRACKING

**Jennifer Keegan, PhD, Peter D. Gatehouse, PhD, Sanjay K. Prasad, MD, David N. Firmin, PhD.** ***Royal Brompton and Harefield NHS Trust, London, United Kingdom.***

*Introduction:* Outputting an inversion pulse 170 ms before the imaging segment of a dark-blood prepared T2-weighted TSE sequence (1) provides suppression of epicardial fat (STIR) and increased sensitivity to the prolonged T1 and T2 of myocardial oedema. The efficacy of this STIR-T2 technique depends upon the heart being in the same position during the slice-selective preparation phases as it is during imaging and poor image quality is often obtained, particularly in the highly mobile basal short axis plane and particularly in subjects with fast heart rates. Although increasing the slice thickness to 15–20 mm (2) reduces the effects of cardiac mis-registration, it increases the unwanted signal from slow-moving blood and reduces the sensitivity for detecting focal areas of oedema.

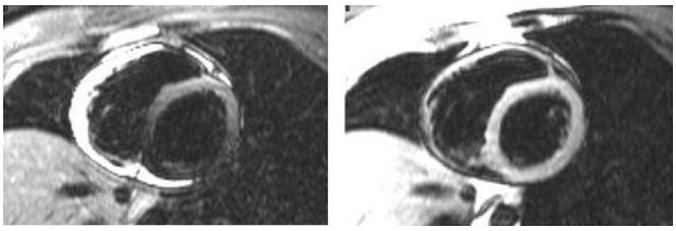

FIG. 1. STIR T2-weighted TSE images both without (left) and with (right) motion tracking.

*Purpose:* To improve thin-slice dark-blood and STIR prepared TSE imaging of the heart, particularly in the basal short axis plane where cardiac mis-registration between the preparation and imaging phases is high.

*Methods:* Ten healthy subjects were studied on a Siemens Sonata 1.5Tesla scanner. Using a modification of the technique of Kozerke (3), interleaved horizontal (hla) and vertical (vla) long axis image planes were acquired during a single breathhold using a cine gradient echo-planar sequence with a labeling pre-pulse. Labeling was performed in basal and mid short axis slices simultaneously by implementing a COMB excitation and the resulting images show the motion of these labeled slices through the cardiac cycle in both the vla and hla planes. A TSE sequence was modified to allow independent positioning of the slice-selective 180 degree dark-blood and STIR preparation pulses on the appropriately timed labeled images. The dark-blood inversion time was calculated to give optimal blood signal suppression and is heart rate dependent. The STIR pulse was output 170 ms before the TSE imaging segment to give optimal fat suppression. The resulting images were scored on a scale of 1 (very poor) to 5 (excellent) by two independent observers and compared with those obtained with the standard untracked STIR-T2 images using a paired Wilcoxon analysis.

*Results:* The labeled images show that the maximal motion of the anterior, inferior, lateral and septal walls of the left ventricular basal short axis plane are 10.0 ± 2.2 mm, 14.7 ± 2.6 mm, 14.0 ± 1.9 mm and 11.8 ± 1.8 mm respectively. The right ventricular basal plane is more mobile than the left with anterior, inferior and lateral maximal motion of 17.0 ± 2.6 mm ($p < .001$), 20.9 ± 3.2 mm ($p < .001$) and 20.9 ± 2.7 mm ($p < .001$). The maximal motion of both left and right mid short axis planes is 50–70% of that in the corresponding basal planes. For the basal plane of both left and right ventricles, tracked images were superior to the untracked images (4.9 ± 0.3 vs 3.3 ± 1.1, $p < .01$ and 3.9 ± 1.0 vs 1.8 ± 0.6, $p < .01$ respectively). For the less mobile mid short axis plane, the image quality of the left ventricle was good (4.8 ± 0.4) and not improved by tracking the motion between preparation and imaging. For the right

ventricle however, motion-tracking continued to significantly improve image quality ($3.8 \pm 0.8$ vs $1.7 \pm 1.0$, $p < 0.01$).

*Conclusion:* Tracking the through-plane motion of the heart between preparation and imaging phases improves the quality of thin-slice TSE images of the heart, particularly in the basal short axis plane and particularly for the more mobile right ventricle. This technique allows imaging of both ventricles at the optimal dark-blood inversion times, even with the thin slice thicknesses necessary for detecting focal abnormalities.

## REFERENCES

1. Simonetti, et al. Radiology 1996.
2. Abdel-Aty, et al. Circulation 2004.
3. Kozerke, et al. Magn Reson Med 1999.

## 532. HIGH RESOLUTION 3D TIME-SERIES IMAGING OF THE CORONARY ARTERIES

**Paul Gurney, Dwight Nishimura.** ***Stanford University, Stanford, CA, USA.***

*Introduction:* The acquisition of high quality 3D images of the heart with fine temporal resolution can provide useful information about the complex movement of the coronary arteries. The 3D Cones trajectory, which is SNR-efficient and robust to motion, was used for this purpose by Irarrazabal et al (1); we now update his method using state-of-the-art gradients and receiver coil to achieve dramatic improvements in spatial and temporal resolution.

*Methods:* The 3D cones trajectory was used to achieve an isotropic FOV of 25 cm and an isotropic resolution of 1 mm. The readout length for each interleaf was 3 ms and a total of 10,000 interleafs are required. We used a steady-state gradient recalled echo sequence with a TR of 7 ms and a flip angle of 60 degrees. The echo time (TE) was set to 1.1 ms, placing the fat and water signals in quadrature. The steady-state was interrupted for 10 ms to play out a navigator (allowing free-breathing acquisition) 200 ms after the reception of the plethysmograph's cardiac trigger. The steady-state was then reentered by ramping the flip angle back up to 60 degrees over 10 TRs. A total of 72 readouts of data, covering 500 ms, were acquired per heartbeat. These were divided into 9 sets of 8 different readouts, resulting in a true temporal resolution of $8 \times 7$ ms $= 56$ ms. The steady-state is then maintained until the next cardiac trigger. The navigator consisted of a single-shot 2D spiral with 5 mm resolution, and acquired a sagittal slice located to the left of the apex of the heart, capable of tracking the S-I movement of the liver as well as the A-P motion of the chest wall. The flip angle for the navigator was 10 degrees, minimizing the effect on the longitudinal magnetization. The Diminishing Variance Algorithm (2) was used with an overscan factor of 50% to reduce the variance of the navigator position and the heart rate for each acquisition, resulting in a total scan time of 1800 heart beats.

FIG. 1. Coronal slice showing the proximal portion of the left main coronary artery.

*Results:* The sequence was implemented on a GE Excite 1.5 T scanner, using an 8-channel cardiac coil for reception. Coronal and axial slices are shown in Figs. 1 and 2. Fig. 3 shows 8 frames from the time series corresponding to the dashed box in Fig. 2.

*Discussion:* This method provides sharp images of the coronary arteries and allows excellent visualization of the subtle motion during diastole (about 350 ms after the cardiac trigger). There is movement (on the order of 1 mm) of the arteries even during the quiescent period. The short readout time used (3 ms) minimizes the off-resonance blurring characteristic of radial trajectories. The use of the 3D Cones trajectory (which is SNR-efficient and robust to motion) allows us to achieve these high

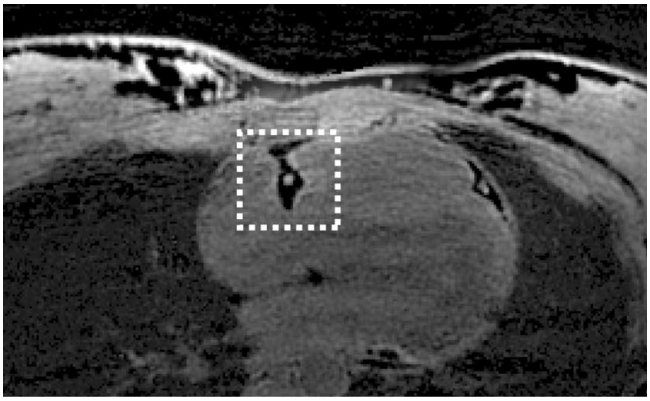

FIG. 2. Axial slice showing a cross-section of the right coronary artery (RCA) and left anterior descending (LAD) artery.

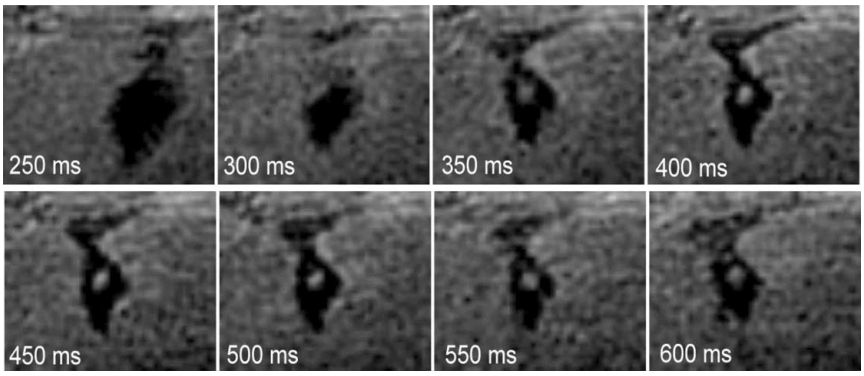


FIG. 3. Motion of the RCA through the time series.

temporal and spatial resolutions with acceptable image quality in a marginally acceptable scan time. The scan time could be reduced to more reasonable levels for clinical use by reducing either the spatial or temporal resolution.

*Conclusions:* Despite the long scan times required, this technique provides valuable information about the motion of the coronary arteries, the understanding of which may lead to more robust and shorter scan time sequences for coronary angiography.

## REFERENCES

1. Irarrazabal, et al. MRM 33:656–662.
2. Sachs, et al. MRM 34:412–422.

## 533. RAPID MEASUREMENT OF LEFT ATRIAL VOLUME BY CARDIAC MAGNETIC RESONANCE

**Caleen Stevens, RT (MR) (N), Nicole T. Smith, MS, Scott E. Bingham, MD.** ***Central Utah Clinic, Provo, UT, USA.***

*Introduction:* Left atrial (LA) volume is an important correlate of diastolic dysfunction, risk of atrial fibrillation, congestive heart failure, cerebrovascular event, and post-myocardial infarction mortality. Due to it's high spatial resolution, uniform volumetric measurements, and cardiac gating, cardiac magnetic resonance (CMR) is ideally suited to quantify LA volume. However, the acquisition of multiple section cine images through the entire left atrium requires time consuming breath-hold imaging and tedious post-processing. A rapid and accurate method to measure LA volume is needed.

*Purpose:* To identify an accurate and easy to use method to determine LA volume by CMR.

*Methods:* After written informed consent, 20 patients who were referred for CMR underwent retrospective gated steady state fast precession imaging and magnetic resonance angiography (3D MRA) with a 1.5T General Electric Twinspeed magnet. Subjects included 10 consecutive patients in normal sinus rhythm (NSR) and 10 consecutive patients in atrial fibrillation (AF). Measurements were performed by Simpson's method with MEDIS workstation software. The following clinical and acquisition parameters were tested for correlation with 4 chamber LA stack volume in diastole (LAVd): Fast LA volume from nongated steady state free precession sagital localizer (Sag Loc), MRA LA volume, age, gender, heart rate, heart rhythm, LA ejection fraction, left ventricular ejection fraction, gating method, central LA area in 4 chamber view, LA anteroposterior diameter, and history of prior ablation. All volume measurements were compared to 4ch LAVd by Bland-Altman analysis. Diameter and area measurements were compared to LAVd by Pearson correlation coefficient. Average time of acquisition and post-processing for each of the three volume methods was compared.

*Results:* Thirteen males and 7 females were tested. Mean LAVd was 120cc (range 59–209). There was an excellent relationship between fast Sag Loc LA volume and LAVd. Bland - Altman mean of differences = 2.1cc (95% CI: −0.6 to 4.7); standard deviation of differences = 6.8cc (Fig.). Agreement with LAVd was high for fast Sag Loc LA volumes (r = 0.99), MRA volumes (r = 0.99), LA systolic volume (r = 0.98), and central LA area (r = 0.97). Agreement was fair for LA diameter (r = 0.86). No other measured parameter correlated with LAVd. No demographic or acquisition factor affected these correlations.

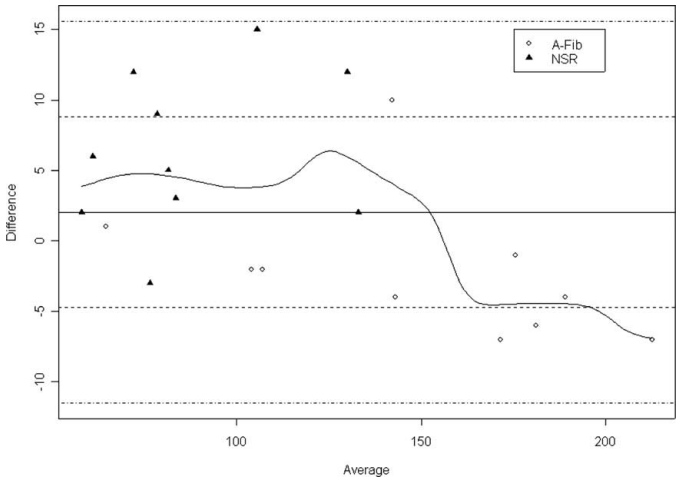

Average acquisition and processing times for fast Sag Loc LA volume were 11 and 100 seconds, for MRA LA volume were 25 and 500 seconds, and for LAVd were 270 and 240 seconds, respectively.

*Conclusion:* Accurate measurement of LA volume can be performed from fast sagital localizer nongated steady state free precession images. The value obtained by this method agrees well with Simpson's method 4 chamber stack diastolic LA volume across a wide range of volumes and regardless of cardiac rhythm. Compared to conventional methods, the new method reduces imaging and processing time by nearly 7 minutes per patient.

## 534. MAGNETIC RESONANCE IMAGING EVALUATION OF SCIMITAR SYNDROME IN EARLY INFANCY

**Muhammad Amar Khan, MD.** ***Children's Hospital of New York, New York, NY, USA.***

*Introduction:* Scimitar Syndrome is a rare and complex congenital anomaly, characterized by partial anomalous pulmonary venous drainage to the inferior vena cava, pulmonary hypoplasia and pulmonary sequestration. Cardiac catheterization with X-ray angiography (XRA) is considered the reference standard for confirmation of the diagnosis and is also used for coil embolization of the systemic arteries supplying the sequestration. However, XRA is an invasive technique involving exposure to ionizing radiation and has a significant risk of complications, especially in infants. Magnetic Resonance Angiography (MRA) is a newer modality that has been shown to be accurate in the diagnosis of pulmonary and systemic venous anomalies and in the identification of aorto-pulmonary collateral arteries in children and adults. However, there are several technical limitations to its use in young infants and its accuracy in the diagnosis of scimitar syndrome in this patient population is unknown. The aim of this study was to evaluate the feasibility, technical aspects and accuracy of MRI in the diagnosis of Scimitar syndrome in early infancy, compared with XRA and/or surgical inspection.

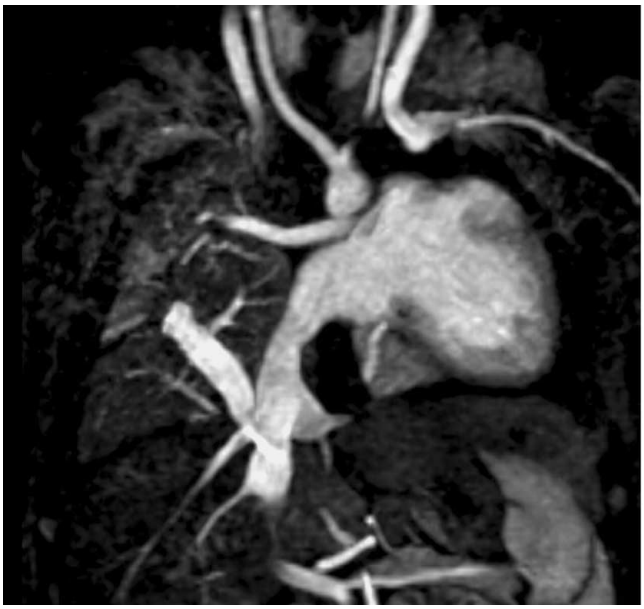

*Methods:* The records of 4 consecutive infants (median age 39 days, range 3–68 ; 1 male and 3 females) with a diagnosis of scimitar syndrome who underwent MRA at a single institution from March to August, 2004 were retrospectively reviewed. Contrast-enhanced 3-D MRA was performed at 1.5 T during suspension of mechanical ventilation. MRA and XRA images were analyzed by separate blinded observers to determine the location and size of the anomalous pulmonary vein, branch pulmonary artery size and architecture and the location and size of systemic-pulmonary collaterals. In addition, the quality of MRA imaging for each of these structures was graded from 1 (poor) to 4 (excellent with well-defined margins). Anatomic measurements on MRA and XRA were compared using correlation and Bland-Altman analysis. Surgical and autopsy reports were analyzed when available.

*Results:* The scimitar vein was right sided in 3 and left sided in 1 subject. Unilateral lung hypoplasia was right sided in 3 and left sided in 1 subject. An aorto-pulmonary collateral artery was seen in 3/4 subjects. Associated cardiac defects included tricuspid atresia ($n = 1$), mixed type total anomalous pulmonary venous return ($n = 1$) and left pulmonary artery sling with ventricular septal defect ($n = 1$). Overall MRA image quality was good in all subjects without imaging artifacts. The imaging quality grade for the main and proximal branch pulmonary arteries, scimitar vein and systemic-pulmonary collateral arteries was 4 (excellent) for every structure in every subject. The median imaging quality grade was 3.7 (range 2–4, $n = 18$) for lobar pulmonary artery branches and 3.9 (range 2–4) for lobar pulmonary veins. Median total duration of magnetic resonance imaging was 7 (range 2–11) minutes. Cardiac catheterization and XRA was performed on 3/4 subjects, all following MRI imaging. There was complete agreement between MRA and XRA in identifying the location and drainage of the scimitar vein (2 subjects) and systemic-pulmonary collaterals (2 subjects). There was close correlation ($r = 0.95$) and agreement (mean difference $0.29 \pm 0.7$ mm) between MRA and XRA in the measurement of the size of proximal pulmonary artery branches, scimitar vein and systemic-pulmonary collaterals. Findings at surgical inspection ($n = 3$) and autopsy ($n = 1$) were in complete agreement with findings on MRA.

*Conclusion:* In this small group of small infants with this rare congenital anomaly, the quality of MRA images was excellent and the results of MRA were in close agreement with the results of cardiac catheterization and surgical or pathologic inspection. MRA may be used for rapid and complete anatomic evaluation of Scimitar syndrome in early infancy, avoiding the need for cardiac catheterization unless embolization of collateral vessels or measurement of pulmonary arterial pressure is indicated.

## 535. STRAIN ENCODED (SENC) IMAGING FOR DETECTION OF REGIONAL DYSFUNCTION IN PATIENTS WITH MYOCARDIAL INFARCTION AT 3T

**Li Pan, MS,[1] Ahmed S. Fahmy, MS,[2] Amy Spooner, MD,[1] Robert G. Weiss, MD,[1] Matthias Stuber, PhD,[1] Nael F. Osman, PhD.[1]** [1]***Johns Hopkins School of Medicine, Baltimore, MD, USA,*** [2]***Johns Hopkins University, Baltimore, MD, USA.***

*Introduction:* SENC imaging (1) is a technique that can directly image and quantify regional myocardial function. It has been demonstrated that SENC imaging on a 3T system provides similar strain measurements in normal subjects as those acquired at 1.5T and offers improvements in SNR (2). In this study, SENC imaging sequences, implemented on 3T MR scanner, have been used to study patients with a history of myocardial infarction. The dysfunctional regions detected by SENC acquisition have been compared with those identified by delayed enhancement imaging.

*Purpose:* To demonstrate that SENC imaging can provide reliable evaluation of regional dysfunction of the heart in patients with a history of myocardial infarction on a 3T MR scanner.

*Methods:* Following informed consent, the studies were performed on a clinical 3T MR whole body scanner (Achieva, Philips Medical System, Best, The Netherlands). Five patients (four males, one female) with a history of myocardial infarction were imaged in both short-axis and four-chamber views. SENC images were acquired in one breath-hold with low-tuning and high-tuning interleaved in one acquisition. A total of 19 to 23 time frames were acquired to cover systole. The tuning spatial frequencies were set as 0.3 $mm^{-1}$ and 0.4 $mm^{-1}$ for low-tuning and high-tuning respectively. The imaging parameters were: slice thickness = 10 mm, FOV = 350 mm, matrix size = $176 \times 176$, spiral interleaves = 12, spiral acquisition window = 12 ms, max ramped flip angle = 40. After SENC acquisition, intravenous contrast, 0.2 $mmol.kg^{-1}$Gd-DTPA, was injected. Fifteen minutes later, an inversion-recovery (IR)-prepared, fast field echo (FFE) pulse sequence with inversion time (TI) = 300 ms was performed to obtain a delayed enhancement image for the localization of the infarct region.

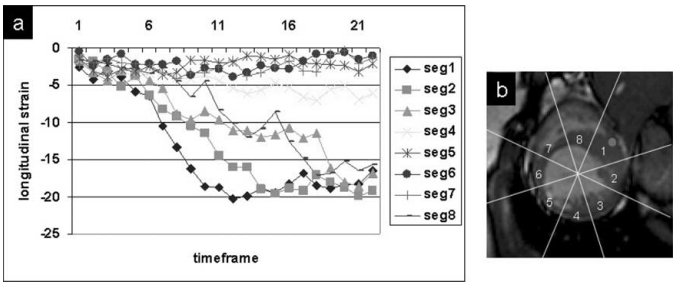


FIG. 2. (a) Longitudinal strain measurments by segments in short-axis view from one patient. (b) The eight segments defined clockwise in the short-axis view, shown on the SSFP image, with the isertion point of the right ventricle (green spot) as mid-point of the first segment.

*Results:* Fig. 1 shows representative results of SENC imaging from two patients, each row represents a different patient. In both four-chamber and short-axis views, the comparison of the areas of myocardial dysfunction detected by SENC imaging (Fig. 1 b,d,f,h) to the nonviable myocardium defined by hyperenhanced tissue in the delayed enhancement images (Fig. 1 a,c,e,g) shows high agreement. Fig. 2a shows representative results of longitudinal strain measurements of eight segments, defined in Fig. 2b, on short-axis SENC images. Segments 5,6,7 are infarcted regions, which show no contraction, segments 3,4,8 are adjacent regions, which show reduced contraction, and segments 1,2 are remote non-infarcted regions, which show normal contraction.

*Conclusions:* Despite the inherent challenges for cardiac imaging at 3T, the SENC imaging has been demonstrated to be able to detect the regional dysfunction of the heart in patients with a history of myocardial infarction. The identified dysfunctional regions show high agreement with those defined

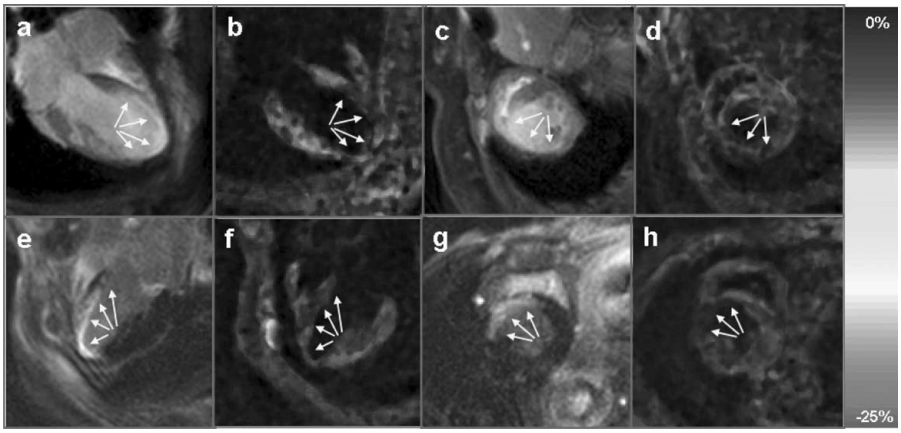


FIG. 1. Representative results from two patients (patient 1: first row, patient 2: second row) in both four-chamber (first two columns) and short-axis view (last two columns). The SENC functional images (b,d,f,h) showing regional dysfunction (arrows) were compared with the delayed-enhancement images (a,c,e,g) showing hyperenhanced nonviable infarcted myocardium (arrows).

by delayed enhancement imaging. SENC imaging on 3T MR system allows determination of regional myocardial function, with high spatial resolution, in infarcted, adjacent, and remote human myocardium.

*Acknowledgements:* This research was supported by grant RO1 HL072704 and by support from the Donald W. Reynolds Foundation.

## REFERENCES

1. Osman NF, et al. Magn Reson Med 2001;46:324–334.
2. Pan L, et al. SCMR 2005, #397.

## 536. BASELINE PATIENT CHARACTERISTICS FOR THE MRI SUBSTUDY TO ONTARGET

**Brett R. Cowan, BE MbChB, Alistair A. Young, BE ME PhD, on behalf of the ONTARGET MRI Substudy Investigators.**
***University of Auckland, Auckland, New Zealand.***

*Introduction:* ONTARGET (ONgoing Telmisartan Alone and in combination with Ramipril Global Endpoint Trial) is a worldwide, multi-center, controlled clinical trial investigating the effects of ramipril and the angiotensin II receptor blocker telmisartan, alone and in combination, in high-risk subjects with vascular disease (1). Major cardiovascular events are being assessed to test for reduction in composite outcome (1). In order to investigate mechanistic pathways in these therapies, a MRI substudy will determine whether the effects of these agents involve direct actions on LV mass and volume, as determined by MRI.

*Purpose:* i) To report the baseline characteristics for subjects enrolled in the MRI substudy to ONTARGET. ii) To examine differences in LV mass and volumes between Asian and non-Asian ethnic groups.

*Methods:* The Cardiac MRI substudy to ONTARGET comprised 28 recruiting centers in 6 countries (Australia, New Zealand, Germany, Canada, Thailand and Hong Kong); 330 patients were enrolled between October 2002 and July 2003. Patients were included with myocardial infarction (MI), coronary or peripheral arterial disease (CAD, PAD), cerebrovascular disease (CVD) or high-risk diabetes mellitus (DM) with end-organ damage (1). Patients were excluded with symptomatic congestive heart failure, significant valvular disease, complex congenital heart disease, syncopal episodes of unknown aetiology, planned cardiac surgery or PTCA within three months of informed consent, uncontrolled hypertension on treatment, heart transplant or stroke due to subarachnoid haemorrhage (1). Substudy exclusion criteria included MRI contraindications. Written informed consent was obtained from all subjects and regulatory authorities of local participating institutions in all countries approved the study protocol. The MR imaging protocol was standardized across 8 imaging centers. Subjects were imaged for the baseline examination during week 3 (plus or minus 1 week) of the run in phase of the trial (ie an average of one week prior to randomization and commencement on study medication). Steady state free precession anatomical cine images were acquired in six equally spaced short axis locations from apex to base and three long axis slices orthogonal to the short axis and orientated at 60 degree increments about the central axis of the LV. Typical imaging parameters were TR/TE/flip/FOV = 30 ms/1.6 ms/60°/360 mm, slice thickness 6 mm, image matrix 256 × 208, 25 frames reconstructed, 8–15 sec breath-hold duration. All MRI studies were digitally recorded onto CD-ROM and sent to the core lab for analysis. LV mass and volumes were determined using guide point modelling (2).

Table 1.

| | |
|---|---|
| Age (yrs) | 66.0 ± 6.6 |
| Height (cm) | 167.1 ± 9.5 |
| Weight (kg) | 77.9 ± 15.3 |
| BSA ($m^2$) | 1.9 ± 0.2 |
| SBP (mmHg) | 131.3 ± 17.4 |
| DBP (mmHg) | 74.6 ± 11.1 |
| HR (bpm) | 64.5 ± 11.7 |

Table 2.

| | n | EDV (mL) | ESV (mL) | LV Mass (g) |
|---|---|---|---|---|
| Gender Male | 255 | 155.9 ± 42.1 | 68.4 ± 37.6 | 156.3 ± 35.5 |
| Female | 75 | 119.9 ± 31.4 | 44.8 ± 23.2 | 117.9 ± 28.8 |
| Age <= 65 | 154 | 151.1 ± 43.4 | 64.5 ± 39.5 | 148.4 ± 35.2 |
| > 65 | 176 | 144.7 ± 41.9 | 61.8 ± 33.2 | 146.9 ± 39.8 |
| Ethnic Asian | 118 | 130.1 ± 37.3 | 53.5 ± 32.9 | 131.8 ± 32.6 |
| non-Asian | 206 | 157.5 ± 42.3 | 68.3 ± 36.7 | 156.4 ± 37.7 |
| MI No | 138 | 131.5 ± 38.6 | 48.5 ± 28.4 | 135.1 ± 34.7 |
| Yes | 192 | 159.3 ± 41.7 | 73.5 ± 37.7 | 156.6 ± 37.3 |
| CAD No | 36 | 131.3 ± 40.7 | 48.4 ± 31.9 | 134.4 ± 37.4 |
| Yes | 294 | 149.7 ± 42.5 | 64.9 ± 36.4 | 149.2 ± 37.5 |
| Hypertension No | 128 | 150.7 ± 47.1 | 68.7 ± 43.0 | 142.3 ± 35.2 |
| Yes | 202 | 145.8 ± 39.5 | 59.5 ± 30.8 | 151.0 ± 38.9 |
| DM No | 219 | 151.8 ± 43.0 | 65.3 ± 36.4 | 148.8 ± 37.7 |
| Yes | 111 | 139.7 ± 41.0 | 58.5 ± 35.6 | 145.2 ± 37.8 |

*Results:* Table 1 shows basic patient characteristics. LV mass and volumes are shown in Table 2. LV mass, EDV and ESV were smaller in Asians vs non-Asians ($p < 0.001$ for each). However, on normalization with the allometric index $Height^{2.7}$, the differences between ethnic groups wereas eliminated (p = NS for each).

*Conclusion:* Baseline characteristics for the MRI substudy to ONTARGET cover a wide range of patient diagnoses. LV mass and volume measurements from these patients provide useful data on population variation in cardiovascular disease. The allometric index $Height^{2.7}$ normalized LV mass and volumes between Asian and non-Asian cohorts.

## REFERENCES

1. Teo KK, et al. Am Heart J 2004;148:52–61.
2. Young AA, et al. Radiology 2000; 216:597–602.

## 537. EFFECT OF 8 WEEKS OF EXERCISE TRAINING ON CARDIAC VOLUMES AND MASS IN OBESE SUBJECTS STUDIED BY MRI

**Thomas W. Vogelsang, MSc,[1] Birgitte Hanel, DMSc,[2] Claus L. Petersen, MD,[3] Andreas Kjaer, MD, DMSc.[2]** [1]***Cluster for Molecular Imaging, Department of Medical Physiology, University of Copenhagen, Copenhagen, Denmark,*** [2]***Department of Clinical Physiology, Nuclear Medicine & PET, Rigshospitalet, Copenhagen, Denmark,*** [3]***Department of Clinical Physiology & Nuclear Medicine, Frederiksberg Hospital, Copenhagen, Denmark.***

*Aim:* The purpose of the present study was to investigate how 8 weeks of intense endurance training influenced cardiac volumes and mass in overweight untrained subjects.

*Methods:* Six overweight subjects (age 19–47 years) with a body mass index of 36 ± 4 kg/m$^2$ underwent 8 weeks of endurance training in a rowing ergometer (Concept II, Morisville, Vermont, USA) with an average training intensity of 72 ± 8% of their maximal capacity. Before and after the period of exercise we measured: End-Diastolic Volume (EDV), End-Systolic Volume (ESV), Left Ventricular Ejection Fraction (LVEF), Stroke Volume (SV) and Left Ventricular Mass (LVM) by Magnetic Resonance Imaging (MRI) using a 1.5 T whole-body scanner (Gyroscan ACS-NT, Philips Medical Systems). To ensure the effect of exercise training we measured the subjects in a submaksimal test at two different workloads (70 W and 110/140 W) before and after the eight weeks of rowing training.

*Results:* The submaksimal heart rate was decreased 14% and 10% respectively after the training period, which indicated a cardiovascular effect of the endurance training. Following eight weeks of rowing training, we found an increase in resting SV of 5% from 100.7 ± 24.6 mL to 105.8 ± 25.3 mL ($p < 0.01$; Fig. 1), and an EDV increase of 7% from 148.3 ± 34.8 mL to 158.7 ± 32.2 ml after the training period ($p < 0.02$). No significant changes were seen in the other parameters measured.

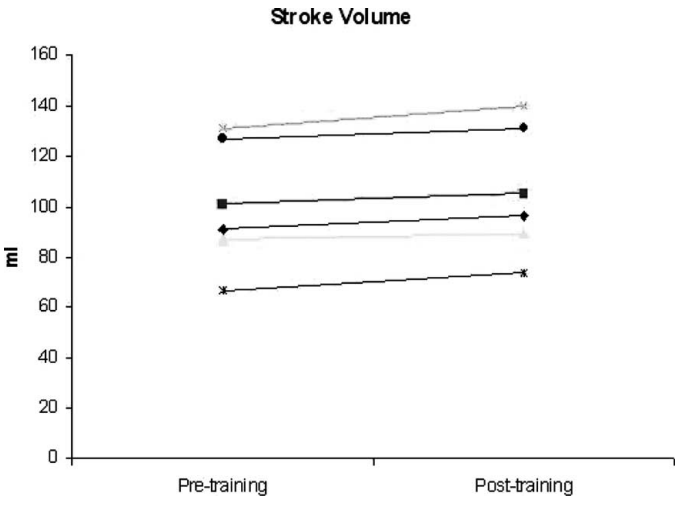


*Conclusion:* Eight weeks of rowing training in obese subjects lead to a significant increase in SV, due to an increase in EDV. We conclude that cardiac MRI is a valuable tool in training studies, since it is possible to detect relatively small changes in cardiac volumes with a high statistical significance.

## 538. EARLY DETECTION OF CARDIAC INVOLVEMENT IN SYSTEMIC SCLEROSIS: PRELIMINARY RESULTS

**Frank Breuckmann, MD,[1] Kai Nassenstein, MD,[2] Alexander Kreuter, MD,[3] Liane Schmidt,[2] Peter Altmeyer, MD,[3] Raimund Erbel, MD,[1] Joerg Barkhausen, MD.[2]** [1]***West German Heart Center Essen, Department of Cardiology, University Duisburg-Essen, Essen, Germany,*** [2]***West German Heart Center Essen, Department of Diagnostic and Interventional Radiology and Neuroradiology, University Duisburg-Essen, Essen, Germany,*** [3]***Department of Dermatology, Ruhr-University Bochum, Bochum, Germany.***

*Introduction:* Progressive systemic sclerosis represents a complex disorder of obscure etiology which affects the skin as well as various organs. Depending on the different subtypes and divergent clinical stages of sclerosis, patients exhibit a variety of clinical symptoms up to even severe systemic manifestations such as myositis or erosive arthropathy, esophageal dysmotility, scleroderma renal crisis, gastrointestinal and pulmonary fibrosis, pulmonary hypertension, and perimyocardial impairment. In the early phase, cardiac involvement seems to be characterized by interstitial inflammatory alterations. Cardiac involvement can be manifested by myocardial disease, conduction system abnormalities, arrhythmias, or pericardial disease. Scleroderma heart disease is virtually always present, though silent, when accurately searched.

*Purpose:* Our current study aimed to assess the potential of contrast enhanced MRI for early detection of cardiac involvement in patients with systemic sclerosis.

*Methods:* The open study included nine patients (male/female 1/8), aged 49 to 76, suffering from severe systemic sclerosis associated with diffuse cutaneous sclerosis, pronounced acral edema and sclerosis. Impairment of internal organs comprised gastrointestinal dysmotility, pulmonary fibrosis and/or hypertension, chronic arthropathy, and renal dysfunction. All examinations were performed on a 1.5T MR scanner equipped with high performance gradients (Magnetom Sonata, Siemens medical solutions, Erlangen, Germany). The MRI protocol included a steady state free precession cine sequence (TrueFISP, TR 3 ms, TE 1.5 ms, FA 60°) for the assessment of the myocardial function in all patients. Based on contiguous short axis scans volumetric measurements were performed using the manufacturer provided software (ARGUS). For assessment of myocardial edema a fat-suppressed T2-weighted turbo spin echo (TR 2 heart beats, TE 49 ms, FA 180°) sequence was performed. Additionally, an inversion recovery fast low angle shot sequence (IR-turboFLASH:

TR 8.0 ms, TE 4.0 ms, TI 180–240 ms, FA 20°) was acquired in short and long axis views 10 min after injection of a 0,2 mmol/kg bodyweight of Gd-DTPA (Schering AG, Berlin, Germany).

*Results:* All patients did not complain about cardiac symptoms during the last six months prior to examination. Adequate image acquisition could be achieved in all but one patient due to severe claustrophobia. Four patients did not show any pathologic abnormalities. Myocardial edema could be detected in none of our patients. MRI analysis revealed a slight decrease of the ejection fraction (EF) in four patients (mean left ventricular EF 50.4%) combined with intraventricular asynchronia in one patient and right ventricular dilatation in another patient. Additionally, one patient showed a pericardial effusion. Delayed enhancement in a spotted subepicardial assortment was detected in one patient.

*Conclusions:* Extent, complexity and severity of internal organ involvement belong to the most important factors influencing outcome and prognosis in systemic sclerosis. Therefore, early diagnosis and accurate staging of visceral involvement are fundamental for appropriate management and therapy. Cardiac MRI has been well-established for the detection of structural and functional myocardial and/or perimyocardial abnormalities. Although, only a limited number of patients have been included so far, our preliminary data show that functional abnormalities can be detected in about 50% of all progressive systemic sclerosis patients using cardiac MRI. Additionally, contrast enhanced MRI allows direct visualization of inflammatory myocardial alterations. However, late contrast enhancement was detected in one of nine patients only. Therefore, larger patient cohorts are mandatory to determine the potential of contrast enhanced MRI for early detection of cardiac involvement in patients with systemic sclerosis. Thus, as to our preliminary results, MRI is feasible to specify potential cardiac comorbidity in scleroderma. In our study cardiac impairment could be assessed in up to 50% of the patients included. However, further studies are mandatory in order to assess a possible correlation between clinical stages of disease and prognosis and perimyocardial involvement detected by contrast enhanced MRI.

## 539. OPEN BIRDCAGE COIL AND PHYSIOLOGICAL CHAMBER FOR MOUSE CARDIAC IMAGING

**Xioabing Fan, PhD, Erica Markiewicz, Muhammad Haque, Marta Zamora, Gregory S. Karczmar, PhD, Brian B. Roman, PhD.** ***University of Chicago, Chicago, IL, USA.***

*Introduction:* The mouse is an extremely important model for studying cardiac disease due to the plethora of transgenic and knock-out/in animals which have been produced. In order to fully appreciate the perturbations generated in these models, physiologically relevant MRI paradigms need to be designed. Mouse cardiac MRI is challenging mainly due to low tissue mass (∼120 mg) and high heart rates (∼500–700 bpm). Surface coils are often used because of the location of heart near the chest wall. A surface coil is often constructed from a single loop which, although simple in design and application, does suffer from poor B1 field uniformity. Volume coils have also been used and although do not suffer from B1 field inhomogeneity, are not optimized for localized cardiac detection and do not provide easy access to the animal. Therefore, to maintain simplicity of application, high B1 field uniformity, and accessibility to the animal, we designed and constructed a low pass open birdcage coil for mouse cardiac MRI. The quality of simple loop surface coil, closed birdcage and open birdcage coil was compared. To complement the open birdcage coil design, a chamber was constructed to maintain the mouse in a good physiological state, obtain clear ECG signals for image gating and isolate the animal from all coil components.

*Material and Methods: Physiological Imaging Chamber:* A clear plexiglass chamber was built to incorporate the open birdcage coil, animal holder, and access ports for ventilation, ECG, temperature and infusion lines. This chamber provides consistent airflow necessary for warming without requiring the animal to be wrapped or covered. This also allows for consistent and clear ECG signals for gating. *Coil Design Open Birdcage:* A six leg low pass open birdcage coil was constructed on a polycarbonate tube with outer diameter 2.6 cm and inner diameter 2.3 cm which was cut in half. The coil width matched the curvature of the tubing at 4 cm long and the length was designed to match the mouse chest at 2 cm in length. In order to reduce the number of solder points, the leads of capacitors (total 1.8 cm long) served as the legs of the birdcage coil and these were attached to the end-ring which was made from copper tape cut into 0.25 cm width. *Single Loop:* The single loop surface coil had the same size and shape as the open birdcage coil but was constructed

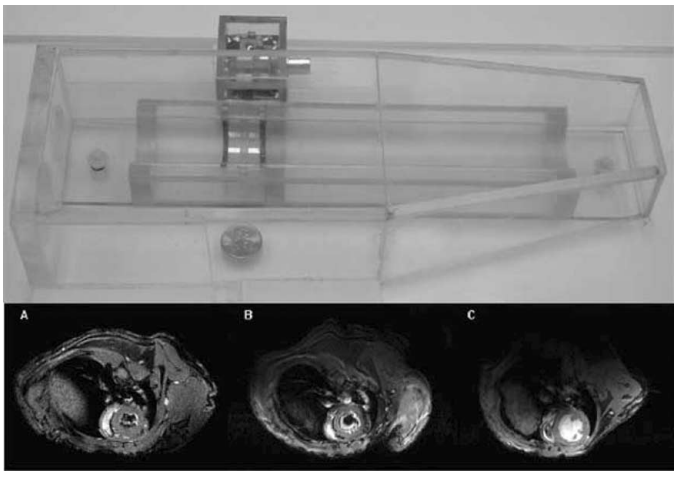


FIG. 1. The top panel shows the mouse physiological imaging chamber. The chamber covers the animal support and coil. It provides for warming air flow over the animal as well as ventilation, ECG, temperature and infusion lines. The bottom panel illustrates the comparative mouse cardiac images at 4.7 T from (A) Body Coil (B) single Loop Coil and (C) Open Birdcage Coil The average SNR with similar heart wall ROT's from each coil are 10, 23, and 32.

from 0.25 cm wide copper tape which was arranged into a 4 × 2 cm rectangle. *Closed Birdcage:* A standard eight leg low pass birdcage coil (3.8 cm × 3.8 cm) was used. Experimental Setup Mice were anesthetized with isoflurane and a SAS physiological monitoring system (Brooklyn, NY) was implemented to acquire ECG signals for gating and to maintain body temperature at 38°C. Image acquisition was triggered 10 ms following the cardiac R wave. All experiments were conducted on a Bruker 4.7 T animal scanner with a 20 G/cm gradient set. Conventional gradient images were acquired using all coils (TR/TE = 16/4.9 ms, slice thickness = 0.5 mm, FOV = 3.0cm, array size = 256 × 256, flip angle = 15, NEX = 4). Image SNR comparisons were determined using comparable ventricular wall ROIs.

*Results and Conclusion:* The SNR obtained from the ventricular wall was 10 for the closed birdcage coil, 23 for the single loop coil, and 32 for the open birdcage coil. Representative images are shown in Fig. 1. The open birdcage coil design for mouse cardiac MRI results in high ventricular wall SNR surpassing that obtained with either the single loop or closed birdcage coil design. When combined with an optimized physiological chamber, this coil design provides excellent mouse cardiac MR images critical for studying transgenic mice.

## 540. VARIABLE DELAYED ENHANCEMENT PATTERNS IN NON-COMPACTION OF THE LEFT VENTRICLE

**Nigel McMillan.** ***Western Infirmary, Glasgow, United Kingdom.***

*Introduction:* Non-compaction of the left ventricle (NCLV) is a rare form of cardiomyopathy. Little is yet known regarding the incidence or significance of late myocardial enhancement on MRI. 6 patients, ages 20–66, exhibited features suggestive of NCLV as part of a wider study of cardiomyopathies in the west of Scotland.

*Purpose:* To review the degree of late Gadolinium enhancement in the myocardium of patients with NCLV.

*Methods:* All patients underwent routine cardiac MRI including cine TrueFisp breathhold sequences for the assessment of cardiac function and LV mass calculations. Further imaging using TurboFlash IR sequences was performed 10 minutes after IV Gadolinium DTPA (0.2 mmol/Kg) to assess myocardial uptake.

*Results:* All 6 patients were shown to have some impairment of cardiac function with reduced ejection fractions (38–51%). 5 patients had a dilated LV. All showed varying degrees of increased myocardial trabeculation in the LV which is the principal feature of the condition. In 4 patients there was no detectable late enhancement of the myocardium; however, in the other two patients (who were sisters), there was a very marked degree of contrast uptake. These two patients had 3 close relatives with HCM which supports the genetic basis for the disease.

*Conclusions:* Gadolinium contrast uptake in NCLV is variable but appears to be more likely in patients with a strong genetic component. More detailed evaluation of the myocardium in these patients is required.

## 541. COMPOSITE STRAIN-ENCODING (C-SENC) IMAGING OF DYSFUNCTIONAL AND SCARRED REGIONS IN PATIENTS' HEARTS

**El-Sayed H. Ibrahim, MSE, Li Pan, MSE, Ahmed S. Fahmy, MSE, Amy Spooner, MD, Matthias Stuber, PhD, Robert G. Weiss, MD, Nael F. Osman, PhD.** ***Johns Hopkins University, Baltimore, MD, USA.***

*Introduction:* Composite Strain-Encoding (C-SENC) MR imaging is a useful method for simultaneous imaging myocardial viability and regional function, with the same spatial resolution, in a single breath-hold (1). Three images result from C-SENC imaging: No-Tuning (NT), Low-Tuning (LT), and High-Tuning (HT) images. Bright regions in the NT, LT, and HT images represent scarred, akinetic, and kinetic myocardium, respectively. No additional time, when compared to standard Inversion-Recovery (IR) Delayed-Enhancement (DE) imaging, is required for acquiring the additional LT and HT functional images. In this work, the method was tested on human volunteers. The viability images showed good agreement with the standard DE images, and the additional functional images gave more understanding of the myocardium condition.

*Methods:* Fig. 1 shows a schematic diagram of the pulse sequence used for C-SENC imaging, where the NT, LT, and HT images were consecutively acquired at end-systole (1). After tagging, the DC and AC signals (the signal components with zero and tagging frequencies, respectively) show different behavior due to $T_1$ relaxation. The AC signals, contributing to the LT and HT images, decay, while the DC signals, contributing to the NT image, increase. At the imaging timepoint, there were enough AC and DC signals to acquire all three images. Fig. 2 shows numerically-simulated AC and DC signal behavior for normal and infarcted myocardium 15 minutes after gadolinium (Gd) injection. The following values were assumed: TRR = 850 ms; TR = 23 ms; TE = 4.9 ms; $T_1$ = 400 ms and 300 ms for normal and infarcted myocardium, respectively; Trigger-Delay (TD) = 300 ms; and flip-angles = 27, 32, and 40 degrees for NT, LT, and HT, respectively. Six volunteers (5 males, average-age = 45) were scanned on a 3T Philips scanner. The subjects were injected with 0.2 mmol/kg of GD-DTPA. Then, 10-15 minutes post injection, C-SENC and DE images were acquired. The imaging parameters were the same as in the simulation. Additional parameters were: TD ≈ 300 ms (depending on heart-rate); BW = 66.68 kHz; scan-matrix = 176×256; and spiral


FIG. 1. The steps, during one cardiac cycle, of the pulse sequence used.

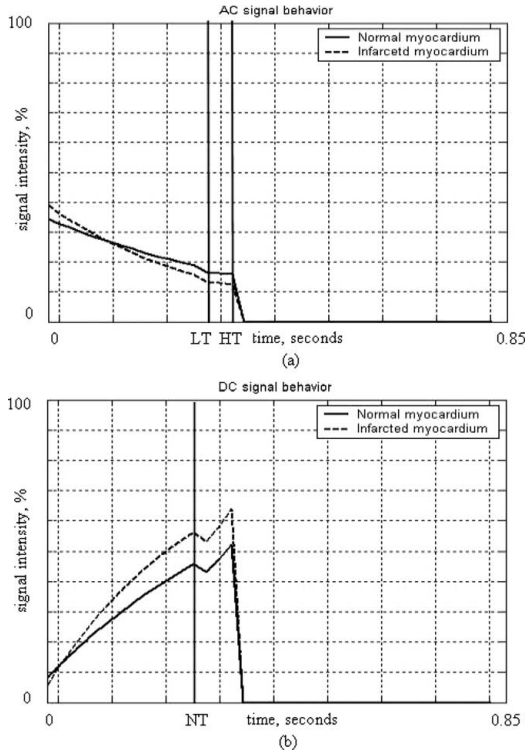


FIG. 2. AC (a) AC and DC (b) signal behaviours through a 850 ms cardiac cycle. The vertical lines represent the time points of images acquisitions NT, LT, and HT. Then, the signals are spoiled and wait till next cardiac cycle.

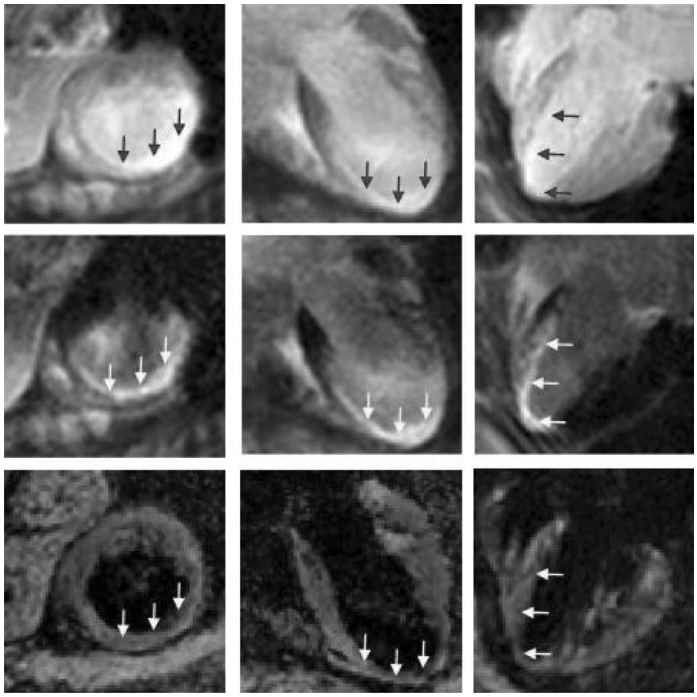

FIG. 3. First, second, and third rows shows NT, DE, and composite images from different volunteers. The arrows point to infarcted myocardium. Contracting and infarcted myocardium are shown in red and blue, respectively, in the composite images. The figure shows good agreement between the NT and DE images.

acquisition-window = 12 ms with 12 interleaves. The resulting NT images were validated against the conventional DE images. The validation of the LT and HT images in evaluating regional function had previously been conducted (2). The infarcted myocardium was automatically extracted from both NT and DE images using the full-width at half-maximum (FWHM) technique (3). The sensitivity and specificity of the C-SENC method, against the gold-standard DE method, for determining the infarcted regions were computed by comparing the extracted infarcted regions from both images. Sensitivity (specificity) was computed as the ratio of the area of the common infarcted region determined from both the DE and NT images to the area of the infarcted region determined from the DE (NT) image.

*Results:* Fig. 3 shows representative slices from different volunteers. The first, second, and third rows show resulting NT images, standard DE images, and composite color-coded images, computed from the LT, HT, and NT images, respectively. The figure shows agreement between the NT and DE viability images: sensitivity and specificity were 82 % and 86 %, respectively. Additionally, using C-SENC, the functional images were obtained without increasing the scan duration.

*Acknowledgements:* Grants: Donald W. Reynolds Foundation and R01-HL072704.

*Conclusions:* We demonstrate that the C-SENC technique is applicable in people and allows high-resolution viability and functional images during the same acquisition. The resulting NT images show good agreement with the standard DE viability images and are complemented by the functional data.

## REFERENCES

EH Ibrahim, et al. Magn Reson Med in press.
J Garot, et al. Radiology 233:596–602.
LC Amado, et al. J Am Coll Cardiol 44:2383–2389.